

Utah State University

DigitalCommons@USU

---

All Graduate Theses and Dissertations

Graduate Studies

---

12-2016

## Design for Manufacturability and Assembly of an Assistive Technician Creeper, Including Single Drive Control of a Multi-Degree of Freedom Kinematic Mechanism

Larry T. Wilde Jr.  
*Utah State University*

Follow this and additional works at: <https://digitalcommons.usu.edu/etd>



Part of the [Mechanical Engineering Commons](#)

---

### Recommended Citation

Wilde, Larry T. Jr., "Design for Manufacturability and Assembly of an Assistive Technician Creeper, Including Single Drive Control of a Multi-Degree of Freedom Kinematic Mechanism" (2016). *All Graduate Theses and Dissertations*. 5049.

<https://digitalcommons.usu.edu/etd/5049>

This Thesis is brought to you for free and open access by the Graduate Studies at DigitalCommons@USU. It has been accepted for inclusion in All Graduate Theses and Dissertations by an authorized administrator of DigitalCommons@USU. For more information, please contact [digitalcommons@usu.edu](mailto:digitalcommons@usu.edu).



DESIGN FOR MANUFACTURABILITY AND ASSEMBLY OF AN ASSISTIVE  
TECHNICIAN CREEPER, INCLUDING SINGLE DRIVE CONTROL OF A  
MULTI-DEGREE OF FREEDOM KINEMATIC MECHANISM

by

Larry T. Wilde, Jr.

A thesis submitted in partial fulfillment  
of the requirements for the degree

of

MASTER OF SCIENCE

in

Mechanical Engineering

Approved:

---

Byard Wood, Ph.D.  
Major Professor

---

Steve Hansen, Ph.D.  
Committee Member

---

Ling Liu, Ph.D.  
Committee Member

---

Mark McLellan, Ph.D.  
Vice President for Research and  
Dean of the School of Graduate Studies

UTAH STATE UNIVERSITY  
Logan, Utah

2016

Copyright © Larry T. Wilde, Jr. 2016

All Rights Reserved

## ABSTRACT

Design for Manufacturability and Assembly of an Assistive Technician Creeper,  
Including Single Drive Control of a Multi-Degree  
of Freedom Kinematic Mechanism

by

Larry T. Wilde, Jr., Master of Science

Utah State University, 2016

Major Professor: Byard Wood, PhD  
Department: Mechanical and Aerospace Engineering

In 2011, a team of senior engineering students at Utah State University, in connection with the university's Center for Persons with Disabilities, designed and prototyped an assistive technician creeper. Building on successful features and resolving issues discovered in design validation testing of the initial prototype, this thesis includes the refined development of a fully assistive technician creeper with emphasis on improvement of kinematic functionality, overall manufacturability, and integration of system safety features. The final design solution is a creeper that transforms a user bi-directionally between the seated position, and a maneuverable supine position, while requiring only simple manual actuation.

New design requirements were established including specifications for user height, weight, and body mass distribution, driven by census and medical data suitable for 95% of individuals. Using 3D modeling software, an iterative design approach was used in conjunction with kinematic, and structural analyses, to generate an improved feature set that can be easily manufactured and assembled. Of particular interest is the modification to the kinematic system, which produces multiple single-degree-of-freedom kinematic motions from a single multi-degree-of-freedom kinematic mechanism. This promotes the use of a single motor to produce separate motions for adjusting upper body inclination, and raising the seat surface. The revised design adheres to principles of design for manufacturability and assembly, by using common economical manufacturing processes, minimizing part asymmetry and maximizing part reuse.

Employment of engineering analyses, including kinematic, finite element, and failure modes and effects analyses quantified design validation and risk mitigation. Static force analysis and computations of fatigue and life expectancy of critical components supplement the analysis set. Analysis suggests all structural components were designed to meet a safety factor of 3.0 or better. This combined with the addition of safety features and system protection redundancies provide confidence in structural integrity and system reliability. This creeper will contribute to the world of assistive technologies by providing new mobility opportunities, improving the quality of life of individuals with certain physical disabilities. It is also well suited for users of all abilities and has potential to become a premium creeper for professionals.

## PUBLIC ABSTRACT

Design for Manufacturability and Assembly of an Assistive Technician Creeper,  
Including Single Drive Control of a Multi-Degree  
of Freedom Kinematic Mechanism

Larry T. Wilde, Jr.

In 2011, a team of engineering students at Utah State University designed and built an assistive technician creeper to assist persons with lower-extremity physical disabilities to work in low-clearance areas. In order to put this technology on the market, a complete product redesign was needed to address safety and functionality concerns. This thesis outlines the specific design needs, presents the detailed design approach, and summarizes the final creeper solution. The mechanisms of the initial prototype were modified to independently incline or recline the upper body, and raise or lower the seat surface with a single motor. This will be especially useful for those wanting to work low to the ground with the backrest up. All components were designed to be fabricated using common manufacturing and assembly processes. Safety features were refined and several specific engineering analyses performed to ensure user safety and system reliability. Results of these analyses suggest all structural components were well designed to provide structural integrity and yield the intended system functionality. The design is mechanically complete, and ready for prototyping. While a good candidate for improving the quality of life of people with physical disabilities, the creeper is also well suited for users of all abilities and has reasonable market potential in the professional world.

## ACKNOWLEDGMENTS

This thesis represents the culmination of a tremendous amount of time, not only spent in the lab, but also sacrificed by many. I want to take a moment to recognize the many individuals and affiliations that have stood by my side and made this possible.

To begin, I express my sincere gratitude to my major professor, Dr. Byard Wood, and my master's committee Dr. Steve Hansen, and Dr. Ling Liu, for their continued patience, support, and guidance. They have been extremely supportive and encouraging. Through their work at USU, this opportunity was available as a thesis project, and it is my hope for them to see the product improve the lives of those who need it.

The work required between classes, exams, and deadlines would have been insurmountable without the flexibility and support of the two employers I have had, Inovar, Inc. and Juniper Systems. In particular, I would like to recognize Craig Rupp, Dave Griffith, Jef Nielsen, Lenoard Sherman, Ryan Harris, and Charles Olson, for their encouragement and mentoring during the course of my graduate school.

Next, I express my appreciation to Christine Spall, for her exceptional graduate advisement and help along the way. She has also had a great deal of patience and has laid the groundwork for me to follow.

Thanks to Terry Zollinger, fabrication of prototype and test parts facilitated the design work, and provided crucial manufacturing and design feedback.

Without Albert LaBounty, and the Utah State University, Dept. of Mechanical & Aerospace Engineering (MAE) and Center for Persons with Disabilities (CPD), the purpose, information, and opportunities for this project and other assistive technology

developments, would not have come to be at this time and place. I issue my sincere thanks to their involvement.

I also recognize the National Science Foundation and the program for Engineering Design to Aid Aging Persons (EDAAP), for the opportunities given to USU.

Although many believe this journey began five years ago, it has in fact been nearly two decades in the making. It all began early in my life when talks with my dad would include his desire for me to go to college and complete a degree. In such discussions, he would often remind me that nothing that meant the most to him in his life, ever came easy. Speaking on life, my dear wife has reminded me on many occasions, in a poem she wrote for me long before she even knew me, that life is not so easy, nor is it meant to be. I certainly didn't know what kind of work it would be 10 years ago after enrolling in my undergraduate program at USU. Among the last promises I made to my dad in this life was that I would finish my undergraduate degree and to go on for a master's degree. My parents were the first to believe in me, and continue to do so, far more than I do in myself. In the last five years life has had to go on, and has refused to slow down for my family and I. We've been blessed and overjoyed with two more sweet little girls. Working more than full time, combined with a few trials, has tested our tenacity, but with those trials have come countless blessings. I thank my dear wife Jana for her support and sacrifice in behalf of this accomplishment. My four beautiful kids, Bela, Patrick, Luciana, and Millee, have had to forego countless hours of daddy time, and will soon be going on their first ever, family vacation. To these special individuals, I owe everything.



## CONTENTS

	Page
ABSTRACT.....	iii
PUBLIC ABSTRACT .....	v
ACKNOWLEDGMENTS .....	vi
LIST OF TABLES .....	x
LIST OF FIGURES .....	xi
NOMENCLATURE .....	xiii
CHAPTER	
1 PROJECT INTRODUCTION & INITIALIZATION .....	1
Background.....	1
Problem Description .....	3
2 DESIGN & DEVELOPMENT .....	9
Key Design Requirements .....	9
Design Approach .....	11
Kinematics .....	14
Kutzbach's Equation.....	17
Design Solution.....	26
3 ANALYSES & DESIGN VALIDATION .....	44
Kinematic Analysis.....	45
Static Force Analysis .....	54
Finite Element Analysis (FEA).....	60
Traditional Theoretical Analysis.....	63
Failure Mode and Effects Analysis (FMEA) .....	64
4 PROJECT FINALIZATION.....	70
Results.....	70
Conclusion .....	72
Future Work .....	74
REFERENCES .....	76
APPENDICES .....	77
Appendix A. Reference Figures.....	78

Appendix B. Kinematics Equations .....	84
Appendix C. Free Body Diagrams .....	89
Appendix D. Static Force Equations .....	102
Appendix E. Kinematics and Static Force Computation Code .....	134
Appendix F. Finite Element Analysis Reports.....	168
Appendix G. Traditional Theoretical Calculations .....	273
Appendix H. Failure Mode and Effects Analysis (FMEA) Table.....	305
Appendix I. Part Level Bill of Materials.....	333
Appendix J. Top-level Mechanical Drawing .....	338

LIST OF TABLES

Table		Page
1	BLAC Inc. Creeper, key product specifications provided in final report [8].....	5
2	Part numbering prefix by manufacturing process .....	26
3	Top-level part and assembly quantities by manufacturing process.....	41
4	Kinematic position, known and unknown values, by vector loop.....	47
5	Kinematic velocity, known and unknown values, by vector loop and motion phase.....	51
6	Number of equations attainable from each link included in the static force analysis for both incline/recline and raise/lower phases .....	57
7	Qualitative FMEA scoring table.....	68
8	Safety factor to OCC scoring chart used to identify the OCC rating by the minimum relevant SF.....	69
9	Numbered list of FEA reports including the part number and description of the analyzed part.....	168
10	FEA information table for all completed finite element analyses, including part names, assumptions, and FEA setup information .....	169
11	FEA results table including material properties, stresses, and safety factors.....	171
12	Complete FMEA table, segmented into 3 columnar sections .....	305
13	Complete component level bill of materials for top-level assembly.....	333

## LIST OF FIGURES

Figure		Page
1	Prototype of BLAC Inc. Creeper.....	6
2	Concept and preliminary design cycle .....	13
3	3D kinematic link stacking of the BLAC Inc. creeper .....	15
4	3D kinematic link stacking of the Creep-Up creeper .....	16
5	Stripped-down view of the main kinematic links, with all other parts hidden from view .....	18
6	Kinematic diagram of linkages with link numbers, and identification of joints .....	19
7	Leg interference force between the two legs where they are in contact during the incline phase .....	21
8	Cutaway view of the back stop and back lock mechanisms that remove rotational degrees of freedom from the backrest kinematic chain.....	22
9	Pushrod axial load plot, across full range of motion.....	24
10	Final Creep-Up design solution shown in three fundamental positions.....	27
11	Welded chassis subassembly of final design solution.....	28
12	Full chassis subassembly of final design solution, including hardware, drive train, and emphasis of belt safety system .....	29
13	Maximum motor shaft speed required for a given torque, superimposed with linear torque/speed performance of Makita drill .....	30
14	Side view of legs, pushrod, and brake in the final design solution .....	32
15	Isolated seat subsection of final design solution .....	34
16	Backrest subassembly of final design solution.....	35

17	Close-up view of footrest locking mechanism (right side) of final design solution .....	37
18	Left-side footrest view: caster leveling strut integrated into final design solution .....	38
19	Vector Loop A: backrest inclination, kinematic chain for kinematics analysis, including link numbers .....	46
20	Vector Loop B: seat raising, kinematic chain for kinematics analysis, including link numbers .....	49
21	Motor shaft speed required to incline the backrest and raise the seat at constant angular and vertical velocities, respectively, in under 20 seconds .....	53
22	Comparison of screw axial loads through the entire phase of motion 2, for hand-prepared calculations and software generated outputs, for the worst-case load conditions .....	60
23	Creep-Up definition of sides/orientations .....	78
24	Creep-Up definition of seated, supine, and transition positions.....	79
25	Creep-Up motion 1 definition: graphical portrayal of the incline/recline motion.....	80
26	Creep-Up motion 2 definition: graphical portrayal of the raise/lower motion.....	80
27	Top-down view of Creep-Up with footrests unlatched and swung out to each side, representing the wheelchair accessibility .....	81
28	Final Creep-Up design solution shown in three fundamental positions, without footrests.....	81
29	PVF Matlab® program flowchart .....	82
30	General FMEA flowchart.....	83

## NOMENCLATURE

Acronym	Description
BOM	bill of materials
<i>CG</i>	center of gravity
<i>DC</i>	direct current power
DET	FMEA rating for failure detection capability
DFMA	design for manufacturability and assembly
DVT	design validation testing
<i>E</i>	Young's modulus
FBD	free body diagram
FEA	finite element analysis
FMEA	failure mode and effects analysis
MDOF	multi-degree-of-freedom
NRE	non-recurring engineering cost
OCC	FMEA rating for probability of occurring
OEM	original equipment manufacturer
PVF	position, velocity, and force
RPM	revolutions per minute

RPN	risk priority number
SDOF	single-degree-of-freedom
SEV	FMEA rating for failure mode severity
$SF$	safety factor
$S_y$	yield strength
$\nu$	Poisson's ratio

## CHAPTER 1

### PROJECT INTRODUCTION & INITIALIZATION

#### **Background**

For over 75 years [4], professionals and hobbyists have employed the use of mechanic's creepers to ease the burden of sliding in and out from under a vehicle or equipment. A creeper's primary function is to provide means whereby one can easily maneuver across a generally smooth surface in the supine position, very low against the ground. Creepers come in a wide variety of shapes, sizes, materials and complexity, however they all share a common limitation of requiring at least some effort from the user to lie down on, and stand up from the device. This limitation inhibits many people from being able to utilize the advantages they offer.

A capstone senior design project [8], assigned in the fall semester of 2010 at Utah State University, targeted the development a mechanics creeper that could be used by a person with little or no use of their legs or trunk. This included providing a design solution that would allow a user to begin in a seated position, lower himself to the ground, function in the supine position underneath a vehicle, and raise himself back up to the seated position. Albert LaBounty, a paraplegic shade-tree mechanic, motivated the project. As the prototype of the design neared completion, it became obvious that paraplegics were not the only ones that could benefit from a creeper with such versatility. In the United States, there were 76.4 million people born between the years of 1946 and 1964, they are now 52-70 years old [5]. There lies a need for more assistive technologies for this large aging generation. Among the assistive devices requested is the mechanics creeper.



The result of the capstone project was a completed proof-of-concept design in which all critical requirements were fulfilled successfully. An integral part of the project's success was the ability to use a single motor to generate two nearly independent motions, lowering and raising the user to and from the ground, and inclining and reclining the upper body. Each of these motions is critical to the functionality of the device through its servicing range of motion. Although the design was functionally successful, in order to provide a marketable product with long-term functionality, there remained the need to solve problems of manufacturability and improve understanding of failure modes and their effects. The scope of this project is to redesign the creeper, improving component manufacturability and survivability, studying failure modes of the creeper components and subsystems, and completing a fully analyzed mechanical design for better market readiness.

The subsequent sections provide a thorough description of the problems that were solved as well as a detailed review of the revised design solution and analyses. The analyses employed for theoretical design validation include kinematic position and velocity computations, static force analysis, structural analysis by theoretical applications as well as finite element methods, and finally a failure modes and effects study was performed for all components and subassemblies. In the subsequent text, "BLAC Inc. creeper" will be in reference to the initial prototype, and "Creep Up" will be used in reference to the new design created as part of this thesis. References to sides, orientations, and relative motions, may be clarified by Figure 23, Figure 25, and Figure 26 in Appendix A.

## **Problem Description**

Technician or mechanic creepers, although a nearly 80 year old technology [4], have found a niche use among amateur and professional technicians alike. Hydraulic lifts and underground bays are also popular options for getting to the bottom side of a vehicle or machinery. However, these require a great deal of space and often substantial financial investments. Since the need for the creeper has out survived the advancements in technology that accomplish a similar task, there remains a sustained demand for the next smaller, lighter, more ergonomic creeper. As years have passed and feature sets have grown, these products have morphed in size, shape, and material for comfort and versatility, including some that can be manually altered into shop stools. Other technologies have implemented the concept of allowing a user to alter their position between supine and seated. Despite the products thus far offered, the feature to carry a user between the seated and supine positions without some effort of their legs and core muscle groups, is a key characteristic of which all are void. A person with a weak or injured back or legs, and especially lower extremity paralysis, needs a solution that will convert simple hand activation, such as pressing a button, or turning a knob, into fully assisted motion between the seated and supine positions. An additional stage in the motion that allows the backrest to remain fully inclined while the seat is low to the ground, may become helpful or necessary for a person to work on tires, brakes, or other work that is close to the ground, yet does not require a user to be lying down.

The BLAC Inc. creeper [8] (See Figure 1), designed in 2011 at Utah State University (USU) by a team of four undergraduate students from the department of

mechanical and aerospace engineering, provided a design concept through which these performance limitations were satisfied. The USU capstone design sequence included a semester segment of design, followed by a semester segment of prototyping and design validation testing (DVT). During the DVT activity, key design limitations became more apparent and would need to be addressed to create a more marketable and manufacturable design. Additionally, a close evaluation of key design features, brought to light many opportunities for improvement to promote overall user experience.

The majority of the materials used in the main structure of the BLAC Inc. prototype included aluminum rectangular tubing. This tubing was cut, machined, and welded or bolted together to form the main frames and structural components. Although the choice of aluminum is wise for its high strength to weight ratio, the welding process voided the heat treatment, resulting in weakened material near the welds. Additionally, the limitation in student equipment and lack of high-volume manufacturing techniques made it difficult to build with materials that could be easily used in economical manufacturing processes. This exposed the need for significant design modification to enable the use of materials and manufacturing processes that are simple to work with and less expensive, while maintaining or improving on the successful design features of the BLAC Inc. creeper.

The next problem considered was the time it takes to move the user from one extreme position to the other, or in this case from the seated position to lying down and vice versa. This transition time for the BLAC Inc. creeper is found in Table 1 to be longer than one minute. In the common event of alternating between the two extreme

positions, the user will likely find it very cumbersome to spend more than two minutes waiting on the creeper to raise them back up and lower them down again. An event as simple as fetching a different tool could result in wasted time, creating a frustrating experience for the user. The design considerations should therefore include a reduced transition time.

**Table 1: BLAC Inc. Creeper, key product specifications provided in final report [8]**

<b>BLAC Inc. Creeper Product Specifications</b>	
<b>Motor</b>	Black & Decker Drill Motor
<b>Power Source</b>	120V A/C
<b>Amps</b>	7 Amps
<b>Frame</b>	Clear Anodized 6061-T6 Aluminum
<b>Drive Screw</b>	ACME 3/8-12
<b>Run Time (extreme to extreme)</b>	66 sec
<b>User Weight Limit</b>	300 lbs.
<b>Empty Weight</b>	70 lbs.

Among the aforementioned parties to which this technology is useful, is also the fully able-bodied technician who needs an assistive creeper to reduce wear and fatigue on the body while working partially elevated in low-clearance areas. It can be seen in Figure 1 that the chain that synchronizes the two lead screws runs underneath the footrest, and in the absence of the footrest, even with the chain covered, there is limited space for the user to place their legs. In this case it is imperative that a footrest be optional or removable and that space is preserved where the user's feet are free to move and propel the creeper about. Also obvious in Figure 1 is the absence of convenient wheelchair access. It is not an option to make such a transition from the front due to the footrest. Accessing the

sides, while a superior option to the accessing the front in this case, is still quite difficult due to the gap created by the casters, chassis, and motor.



**Figure 1: Prototype of BLAC Inc. Creeper**

There are also a number of items to address to improve the long-term reliability and user experience. Firstly, the drive mechanism used in the BLAC Inc. creeper is two acme threaded rods that remain synchronized by the chain. These drive rods must be accessible for preventative maintenance procedures, but perhaps they are too accessible in the BLAC Inc. design. The entire length of the rod is enclosed in the chassis, however, the tops of the tubes that contain them are open on nearly the entire length. This presents an obvious hazard to the system as debris or loose hardware such as a rogue nut could easily fall into the tube and interfere with the crucial components of the drive system.

The slenderness of the legs and pushrods, the bearing types at their respective pivot points, and component attachment methods all contribute to a wobbly seat. Although not an imminent structural concern, the significant deflection of the seat contributes to a subpar user experience and extraneous rubbing and catching of components as they pass one another.

The use of A/C power, although generally available in normal work conditions, is not an optimal option for a motor due to the need of a power cord. A/C motors are very cheap and powerful, which is the primary motive for the A/C drill motor selection during the initial prototype. In an effort to better satisfy user needs, removing the need for corded power is an important task to complete.

Perhaps the most important of all the features to consider is user safety. In the BLAC Inc. prototype, ample opportunity was left for improvement in isolating the user from any inadvertent pinch hazards. This remains a topic of critical importance throughout the redesign process within the scope of this project. Secondary to the pinch point concerns is the need to protect a user from falling due to the creeper rolling in the seated position in the event of making the transition from a wheelchair to the creeper. The brake system provided in the BLAC Inc. design was inadequate, oversized and cumbersome to access.

Finally, a comprehensive analysis is critical to understand the effect each component and subassembly has on the performance of the overall system. A failure mode and effects analysis combined with force and stress analyses are necessary to provide a safe and reliable user experience.

In summary, the design solution will include a manufacturable mechanical design of an assistive creeper technology, capable of transforming a person bi-directionally between the seated and supine positions. This includes the employment of successful design features from the BLAC Inc. creeper design, and generating an improved design feature set that will address the problems discovered in DVT of the first prototype. Finally, all appropriate analyses must be performed to ensure the highest level of user safety and product integrity, in order to minimize and mitigate user and system risk, and prevent expensive system design changes after future prototyping.

## CHAPTER 2

### DESIGN & DEVELOPMENT

#### **Key Design Requirements**

Prior to beginning the initial development, it was necessary to understand what the key driving requirements were, to ensure that the needs of the manufacturer and ultimately the user are met, and the end product can be manufactured economically. In considering the cost of product development from concept to production, it is always best to spare late modification and resolve major design issues in concept and preliminary design. Specific design requirements were prescribed to facilitate successful completion of the design initiatives. These design requirements are as follows:

- Safely raise and lower a person from seated to the supine position and back seated again, requiring only simple user activation. The positions must be achievable by a person with no use of their legs or trunk.
- User size requirements: 300 lb. maximum weight capacity, 6'4" maximum user height. According to the US Census Bureau, 96.9% of males of all ages are 300 lb. or less, and 97.6% of them are shorter than 6'4" [10].
- Base product weight less than 60 lb. (exclusive of the footrest). Costs associated with product shipments and user handling, merit the need to drive weight as low as possible. This requirement was given from feedback acquired from Albert LaBounty, and is equivalent to the amount of weight he is able to handle with relative ease.



- Work surface in supine position less than 3 in. off the ground. Although creepers come in a variety of heights, this requirement allows the product to remain competitive with a large majority of the existing creeper products.
- Ability to transition from a wheelchair from the front. In order to make this possible, the seat must rise to greater than 20" off the ground, coming level with the seat of a wheelchair. This was determined by consulting with Albert LaBounty, and taking measurements of his wheelchair.
- Creeper speed or time to transition from one extreme to the other is desired to be less than 20 seconds. This would reduce the run time by 70% from the initial prototype.
- Brake system to prevent chair movement in seated position. Though it may be useful to have the ability to immobilize the creeper manually in any position, the scope of this design only demands a reliable solution to immobilize the creeper in the fully seated position. The application method is unspecified.
- Removable leg/foot rest with no obstructions to the feet/legs in the absence of the footrest. This will allow the product to be used as a traditional creeper by persons that have the use of their legs.
- Onboard power supply (battery operated). A tethered power option is not an acceptable solution for the nature of the work this serves. The mechanisms must be activated by a D/C power source that is easily replaceable in any position.
- Cover all pinch hazards internal to the user contact area. A user's body must not be at risk of being pinched anywhere within normal hand or body placement.

- Generate smooth constant velocities with variable motor speed. Due to the nature of the mechanisms that actuate the creeper's motion, a constant speed motor will deliver variable angular and linear velocities to the user. In the analyses, it is desired that the motor speed be variable to achieve constant angular and linear outputs.

### **Design Approach**

The design approach used began with clearly defined design requirements. These requirements acted as drivers for high-level design decisions and were referred to often as a tool to calibrate design direction and focus. Consideration of these requirements fueled the concept and preliminary design cycle until a solid design foundation was in place and finer details were implemented.

As concepts were considered to fulfill a specific design requirement, the next step was to evaluate the concept's compatibility with the complex kinematics. The general kinematic design is one of the features from the BLAC Inc. project that serves important purposes discussed later. This kinematic system is very sensitive to even small changes in design of the kinematic links. Due to the extensive range of motion of these links, the system may quickly lose function or range of motion by the sequence in which they are stacked, and especially by having other components or design features encroach into the space needed in the course of their motion. There must be careful consideration of the impact any given design decision has on the system's kinematic synthesis.

Once a design modification or addition was determined to cohabitate with the kinematics, further consideration was given to whether or not the design requirements

and user needs were fulfilled. If a need was positively fulfilled, the appropriate design decisions were implemented. If a change made at this point had any effect on kinematic function including the length or shape of any link, the geometric inputs were changed appropriately in a kinematics computation input file. This input file was created in Microsoft Excel and contained all inputs necessary to complete the kinematic computations. Matlab® was then used to run the position, velocity, force (PVF) program found in Appendix E. The program is described later in detail. Position, velocity, and joint force outputs were obtained for the new design changes. At that point, if the structural integrity was in question for any of the new or existing components, a preliminary structural analysis was done to provide confidence to move forward in the design process. A preliminary structural analysis is defined as a quick hand calculation or a crude finite element analysis. This is not intended to be a significant time consuming activity but rather an approximation to verify that there is not a design altering problem further down the design cycle that could otherwise have been avoided at this stage.

An informal design review was then used to identify the need, and prioritize efforts for any additional changes. If subsequent work was required to address issues, then the cycle began anew. This cycle is illustrated graphically by Figure 2. When design changes became smaller and much less impactful, requiring no reanalysis, this cycle began to break down and it was at this point that a bill of materials was generated and the development phase moved into the critical design stages where more thorough analysis were completed. With the bill of materials largely in place, the failure modes could be

populated in a FMEA table. This table ultimately drove the analyses regarding what kind and to what extent the computations needed to be completed.

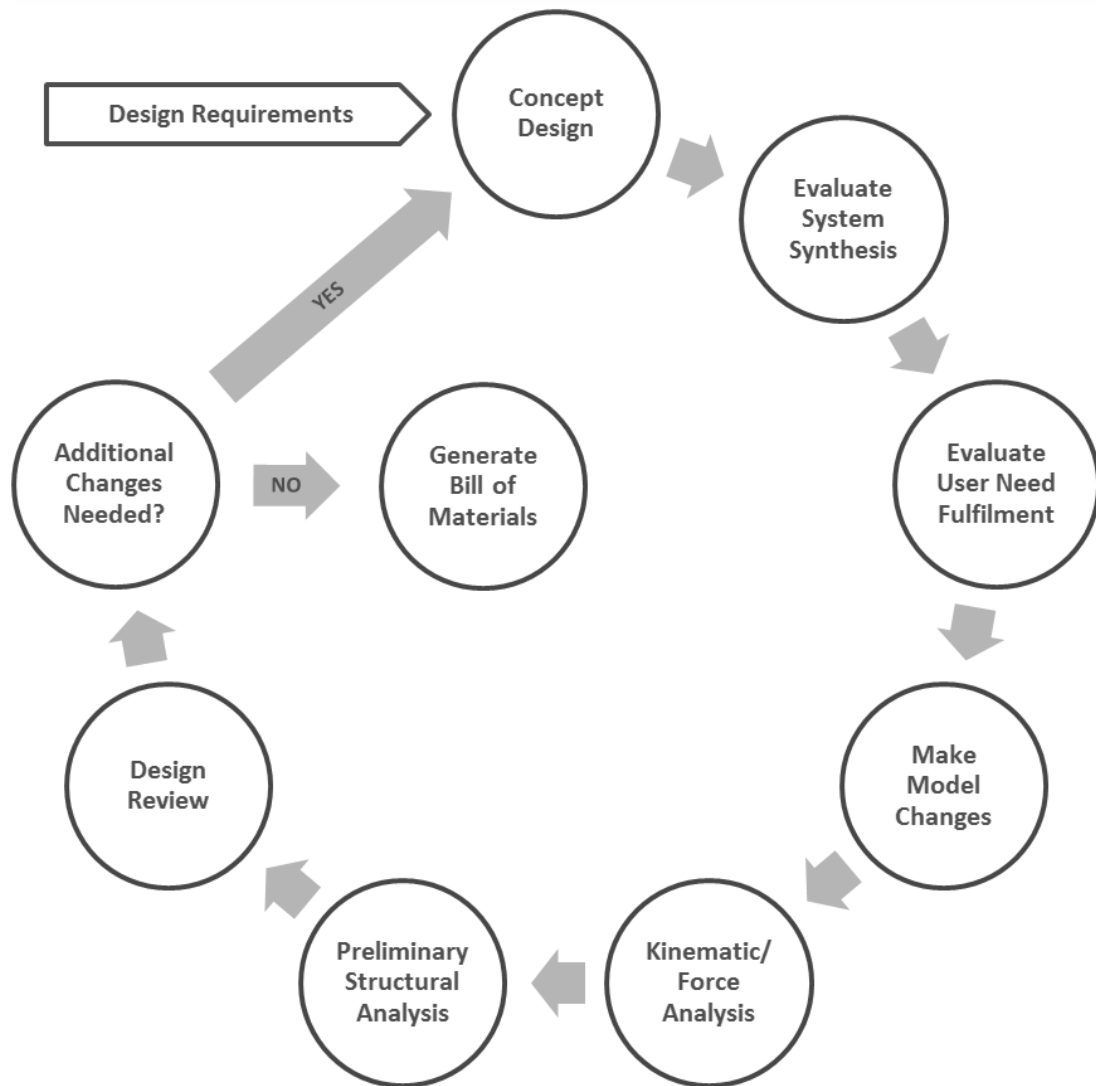


**Figure 2: Concept and preliminary design cycle**

In the course of the design cycle, principles of design for manufacturability and assembly were employed to ensure that each design change was not only functional but also manufacturable and cost effective. Professionals and manufacturers were often

consulted, and feedback procured on how to improve the design or geometry to optimize the part for manufacturability. This feedback was also received on a quantitative level as quotes were requested and compared for both prototype and production quantities. Tooling amortization and piece part costs were considered together where manufacturing processes with expensive non-recurring engineering costs (NRE). These costs, and pricing estimates were obtained only on selective components for assistance in making sound decisions regarding the selection of a manufacturing process. These costs procured do not contain adequate information on all parts to provide estimates for prototyping or production volume cost of goods.

The critical design phase was a much more analysis intensive phase where only fine adjustments were made to parts and assemblies to fine tune kinematic performance, manufacturing methods, and structural integrity. When applicable analyses were completed, their results were reviewed for adequacy and accuracy, and small design modifications were made to attend to the demands of the analyses.

### **Kinematics**

The nature of this development project is kinematics intensive. The kinematic chains used in the design were critical in satisfying several main objectives. To begin, the primary function of an assistive technology of this type is to do work, or in other words to apply forces that will provide movement of a person that the individual is otherwise unable to do for himself. The motions generated in the case of the creeper, use specific paths and must end at particular positions in order to fulfill the needs of the technician. While this objective must be fulfilled, it must also be completed while giving

sound regard to the user's ability to transfer to the device from their current position, and provide general support and comfort for the body. Therefore, the kinematic components must integrate with other structural and ergonomic components. Additionally, kinematic linkages often yield pinch points where fingers, hands, or even limbs may inadvertently enter and be easily injured. And finally, the lengths, angles and positions of each link may drastically affect the forces, speeds and accelerations in the mechanism. The kinematics in the design must have the right balance to satisfy all of these key objectives.

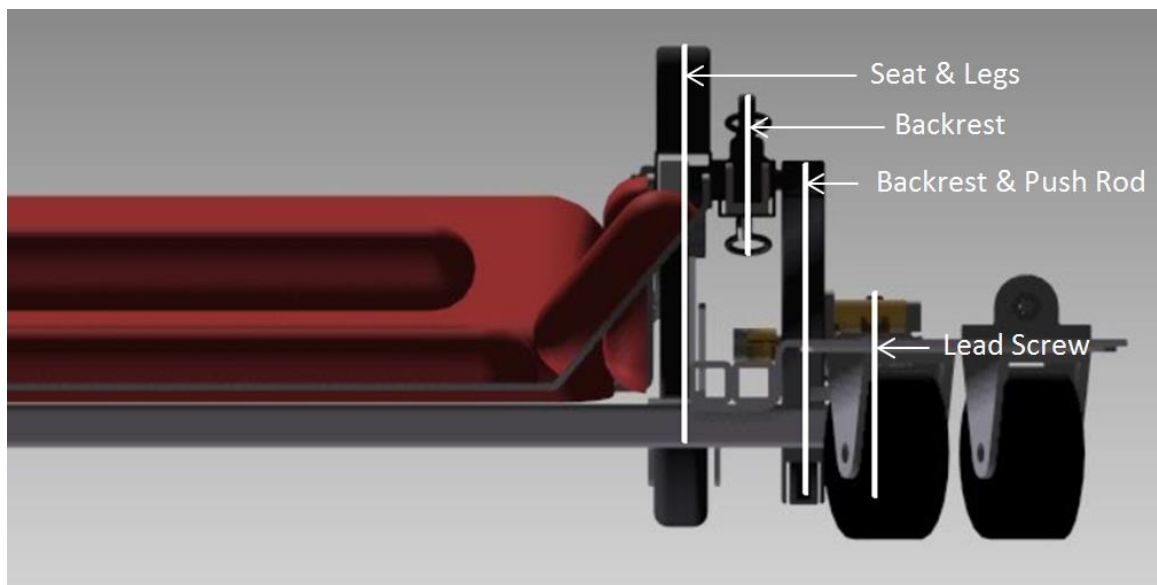


**Figure 3: 3D kinematic link stacking of the BLAC Inc. creeper, showing how the respective links of the 2D kinematic chain are layered**

In the design process there was considerable time, effort, and analysis expended to meet these needs. Although the majority of the kinematic motion is a direct result of the two-dimensional layout of the linkages, the three-dimensional aspect is also an important detail to consider. One of the weaknesses of the BLAC Inc. kinematic design

was the component stacking sequence, or the three-dimensional layering of the linkages. The stacking, shown in Figure 3 illustrates the wide spread stacking of components in the BLAC Inc. design. Aside from the excess space consumed, the large moments created on the kinematic system are the primary problem with such stacking. In particular, the seat and legs, relative to the push rod and lead screw, are a great distance apart. The forces in the push rod and legs are some of the greatest axial loads seen in the system. These loads oppose each other in order to create the lifting forces on the seat. The push rod and backrest also experience significant loads. Large opposing forces that act offset from one another generate undesirable moments that lead to lateral deflections of the kinematics, and spurious bending of axial loaded links.



**Figure 4: 3D kinematic link stacking of the Creep-Up creeper, showing how the respective links of the 2D kinematic chain are layered**

To remedy these problematic moments, the kinematic stack-up was redesigned to place as many links as possible in direct line with one another. When the mid-planes of two or more pivoting components are coplanar, the stresses on the pins at the joints are

purely shear stresses. The end design resulted in co-planarity of all kinematic component mid-planes, with the exception of the legs, which are placed in close proximity to the other links. This effectively reduced the number of layers from four to two, a significant design improvement, shown in Figure 4.

### **Kutzbach's Equation**

A topic of particular interest in this creeper design is that of being able to isolate the independent motions of a multi-degree-of-freedom (MDOF) kinematic system. There are many ways in which MDOF can be reduced to resemble the behavior of a single degree of freedom (SDOF) system. Two specific methods apply to the control of this creeper: (1) utilize gravity and motion inhibiting stops, and (2) completely remove a degree of freedom by selective integration of an additional component.

The Kutzbach equation, also known as Grübler-Kutzbach criterion [9], indicates the number of degrees of freedom in any kinematic chain, with the exception of a few paradoxes. The result is known as the “M” value, which directly corresponds to the number of degrees of freedom remaining after considering the number of links in the kinematic chain, and the quantity and type of each joint or connection. This equation can be considered in spatial form including 6 degrees of freedom, or in planar form including only 3 degrees of freedom. The nature of the kinematic chain used in this design is of planar type, therefore the following equation applies:

$$M = 3(N - 1) - 2J_1 - J_2 \quad (1)$$



where,  $N$  is the number of links in the kinematic chain,  $J_1$  is the number of joints in which only 1 degree of freedom remains, and  $J_2$  is the number of joints in which 2 degrees of freedom remain.

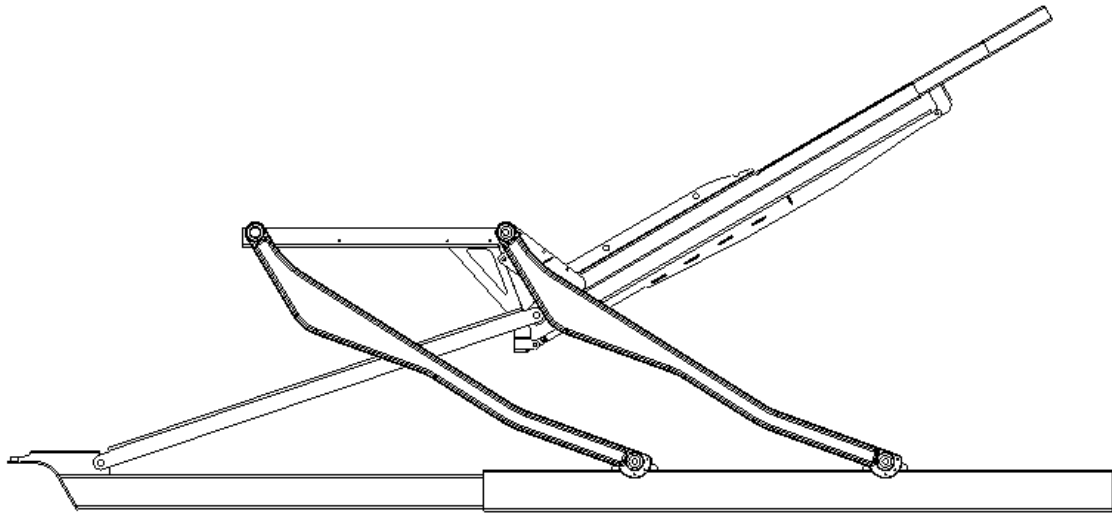


**Figure 5: Stripped-down view of the main kinematic links, with all other parts hidden from view**

The base kinematic frame is illustrated in Figure 5. This shows the minimum number of components that form the basic kinematic chain that is responsible for providing the motions that will take a user from the supine position up to the seated position. Furthermore, Figure 6 shows the links distinctly separated for component identification, and the type of connection made at each link interface. From this figure, 9 links (link numbers are denoted by the circled numbers) are noted along with 11  $J_1$  connections, and no  $J_2$  connections. By applying equation (1) to this kinematic chain, it follows that  $M = 2$ .

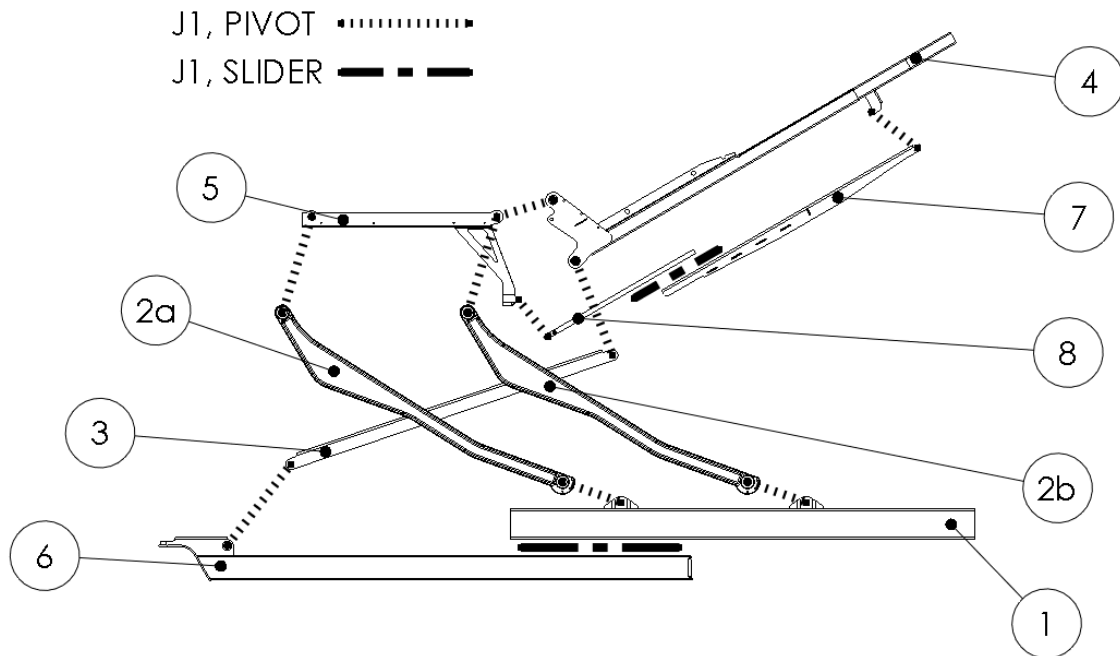


**Figure 6: Kinematic diagram of linkages with link numbers, and identification of joints**

With an “M” value of 2, this system is capable of producing 2 independent motions from a single given input. In the case of this design, link 1 is part of the chassis that remains in contact with the ground. Consider link 1 to be the ground link, and link 6 to be the input. Link 6 is a slider member that telescopes out of the ground link and is driven in and out by a lead screw. Attached to the ground link are 2 legs, links 2a, and 2b, which in turn attach to the seat frame, link 5, where the user sits. Links 4, 7, and 8 compose the backrest. The backrest is driven at link 4 by a push rod, link 3, and pivots about the link4/5 connection point. It can be noted that by removing the backrest’s rotational degree of freedom, the system is left with a SDOF chain in which the legs and seat are free to be moved up and down. Likewise, by not allowing the legs and seat to

rise, the system again reduces to a SDOF and only the backrest is free to rotate. A more thorough derivation of these SDOF systems is found in the Kinematic Analysis section of Chapter 3.

Since these two remaining degrees of freedom are both desired, one for inclining and reclining the users upper body, and another for raising and lowering the seat surface, it is not desirable to completely remove a degree of freedom. Instead, in order to produce both motions independently with the actuation of a single drive system, it is desired to maintain both degrees of freedom, and employ additional components and force balancing to control when a degree of freedom is used.

When the user is in the supine position, the creeper is at the lower extreme, see Figure 24 in Appendix A for referencing the views referred to here. At this instant, when the slider begins to pull into the chassis, the response from the available degrees of freedom may be either of the two following motions:

- 1) the seat rises, which is a result of the legs pivoting clockwise at the chassis pivots per the reference configuration of Figure 5, or
- 2) the backrest inclines, as a result of the counter-clockwise pivoting of the backrest frame about the rear pivot of the seat frame.

Both degrees of freedom available at this moment are only capable of producing movement away from the ground. The legs cannot move toward the ground because their geometry nests them together and prevents rotation past that seen in the supine or transition positions. The backrest is also confined to sole counter-clockwise rotation, due to physical restrictions of the backrest resting on top of the chassis. Aside from the

physical impossibilities of moving toward the ground, the system was also designed with redundant limit switches that stop all electric actuation in that direction.

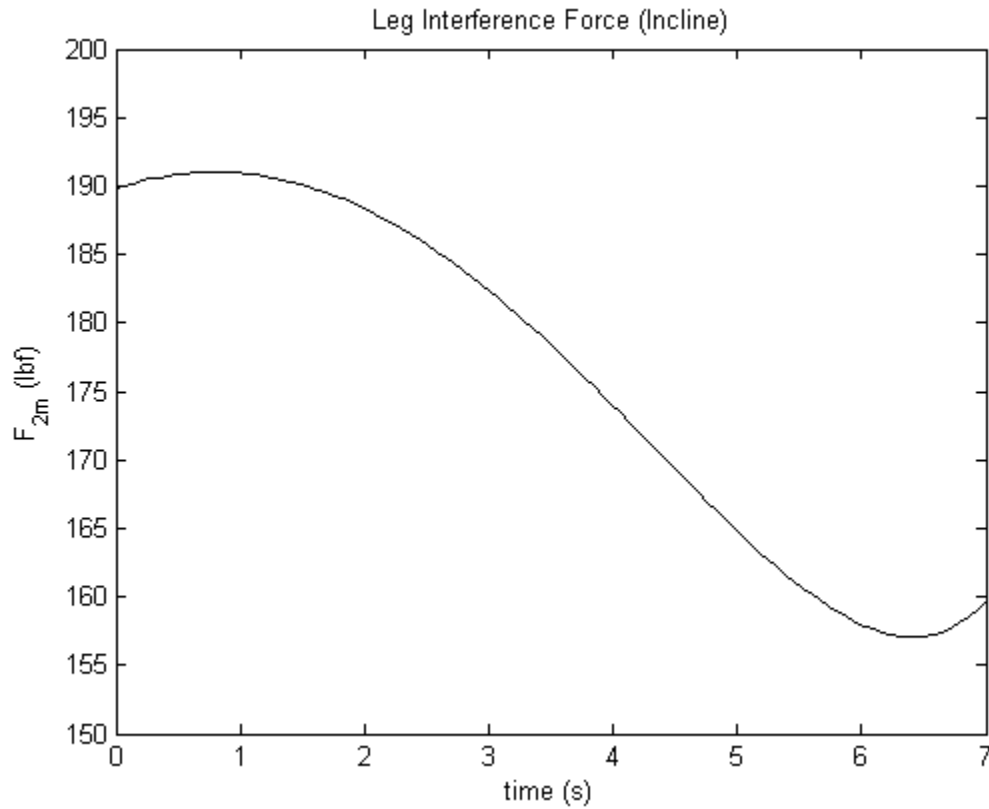


**Figure 7: Leg interference force between the two legs where they are in contact during the incline phase. This load is seen by both sets of legs on each the left and right side of the creeper; external loads set at maximum of 300 lbf, distributed per de Leva body segment measurements [1]**

Considering then, only movement away from the ground, using a balance of forces in the design, one degree of freedom may override the other. With the user's weight distributed across the creeper, by design it requires a different amount of actuation force to incline the backrest than it does to lift the seat at any given time throughout the inclining motion. During the preliminary design cycle, iterative design adjustments

combined with periodic kinematic and force analyses resulted in the ability to find and maintain a force balance that prevents the seat from rising while the backrest inclines or reclines. Figure 7 illustrates that the contact force between the two legs remains positive throughout the entire 7 second duration of incline motion. A second witness to this can also be evaluated in Figure 9, where a significant jump in the push rod axial load occurs at the transition position from incline to raising the seat. This load is more than 75% higher than the maximum load required at any point during the incline motion.

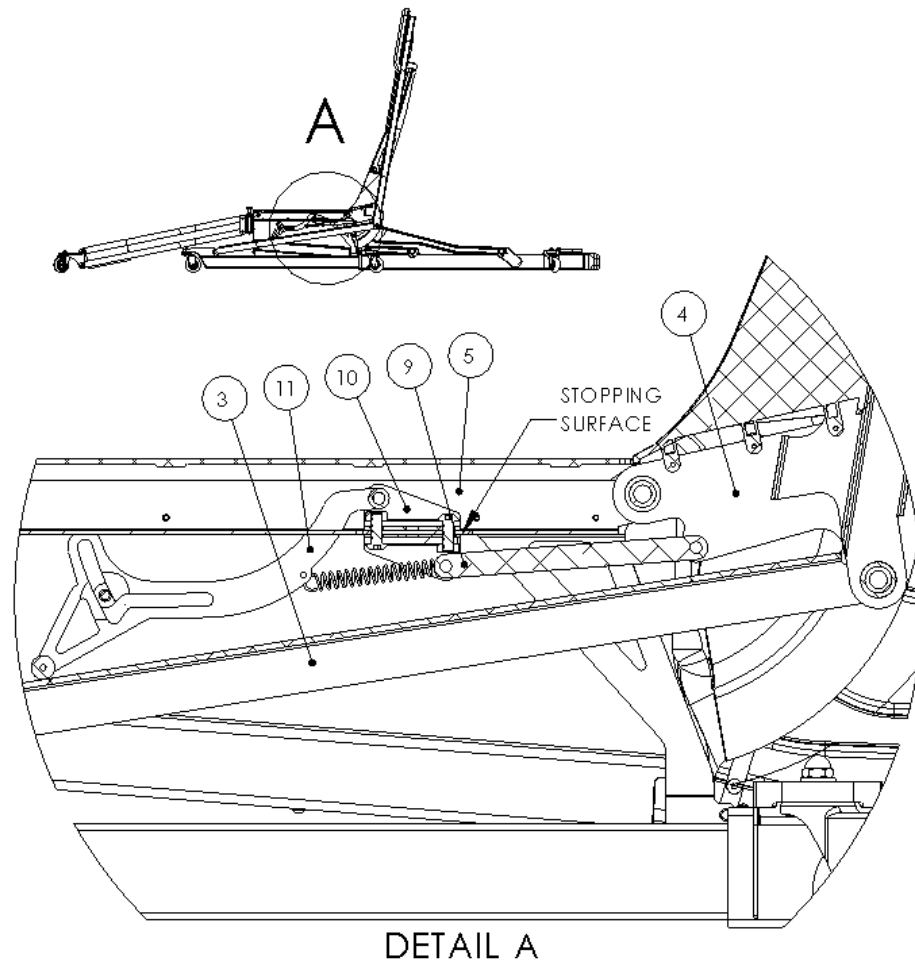


**Figure 8: Cutaway view of the back stop and back lock mechanisms that remove rotational degrees of freedom from the backrest kinematic chain**

When the backrest becomes fully inclined the system reaches position 2, the transition point where it is desired to direct the systems actuation energy toward raising the seat. It is necessary then for the backrest to cease further rotation at the desired incline angle. This is accomplished by adding a subsystem that inhibits the counter-clockwise backrest rotation. Link 9 in Figure 8 is a tensile member attached to item 10 which stops against the surface indicated in the same figure. Item 10 is allowed to slide freely to the right as the backrest inclines until it reaches the end of the slot at which point it removes the counter-clockwise rotational degree of freedom of the backrest. This is defined in Figure 24 as position 2 or the transition position. This position marks the end of the incline phase and the beginning of the raise phase.

As the lead screw continues to retract the slider into the chassis, the push rod continues to drive the system by the backrest. Because the backrest's counter-clockwise rotation is now fixed, the force in the pushrod is allowed to increase and overcome the gravitational forces that have held the seat down, and the seat begins to rise. This is the point at which the second phase or motion begins. As the seat rises, the forces required to raise the user decrease due to the increase in the vertical components of force in both the push rod, and the legs. Recall link 9 and item 10 in Figure 8 that are used to constrain the counter-clockwise rotational degree of freedom of the backrest. At the point of transition, there is nothing constraining the clockwise rotational degree of freedom, therefore the forces on the backrest applied by the pushrod are crucial to the stability of the backrest.

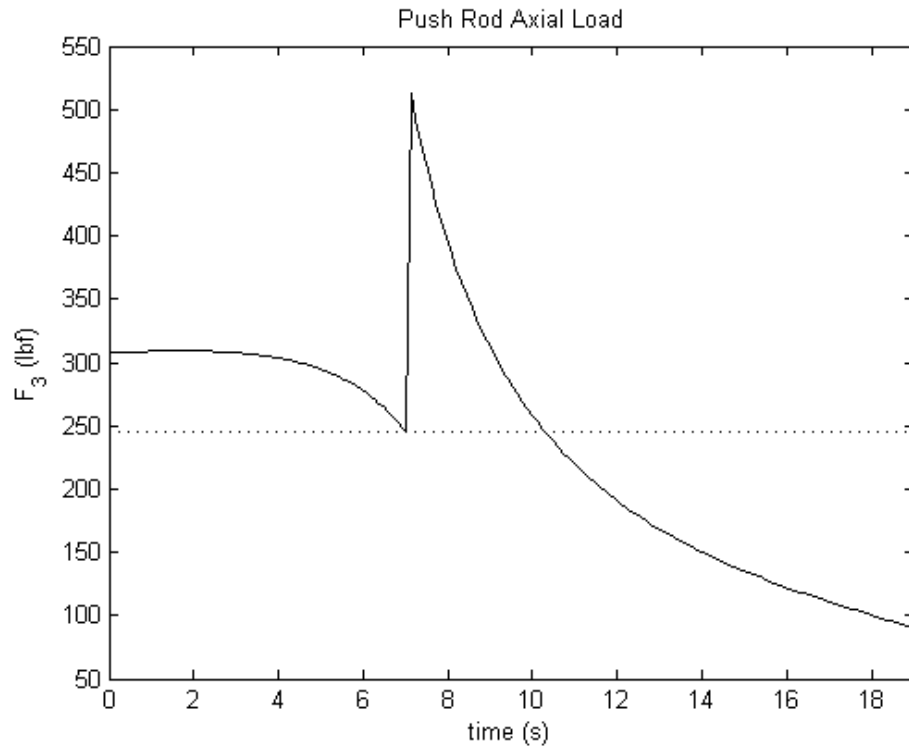


**Figure 9: Pushrod axial load plot, across full range of motion: contains the static axial load seen by each push rod on each the left and right side of the creeper; external loads set at maximum of 300 lbf, distributed per de Leva body segment measurements [1]**

As the seat rises and the force applied by the pushrod decreases, there comes a point at which the force required to lift the seat falls below the force required to hold the backrest up. This point occurs at approximately the 10.5 second mark and is evident at the intersection point shown in Figure 9. Such a point would result in the backrest falling backward at some point between the transition point and the seated position, thus becoming a potential critical design flaw and a concern for the user's safety. In order to prevent this from occurring, the clockwise rotational degree of freedom must be removed. It must however, be removed sometime soon after the seat begins to rise. Conversely, on

the way back down, it is equally important that the mechanism completely release before the seat bottoms out in order to prevent system binding and damage when the backrest needs to rotate backward.

This is accomplished with the addition of a spring loaded laser cut part that locks the backrest as the seat lifts off from above the push rod. This occurs automatically as the seat rises, and the distance increases between the seat and the push rod, allowing the spring to pull the lock into place. Just the opposite, when the seat is lowering, a bumper on the part runs into the top of the push rod, overcoming the spring and forcing the lock mechanism out of the way, leaving the backrest free to rotate. This part is item 11 shown in Figure 8, and is displayed in its locked state with the bumper just in contact with the top of the push rod, link 3. From this position the seat may lower just enough to release the catch, or as the seat rises, the bumper will separate from the push rod. Because this is a critical link to the safety of the user, this system is integrated into both sides of the creeper as a redundancy.

With the integration of the back lock mechanism, the backrest locking features, and the use of force balancing, this MDOF kinematic chain is able to be distinctly separated into two independent SDOF kinematic chains. Motors or other drive sources are the most expensive components in the bill of materials, therefore to successfully drive the system with one motor is especially desirable. The successful isolation of these motions saves a tremendous amount of cost since a second drive source is not needed. Additional detail on the individual SDOF kinematic chains can be found in the Kinematic Analysis portion of Chapter 3.



## Design Solution

The final design solution was completed with satisfactory kinematic synthesis, structural integrity and sound manufacturability. Among others found in Appendix A, Figure 10 shows the final design solution poised in the three distinct positions. This same detail is shown without the footrests in Figure 28. The bill of materials for the Creep-Up design can be seen in detail, broken down by component, in Appendix I. Part numbering in the BOM is organized by a 3-digit prefix that corresponds to general manufacturing process categories. These prefixes are defined in Table 2.

**Table 2: Part numbering prefix by manufacturing process**

<b>Prefix</b>	<b>Associated Manufacturing Processes</b>
<b>P00</b>	Consumer off-the-shelf components
<b>P01</b>	Customized COTS components
<b>P02</b>	3D machined/turned, 2D waterjet/laser cut or basic fabrication
<b>P03</b>	Sheet metal, stamped/formed
<b>P04</b>	Cast, injection molded, thermoformed, rotational molded
<b>P05</b>	Sewn, upholstered
<b>A00</b>	Top-level Assembly
<b>A01</b>	General Mechanical Subassemblies
<b>A02</b>	Welded Subassemblies

Overall dimensions of the final design can be found in the top-level mechanical drawing located in Appendix J. High-level assembly detail, including subsections and large subassemblies are included in the drawing.

Since it is not feasible to examine every component and subassembly in detail, a more general discussion of key design features is provided. This design overview is done

by looking at the system as a whole as well as looking at the design broken down into subsections. The design summary is discussed in the following categories:

- Chassis & drive train
- Legs & push rods
- Seat
- Backrest
- Footrest
- Bill of Materials Overview

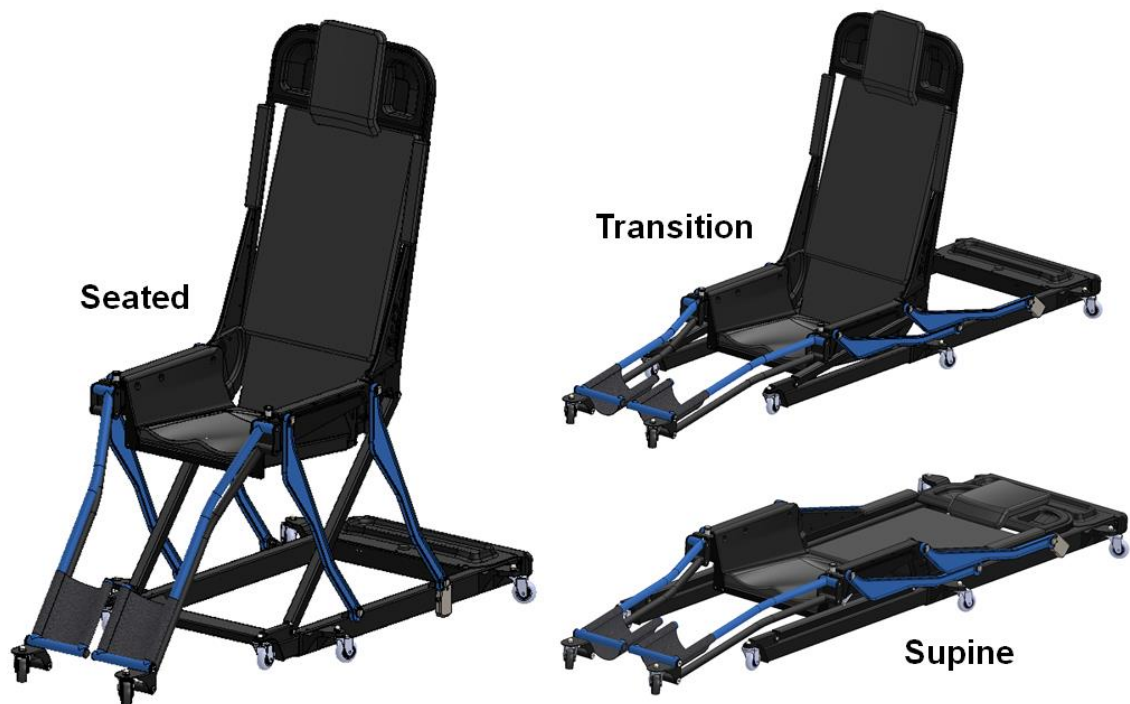


**Figure 10: Final Creep-Up design solution shown in three fundamental positions**

#### Chassis & Drive Train

The chassis, shown in Figure 11 is a welded subassembly and is the main foundation on which the rest of the mechanics attach and rely. It includes the motor and drive train attachment geometry, caster brackets, structural cross members, and screw and slide housing. The Creep Up solution was completely redesigned from the BLAC Inc.

solution and includes all steel components that are welded together. The steel members, although heavier than aluminum, are capable of weld strengths far superior to aluminum. Steel tubing in appropriate sizes and with rounded corners, is also much more available and cost effective than aluminum.

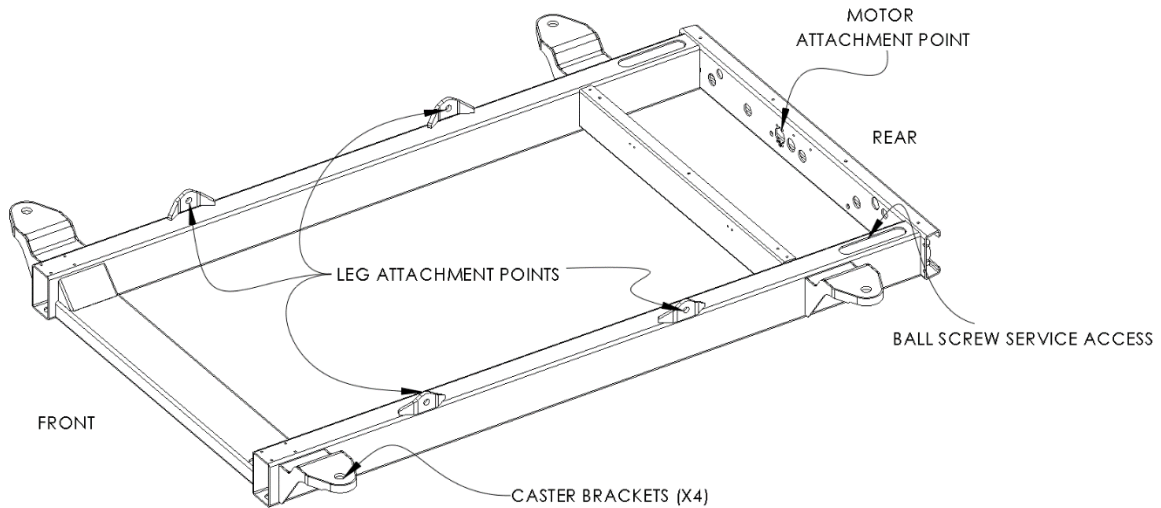


**Figure 11: Welded chassis subassembly of final design solution**

The welded frame then receives a number of other components and subassemblies that make up the rest of the creeper's drive train. During the design process, a significant amount of time was spent in cost and weight reduction efforts to reduce the need for dual lead screws to a single screw. However, the result from the activities was increased weight and break-even costs due to the other components that were involved in removing off-axis torque on the lead screw and preventing binding. Two screws were again introduced and this is how the final solution stands. Two additional changes involving the screw are also significant. The first being that the lead screws in the BLAC Inc. design were exposed on the top side, which opened opportunities for debris, tools, or

hardware to inadvertently interfere with the main drive mechanism. The Creep Up chassis was designed to completely enclose the screws, leaving a small opening at the rear, concealed by the motor cover, where lubrication and other preventative maintenance can be performed, as indicated in Figure 11. Secondly, a 4 mm pitch ball screw, twice the pitch of the BLAC Inc. acme screw, provides a low friction drive option that moves the nut along the screw much faster.

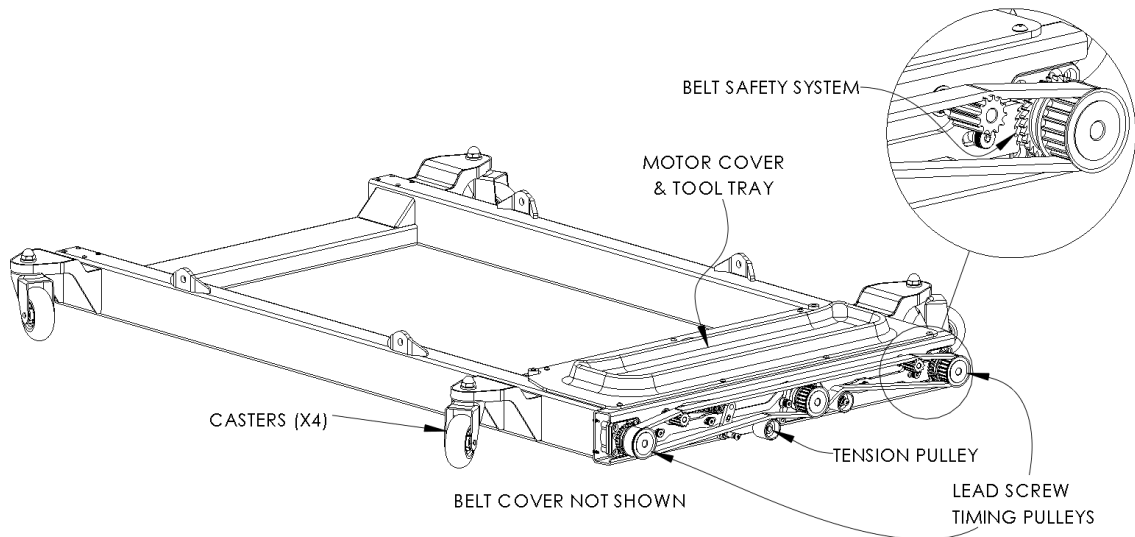


**Figure 12: Full chassis subassembly of final design solution, including hardware, drive train, and emphasis of belt safety system**

Because each screw is responsible for moving one of the sliders, it is crucial that the screws remain synchronized to avoid binding and tilting of the chair or backrest. This is accomplished by the timing belt system shown in Figure 12. In the BLAC Inc. design, this was done similarly with a chain at the front of the creeper chassis. A number of benefits resulted from these changes implemented in the Creep-Up design; first off, by moving this system to the rear of the creeper, space under the feet was vacated,

contributing to front-side wheelchair accessibility and successful functionality as a traditional creeper without the footrest. Secondly, the timing belt option will also create less noise and general maintenance than the chain solution.

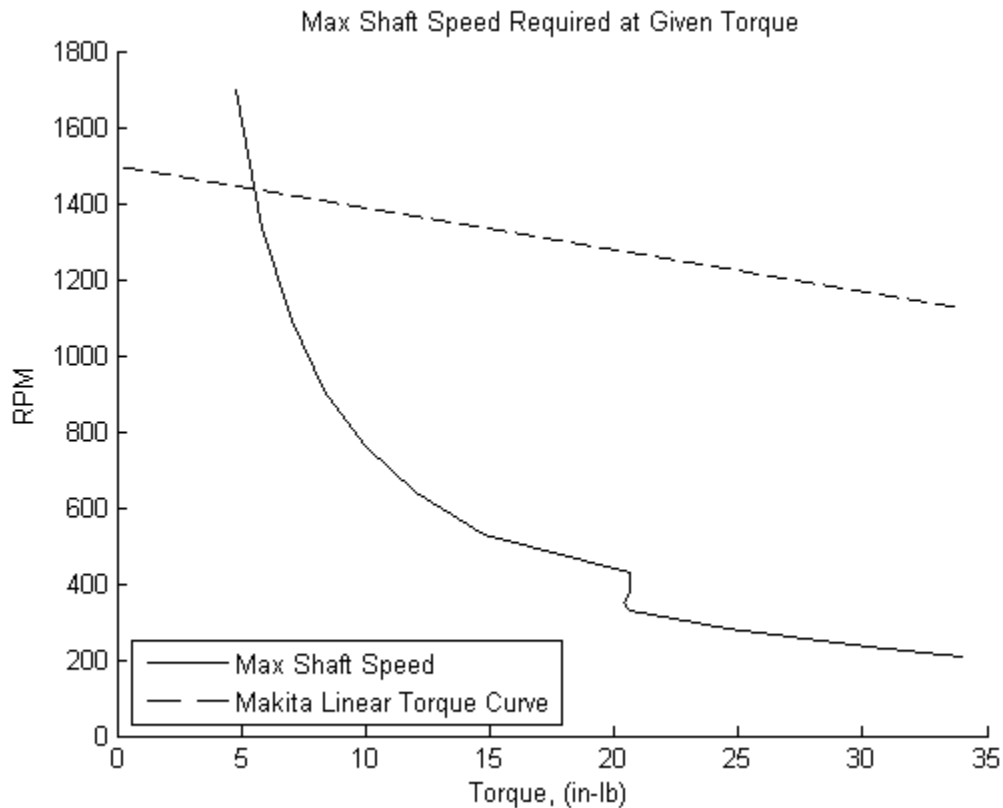


**Figure 13: Maximum motor shaft speed required for a given torque, superimposed with linear torque/speed performance of Makita drill**

Although the belt working tension is well under the belt breaking strength, the belt is still prone to wearing out and potentially breaking if not replaced as needed. Because ball screws are used, a high enough axial load on the screws will cause the screws to rotate. Hence, if the belt breaks, the creeper will lose its position and the user will potentially fall. To avoid such, a belt safety system was designed with a gear and pawl that activate when the belt loses tension. As seen in Figure 12, if the belt breaks,

the tension pulley will rotate counter-clockwise by the spring force. Attached to the tension pulley arm is a small system of linkages that will drive two pawls up against the two gears on each lead screw. These pawls will then stop the creeper from any motion in the downward direction.

Motor selection was a considerable design challenge. In order to satisfy the maximum torque requirements and the speed requirements, it is the best option to use a DC gear motor. Figure 13 shows the maximum speed required at any given torque value in order to maintain constant angular velocity of the backrest during incline and constant vertical velocity of the seat during raise. It can be noted that this curve is exactly as desired with high torques only demanding low RPMs and as torque decreases, the needed RPMs grows. This is the standard performance that a motor can deliver. The most cost competitive motor (which conveniently included two batteries and a charger) that closely satisfied the speed and torque requirements was a Makita 18V lithium ion cordless drill motor, with the speed setting in the high gear. The motor evaluated has a maximum (no load, or zero torque) speed of 1500 RPM and a maximum torque (stall, or zero RPM) of 135 in-lbf. Assuming a linear digression of speed as torque is applied, then using the two Makita specifications, a linear torque curve can be deduced. Although this motor does not reach the maximum RPM desired, it remains a decent option that satisfies the requirement for a battery operated system.

#### Legs & Push Rods

The entire upper assembly, from the footrest to the headrest, is raised from the ground by the joint work of the legs and push rods. The push rods are attached to the

slider assembly which is acted upon by the screw to drive the system up and down.

These structural members are the most heavily loaded and are primary kinematic links.

Both the leg and push rod components are symmetric and intended to be used on right or left sides. Although the leg itself is symmetric, the four legs used in the assembly will become part of two different subassemblies, one subassembly for the legs on the left, and the other subassembly for the right side. All four leg subassemblies contain the same parts in identical quantities, they only become distinct by the way in which the bearing components are inserted.

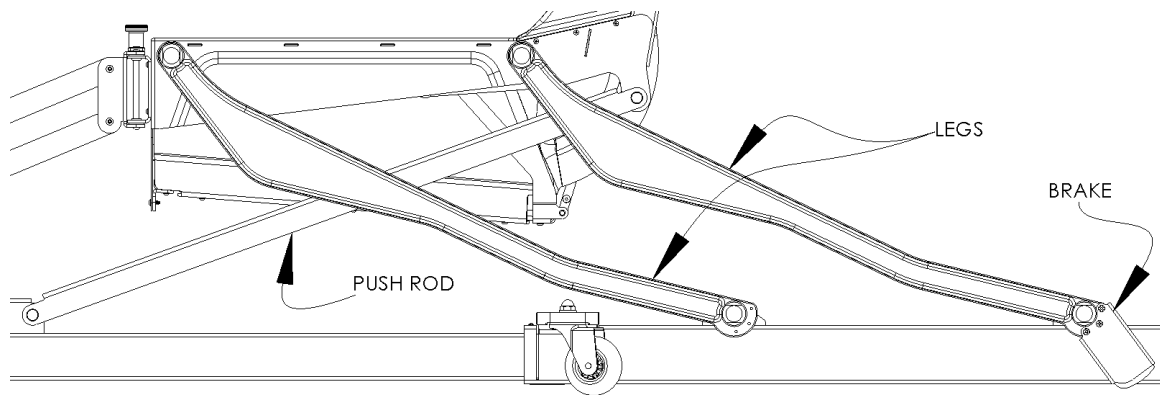


**Figure 14: Side view of legs, pushrod, and brake in the final design solution**

The push rod was designed as a simple sheet metal part with a U bend, and its structure was analyzed to be made from 5052-H32 aluminum, a common sheet metal alloy. The legs are cast A380 aluminum, with post machining processes to provide high precision bearing surfaces and nesting ability. It is anticipated that by attaching the legs to the seat and chassis using bolts that sandwich thrust bearings at each sliding interface, the lateral stability will significantly improve since the BLAC Inc. legs were simply pinned to the side of the chassis. To aid further in lateral stability, and provide smooth

motion and longevity in the joints, the legs are equipped with needle bearings and the pushrods with high load bushings.

Immobilization of the creeper is important, especially in the upper-seated position where transfer from a wheelchair or sitting from the standing position will occur. The brake designed includes a custom steel sleeve that holds a rubber boot and is rigidly attached to the rear legs. As the legs rotate clockwise at the chassis, as shown in Figure 14, the brake will drive lower than the ground plane, ultimately lifting the rear casters off the ground slightly and immobilizing the creeper. This creates a far superior brake to that found in the BLAC Inc. design.

#### Seat

The seat assembly is the main hub for kinematic attachments. The backrest frame, legs, back bridge and back stop and lock mechanisms are all connected to the seat area. The nature of the kinematic design requires vertical space for all these attachment points. In order for the seat surface to be low to the ground, this requires that kinematic links use space to either side of the user, as seen in Figure 15. This vertical space creates a wall that would make it very hard for someone who is a paraplegic to make the transfer from their wheelchair. With footrests that can be moved out to the sides, the opportunity and ease for a person in a wheelchair to access and transfer into the creeper from the front is drastically improved.

With all the kinematic links that pivot at the seat, this also becomes a prime location for pinch hazards. There are many moving parts in this area that the user needed to be isolated from. The design and integration of the seat side shrouds combined with



the welded seat structure, offer complete coverage of acute pinch points and reasonable clearances to the legs that pinches are very unlikely to occur. These seat shrouds integrate tightly with the backrest shrouds to create a safe environment where the user is in contact with the creeper.

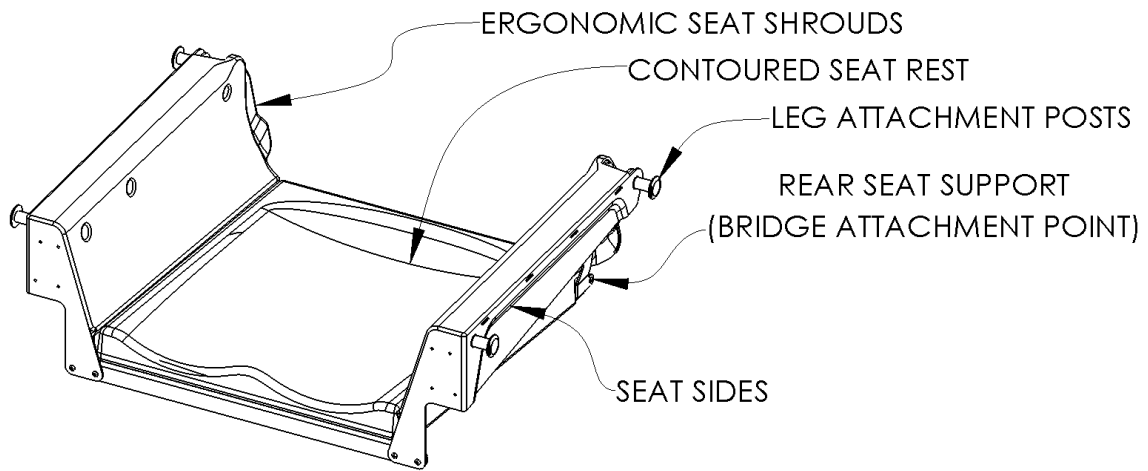


**Figure 15: Isolated seat subsection of final design solution**

### Backrest

The backrest is a crucial member of the assembly and is comprised mainly of the backrest pad, structural frames, bridge and headrest. The backrest pad is carried by a support frame, which attaches with two pinned joints to the main backrest frame. The backrest pad is the surface that the user lies on and is a padded, upholstered piece. The bridge interfaces with the pad's support frame by sliding in two slots out at the left and right edges of the bridge. While in the supine position, the bottom of the backrest pad and the rear side of the seat pad are in close proximity to one another. As the creeper's backrest inclines, the space between the bottom of the backrest pad and the rear edge of

the seat pad widens. The bridge is the critical component that closes this gap, giving support to the lower back while in the seated position and protecting the user from being pinched as the backrest reclines.

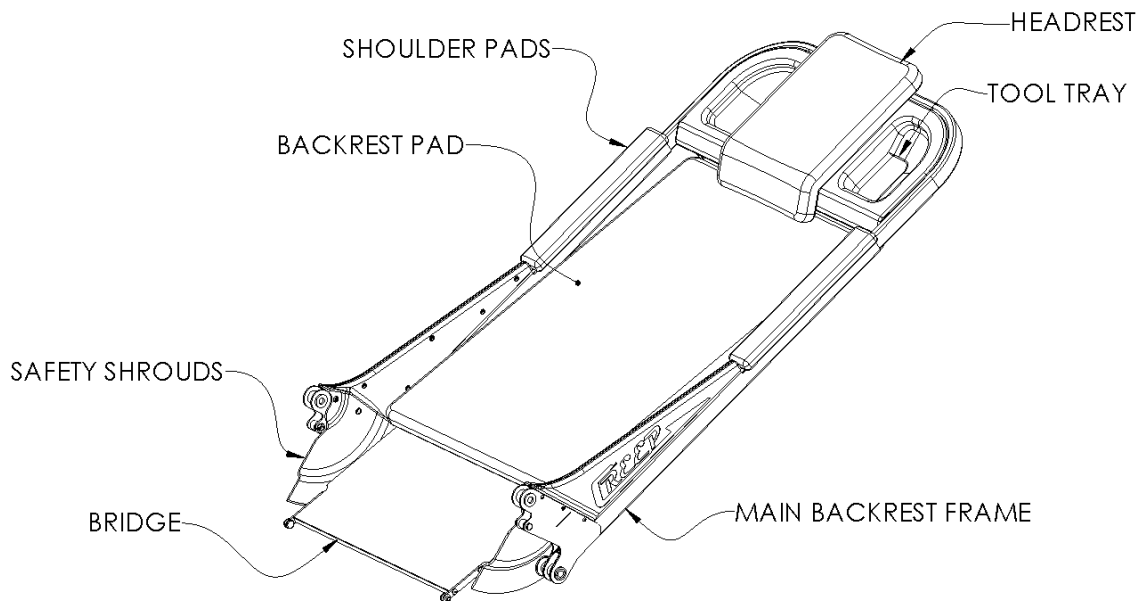


**Figure 16: Backrest subassembly of final design solution**

Due to the sliding relationship between the bridge and the backrest support frame, it is necessary to have a pivoting joint where the backrest support frame meets the main backrest frame. The main frame attaches to the seat and is the primary link for inclining the user's upper body. When in the supine position, due to the recessed nature of this pad, the work surface is approximately 2.9 inches off the ground, see the mechanical drawing in Appendix J. This successfully satisfies the design requirement to provide a work surface at a maximum distance of 3 inches from the ground.

Given how the backrest pad is recessed in the main backrest frame, this made it quite simple to design an elevated head support. The headrest was also designed as an

upholstered piece that can be adjusted to accommodate a variety of user heights. To determine the headrest position, several men near 6'4" in height were measured while sitting down. The maximum value of these measurements was used to quantify the distance from the seat to the top of the headrest, when the headrest is in its highest position. Similar measurements were also taken to determine the lengths needed for the footrests and seat pad.

A thermoformed headrest tray designed to be fastened onto the main frame of the backrest assembly supports the headrest. This tray utilizes the space to each side of the headrest to provide a temporary parts or tool tray. The location of the tray pockets is a very convenient, reachable location where hardware or tools can be kept while working in the supine or semi-reclined positions.

The primary manufacturing processes used in the framework of the backrest were simple fabrication of tube steel and sheet metal processes where several thin pieces are spot welded together. All sheet metal parts used in the main frame are assembled in a symmetric fashion, which makes the left identical to the right, cutting down on side-specific parts.

The pinch hazards at the sides near the backrest pivot location are covered using symmetric injection molded ABS covers. These covers nest together with the sides of the seat to form a complete isolation of the user from pinch hazards in the user contact area. Because one side's cover is symmetrical with the opposite side, these components are good candidates for family molding, which, while including the seat side covers, reduces

the number of mold tools needed from six to three. This saves a significant expense in non-recurring engineering (NRE) costs.

### Footrest

Due to the potential market for an assistive creeper utilized by individuals that have the ability to propel themselves in a traditional manner, using their legs and feet, the footrest was designed to be an optional and quite simply removable feature. In this case, the creeper functions much as a traditional creeper when in the supine position, and is quite similar in size. Each side of the footrest is attached to the seat assembly of the creeper with four self-tapping screws.

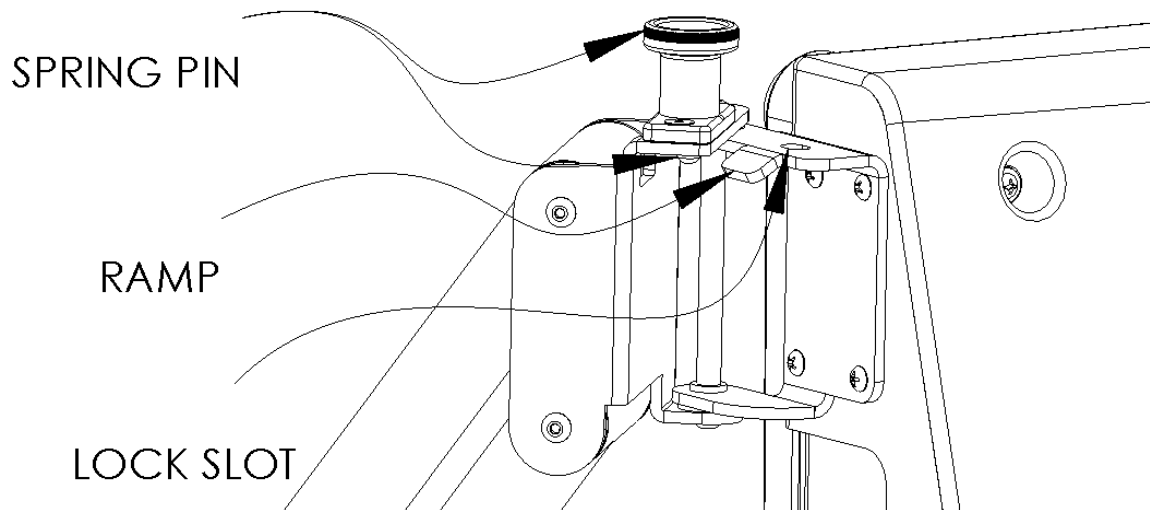


**Figure 17: Close-up view of footrest locking mechanism (right side) of final design solution**

The primary need for a footrest is for people with physical disabilities that need their legs to be supported. For those individuals, who are likely going to be transferring into the creeper from a wheelchair, the footrests were designed to easily swing out of the

way to allow access to the front of the creeper; Figure 27 of Appendix A demonstrates this from a top down view. This is done by lifting a spring pin, easily accessed at the front and top of the seat sides, and pushing the footrest out to its corresponding side, shown partially in Figure 17. Each footrest is capable of rotating outward approximately  $120^\circ$ , which easily clears the path in front, shown in Figure 27. Conversely, when the footrests are out to the sides, the user needs only to swing them back in front. The spring pin will ride up a small ramp on the bracket that attaches to the seat and eventually fall into place in the slot on the top of the same bracket. This makes engagement and disengagement of each footrest a single-handed operation.

The user's foot rests on the horizontal bar, with the back of the foot resting in the cloth stirrup. This design should allow for secure containment of the user's legs, however if additional securement is needed, a shin strap may easily attach to the main upper footrest member

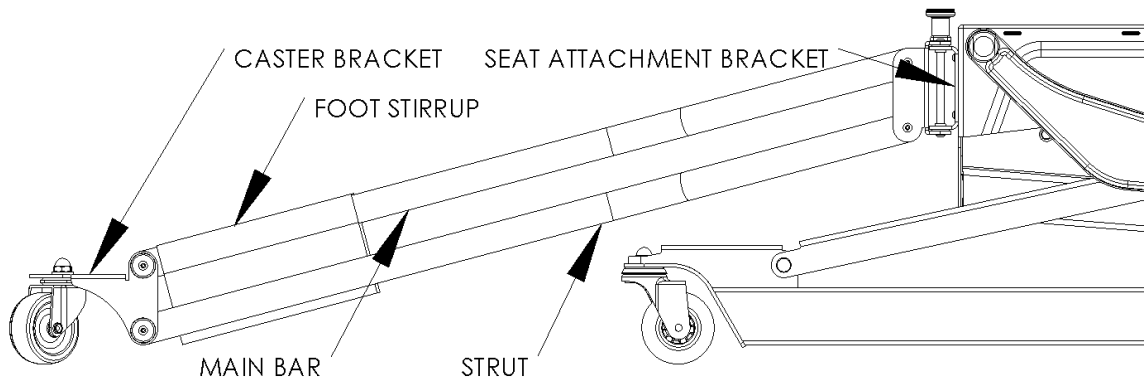


**Figure 18: Left-side footrest view: caster leveling strut integrated into final design solution**

Because the footrest goes through a dramatic angle change while the seat is raising or lowering, it is important to maintain the footrest's casters level. If the casters

are not level, they will favor sitting in one direction and will not allow satisfactory maneuverability. To accomplish this, the footrests were designed with an additional strut, shown in Figure 18 that functions much the same as the legs do in order to keep the seat level. Therefore, regardless of the vertical position in which the user stops the creeper, the casters will roll the same, as shown in Figure 18.

Lastly, the main custom components to the footrest are the caster brackets, footrest bars and attachment brackets. These primary components can be manufactured by sheet metal forming and basic fabrication processes such as pipe bending, cutting and welding. The majority of the additional components involved are economical consumer off-the-shelf (COTS) components.

#### Bill of Materials Overview

The bill of materials for the completed design is summarized in Table 3 and categorized by general manufacturing and assembly processes. This table offers simple visualization of the number of parts included in the top-level assembly. The total number of components is defined as the number of purchased or fabricated components within the entire assembly, before any assembly is done. The number of unique components is defined as the number of parts that differ from any other part in the assembly. This terminology clarification is also pertinent to the assemblies' breakdown. A complete parts level bill of materials can be accessed in Appendix I.

Table 3 indicates that exactly half of the components included in the assembly are COTS components. The other half is custom manufactured parts, and quantities are broken down into respective groups by manufacturing process. Perhaps the most

expensive manufacturing process in terms of labor cost per part is machined components. Although 35 components fall under this category, machining processes only account for nine of these components. Of these nine parts, all of them are turned components, made from stock very close to the size of the finished part. Therefore, the machining processes needed are simple and will not involve expensive 3D machining. Laser and waterjet processes involve simple 2D profile cuts out of metallic, rubber, and polymeric materials. Depending on the production quantities, many of these components are also good candidates for punching and potentially even stamping processes. However, due to the tooling costs associated with these processes, lasers and waterjets are often used for prototype or low production quantities. Basic fabrication refers to components that are merely sawn or cut, or have holes drilled and/or tapped. Many of the tubular steel chassis components fall into this category.

Sheet metal and formed components are also likely to include laser processing for low quantities. However, what differentiates these sheet metal components from the prior group is the forming and bending that these components undergo. With specialized tooling, these components can be made economically, and when combined with the prior category, these simple processes account for 75% of the custom components, which is a good sign in terms of DFMA principles.

Injection molding, thermoforming, and casting processes is another category of manufacturing that requires expensive tooling, but when amortized across the shooting of high part volumes, is very cost effective. This is a process used on the shrouds and covers in the Creep Up design. The legs in the assembly are the only component that is

cast, which is done from A380 aluminum alloy. While tooling for die casting is very expensive, these important structural members can be made for around \$12 each. A cost reducing effort done for the legs was to make all 4 legs the same. By designing the legs to nest together and be the same for front, back left and right, the piece part cost was minimized. When considering the plastic components designed for injection molding processes, due to high tooling costs, it is crucial to note the possibility of family tooling. When two plastic components are mirror images, they can often be molded in mirror form with the injection site and gating centrally placed between the two parts. Wherever a molded part is used only once in the design, there is a mirror image to the part that may be molded with its mirrored counterpart using a single mold tool. All other injection molded components are used multiple times in the assembly, making the parts and tool amortization more cost effective.

**Table 3: Top-level part and assembly quantities by manufacturing process**

<b>Metric</b>	<b>Quantity</b>
<b>Total Parts (if every individual part counted)</b>	<b>593</b>
<b>Unique Parts (excludes multiples of the same component)</b> <i>Listed in Appendix I</i>	<b>170</b>
Consumer off-the-shelf (COTS) components	85
Machined/turned, laser/waterjet, basic fabrication	35
Sheet metal, stamped/formed components	29
Cast, Injection Molded, Thermoformed Parts	16
Sewn, upholstered components	5
<i>Average number of times each unique part is used</i>	<b>3.5</b>
<b>Total Subassemblies</b>	<b>69</b>
<b>Unique Subassemblies</b>	<b>45</b>
Mechanical Subassemblies	29
Welded Subassemblies	16



Lastly, the sewn and upholstered parts are fewest in number and include the seat pad, backrest pad, headrest, footrest stirrup, and two shoulder pads. These components are primarily for the comfort of the user but are also important components that give the creeper structural shear support.

An interesting metric to consider when comparing designs for manufacturability, is the average number of times that a unique component is used in the assembly. This is computed by the following relationship:

$$\text{Average Component Qty} = \frac{\text{Total Number of Parts}}{\text{Number of Unique Components}} \quad (2)$$

The average component quantity is the quantity of each individual part number that would be required in order to build one complete creeper assembly if every component was used the exact same number of times.

When components are purchased for an assembly, generally the greater the purchase quantities the lower the piece part cost. Therefore, if there are 50 locations that need a washer, using 5 different washers, 10 times each, is inferior to designing the use of only 2 different washers used 25 times each. It is not reasonable to expect that every component be used the same number of times, but the idea is to minimize the number of unique components, thus driving the average component quantity as high as possible. The BLAC Inc. design finished with 254 total parts, with 89 being unique components. This yields an average component quantity of 2.9. As noted in Table 3, the Creep-Up mechanical design was finished with a total of 593 parts, with 170 unique components. This design has an average component quantity of 3.5, which is an improvement over the BLAC Inc. design.

At the same time, minimizing the total number of components is also desirable. The BLAC Inc. design is not a fair basis for comparison to the Creep-Up design in regard to the total number of components. This is because the BLAC Inc. design was a proof-of-concept project in which the final design lacked a significant number of parts that would make the detail of the design manufacturable and suitable for consumer safety.

## CHAPTER 3

### ANALYSES & DESIGN VALIDATION

In order to validate the design decisions and solutions discussed in Chapter 2, a thorough set of analyses was performed. The purpose for the analyses was twofold:

- 1) Provide design performance feedback during concept and preliminary design phases to justify design decisions and identify unmet needs, and
- 2) Analyze the design in the critical design phase to promote a greater level of confidence in the integrity of the final solution through refined design validation analysis.

The sum of the analyses consisted of five key methods, each fulfilling an important role, some of which were only done as preparatory calculations for subsequent analyses.

Nonetheless, all were necessary to instill adequate confidence in the integrity, and thus the overall safety of the system. These five analyses are done in relative order and consist of the following:

- Kinematics Analysis
- Static Force Analysis
- Finite Element Analysis (FEA)
- Theoretical Analysis
- Failure Mode and Effects Analysis (FMEA)

Although these analyses produce a reasonable compilation of theoretical behaviors and failure modes, they do not serve as a replacement for design validation testing. It is very difficult to perfectly predict the dynamic and structural behavior of the

system, however, these analyses justify the design's readiness for prototyping.

Ultimately, prototyping and design validation testing are still critical parts of the design cycle that must be completed before production.

### **Kinematic Analysis**

During the course of preliminary design, it was important to choose link lengths and angle ranges that kept the forces and speeds of the links manageable. Hence, the ability to quickly review kinematic positions and velocities was necessary. To accomplish this, a kinematics analysis was done in which the positions and velocities of all links in the kinematic chains were determined. The values solved for in this analysis were transient values that changed with each movement of the creeper, whether in the incline/recline phase or the raise/lower phase. To facilitate rapid design feedback given geometric inputs, a custom program was written in Matlab® where equations for solving all kinematic unknowns were computed. Solutions were found and stored for all positions between supine and full seated at increments of approximately ¾° incline of the backrest and ½° rotation of the legs. This translates to 201 positions between the two extremes.

To begin, the kinematics analysis was done using closed-loop vector addition in that, the sum of any closed loop of vectors is equal to zero.

$$\sum_{i=1}^n \vec{R}_i = 0 \quad (3)$$

The kinematic solutions were broken up into two vector loops; vector loop A and vector loop B, shown in Figure 19 and Figure 20, respectively. This was necessary due

to the complex set of linkages associated with the two independent motions. There were four transient unknown position values during the incline/recline phase. When split into two loops the unknowns were divided as a result, so the kinematics analysis could then provide sufficient equations to solve for the unknowns. Each loop shares a joint where the backrest frame pivots on the seat link, best understood as the pivot between links 4 and 5 as indicated in Figure 6.

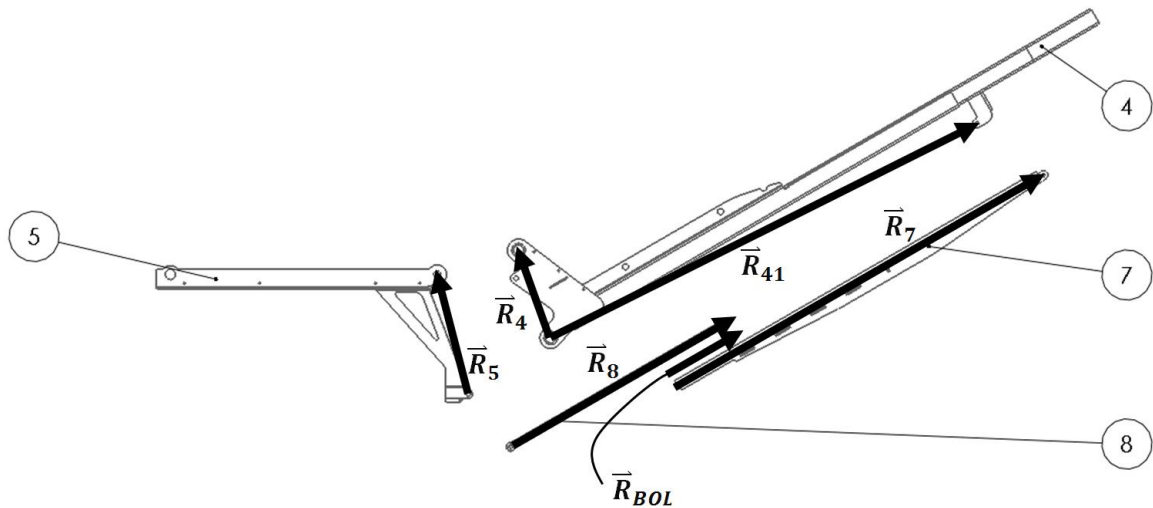


**Figure 19: Vector Loop A: backrest inclination, kinematic chain for kinematics analysis, including link numbers**

Vector loop A (Figure 19) was used to solve for kinematic outputs in all backrest members. In this case, the seat member, link 5, was treated as a ground link and the backrest frame, link 4, was considered to be the input link where the initial conditions were known as well as the total sweep angle. All physical link lengths were treated as known inputs to the analysis. The vector  $\vec{R}_{41}$  references a secondary location on link 4 where the backrest pad attaches, and its angle is measured counter-clockwise from the

vector  $\vec{R}_4$ . The angle for this vector is fixed, and because link 5 remains the same angle by nature of the design, this leaves two unknown transient values. The vectors  $\vec{R}_7$ ,  $\vec{R}_8$ , and  $\vec{R}_{BOL}$  share the same angle, which is the angle of the bridge and backrest pad, shown in the free body diagrams as  $\theta_{78}$ . This is one of the unknowns, and the second is the overlap distance of the bridge and backrest pad,  $L_{BOL}$ , or the length of the virtual link  $\vec{R}_{BOL}$ . Table 4 summarizes which position values are known and unknown for each vector loop.

**Table 4: Kinematic position, known and unknown values, by vector loop**

<i>Kinematic Position Values</i>		
Vector Loop	A	B
Known	$L_4, \theta_4$ $L_5, \theta_5$ $L_{41}, \delta_{41}$ $L_7$ $L_8$	$L_4, \theta_4$ $L_{2b}, \theta_{2b}$ $L_{12}, \theta_{12}$ $\theta_{11}$ $L_6, \theta_6$ $L_3$
Unknown	$L_{BOL}$ $\theta_{78}$	$L_{11}$ $\theta_3$

Finding these two unknowns requires two equations. Each of the vectors in the vector loop sum can be written in terms of link length, and the exponential of the link angle, in the following way:

$$\vec{R}_i = L_i e^{j\theta_i} \quad (4)$$

This equation when applied to equation (3) for vector loop A, yields the following governing position equation for vector loop A in the incline/recline phase:

$$L_4 e^{j\theta_4} - L_5 e^{j\theta_5} + L_8 e^{j\theta_{78}} - L_{BOL} e^{j\theta_{78}} + L_7 e^{j\theta_{78}} - L_{41} e^{j(\theta_4 + \delta_{41})} = 0 \quad (5)$$

The individual terms of this equation can then be expanded further as

$$L_i e^{j\theta_i} = L_i \cos(\theta_i) + jL_i \sin(\theta_i) \quad (6)$$

By applying the above relationship to the vector sum, then separating out the real and imaginary parts, two equations containing the relationships of unknown variables to the known are derived. The entire derivation can be found in Appendix B, whereas the two equations for solving for the unknown positions of vector loop A are as follows:

$$\begin{aligned} L_4 \cos(\theta_4) - L_5 \cos(\theta_5) + (L_8 - L_{BOL} + L_7) \cos(\theta_{78}) \\ - L_{41} \cos(\theta_4 + \delta_{41}) = 0 \end{aligned} \quad (7)$$

$$\begin{aligned} L_4 \sin(\theta_4) - L_5 \sin(\theta_5) + (L_8 - L_{BOL} + L_7) \sin(\theta_{78}) \\ - L_{41} \sin(\theta_4 + \delta_{41}) = 0 \end{aligned} \quad (8)$$

Because  $\theta_{78}$  and  $L_{BOL}$  appear in both equations and cannot be eliminated or substituted algebraically, Newton's method was used to determine the solution [7]. Initial guesses for Newton's method were  $L_{BOL} = 6 \text{ inches}$  and  $\theta_{78} = 40^\circ$ , each of these values representing approximately the middle value of the variables' ranges.

Positions for vector loop B (Figure 20) were computed in the same manner, again using the backrest, link 4, as the input link. In this case however, the seat component, link 5, was no longer considered the ground link as it was not a part of vector loop B. The chassis component, link 1, was taken to be the new ground and remained the ground link through the kinematics analysis of the raise/lower phase. Application of the vector loop equations to vector loop B yielded the following governing position equation:

$$L_{11} e^{j\theta_{11}} + L_{12} e^{j\theta_{12}} - L_4 e^{j\theta_4} - L_3 e^{j\theta_3} - L_6 e^{j\theta_6} + L_{2b} e^{j\theta_{2b}} = 0 \quad (9)$$

This in turn produced the two relationships:

$$L_{11} + L_{12} \cos(\theta_{12}) - L_4 \cos(\theta_4) - L_3 \cos(\theta_3) - L_6 \cos(\theta_6) + L_2 \cos(\theta_2) = 0 \quad (10)$$

$$L_{12} \sin(\theta_{12}) - L_4 \sin(\theta_4) - L_3 \sin(\theta_3) - L_6 \sin(\theta_6) + L_2 \sin(\theta_2) = 0 \quad (11)$$

Equation (11) could be solved algebraically for  $\theta_3$  since it was the only unknown in that equation. The now known value for  $\theta_3$ , applied to equation (10) made  $L_{11}$  a simple algebraic problem as well.

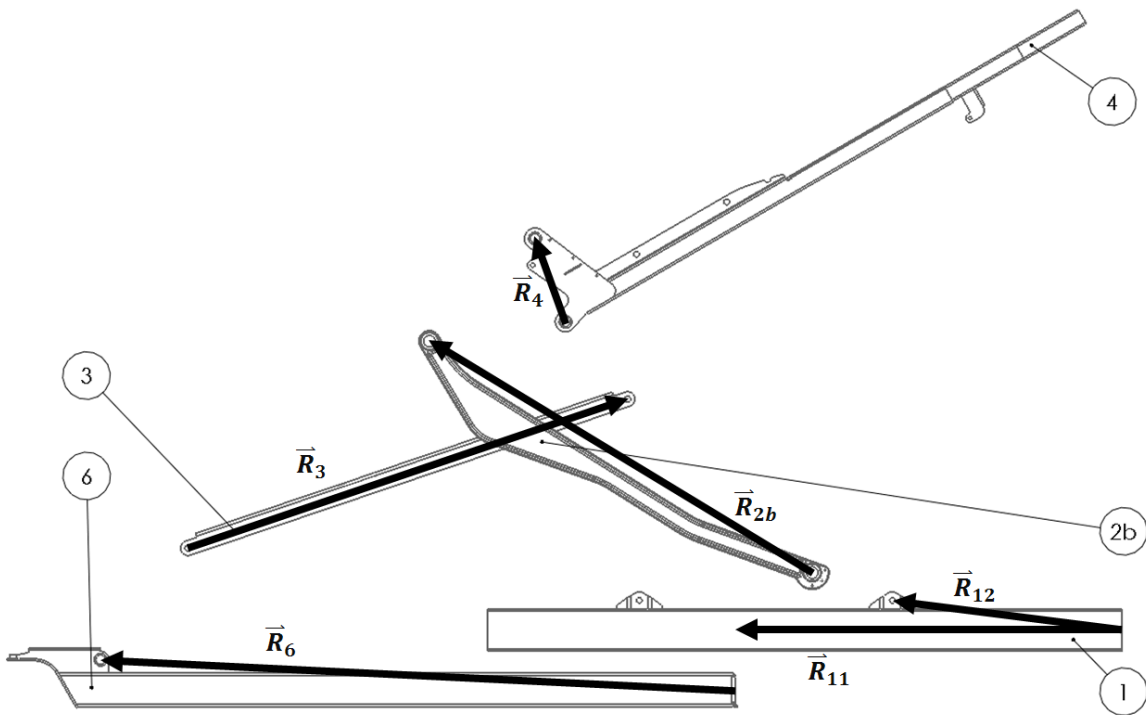


**Figure 20: Vector Loop B: seat raising, kinematic chain for kinematics analysis, including link numbers**

During the raise/lower phase, the backrest is no longer a transient part of the kinematic positions, therefore, vector loop A does not apply to this phase. Vector loop B, however, was applicable to the raise/lower motion as well. There was a minor difference in input links between the incline/recline and raise/lower kinematics of vector loop B.



Recall in the incline/recline phase, the leg, link 2b, was kept at a known angle while the backrest frame, link 4, was moved as the input link. In the raise/lower phase, the backrest frame was held stationary by the additional mechanics explained in Chapter 2, and the leg was allowed to move, ultimately raising the seat. In the position analysis, this difference was only clerical as to ground and input link titles because all knowns and unknowns remained the same.

Determining the retraction and extension velocity of the slider is crucial for determining motor speed. This has a direct effect on motor and lead screw selection, hence the reason for the kinematics analysis to include link velocities. These velocities were computed in a similar fashion to the positions. Since velocity is the time derivative of position, the necessary governing velocity equations could be found by differentiating the governing position equations. The change in the stationary and transient input links referred to above in the position analyses for the incline/recline and raise/lower phases, also affected the kinematic velocity equations. An example of this is, the velocity of link 4 is non-zero in the incline/recline phase, and becomes zero in the raise/lower phase. Therefore, the two phases of vector loop B used the same governing velocity equation, but their inputs produced two unique sets of kinematic equations. The velocity equation for vector loop A was derived as

$$\begin{aligned}
 jL_4\omega_4e^{j\theta_4} + j(L_8 - L_{BOL} + L_7)\omega_{78}e^{j\theta_{78}} - \dot{L}_{BOL}e^{j\theta_{78}} \\
 - jL_{41}\omega_4e^{j(\theta_4+\delta_{41})} = 0
 \end{aligned} \tag{12}$$

Likewise, the governing velocity equation for vector loop B became

$$\dot{L}_{11} - jL_4\omega_4e^{j\theta_4} - jL_3\omega_3e^{j\theta_3} + jL_{2b}\omega_{2b}e^{j\theta_{2b}} = 0 \tag{13}$$

These equations were then separated into real and imaginary parts by employing equation (6), again producing two kinematic equations per governing equation. The kinematic equations for vector loop A in the incline/recline phase, from equation (12) are

$$L_4\omega_4\cos(\theta_4) + (L_8 - L_{BOL} + L_7)\omega_{78}\cos(\theta_{78}) - \dot{L}_{BOL}\sin(\theta_{78}) - L_{41}\omega_4\cos(\theta_4 + \delta_{41}) = 0 \quad (14)$$

$$-L_4\omega_4\sin(\theta_4) - (L_8 - L_{BOL} + L_7)\omega_{78}\sin(\theta_{78}) - \dot{L}_{BOL}\cos(\theta_{78}) + L_{41}\omega_4\sin(\theta_4 + \delta_{41}) = 0 \quad (15)$$

From the positions analysis, all lengths and angles of each link are known values. During this phase, the angular velocity of the backrest was also known since it was the input, or driver link. This angular velocity was set at a constant value, which was calculated from an arbitrary time duration assigned to the inclination of the backrest. A constant rotation speed of the backrest contributes to a better user experience. A summary of knowns and unknown values can be found in Table 5. Newton's method was employed again with equations (14) and (15) to determine the two unknown values.

**Table 5: Kinematic velocity, known and unknown values, by vector loop and motion phase**

<i>Kinematic Velocity Values</i>			
Vector Loop, Phase	A, 1	B, 1	B, 2
Known	$L_4, \theta_4, \omega_4$ $L_7, L_8, L_{BOL}, \theta_{78}$ $L_{41}, \delta_{41}$	$L_4, \theta_4, \omega_4$ $L_3, \theta_3$ $L_2, \theta_2, \omega_2$	$L_4, \theta_4, \omega_4$ $L_3, \theta_3$ $L_2, \theta_2$
Unknown	$\dot{L}_{BOL}$ $\omega_{78}$	$\dot{L}_{11}$ $\omega_3$	$\dot{L}_{11}$ $\omega_3$ $\omega_2$

Next, the kinematic equations for vector loop B in the incline/recline phase, from equation (13) are

$$-L_4\omega_4 \cos(\theta_4) - L_3\omega_3 \cos(\theta_3) = 0 \quad (16)$$

$$\dot{L}_{11} + L_4\omega_4 \sin(\theta_4) + L_3\omega_3 \sin(\theta_3) = 0 \quad (17)$$

Note that from the governing velocity equation for vector loop 2, the link 2 terms are missing in the kinematic equations. This is due to zero angular velocity of the leg during the incline/recline phase. Likewise, in the following equations for the raise/lower phase, link 4 terms are removed since there is no rotation in the backrest during this phase.

$$-L_3\omega_3 \cos(\theta_3) + L_2\omega_2 \cos(\theta_2) = 0 \quad (18)$$

$$\dot{L}_{11} + L_3\omega_3 \sin(\theta_3) - L_2\omega_2 \sin(\theta_2) = 0 \quad (19)$$

Equations (16) and (17) were solved algebraically for the two unknowns in phase 1 of vector loop B. It is important to note that the number of unknowns listed for the raise/lower phase of vector loop B is three. The angular velocity of the leg,  $\omega_2$ , is listed as the third unknown. Although this link was used as the input for the phase 2 motion, it was not given an arbitrary velocity value as was link 4 for phase 1. Instead, a transition analysis was included to compute the initial raise rate of the seat, given the motor speed at the end of phase 1. This was done by using equation (19) to solve for  $\omega_2$  using  $\dot{L}_{11}$  from the end of phase 1. The vertical component of velocity at this instant was computed by the following relationship:

$$L_2\omega_2 \cos(\theta_2) = \text{constant seat raise rate} \quad (20)$$

Once the seat raise rate was known at the start of phase 2, equation (20) was rearranged and used in each raise step to compute a new value for  $\omega_2$ , which increased as  $\theta_2$

decreased in order to maintain a constant vertical velocity of the seat. With the value of  $\omega_2$  for each position, equations (18) and (19) could then be used to solve algebraically for the other two unknown values in phase 2 of vector loop B. Ultimately, the vertical component of velocity of the seat was held constant to improve the user experience. In order to maintain constant angular velocity of the backrest in phase 1 and constant vertical velocity of the seat in phase 2, the motor must be driven at variable speeds. Using a 4mm pitch ball screw, the speeds required to generate a total transition time of 20 seconds or less are evident in Figure 21. It can be seen that a motor speed of about 200 RPM is shared at the interface of the two phases, evident by the piecewise continuity. The maximum speed required by the motor to achieve a time from supine to full seated of less than 20 seconds is 1750 RPM, a reasonable speed requirement from a DC gear motor.

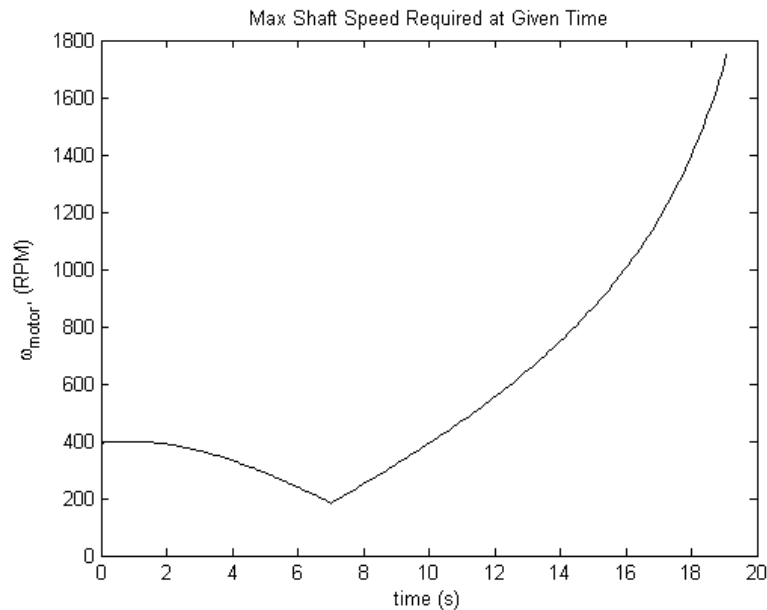


**Figure 21: Motor shaft speed required to incline the backrest and raise the seat at constant angular and vertical velocities, respectively, in under 20 seconds**

Positions, velocities, and subsequent static forces computed by the PVF program were stored in vectors for all kinematic positions and are accessible to review with respect to time. A high-level flow chart of the PVF program written for these computations can be found in Figure 29 of Appendix A.

Accelerations were not computed as part of this analysis. Comfortable accelerations on the human body top out at around 0.15g [6]. Because electronics will be used to control motor speed, these electronics may also be used to implement soft start and stop features to create a better user experience and avoid accelerations that will result in significant reaction loads on the system. There will however, be small accelerations that are considered to be handled by the safety factors adhered to in the subsequent analyses.

### **Static Force Analysis**

The purpose for the static force analysis was to compute the reaction forces at the joints of all the kinematic links, and to post process these and any pertinent force computations. All outputs from this analysis are important inputs for the subsequent structural analyses.

As shown in the flow chart in Figure 29, the position solutions of all kinematic links were used as inputs for the static force calculations, which were performed in the same PVF program. These inputs supplied critical angle and distance information regarding the direction of applied loads. Additionally, externally applied loads on the system, and individual component weights and centers of gravity, were inputs to this analysis. Component weights and CG information was available in SolidWorks after

applying material properties for each component. External loads considered are purely static loads induced by the user. In order to nominally apply the loads to the creeper as realistically as possible, de Leva's body segment data was used [1]. Average values for percent body weight and center of gravity measured from the user's proximal end (top of head), were applied to a user weight of 300 lbf and height of 6'4". This provided an average weight distribution in the worst-case load configuration per the prescribed design requirements. These loads were estimated and applied to the backrest and seat pad, and include friction and normal loads. For analysis of kinematic joint reaction forces, the anatomical loads were separated into  $W_{ub}$  and  $W_{lb}$ , representing the weight of the upper body and lower body, respectively. Because the kinematic system is mirrored on either side of the user, and the user is forced to be reasonably centered on the creeper, these loads were halved and applied to one side only.

The kinematic link subassembly was broken out, and equal and opposite forces at all points of contact were drawn on individual free body diagrams (FBD). All applicable FBDs can be found in Appendix C. Note that components with anatomical loads applied, also include these external forces on the FBD. Separate analyses were done for phase 1 and phase 2, and all unknown reaction forces were identified and organized into vectors in equation (21).

In each phase there turned out to be 25 unknown force values, thus requiring 25 equations to determinately solve the static solution. The static force equations were derived from the use of the static equilibrium equations on each of the components involved in the FBDs.

$$F_{Phase1} = \left\{ \begin{array}{l} F_{2aCx} \\ F_{2aCy} \\ F_{2aSx} \\ F_{2aSy} \\ F_{2bCx} \\ F_{2bCy} \\ F_{2bSx} \\ F_{2bSy} \\ F_{2m} \\ F_{3x} \\ F_{3y} \\ F_{4Ax} \\ F_{4Ay} \\ F_{78L} \\ F_{78U} \\ F_{Cx} \\ F_{Cy} \\ F_{Dx} \\ F_{Dy} \\ F_{5front} \\ F_{5Ax} \\ F_{5Ay} \\ F_{seatx} \\ F_{seaty} \\ F_{hangscrew} \end{array} \right\} \text{ and } F_{Phase2} = \left\{ \begin{array}{l} F_{2ax} \\ F_{2ay} \\ F_{9x} \\ F_{9y} \\ F_{2bx} \\ F_{2by} \\ F_{9screwx} \\ F_{9screwyfront} \\ F_{9screwyrear} \\ F_{3x} \\ F_{3y} \\ F_{4Ax} \\ F_{4Ay} \\ F_{78L} \\ F_{78U} \\ F_{Cx} \\ F_{Cy} \\ F_{Dx} \\ F_{Dy} \\ F_{5front} \\ F_{5Ax} \\ F_{5Ay} \\ F_{seatx} \\ F_{seaty} \\ F_{hangscrew} \end{array} \right\} \quad (21)$$

$$\sum M_A = 0 \quad (22)$$

$$\sum F_x = 0 \quad (23)$$

$$\sum F_y = 0 \quad (24)$$

If components were purely axially loaded members, then only one equilibrium equation could be derived using the sum of the moments, equation (22). The other two equations would only produce trivial solutions. In components where there is composite loading, three equations could be extracted by employing equations (22) through (24). Nine

components made up the free body static force analysis for phase 1, while two additional parts involved with the backrest stop mechanism were included in phase 2. The complete static force analysis for both phases can be found in Appendix D, however, Table 6 gives a summary of the number of equations extracted from each FBD. The key difference between the two phases, aside from the number of components involved in the analysis, was the number of equations attainable from the FBDs of the legs. In phase 1, the legs are nested together and gravity creates a non-axial load between the two members. On the other hand, in phase 2, the two legs lose contact and become purely axial members. Hence, in phase 1, the legs account for three equations each and in phase 2, they only account for one each.

**Table 6: Number of equations attainable from each link included in the static force analysis for both incline/recline and raise/lower phases**

<b>Part No. Component (FBD)</b>	<b>No. of Eqns (Phase 1)</b>	<b>No. of Eqns (Phase 2)</b>
P03-00025 Middle Seat Brace	3	3
P03-00026 Rear Seat Hanger	3	3
P03-00027 Sheet Metal Push Rod	1	1
A02-00016 Welded Backrest Frame Subassembly	3	3
A01-00003 Bridge Subassembly	3	3
A01-00011 Back Rest Subassembly	3	3
P04-00008 Leg (front)	3	1
P04-00008 Leg (rear)	3	1
P05-00004 Upholstered Seat Subassembly	3	3
*P03-00004 Back Slider Bracket	N/A	3
*P02-00006 Back Tension Bar	N/A	1
<b>Total Equations</b>	<b>25</b>	<b>25</b>

\* Only applicable to Phase 2

The 25 equations generated in each phase, were arranged by coefficients of the unknown terms in equation (21) for their respective phase. This arrangement was done in the form



$$\begin{bmatrix} A_{1,1} & \cdots & A_{1,25} \\ \vdots & \ddots & \vdots \\ A_{25,1} & \cdots & A_{25,25} \end{bmatrix} \{F_{Phase1}\} = \{P\} \quad (25)$$

and

$$\begin{bmatrix} B_{1,1} & \cdots & B_{1,25} \\ \vdots & \ddots & \vdots \\ B_{25,1} & \cdots & B_{25,25} \end{bmatrix} \{F_{Phase2}\} = \{Q\} \quad (26)$$

where  $\{P\}$  and  $\{Q\}$  are the external load vectors for phase 1 and phase 2, respectively.

The reaction force vectors were simply solved by inverting the square matrices and multiplying them by their respective external load vectors. As an example, the phase 1 reaction forces were found in the following way:

$$\{F_{Phase1}\} = [A]^{-1}\{P\} \quad (27)$$

In addition to the computations done for the main system kinematics, an additional set of six equations was used to solve for the caster bracket loads and slider contact forces of the chassis and slider members. Because there are three casters per side in contact with the ground, this solution is statically indeterminate, and additional assumptions were made regarding the sharing of the loads. These assumptions included position dependent load distribution based on the estimated location of the combined user and creeper CG. If the combined CG fell between the front and middle casters, then it was assumed that the rear casters only supported 25% of the total combined weight. Similarly, if the combined CG fell between the middle and rear casters, then it was assumed that the front casters were responsible for 25% of the total combined weight.

While the majority of the terms in the square matrices were zero, all non-zero terms derived, along with expressions for the external load vectors terms, are listed in

Appendix D. The process of computing the reaction loads was performed for every kinematic position immediately following the position and velocity analyses. Similar to the positions and velocities, the reaction forces were stored into vectors to be used to view and extract meaningful data such as those seen in Figure 7 and Figure 9. Outputs from this section of the analyses were combined with the external load values to form a complete load input set for analyzing individual component integrity by finite element and theoretical methods.

The following key assumptions were used in the static force analysis:

- Frictionless pivots; justified by the use of ball, roller, and/or thrust bearings at all pivoting joints
- Frictionless slider contact; justified by the use of Delrin or ABS plastic against smooth aluminum or steel surfaces at low speeds
- Uniform distribution of external loads on contact surfaces
- Anatomical inputs use loads per de Leva's percentages of total body weight and centers of gravity for maximum user weight and height

To establish confidence in the validity of the output values in the static force analysis, a comparison was done in SolidWorks Motion. For this comparison the full upper and lower body weights were applied to the solid model assembly and the axial lead screw force was computed by the software for phase 2. The screw load computed by SolidWorks was superimposed with that from the PVF program, and the results are in Figure 22. It can be seen that the curves differ from one another, but that the general shape and values are very similar. These differences were anticipated due to the

estimations of user contact dimensions and CGs used in the hand calculations. It is also satisfactory to note that in the highest load region, the hand calculations are more conservative. Considering this evaluation, acceptable agreement between the two analyses can be concluded.

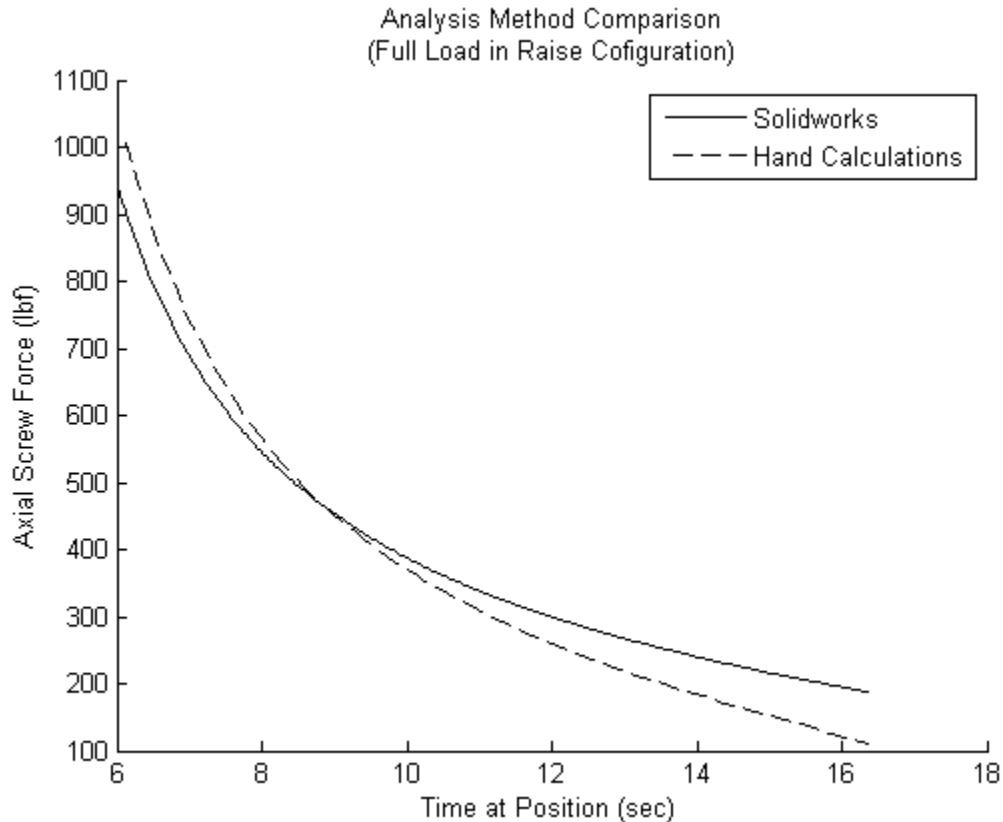


**Figure 22: Comparison of screw axial loads through the entire phase of motion 2, for hand-prepared calculations and software generated outputs, for the worst-case load conditions**

### Finite Element Analysis (FEA)

If the failure of a component due to stress or fatigue would result in the failure of the creeper or harm to the user, then finite element methods were employed to find locations and magnitudes of the peak stresses. FEA was also used on select components

to quantify compliance before yield occurs. In some cases, conventional theory provided highly reliable results, however, the large majority of the components and subassemblies that required analysis were more complex and required that finite element be used. The majority of the studies were performed in Femap/NX Nastran software.

Most of the components analyzed were made of sheet metal or thin walled tubing that was welded together. As a general rule, the material thickness was used as the base mesh size. As a study completed, stresses were analyzed, and if there was any indication of stress potentially high enough to produce a safety factor (SF) less than 3.0 against yielding, then additional mesh refinement was applied in those high stress regions. In cases of complex welded subassemblies, the individual components were assembled together and joined as solid parts with fillets applied to the solid geometry to represent the location, throat size, and lengths of the intended welds. Some simple welded subassemblies were not analyzed here, but rather by conventional theory for weld analysis [3].

Inputs used were the externally applied loads and joint forces calculated in the static force analysis. Additionally, each run required that the material be selected from a preset list, or a minimum of Young's modulus, yield strength, and Poisson's ratio were entered manually. Loads were applied to axially loaded members, or pivot joint reaction forces using rigid elements that distributed the point load to the bearing surface.

Outputs taken from these analyses were primarily safety factors against yielding, however deflections, 3D buckling modes and loads, and stress values were also important. In some cases, like the rotating shafts that were prone to cyclic loading and

unloading, the stress outputs from FEA were used in further hand calculations for infinite life and fatigue failure. In any case, each study produced meaningful results that were used to validate the integrity of the design components and subassemblies. The results were then tabulated in Table 10 and Table 11 in Appendix F, with a summary of file names, assumptions and the end SF calculated for each analyzed failure mode. The safety factors were calculated using the yield stress,  $S_y$  and the maximum stress,  $\sigma_{max}$  in the following way:

$$SF = \frac{S_y}{\sigma_{max}} \quad (28)$$

These safety factors became important input to the failure mode and effect analysis (FMEA).

A total of 24 finite element studies were completed, and with each a manual report was generated to summarize the analysis performed. Included in each report is the following information:

- Solid model file name, part number and revision of the analyzed part or subassembly
- Femap or SolidWorks file name from the final analysis
- Brief purpose for the analysis
- Material name and respective properties,  $E$ ,  $S_y$ ,  $\nu$
- Input load definitions and applied constraints as applied to the geometry per the coordinate system of the part in Femap
- Relevant outputs including maximum stresses, deflections, and buckling loads

- Images of the complete part, the initial and final analyzed geometry, initial and refined mesh, stress distribution, location of maximum stress, and deflection or buckling if applicable

These 24 reports can be found in Appendix F and are organized by Table 9.

### **Traditional Theoretical Analysis**

When FEA was impractical, hand calculations were performed using conventional theoretical applications. Mathcad software was used to organize preliminary calculations for other analyses, to determine safety factors on COTS components, and to perform post processing of information from other analyses. Hence, the inputs used in these analyses included product specifications, outputs from the static force analysis, and stresses and deflections acquired during FEA. The detailed analyses can be found in Appendix G.

It was assumed that COTS components were pre-designed with a safety factor of 3.0, therefore computation of the creeper design safety factors were scaled accordingly, as indicated in equation (29). This allowed for COTS components to be used up to their rated specifications without adversely affecting the OCC rating in FMEA.

$$SF = 3.0 \cdot \frac{\text{COTS Component Rating or Specification}}{\text{Calculated Load on Component}} \quad (29)$$

Components analyzed in this way included bearings, casters, lead screw components, springs, motor, and hardware such as screws and fasteners.

Several components such as the lead screws and rotating shafts, will undergo cyclic stress loading. The loading and unloading of stress on materials can cause fatigue failure. For this reason, additional computations were done regarding the infinite life and

fatigue failure limits associated with these components. These failure modes were included in the FMEA portion and demanded a safety factor against such. On the other hand, FEA required load inputs that were not part of the static force analysis. Although these were few, preparatory calculations were crucial for structurally analyzing some components with unknown loads.

Finally, in a few cases, FEA methods would have been more laborious to determine stresses and safety factors where simple loading and geometry prevailed. In this case, equations prescribed for mechanical design analysis were employed [3]. Several pins used in the Creep-Up assembly are subjected to a pure stress-like condition which stress could quickly and easily be solved, and a safety factor computed. Likewise, several welds were analyzed using theoretical equations that took into account weld material, electrode, and throat depth.

### **Failure Mode and Effects Analysis (FMEA)**

In an effort to prevent expensive design changes and potential harm to a user, a failure mode and effects analysis was performed. This process did not begin until the critical design phase when the bill of materials was complete. Some components and subassemblies were labeled to not have any failure modes identified, or that failure modes of a particular component were captured by the FMEA of another component or subassembly. Nonetheless, every subassembly along with each item in the BOM was listed in the FMEA table, which is found in Appendix H. In other cases, some components have multiple failure modes identified and addressed.

The table in Appendix H is broken into three columnar subsections with line numbers listed in each to be able to identify all sections of the table for a given component or subassembly. The table begins with the identification of subassemblies and is followed by the individual components and their respective descriptions. In some cases, a given component may be used in different locations under differing load conditions. This was handled by a column where the context used was described. From this context, failure modes were identified, effect of the failure theorized, and the root cause of the failure predicted. Given the type of failure, a column was populated with the type of analysis best fit for validating the design. Finally, two sets of columns were used to compute the initial and final risk priority numbers (RPN) from the severity (SEV), probability of occurrence (OCC), and detection (DET) ratings. A second RPN was only computed if additional action needed to be taken. The SEV, OCC, and DET ratings were given on a scale of 1 to 10, and the RPN was computed by the product of the three ratings, as indicated by equation (30) [2].

$$RPN = (SEV)(OCC)(DET) \quad (30)$$

The need for action to be taken was determined by the magnitude of the RPN value. The risk priority number is meaningless unless an acceptable criterion is designated. The threshold in analyzing the creeper was determined by worst-case comparisons. When considering a failure situation that has the most catastrophic effects and is impossible to detect before it is too late, this would yield SEV=10 and DET=10. Therefore, because user safety and system reliability are concerns, an OCC=1 rating, indicating the lowest probability of occurring, should yield an acceptable RPN, which in



this case would be RPN=100. Furthermore, consider OCC=2 in the same catastrophic case, making RPN increase to 200. While considering the OCC=1 case to be acceptable, and the OCC=2 case to be unacceptable, the RPN threshold where action must be taken, was set between these two cases at RPN=150. Any failure modes yielding an RPN greater than or equal to 150 were addressed and reanalyzed.

To score the SEV value in the FMEA table, a conscientious selection was made from the SEV column of Table 7. The scale from 1 to 10 outlines a gradual change from an effect unperceivable to the system functionality and extremely low risk to the user, to a high risk of injury to the user and catastrophic system failure. A hierarchy of risks was used to eliminate uncertainty in the selection process. Of greatest significance was the user safety. If at any point in a failure mode, the user could or could not be injured, this was the primary driver for selection. After this selection, the potential level of part damage was considered. Part damage resulting in only cosmetic effects up to damage that causes a complete loss of use, was evaluated. Then the likelihood of failure propagation was scrutinized to account for other possible failures that result from the primary failure. Lastly, the nature of the function loss was compared between unperceivable to significant.

Selection of a DET score was very similar to the SEV score. This time, three considerations were made: how the issue is detected, how the problem is mitigated, and how much harm may result between the time of detection and mitigation. Exercising sound engineering judgement and having a complete working knowledge of the creeper design were critical in the selection process.

The SEV and DET scores were extracted exclusively from Table 7, whereas the OCC score was determined either by best judgement consulting Table 7, or by extracting the exact value from Table 8. If a safety factor could not be determined, then the OCC value was identified by selecting the best-fit scenario from the OCC column of Table 7. If a safety factor was determined, then inputting the safety factor into Table 8 would yield an OCC score. Table 8 was created by identifying two thresholds: firstly, the point at which a failure mode is very likely to occur under the worst-case load conditions, and on the other end of the scale, where a reasonable margin of safety is applied against common failure modes. To satisfy these considerations,  $SF \leq 1$  was linked to the highest probability of occurrence, or  $OCC=10$ , and  $SF > 3$  was represented by  $OCC=1$ , in that a safety factor greater than 3 would account for all anomalies and uncertainties. All other OCC values were filled into Table 8 linearly between the OCC and SF extremes.

When all three scores were assigned, the RPN was computed. If the RPN was under 150 then no further work was done to that component and it was considered complete. Any further changes to that component were avoided, and if necessary, were carefully made to avoid the possibility of voiding the analysis. If the RPN reached at least 150, then further action was taken. To determine the action necessary, the simplest change was considered first that would lower any one of the three scores. Before making the change, a target score on the category to be changed was calculated, and the extent of the changes made were decided based on the target score. Figure 30 shows this FMEA cycle, including how FMEA integrated with the other analyses.

**Table 7: Qualitative FMEA scoring table**

<b>FMEA SCORING DESCRIPTION</b>			
<b>Rating</b>	<b>SEVERITY</b>	<b>OCCURRENCE*</b>	<b>DETECTION</b>
<b>1</b>	<b>User Risk for Injury:</b> Extremely Low <b>Repair Needed:</b> Mild/Cosmetic <b>Leads to Other Failure:</b> No <b>System Function Loss:</b> Unperceivable	Extremely unlikely to occur even if used incorrectly	Detection and problem mitigation is independent of the user, before any user harm or equipment damage can be done
<b>2</b>	<b>User Risk for Injury:</b> Extremely Low <b>Repair Needed:</b> Mild <b>Leads to Other Failure:</b> No <b>System Function Loss:</b> Mild	Very unlikely to occur even if used incorrectly	Detection is independent of the user, before any user harm is done, but may be after mild equipment damage is done
<b>3</b>	<b>User Risk for Injury:</b> Low <b>Repair Needed:</b> Mild <b>Leads to Other Failure:</b> No <b>System Function Loss:</b> Mild	Unlikely to occur even if used incorrectly	Detection must be done by user, however, clear and obvious for the user to detect if looked for. Ignorance will not cause user harm but may result in mild equipment damage
<b>4</b>	<b>User Risk for Injury:</b> Low <b>Repair Needed:</b> Mild <b>Leads to Other Failure:</b> Potentially <b>System Function Loss:</b> Moderate	Very unlikely to occur under normal use	Detection is independent of the user, before any user harm is done, but may be after moderate equipment damage is done
<b>5</b>	<b>User Risk for Injury:</b> Low <b>Repair Needed:</b> Moderate <b>Leads to Other Failure:</b> Potentially <b>System Function Loss:</b> Moderate	Unlikely to occur under normal use	Detection must be done by user, however, clear and obvious for the user to detect if looked for. Ignorance will not cause user harm but may result in moderate equipment damage
<b>6</b>	<b>User Risk for Injury:</b> Low <b>Repair Needed:</b> Moderate <b>Leads to Other Failure:</b> Potentially <b>System Function Loss:</b> Significant	Likely to occur if used incorrectly	Detection is independent of the user, before any user harm is done, but may be after major equipment damage is done
<b>7</b>	<b>User Risk for Injury:</b> Moderate <b>Repair Needed:</b> Moderate <b>Leads to Other Failure:</b> Potentially <b>System Function Loss:</b> Moderate	Very likely to occur if used incorrectly	Detection must be done by user, however, clear and obvious for the user to detect if looked for. Ignorance will not cause user harm but may result in major equipment damage
<b>8</b>	<b>User Risk for Injury:</b> Moderate <b>Repair Needed:</b> Significant <b>Leads to Other Failure:</b> Potentially <b>System Function Loss:</b> Significant	Likely to occur under normal use	Difficult for the user to detect and correct the issue before user harm or major equipment damage is done
<b>9</b>	<b>User Risk for Injury:</b> High <b>Repair Needed:</b> Significant <b>Leads to Other Failure:</b> Potentially <b>System Function Loss:</b> Significant	Very likely to occur under normal use	Very difficult for the user to detect and correct the issue before catastrophic harm or damage is done
<b>10</b>	<b>User Risk for Injury:</b> Extremely High <b>Repair Needed:</b> Significant <b>Leads to Other Failure:</b> Potentially <b>System Function Loss:</b> Significant	Extremely likely to occur under normal use	Impossible for the user to detect and correct the issue before catastrophic harm or damage is done

**\*\* If a safety factor was quantified by analysis for the failure mode, then refer to the other chart for the OCC rating**

**Table 8: Safety factor to OCC scoring chart used to identify the OCC rating by the minimum relevant SF**

Safety Factor	OCC Rating
$SF \leq 1$	10
$1 < SF \leq 1.25$	9
$1.25 < SF \leq 1.5$	8
$1.5 < SF \leq 1.75$	7
$1.75 < SF \leq 2$	6
$2 < SF \leq 2.25$	5
$2.25 < SF \leq 2.5$	4
$2.5 < SF \leq 2.75$	3
$2.75 < SF \leq 3$	2
$3 < SF$	1

This analysis was completed for all BOM components and subassemblies and after all actions were taken, the highest RPN value was 144, indicating a high-confidence design against all failure modes listed in Appendix H.

## CHAPTER 4

### PROJECT FINALIZATION

#### **Results**

To summarize, the BLAC Inc. creeper has been completely redesigned to facilitate manufacturability utilizing the most economical and up to date manufacturing and assembly processes. The completed design was thoroughly analyzed through five distinct engineering analyses. The results can be viewed best by reconciliation of the design requirements.

*Safely raise and lower a person from seated to the supine position and back seated again, requiring only simple user activation.* This requirement was satisfied by the successful completion of FMEA, and motor selection within speed and torque requirements.

*User size requirements: 300 lbf. maximum weight capacity, 6'4" maximum height capacity.* In all analyses where loads and CG locations were applied, only the worst-case scenarios were evaluated, therefore this requirement was satisfied.

*Base product weight less than 60 lbf. (exclusive of the footrest).* The final product weight without the footrest was 88 lbf. This requirement was not satisfied, yet remains an important target to hit in future revisions. The origin of the requirement stems from the weight that Albert is able to curl with one arm. There were two key design changes that contributed to the increase in weight. First, because the user accessing Creep-Up from a wheelchair does so from the front instead of the side, the seat must raise about 5 inches higher. This added length to the steel chassis and most of the kinematic members.

Secondly, the change in material from aluminum to steel resolved many manufacturability concerns that were trade-offs for weight. Despite the miss on this requirement, UPS considers packages under 150 lbf. candidates for traditional shipping methods, without the use of expensive freight [11].

*Work surface in supine position less than 3 inches off the ground.* The top of the padded surface of the backrest, in the supine position, was 3.1 inches from the ground, however, with ½ inch of foam padding, an assumption of ¼ inch foam compression yielded a final surface height of 2.85 inches, thus satisfying the requirement.

*Ability to transition from a wheelchair from the front; seat must rise to greater than 20" off the ground.* The maximum seat height in the final design was 22.5 inches, exceeding the prescribed requirement. Additionally, the footrests have been made to pivot entirely out of the way to ensure close front access.

*Creeper speed or time to transition from one extreme to the other is desired to be less than 20 seconds.* Using a motor with a 1750 RPM maximum speed, common in DC gear motors, the estimated transition time was 19.1 seconds, adequately satisfying this requirement.

*Brake system to prevent chair movement in seated position.* An optional brake system was integrated into the rear leg subassemblies in which the creeper is immobilized while in the seated position. This satisfies the immediate need, however future efforts can be spent in development of a brake that could be applied in any position.

*Removable leg/foot rest with no obstructions to the feet/legs in the absence of the footrest.* As designed, the footrests can be detached from the main creeper by removing 2

screws. When the footrest is not used, there is ample space beneath the feet to allow the use of a person's feet and legs to propel and manipulate the creeper's location. These features satisfy this design requirement.

*Onboard power supply (battery operated).* This requirement was fulfilled when evaluation of torques and speeds required in the system could easily be satisfied by using an 18V DC drill motor. This common brushed DC gear motor is readily available.

*Cover all pinch hazards internal to the user contact area.* As seen in Figure 10, the region with which the user is in normal contact, was finished with several shrouds that tightly nest, protecting the user from the pinch hazards induced by the kinematic mechanisms.

*Generate smooth constant velocities with variable motor speed.* Indicated in Figure 21, the kinematic analysis was completed using constant angular and linear velocities as inputs, and computing the linear speed of the drive screw as the output. This allows for known electronic control parameters for motor speed to generate the desired user experience.

## **Conclusion**

The Creep-Up design project was a continuation of the BLAC Inc. prototype in which a complete redesign was successfully completed to address the issues discovered in the Design Validation Testing phase. All functionality, reliability, and safety concerns were addressed including crucial improvements to the kinematic mechanisms, ultimately providing a design solution that allows two independent motions with a single motor.

Kinematic analysis provided complete position and velocity output for the useful range of the system, and static force analysis output all structural component forces for each position under conservative loading conditions. Theoretical and finite element methods validated design structural integrity, while a thorough failure modes and effects analysis provided high confidence in overall system performance and user experience. These analyses combine to promote user and system safety, and to prevent major, expensive design changes after prototyping.

Attention given to the manufacturability of individual components and assemblies, yielded a design solution not only functional but also ready to prototype, perform design validation testing, and produce. The final design solution employs the use of modern standardized manufacturing and assembly processes, at the same time showing off aesthetics for a marketable premium creeper solution.

All engineering objectives were satisfied, and the most critical design requirements were fulfilled, while leaving room for improvement of the overall product weight.

It may seem that the need for this technology is limited to only those in a wheelchair, in need of full assistance. However, due to the high population of the aging generation of baby-boomers, there exists a market of many technicians, mechanics, and hobbyists, that may have a need for partial assistance. Even younger, able-bodied techs may find this technology useful in working in low-clearance areas that would otherwise be strenuous positions. Amidst all these application possibilities, perhaps the most



significant is the potential for improving the quality of life of individuals in the work place.

### **Future Work**

Several areas of improvement remain, upon which future work may be based. To begin, the only design requirement in this project that was not adequately satisfied was the product weight. Weight reducing design and material modifications should be considered in future work. Additionally, while the brake system designed fulfilled the original design intent, it has been noted that a separate, manual brake system that is independent of the backrest position or seat height is desirable.

The motor selected to fulfill the needs of this design was ultimately from a lithium ion 18V Makita drill motor. This was the most economical option for a motor which included the motor and gearbox, batteries, and a charger. Despite the functionality, stripping down off-the-shelf drills for the assembly is wasteful and impractical. A different motor selection and battery design, or establishment of partnerships with original equipment manufacturers (OEM) to minimize motor and battery cost would be of notable significance.

Because the scope of this project was purely mechanical, with the exception of the motor and limit switch placement, an electrical design needs to be done. Following electrical design, the next step in the development cycle involves a refined tolerance analysis of all critical fits and functions, so that mechanical drawings can be done with appropriate reference data and critical dimensions and tolerances. These mechanical drawing will then be used for prototyping the Creep-Up design. Following prototyping,

design validation testing, should be done to verify accomplishment of original design intent and safe operation.

Lastly, when the design has been adequately tested and deemed safe and reliable for consumer use, the product will need to be introduced to the world of assistive technologies. Marketing and commercialization activities will be necessary to take the product to the broad spectrum of potential buyers.

## REFERENCES

- [1] “Body Segment Data,” Exercise Prescription, last accessed July 24, 2016, <http://www.exrx.net/Kinesiology/Segments.html>.
- [2] “Capstone Design I: Failure Modes & Effects Analysis (FMEA)” (Lecture 13 of Capstone Design Class, Utah State University, November 5, 2013).
- [3] Richard G. Budynas and J. Keith Nisbett, *Shigley's Mechanical Engineering Design, Eighth Edition* (New York, NY: McGraw Hill, 2008).
- [4] Heckman, Joseph H. “Mechanic’s Creeper” Accessed April 15, 2014, [www.uspto.gov](http://www.uspto.gov). United States Patent and Trademark Office (US002148199, February 21, 1939).
- [5] History.com Staff, “Baby Boomers,” History.com, A+E Networks (2010), accessed April 26, 2014, [www.history.com/topics/baby-boomers](http://www.history.com/topics/baby-boomers).
- [6] Jacob Ward, “Bodies In Motion: Exploring The Human Limits of Future Travel,” Popular Science, May 15, 2011, accessed May 21, 2016, <http://www.popsci.com/science/article/2011-04/future-travel>.
- [7] Joe D. Hoffman, *Numerical Methods for Engineers and Scientists, 2nd Edition* (New York, NY: Marcel Dekker, 2001).
- [8] Nick Clifford, L.J. Wilde, Stewart Goble, and Andy Shupe, “Wheelchair Creeper” (Capstone Design Class, Utah State University, 2011).
- [9] Robert L. Norton, *Design of Machinery, 5th Edition* (New York, NY: McGraw-Hill, 2012).
- [10] “Statistical Abstract of the United States: 2011,” Last accessed July 30, 2016, [www2.census.gov](http://www2.census.gov). (U.S. Census Bureau Tables 205 and 206).
- [11] “What are the weight and size limits for shipping using UPS?,” United Parcel Service, accessed May 30, 2016, <https://www.ups.com/content/us/en/resources/sri/size2.html>.

## APPENDICES

Appendix A. Reference Figures

# ORIENTATION VIEWS

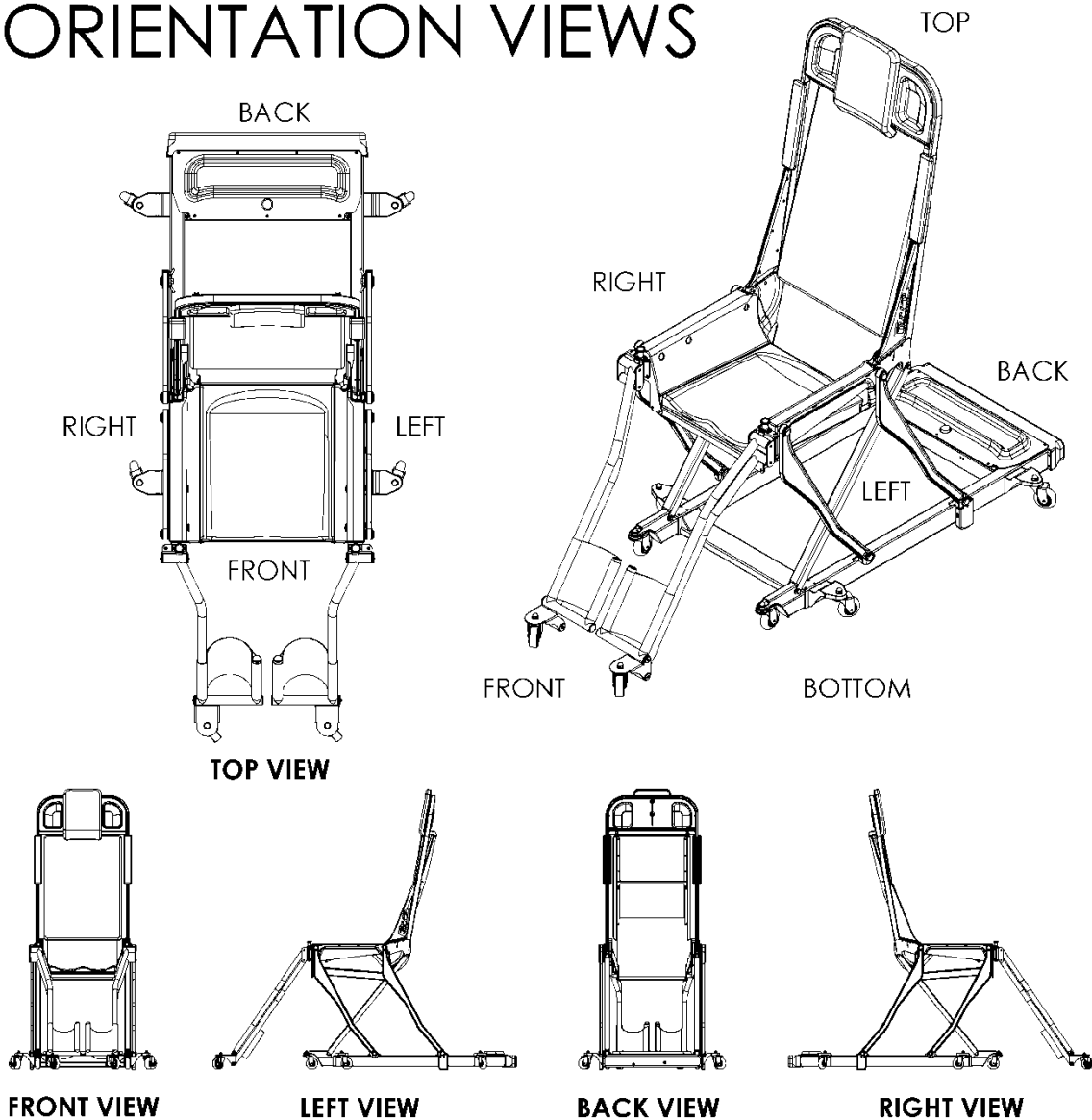
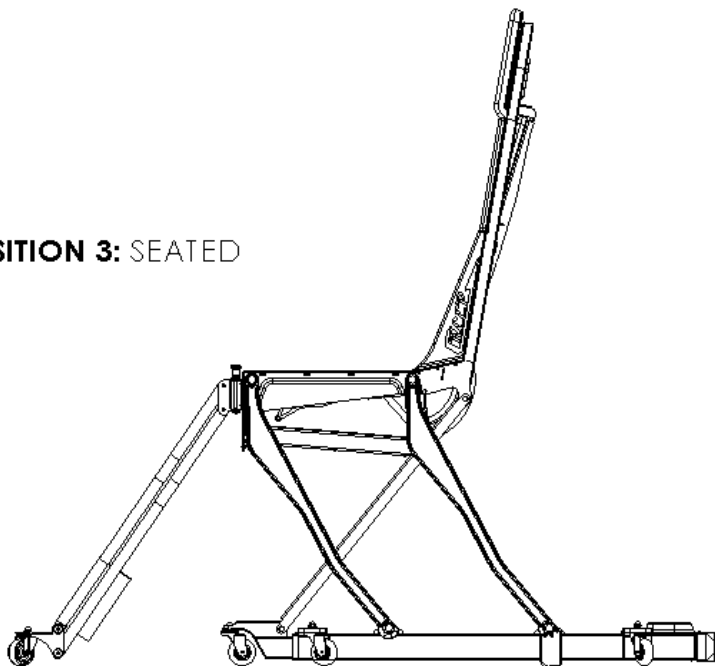
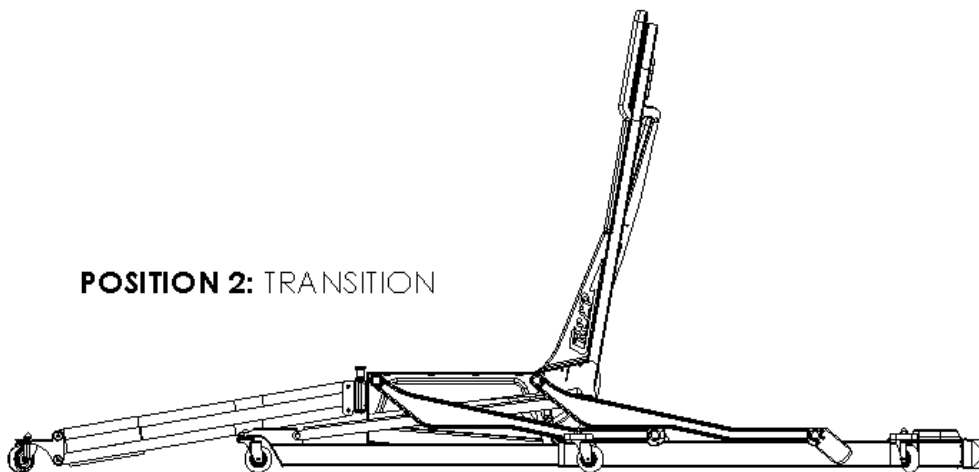
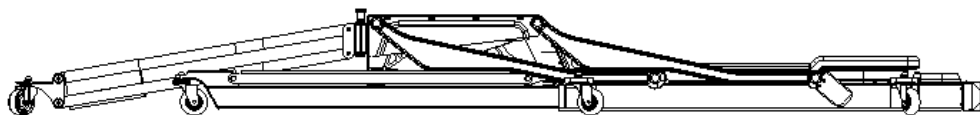
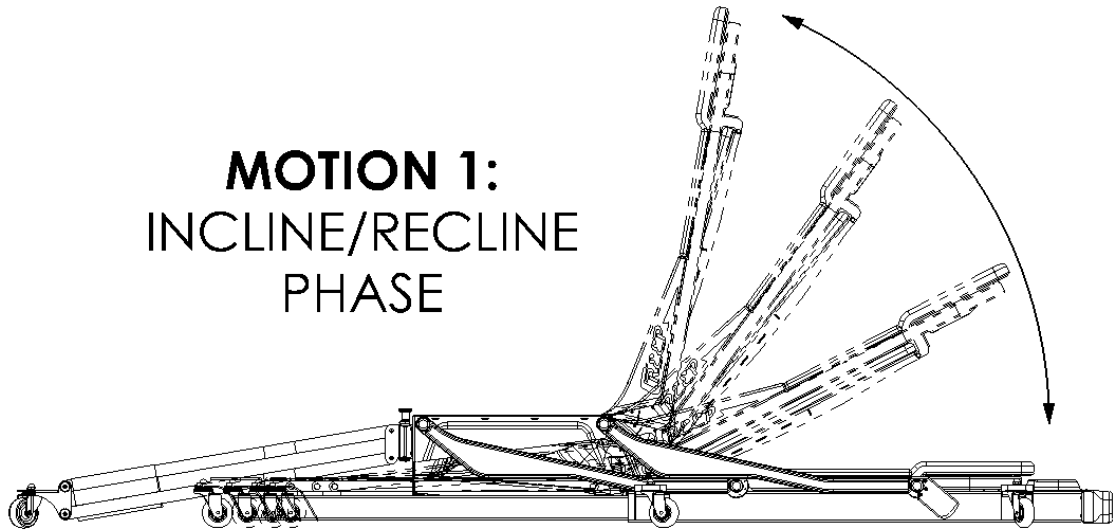


Figure 23: Creep-Up definition of sides/orientations

**POSITION 3: SEATED****POSITION 2: TRANSITION****POSITION 1: SUPINE****Figure 24: Creep-Up definition of seated, supine, and transition positions**

**MOTION 1:  
INCLINE/RECLINE  
PHASE**



**Figure 25: Creep-Up motion 1 definition: graphical portrayal of the incline/recline motion**

**MOTION 2:  
RAISE/LOWER  
PHASE**

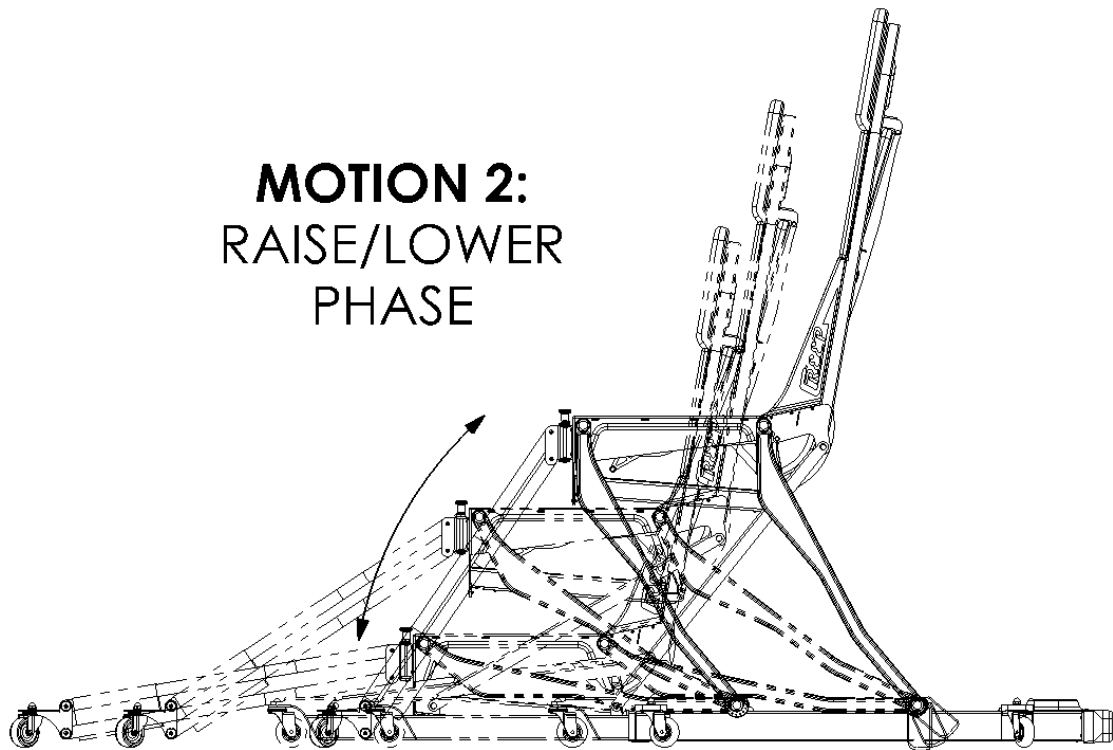


**Figure 26: Creep-Up motion 2 definition: graphical portrayal of the raise/lower motion**

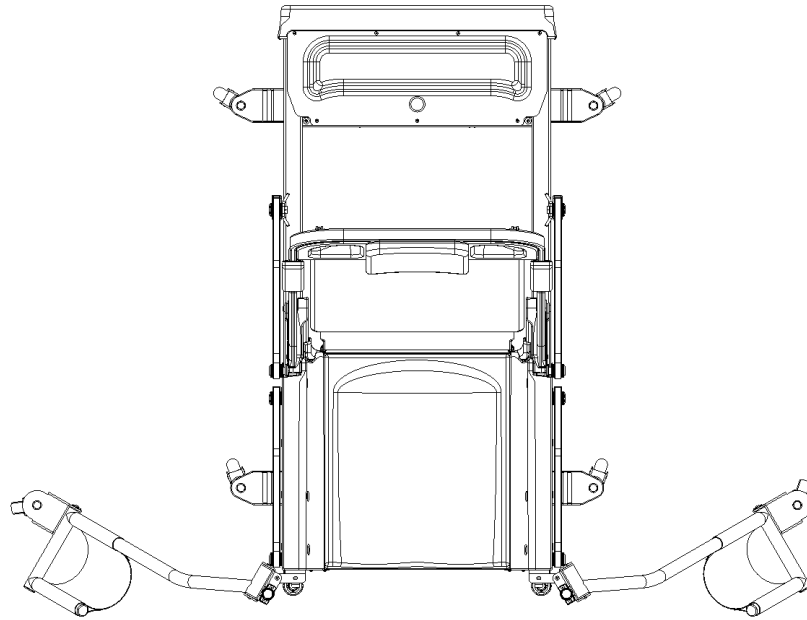


**Figure 27: Top-down view of Creep-Up with footrests unclashed and swung out to each side, representing the wheelchair accessibility**

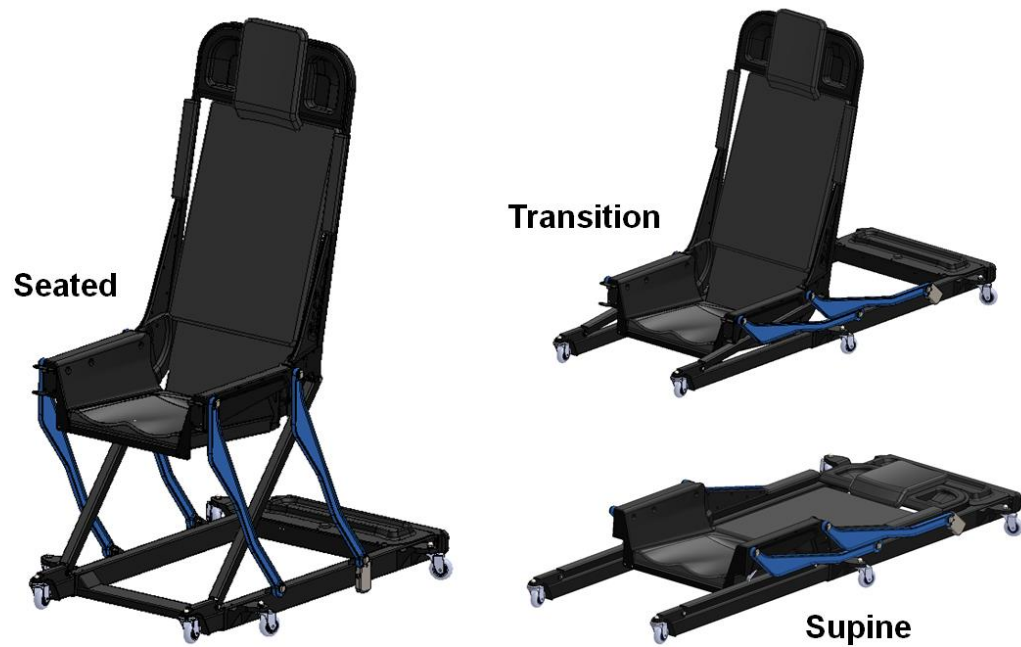


**Figure 28: Final Creep-Up design solution shown in three fundamental positions, without footrests**



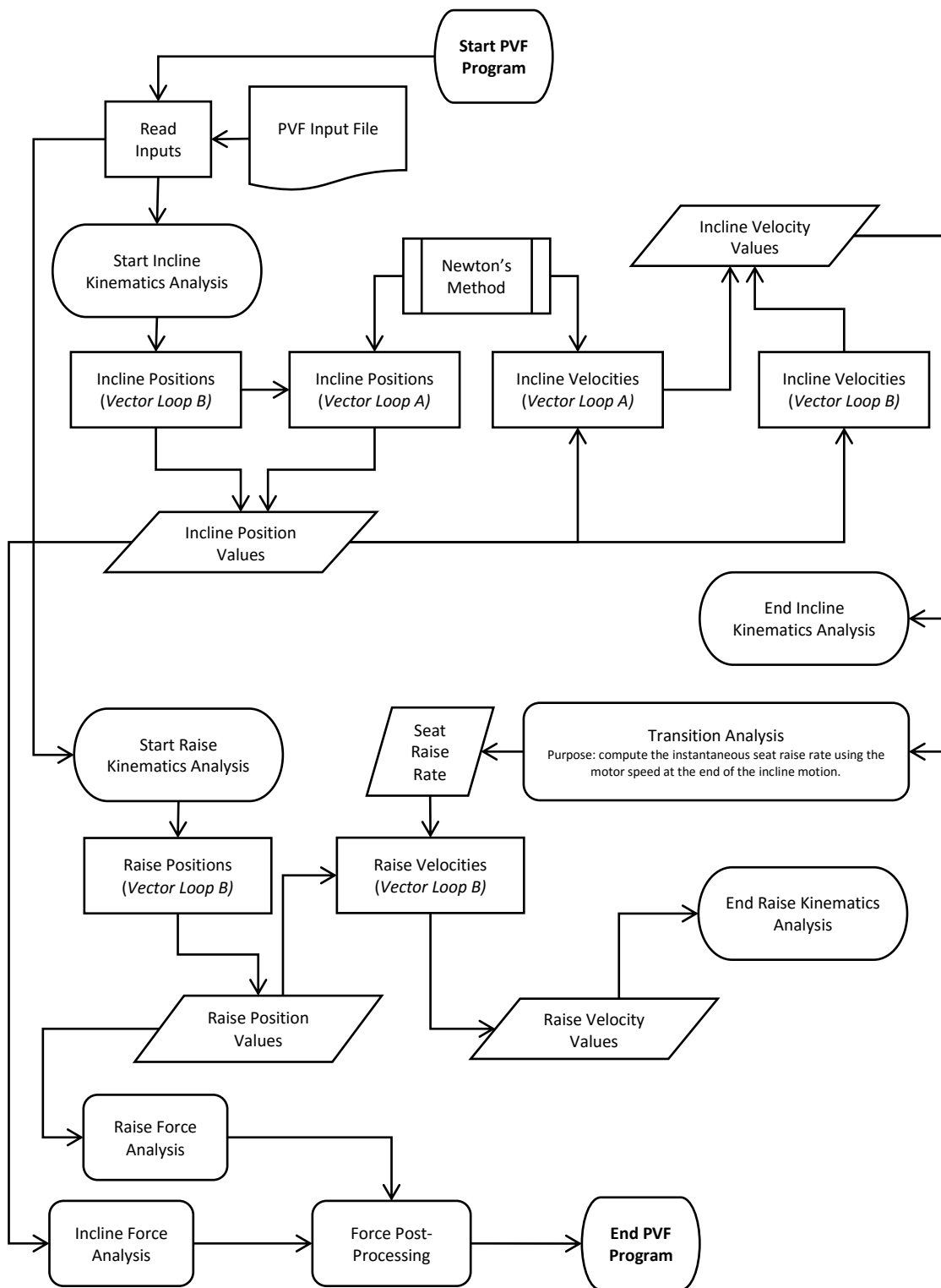


Figure 29: PVF Matlab® program flowchart

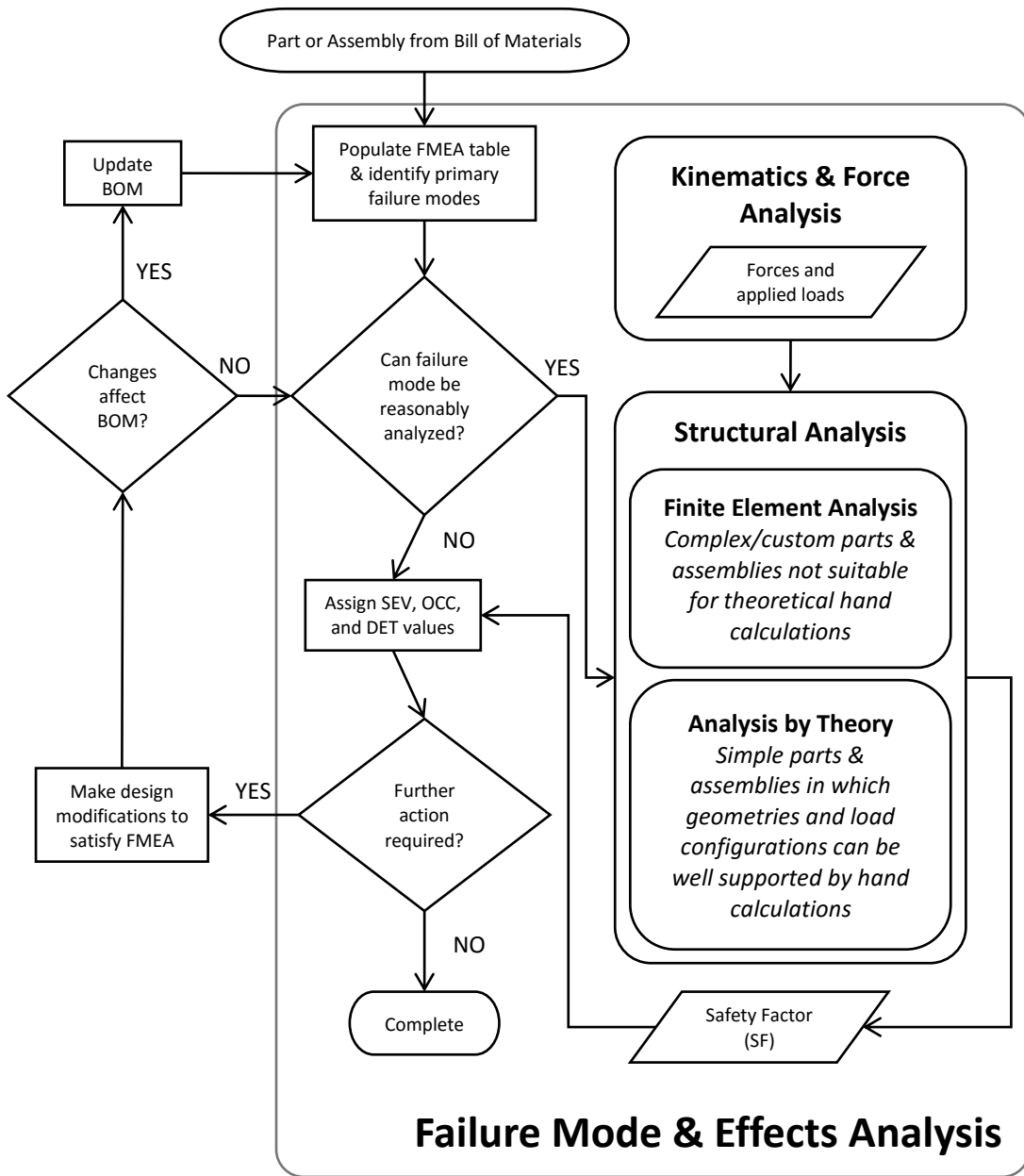


Figure 30: General FMEA flowchart

## Appendix B. Kinematics Equations

Vector Loop A Position Analysis

By applying equation (3) to Figure 18, the following equation is deduced:

$$\vec{R}_4 - \vec{R}_5 + \vec{R}_8 - \vec{R}_{BOL} + \vec{R}_7 - \vec{R}_{41} = 0$$

By applying equation (4) to the above, equation (5) results. Then by applying equation (6), and separating real and imaginary parts, equation (7) and (8) are derived.

Since the two unknowns cannot be solved for algebraically using these two equations,

Newton's method is applied to (7) and (8) in the following way:

$$\begin{aligned} f(L_{BOL_0}, \theta_{78_0}) &= L_4 \cos(\theta_4) - L_5 \cos(\theta_5) + (L_8 - L_{BOL} + L_7) \cos(\theta_{78}) \\ &\quad - L_{41} \cos(\theta_4 + \delta_{41}) \end{aligned}$$

$$\begin{aligned} g(L_{BOL_0}, \theta_{78_0}) &= L_4 \sin(\theta_4) - L_5 \sin(\theta_5) + (L_8 - L_{BOL} + L_7) \sin(\theta_{78}) \\ &\quad - L_{41} \sin(\theta_4 + \delta_{41}) \end{aligned}$$

where initial values used are

$$L_{BOL_0} = 6 \text{ inches}$$

$$\theta_{78_0} = 45^\circ$$

Partial derivative terms for Newton's Method for these are:

$$f_{L_{BOL}} = -\cos \theta_{78}$$

$$g_{L_{BOL}} = -\sin \theta_{78}$$

$$f_{\theta_{78}} = (L_{BOL} - L_7 - L_8) \sin \theta_{78}$$

$$g_{\theta_{78}} = (-L_{BOL} + L_7 + L_8) \cos \theta_{78}$$

Applying Hoffman's Equations 3.176 A and B

$$f_{L_{BOL}}(L_{BOL_0}, \theta_{78_0})\Delta L_{BOL} + f_{\theta_{78}}(L_{BOL_0}, \theta_{78_0})\Delta\theta_{78} = -f(L_{BOL_0}, \theta_{78_0})$$

$$g_{L_{BOL}}(L_{BOL_0}, \theta_{78_0})\Delta L_{BOL} + g_{\theta_{78}}(L_{BOL_0}, \theta_{78_0})\Delta\theta_{78} = -g(L_{BOL_0}, \theta_{78_0})$$

and solving the linear system

$$\begin{bmatrix} f_{L_{BOL}} & f_{\theta_{78}} \\ g_{L_{BOL}} & g_{\theta_{78}} \end{bmatrix} \begin{Bmatrix} \Delta L_{BOL} \\ \Delta\theta_{78} \end{Bmatrix} = \begin{Bmatrix} -f(L_{BOL_0}, \theta_{78_0}) \\ -g(L_{BOL_0}, \theta_{78_0}) \end{Bmatrix}$$

for the delta values, and applying them to the following gives new guess values.

$$L_{BOL_1} = L_{BOL_0} + \Delta L_{BOL}$$

$$\theta_{78_1} = \theta_{78_0} + \Delta\theta_{78}$$

Apply these new values to the system again and repeat the computations until both of the

following criteria are met

$$\Delta L_{BOL} \leq 10^{-6}$$

$$\Delta\theta_{78} \leq 10^{-6}$$

### Vector Loop A Velocity Analysis

Compute the time derivative of equation (5)

$$\frac{d}{dt} [L_4 e^{j\theta_4} - L_5 e^{j\theta_5} + L_8 e^{j\theta_{78}} - L_{BOL} e^{j\theta_{78}} + L_7 e^{j\theta_{78}} - L_{41} e^{j(\theta_4 + \delta_{41})}] = 0$$

which yields equation (12). By again applying equation (6) and separating real and imaginary parts, this yields equations (14) and (15). By again applying Newton's method, these are used in the following way

$$\begin{aligned} f(\dot{L}_{BOL_0}, \dot{\theta}_{78_0}) &= L_4 \omega_4 \cos(\theta_4) + (L_7 + L_8 - L_{BOL}) \omega_{78} \cos(\theta_{78}) - \dot{L}_{BOL} \sin(\theta_{78}) \\ &\quad - L_{41} \omega_4 \cos(\theta_4 + \delta_{41}) \\ g(\dot{L}_{BOL_0}, \dot{\theta}_{78_0}) &= -L_4 \omega_4 \sin(\theta_4) - (L_7 + L_8 - L_{BOL}) \omega_{78} \sin(\theta_{78}) \\ &\quad - \dot{L}_{BOL} \cos(\theta_{78}) + L_{41} \omega_4 \sin(\theta_4 + \delta_{41}) \end{aligned}$$

Partial derivative terms for Newton's Method for these are:

$$f_{L_{BOL}} = -\sin(\theta_{78})$$

$$g_{L_{BOL}} = -\cos(\theta_{78})$$

$$f_{\omega_{78}} = (L_7 + L_8 - L_{BOL}) \cos(\theta_{78})$$

$$g_{\omega_{78}} = (L_{BOL} - L_7 + L_8) \sin(\theta_{78})$$

These are used in the same way as the position analysis to solve for the two unknown velocities.

### Vector Loop B Position Analysis

By applying equation (3) to Figure 19, the following equation is deduced:

$$\vec{R}_{11} + \vec{R}_{12} - \vec{R}_4 - \vec{R}_3 - \vec{R}_6 + \vec{R}_{2b} = 0$$

By applying equation (4) to the above, equation (9) results. Then by applying equation (6), and separating real and imaginary parts, equation (10) and (11) are derived.

The two unknowns can be solved for algebraically using the following two equations:

$$\theta_3 = \sin^{-1} \left( \frac{L_{12} \sin \theta_{12} - L_4 \sin \theta_4 - L_6 \sin \theta_6 + L_{23} \sin \theta_{23}}{L_3} \right)$$

$$L_{11} = -L_{12} \cos \theta_{12} + L_4 \cos \theta_4 + L_3 \cos \theta_3 + L_6 \cos \theta_6 - L_{23} \cos \theta_{23}$$

### Vector Loop B Velocity Analysis

Compute the time derivative of equation (9)

$$\frac{d}{dt} [L_{11}e^{j\theta_{11}} + L_{12}e^{j\theta_{12}} - L_4e^{j\theta_4} - L_3e^{j\theta_3} - L_6e^{j\theta_6} + L_{2b}e^{j\theta_{2b}}] = 0$$

which yields equation (13). Applying equation (6) again produces the following:

$$\begin{aligned} \dot{L}_{11} - L_4\omega_4(j \cos \theta_4 - \sin \theta_4) - L_3\omega_3(j \cos \theta_3 - \sin \theta_3) + L_{2b}\omega_{2b}(j \cos \theta_{2b} - \sin \theta_{2b}) \\ = 0 \end{aligned}$$

Separation of real and imaginary parts yields

$$-L_4\omega_4 \cos(\theta_4) - L_3\omega_3 \cos(\theta_3) + L_{2b}\omega_{2b} \cos(\theta_{2b}) = 0$$

$$\dot{L}_{11} + L_4\omega_4 \sin \theta_4 + L_3\omega_3 \sin \theta_3 - L_{2b}\omega_{2b} \sin \theta_{2b} = 0$$

Applying known values to the above two equations, the incline velocities are solved for algebraically as

$$\omega_3 = \frac{L_{2b}\omega_{2b} \cos(\theta_{2b}) - L_4\omega_4 \cos(\theta_4)}{L_3 \cos(\theta_3)}$$

$$\dot{L}_{11} = L_{2b}\omega_{2b} \sin(\theta_{2b}) - L_3\omega_3 \sin(\theta_3) - L_4\omega_4 \sin(\theta_4)$$

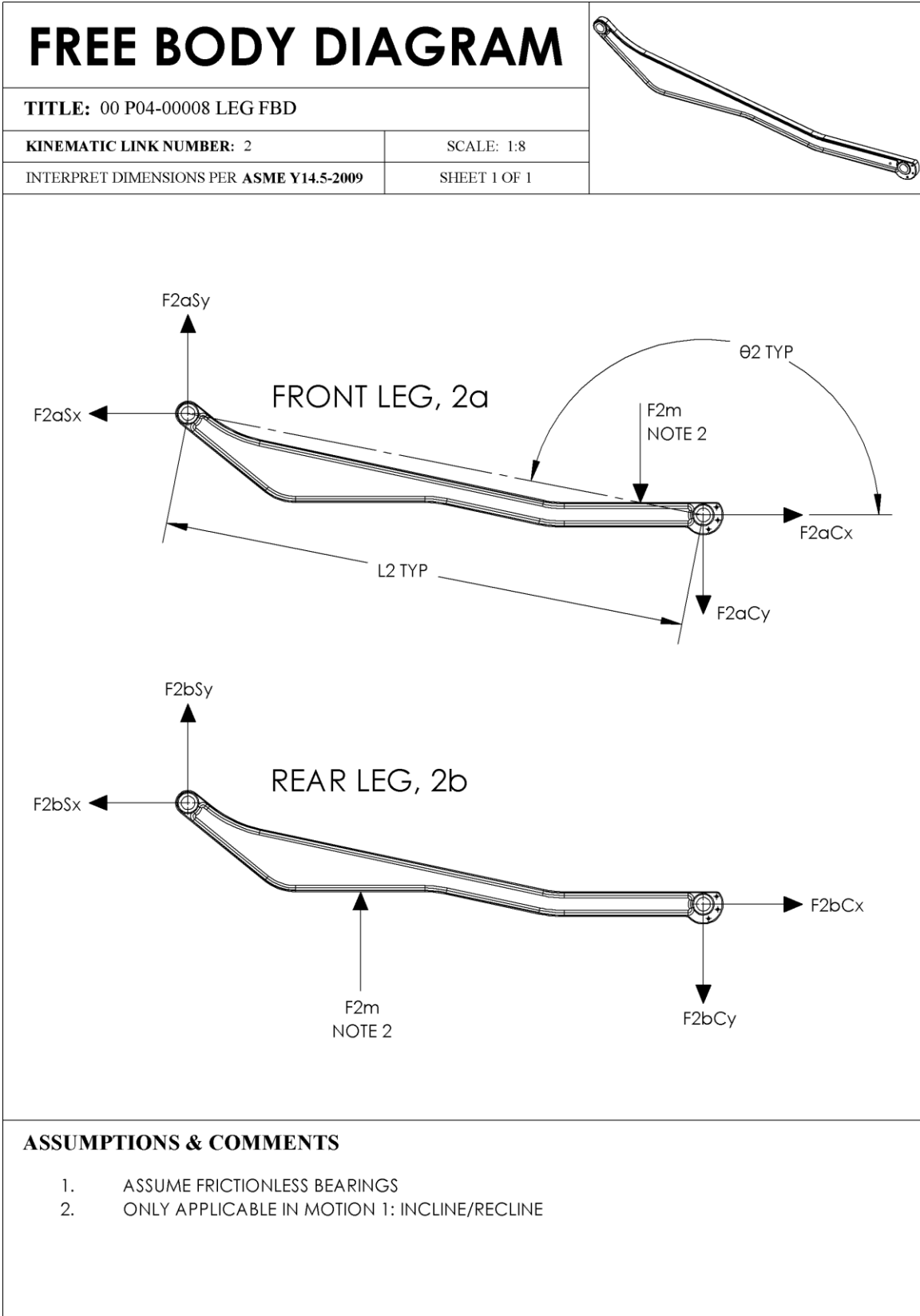
## Appendix C. Free Body Diagrams

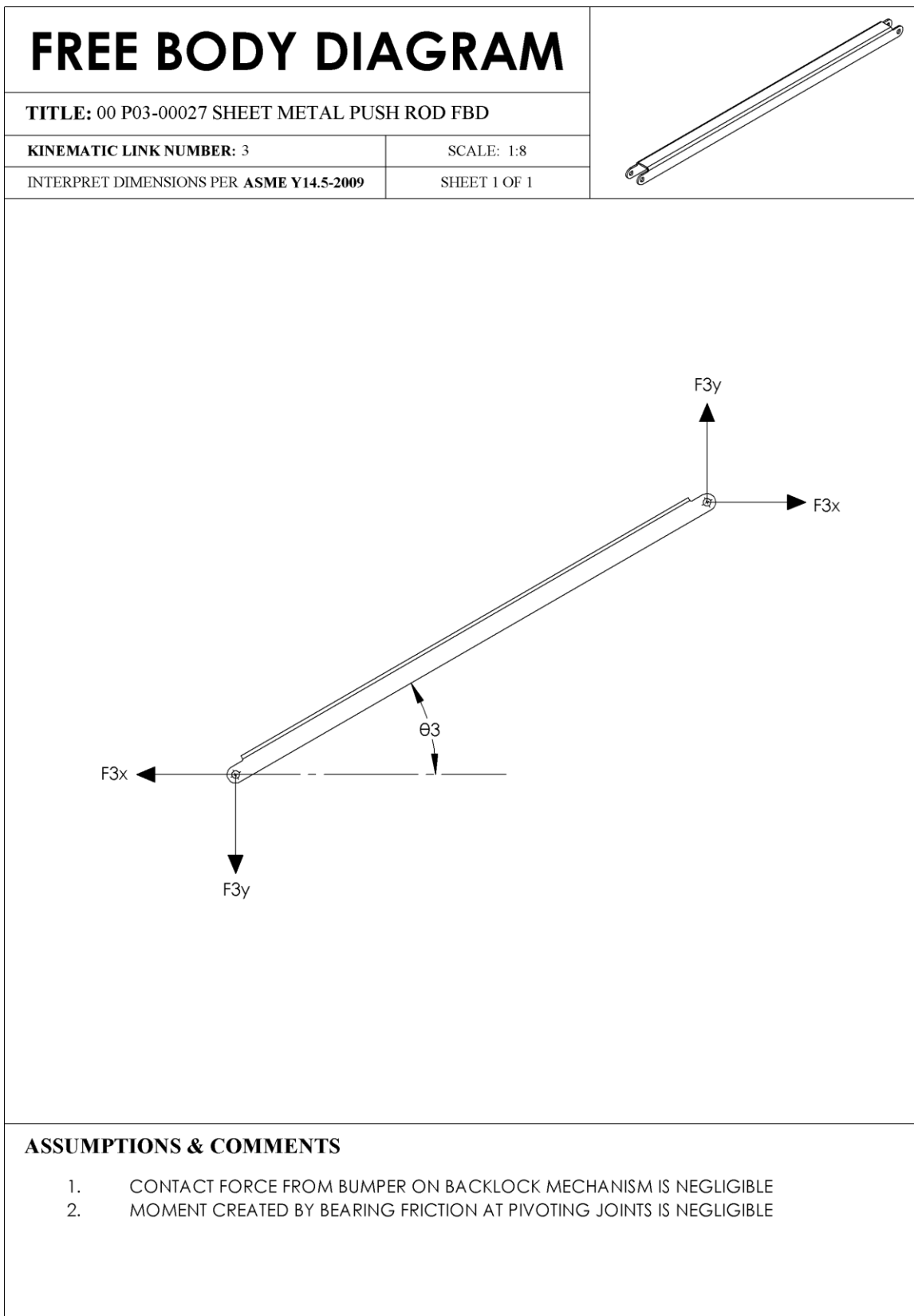
All static force analyses and sign convention are in accordance with the free body diagrams contained herein. The diagrams are shown below, ordered by link number in the kinematics analysis. Each title block contains the part number and description, link number, FBD scale and the number of sheets associated with that FBD. The following is a list of all FBDs:

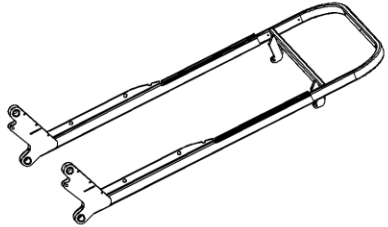
<u>Link</u>	<u>Title</u>
1	00 A02-00008 Chassis Welded Subassembly FBD
2	00 P04-00008 Leg FBD
3	00 P03-00027 Sheet Metal Push Rod FBD
4	00 A02-00016 Welded Backrest Frame FBD
5	00 P03-00025 Middle Seat Brace FBD
5	00 P03-00026 Rear Seat Hanger FBD
5	00 P05-00004 Upholstered Seat Subassembly FBD
6	00 A02-00015 Slider Welded Subassembly FBD
7	00 A01-00011 Back Rest Subassembly FBD
8	00 A01-00003 Bridge Subassembly FBD
9	00 P02-00006 Back Tension Bar FBD
NA	00 P03-00004 Back Slider Bracket FBD

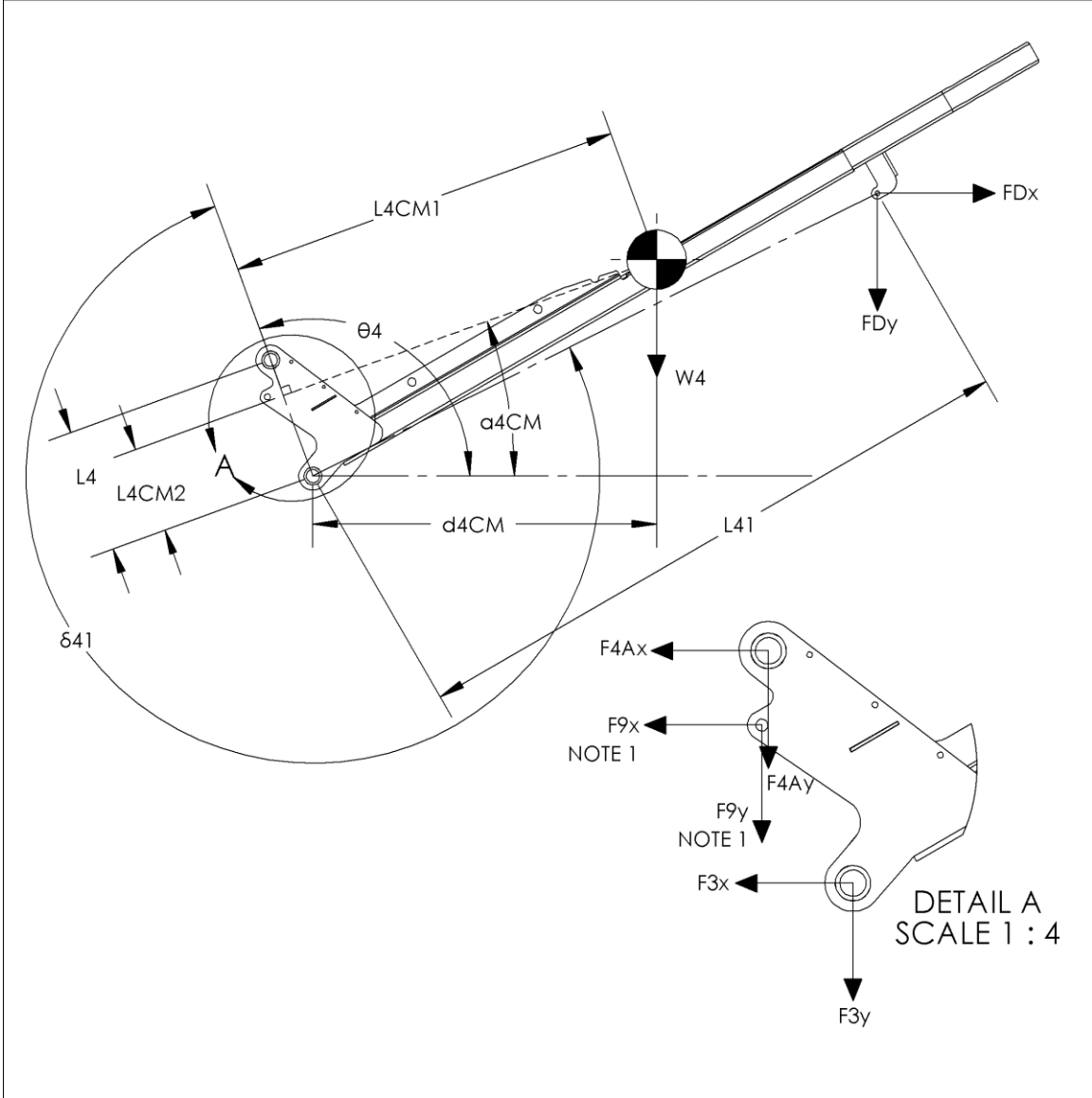






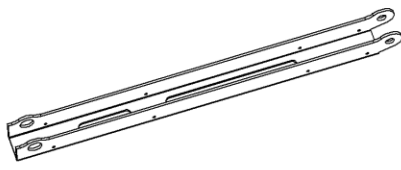


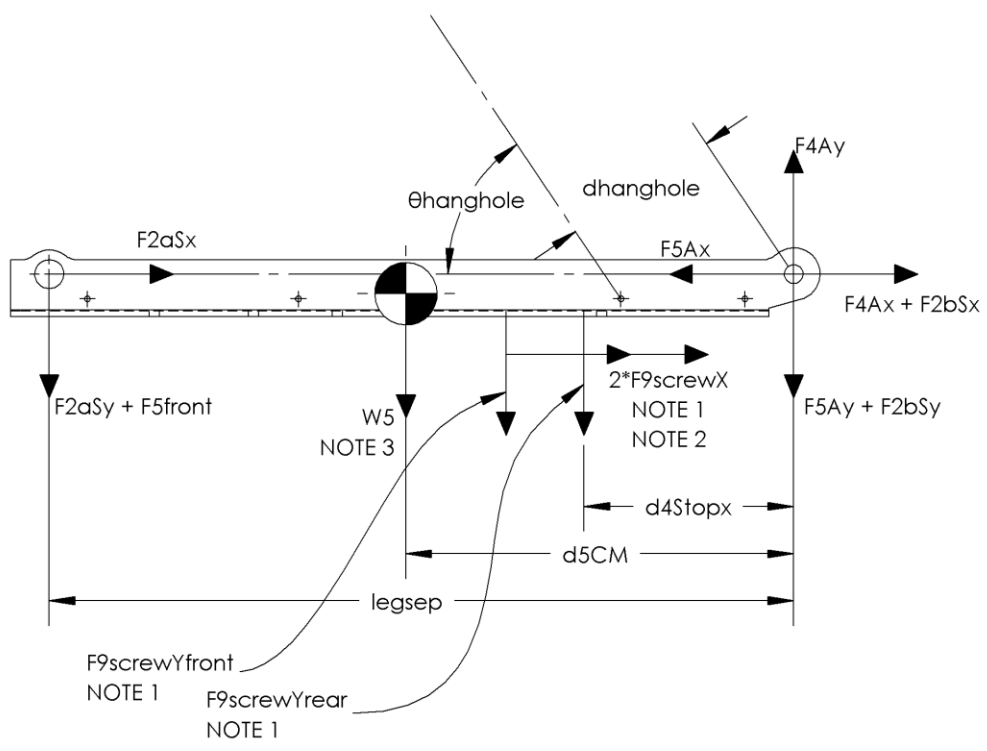
<h1>FREE BODY DIAGRAM</h1>		
<b>TITLE:</b> 00 A02-00016 WELDED BACKREST FRAME FBD		
<b>KINEMATIC LINK NUMBER:</b> 4	SCALE: 1:8	
INTERPRET DIMENSIONS PER <b>ASME Y14.5-2009</b>	SHEET 1 OF 1	



**ASSUMPTIONS & COMMENTS**

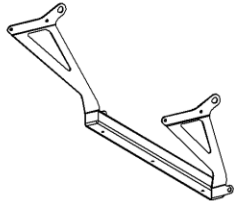
1. THESE FORCES ONLY APPLY TO MOTION 2: RAISE/LOWER CONFIG.
2. ASSUME FRICTIONLESS PIVOTS

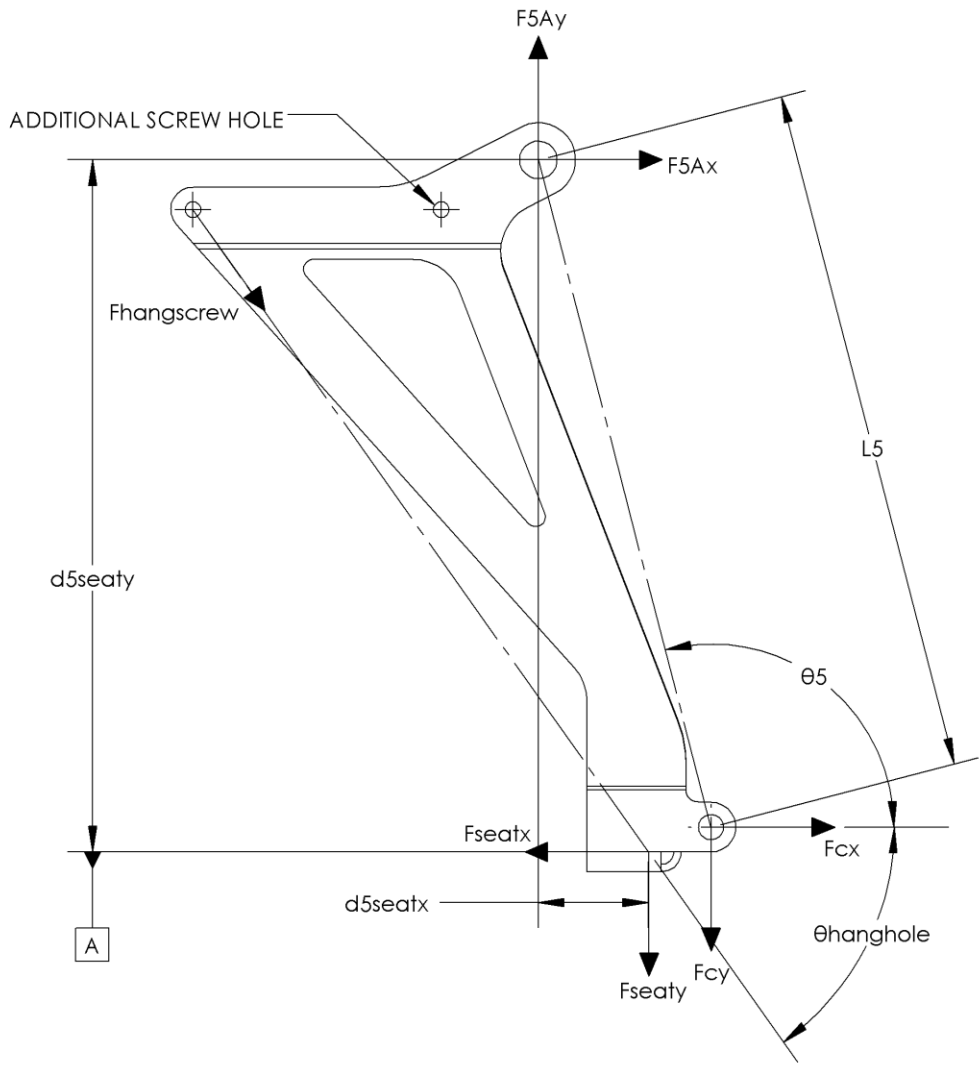
<h1>FREE BODY DIAGRAM</h1>		
<b>TITLE:</b> 00 P03-00025 MIDDLE SEAT BRACE FBD		
<b>KINEMATIC LINK NUMBER:</b> 5	SCALE: 1:4	
INTERPRET DIMENSIONS PER <b>ASME Y14.5-2009</b>	SHEET 1 OF 1	



**ASSUMPTIONS & COMMENTS**

1. THESE FORCES ONLY APPLY TO MOTION 2: RAISE/LOWER CONFIGURATION
2. ASSUME THE 2 SCREWS SHARE THE SHEAR LOAD EVENLY
3. CG AND W5 ARE FOR ENTIRE SEAT ASSEMBLY AND NOT JUST THIS COMPONENT

<h1>FREE BODY DIAGRAM</h1>		
<b>TITLE:</b> 00 P03-00026 REAR SEAT HANGER FBD		
<b>KINEMATIC LINK NUMBER:</b> 5	SCALE: 1:2	
INTERPRET DIMENSIONS PER <b>ASME Y14.5-2009</b>	SHEET 1 OF 1	



**ASSUMPTIONS & COMMENTS**

1. ADDITIONAL SCREW HOLE IS NOT LOAD BEARING, REDUNDANCY ONLY
2. SEAT CONTACTS SURFACE AS A EVENLY DISTRIBUTED ON A
3. USER SITTING SUCH THAT EACH SIDE TAKES EQUAL LOAD

# FREE BODY DIAGRAM

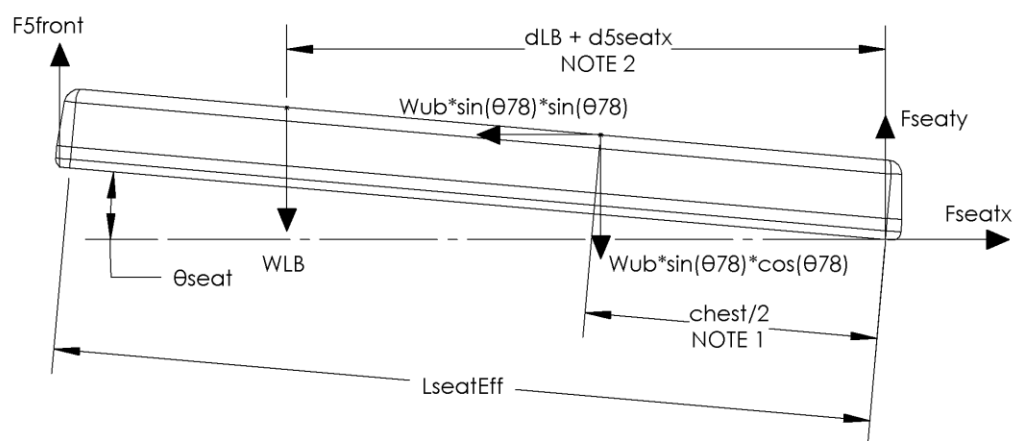
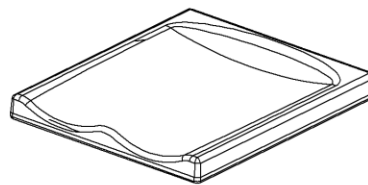
**TITLE:** 00 P05-00004 UPHOLSTERED SEAT SUBASSEMBLY FBD

**KINEMATIC LINK NUMBER:** 5

SCALE: 1:4

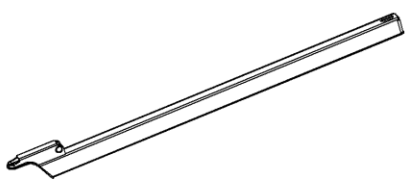
INTERPRET DIMENSIONS PER **ASME Y14.5-2009**

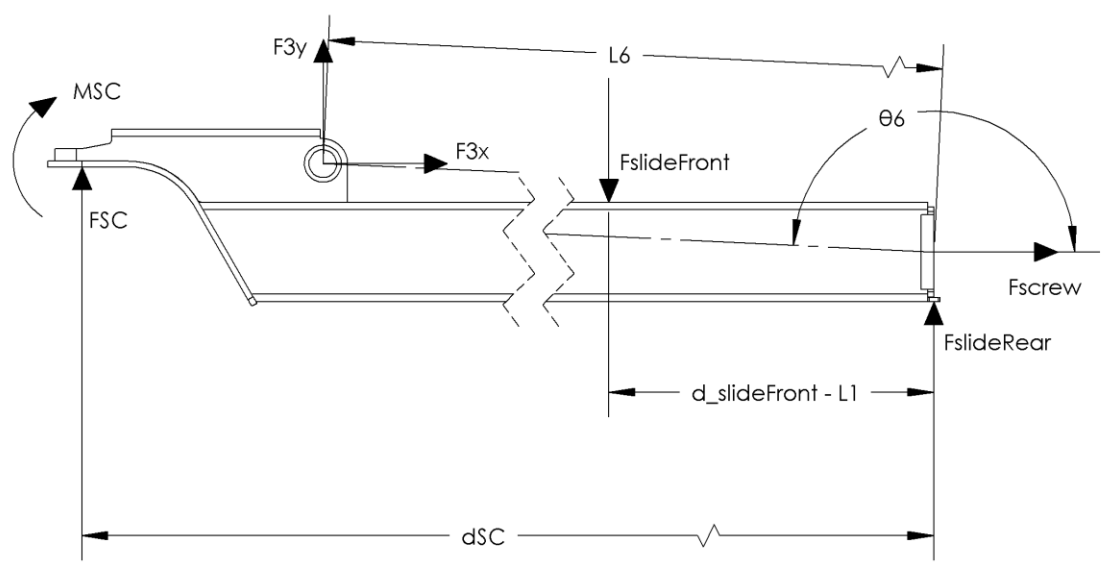
SHEET 1 OF 1



## ASSUMPTIONS & COMMENTS

1. ASSUME THAT THE ACTION PATH OF THE UPPER BODY FORCE IS HALF THE USER CHEST THICKNESS
2. IF THIS LENGTH GOES BEYOND THE LEFT END OF THE SEAT (AS SHOWN IN THIS DIAGRAM), THEN SET THIS LENGTH VALUE TO  $L_{seatEff} * \cos(\theta_{seat})$

<h1>FREE BODY DIAGRAM</h1>		
<b>TITLE:</b> 00 A02-00015 SLIDER WELDED SUBASSEMBLY FBD		
<b>KINEMATIC LINK NUMBER:</b> 6	SCALE: 1:4	
INTERPRET DIMENSIONS PER <b>ASME Y14.5-2009</b>	SHEET 1 OF 1	



**ASSUMPTIONS & COMMENTS**

1. ASSUME FRICTIONLESS SLIDING AND ROTATION OF INTERFACING MEMBERS



# FREE BODY DIAGRAM

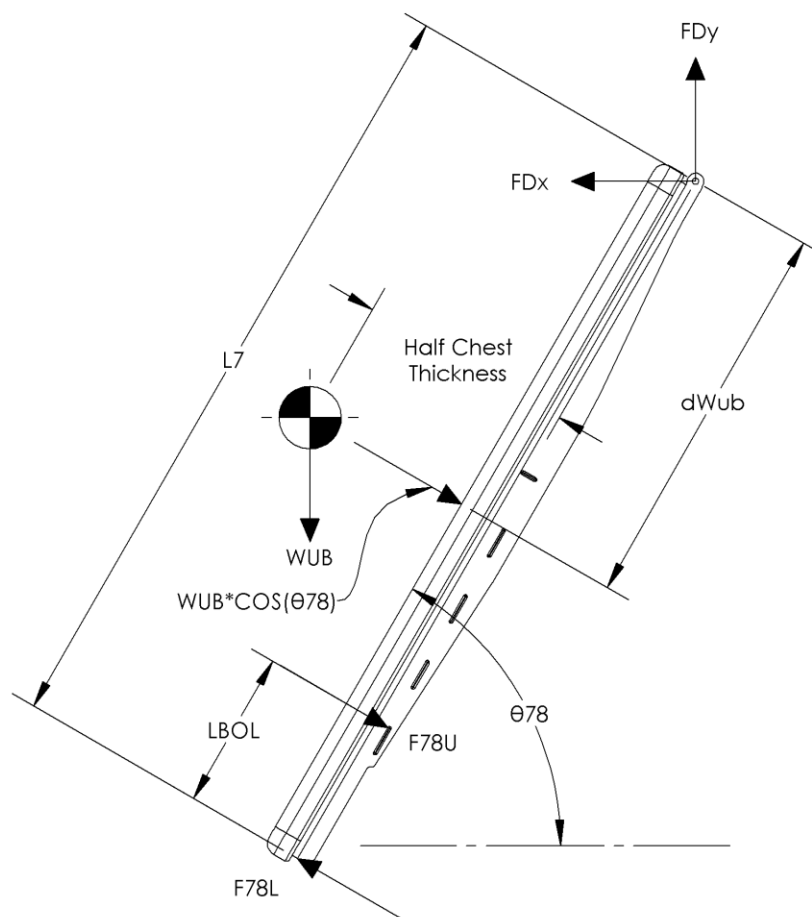
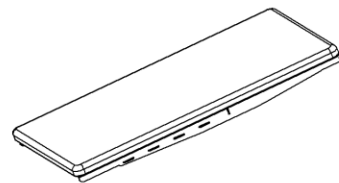
**TITLE:** 00 A01-00011 BACK REST SUBASSEMBLY FBD

**KINEMATIC LINK NUMBER:** 7

SCALE: 1:6

INTERPRET DIMENSIONS PER ASME Y14.5-2009

SHEET 1 OF 1



## ASSUMPTIONS & COMMENTS

1. ASSUME FRICTIONLESS SLIDER AND PIVOT JOINTS
2. ASSUME CG OF USER UPPER BODY IS LOCATED HALF OF THE USER CHEST THICKNESS WHICH IS ASSUMED TO BE 12"
3. ASSUME BROAD SURFACE CONTACT OF THE USER'S BACK, WHERE THE APPLIED FORCE SHOWN REPRESENTS THE DISTRIBUTED LOAD

# FREE BODY DIAGRAM

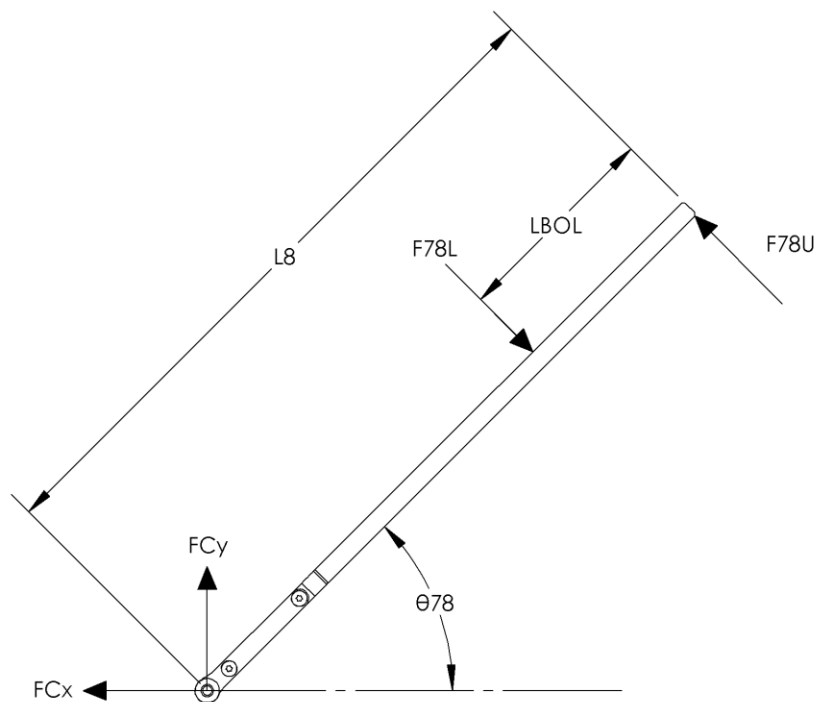
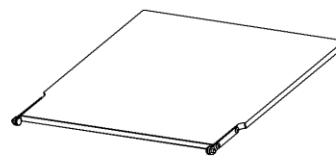
**TITLE:** 00 A01-00003 BRIDGE SUBASSEMBLY FBD

**KINEMATIC LINK NUMBER:** 8

SCALE: 1:4

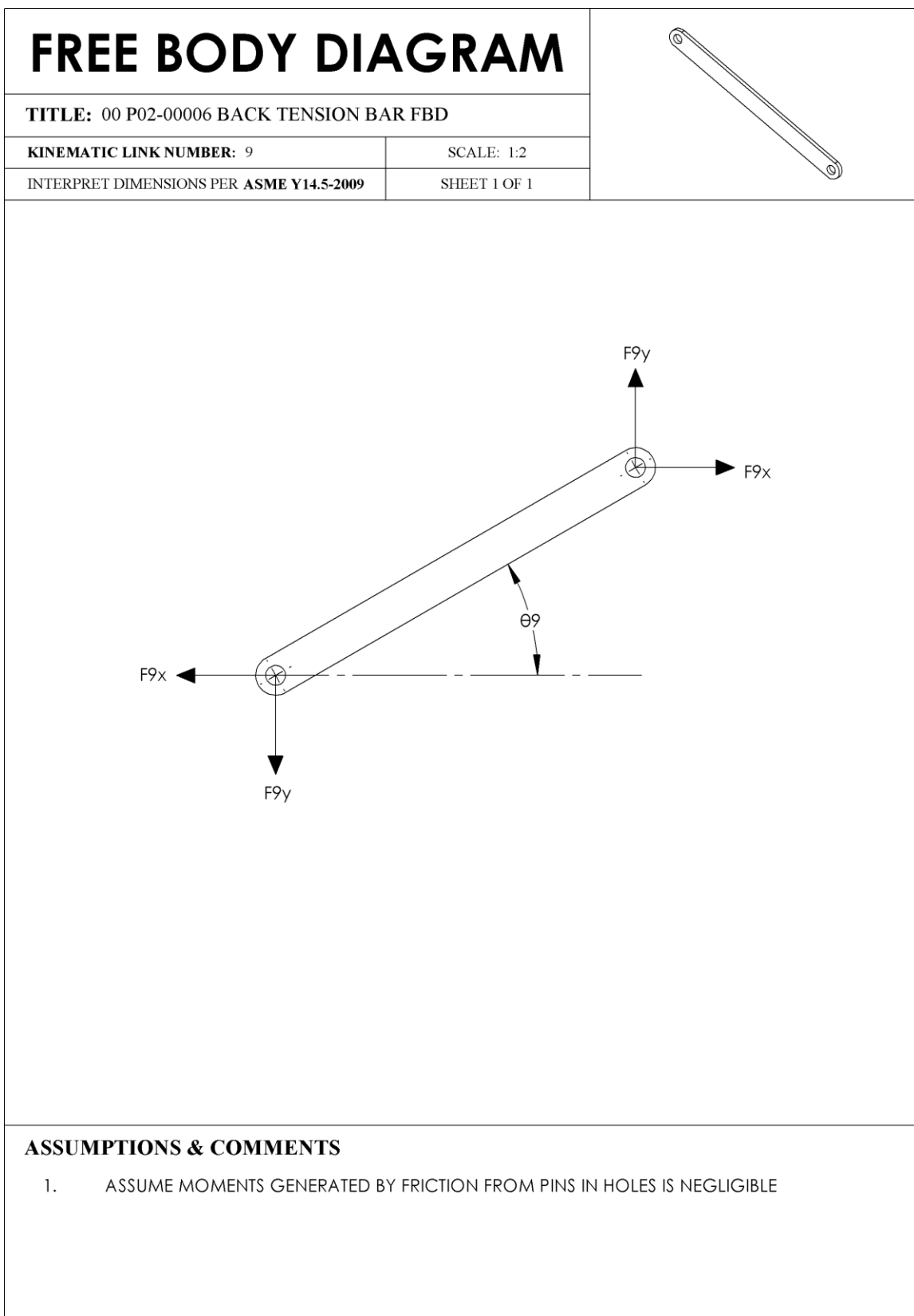
INTERPRET DIMENSIONS PER **ASME Y14.5-2009**

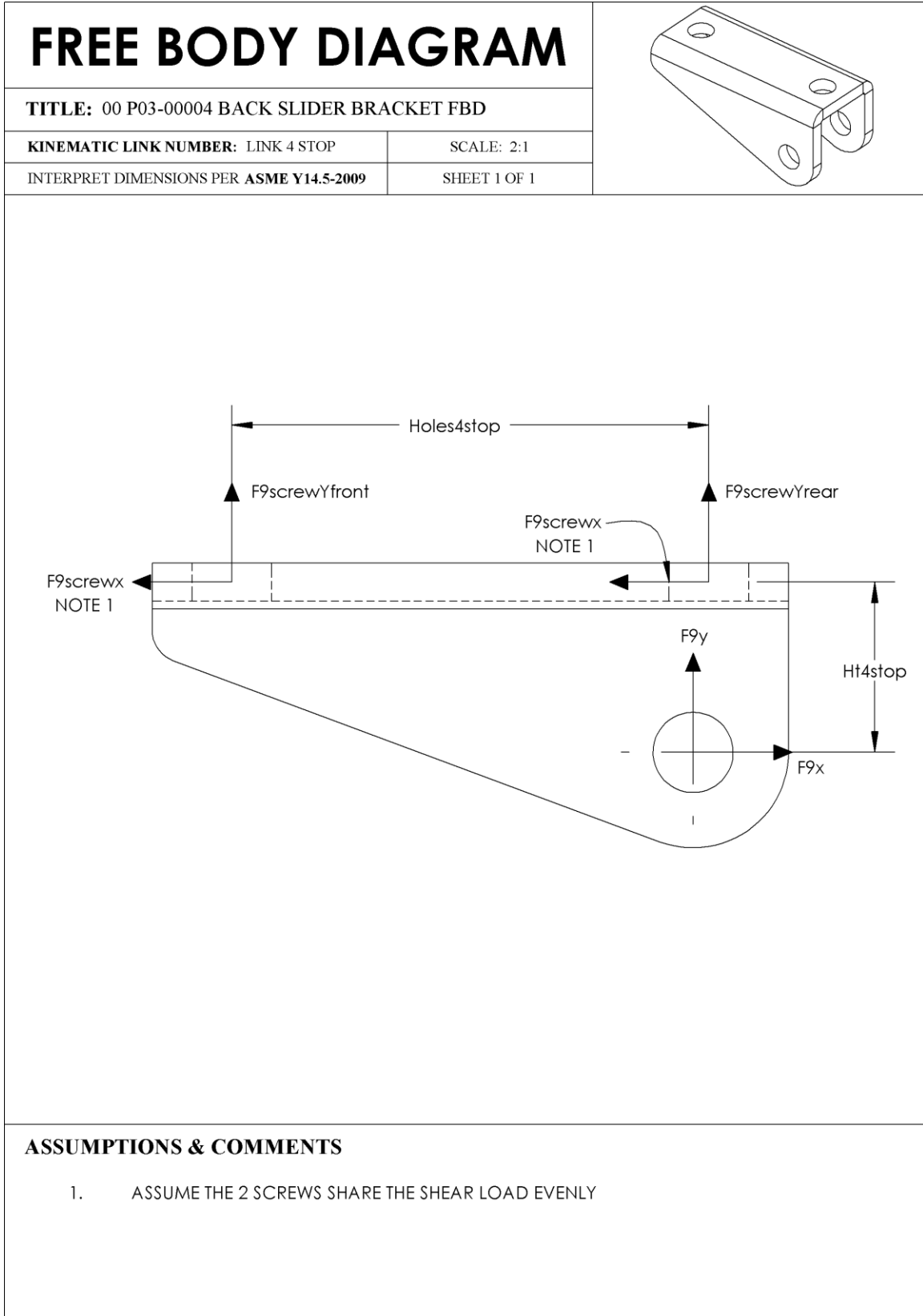
SHEET 1 OF 1



## ASSUMPTIONS & COMMENTS

1. ASSUME FRICTIONLESS SLIDING AND PIVOTING JOINTS





## Appendix D. Static Force Equations

Incline/Recline Motion Static Force Analysis

Link 7 Equilibrium Equations per the FBD

Moment equation:  $\sum M_D = 0$

$$-F_{78L} \cdot L_7 + F_{78U} \cdot (L_7 - L_{BOL}) + W_{uB} \cos(\theta_{78}) \cdot dW_{uB} = 0$$

$$dW_{uB} = d_{uB,Proximal} - L_{head,neck}$$

where  $d_{uB,Proximal}$  is defined as the distance from the top of the head to the center of mass of the upper body, and  $L_{head,neck}$  is the length of the head and neck.

Rearranging the coefficients for the force matrix yields,

$$A_{1,14} \cdot F_{78L} + A_{1,15} \cdot F_{78U} = P_1 \#(i)$$

where the coefficients are as follows:

$$A_{1,14} = \frac{L_7}{dW_{uB} \cos(\theta_{78})}$$

$$A_{1,15} = \frac{L_{BOL} - L_7}{dW_{uB} \cos(\theta_{78})}$$

$$P_1 = W_{uB}$$

y' Force equation:  $\sum Fy' = 0$

$$F_{78L} - F_{78u} - W_{uB} \cos(\theta_{78}) + F_D = 0$$

Rearranging the coefficients for the force matrix yields,

$$A_{2,14} \cdot F_{78L} + A_{2,15} \cdot F_{78u} + A_{2,18} \cdot F_{Dx} = P_2$$

where the coefficients are as follows:

$$A_{2,14} = \frac{1}{\cos(\theta_{78})}$$

$$A_{2,15} = \frac{-1}{\cos(\theta_{78})}$$

$$A_{2,18} = \frac{1}{\cos(\theta_{78}) \sin(\theta_{78})}$$

$$P_2 = W_{uB}$$

Assuming low friction, there is no x' force equation; due to the slider joint, this member is unable to take an axial load. However, the  $F_D$  force is in the y' direction and the unknown forces to be solved are in the x and y direction. Therefore, relationships for  $F_{Dx}$  and  $F_{Dy}$  are as follows:

$$F_{Dy} = F_D \cos(\theta_{78})$$

$$F_D = \frac{F_{Dy}}{\cos(\theta_{78})}$$

$$F_{Dx} = F_D \sin(\theta_{78})$$

$$F_D = \frac{F_{Dx}}{\sin(\theta_{78})}$$

$$F_{Dx} = F_{Dy} \cdot \tan(\theta_{78})$$

Rearranging the coefficients for the force matrix yields,

$$A_{3,18} \cdot F_{Dx} + A_{3,19} \cdot F_{Dy} = P_3$$

where the coefficients are as follows:

$$A_{3,18} = 1$$

$$A_{3,19} = -\tan(\theta_{78})$$

$$P_3 = 0$$

Link 8 Equilibrium Equations per the FBD

Moment equation:  $\sum M_C = 0$

$$F_{78u} \cdot L_8 - F_{78L}(L_8 - L_{BOL}) = 0$$

Rearranging the coefficients for the force matrix yields,

$$A_{4,14} \cdot F_{78L} + A_{4,15} \cdot F_{78u} = P_4 \#(iv)$$

where the coefficients are as follows:

$$A_{4,14} = L_{BOL} - L_8$$

$$A_{4,15} = L_8$$

$$P_4 = 0$$

y' Force equation:  $\sum F_{y'} = 0$

$$F_C - F_{78L} + F_{78u} = 0$$

The x and y components of  $F_c$  are:

$$F_{cx} = F_c \sin(\theta_{78})$$

$$F_{cy} = F_c \cos(\theta_{78})$$

Rearranging the coefficients for the force matrix yields,

$$A_{5,16} \cdot F_{cx} + A_{5,14} \cdot F_{78L} + A_{5,15} \cdot F_{78u} = P_5$$

where the coefficients are as follows:

$$A_{5,16} = \frac{1}{\sin(\theta_{78})}$$

$$A_{5,14} = -1$$

$$A_{5,15} = 1$$

$$P_5 = 0$$

Similar to the relationships found in link 7, the x and y components of  $F_c$  can be arranged

in an additional equation:

$$F_{cx} = F_{cy} \cdot \tan(\theta_{78})$$

Rearranging the coefficients for the force matrix yields,

$$A_{6,16} \cdot F_{cx} + A_{6,17} \cdot F_{cy} = P_6$$

where the coefficients are as follows:

$$A_{6,16} = 1$$

$$A_{6,17} = -\tan(\theta_{78})$$

$$P_6 = 0$$

Link 4 Equilibrium Equations per the FBD

Applicable geometric relationships for the *CG* of the backrest are:

$$\alpha_{4CM} = \theta_4 - \frac{\pi}{2}$$

$$d_{4CM} = L_{4CM_1} \cos(\alpha_{4CM}) - L_{4CM_2} \cos(\pi - \theta_4)$$

Moment equation:  $\sum M_3 = 0$

$$\begin{aligned} -F_{CMBack} \cdot d_{4CM} - F_{Dx} [L_{41} \sin(\delta_{41} - \theta_4)] - F_{Dy} [L_{41} \cos(\delta_{41} - \theta_4)] \\ + F_{4Ax} \left[ L_4 \cos \left( \theta_4 - \frac{\pi}{2} \right) \right] + F_{4Ay} \left[ L_4 \sin \left( \theta_4 - \frac{\pi}{2} \right) \right] = 0 \end{aligned}$$

Rearranging the coefficients for the force matrix yields,

$$A_{7,18} \cdot F_{Dx} + A_{7,19} \cdot F_{Dy} + A_{7,12} \cdot F_{4Ax} + A_{7,13} \cdot F_{4Ay} = P_7$$

where the coefficients are as follows:

$$A_{7,18} = -L_{41} \sin(\delta_{41} + \theta_4)$$

$$A_{7,19} = -L_{41} \cos(\delta_{41} + \theta_4)$$

$$A_{7,12} = L_4 \cos \left( \theta_4 - \frac{\pi}{2} \right)$$

$$A_{7,13} = L_4 \sin \left( \theta_4 - \frac{\pi}{2} \right)$$

$$P_7 = W_4 \cdot d_{4CM}$$

X force equation:  $\sum F_x = 0$

$$F_{Dx} - F_{4Ax} - F_{3x} = 0$$

Rearranging the coefficients for the force matrix yields,

$$A_{8,18} \cdot F_{Dx} + A_{8,12} \cdot F_{4Ax} + A_{8,10} \cdot F_{3x} = P_8$$

where the coefficients are as follows:

$$A_{8,18} = 1$$

$$A_{8,12} = A_{8,10} = -1$$

$$P_8 = 0$$

Y force equation:  $\sum F_y = 0$

$$-F_{Dy} - F_{4Ay} - F_{3y} - W_4 = 0$$

Rearranging the coefficients for the force matrix yields,

$$A_{9,19} \cdot F_{Dy} + A_{9,13} \cdot F_{4Ay} + A_{9,11} \cdot F_{3y} = P_9$$



where the coefficients are as follows:

$$A_{9,19} = A_{9,13} = A_{9,11} = -1$$

$$P_9 = W_4$$

Link 5 (Main Seat Member) Equilibrium Equations per the FBD

Moment equation:  $\sum M_A = 0$

$$(F_{2aSy} + F_{5front}) \cdot legsep + W_5 \cdot d_{5CM} - d_{hanghole} \cdot F_{hangscrew} = 0$$

Rearranging the coefficients for the force matrix yields,

$$A_{10,25} \cdot F_{hangscrew} + A_{10,4} \cdot F_{2aSy} + A_{10,20} \cdot F_{5front} = P_{10}$$

where the coefficients are as follows:

$$A_{10,25} = -d_{hanghole}$$

$$A_{10,4} = A_{10,20} = legsep$$

$$P_{10} = -W_5 \cdot d_{5CM}$$

X force equation:  $\sum F_x = 0$

$$F_{2aSx} + F_{4Ax} + F_{2bSx} - F_{5Ax} - F_{hangscrew} \cos(\theta_{hanghole}) = 0$$

Rearranging the coefficients for the force matrix yields,

$$A_{11,3} \cdot F_{2aSx} + A_{11,12} \cdot F_{4Ax} + A_{11,7} \cdot F_{2bSx} +$$

$$A_{11,25} \cdot F_{hangscrew} + A_{11,21} \cdot F_{5Ax} = P_{11}$$

where the coefficients are as follows:

$$A_{11,3} = A_{11,12} = A_{11,7} = 1$$

$$A_{11,21} = -1$$

$$A_{11,25} = -\cos(\theta_{hanghole})$$

$$P_{11} = 0$$

Y force equation:  $\sum F_y = 0$

$$-F_{5front} - F_{2aSy} + F_{hangscrew} \sin(\theta_{hanghole}) + F_{4Ay} - F_{5Ay} - F_{2bSy} - W_5 = 0$$

Rearranging the coefficients for the force matrix yields,

$$A_{12,20} \cdot F_{5front} + A_{12,4} \cdot F_{2aSy} + A_{12,25} \cdot F_{hangscrew} +$$

$$A_{12,13} \cdot F_{4Ay} + A_{12,22} \cdot F_{5Ay} + A_{12,8} \cdot F_{2bSy} = P_{12}$$

where the coefficients are as follows:

$$A_{12,20} = A_{12,4} = A_{12,22} = A_{12,8} = -1$$

$$A_{12,13} = 1$$

$$A_{12,25} = \sin(\theta_{hanghole})$$

$$P_{12} = W_5$$

Link 2a (Front Leg) Equilibrium Equations per the FBD

Moment equation:  $\sum M_A = 0$

$$F_{2m} \cdot L_{2am} + F_{2asx} \cdot L_2 \sin(\pi - \theta_2) - F_{2asy} \cdot L_2 \cos(\pi - \theta_2) = 0$$

Rearranging the coefficients for the force matrix yields,

$$A_{13,9} \cdot F_{2m} + A_{13,3} \cdot F_{2asx} + A_{13,4} \cdot F_{2asy} = P_{13}$$

where the coefficients are as follows:

$$A_{13,3} = L_2 \sin(\pi - \theta_2)$$

$$A_{13,4} = -L_2 \cos(\pi - \theta_2)$$

$$A_{13,9} = L_{2am}$$

$$P_{13} = 0$$

Y force equation:  $\sum F_y = 0$

$$F_{2asy} - F_{2m} - F_{2acy} = 0$$

Rearranging the coefficients for the force matrix yields,

$$A_{14,4} \cdot F_{2asy} + A_{14,9} \cdot F_{2m} + A_{14,2} \cdot F_{2acy} = P_{14}$$

where the coefficients are as follows:

$$A_{14,2} = A_{14,9} = -1$$

$$A_{14,4} = 1$$

$$P_{14} = 0$$

X force equation:  $\sum F_x = 0$

$$-F_{2asx} + F_{2acx} = 0$$

Rearranging the coefficients for the force matrix yields,

$$A_{15,3} \cdot F_{2asx} + A_{15,1} \cdot F_{2acx} = P_{15}$$

where the coefficients are as follows:

$$A_{15,1} = 1$$

$$A_{15,3} = -1$$

$$P_{15} = 0$$

Link 2b (Rear Leg) Equilibrium Equations per the FBD

Moment equation:  $\sum M_A = 0$

$$F_{2m} \cdot L_{2bm} + F_{2bcx} \cdot L_2 \sin(\pi - \theta_2) - F_{2bcy} \cdot L_2 \cos(\pi - \theta_2) = 0$$

Rearranging the coefficients for the force matrix yields,

$$A_{16,9} \cdot F_{2m} + A_{16,5} \cdot F_{2bcx} + A_{16,6} \cdot F_{2bcy} = P_{16}$$

where the coefficients are as follows:

$$A_{16,5} = L_2 \sin(\pi - \theta_2)$$

$$A_{16,6} = -L_2 \cos(\pi - \theta_2)$$

$$A_{16,9} = L_{2bm}$$

$$P_{16} = 0$$

Y force equation:  $\sum F_y = 0$

$$F_{2bsy} + F_{2m} - F_{2bcy} = 0$$

Rearranging the coefficients for the force matrix yields,

$$A_{17,8} \cdot F_{2bsy} + A_{17,9} \cdot F_{2m} + A_{17,6} \cdot F_{2bcy} = P_{14}$$

where the coefficients are as follows:

$$A_{17,6} = -1$$

$$A_{17,8} = A_{17,9} = 1$$

$$P_{17} = 0$$

X force equation:  $\sum F_x = 0$

$$-F_{2bsx} + F_{2bcx} = 0$$

Rearranging the coefficients for the force matrix yields,

$$A_{18,7} \cdot F_{2bsx} + A_{18,5} \cdot F_{2bcx} = P_{18}$$

where the coefficients are as follows:

$$A_{18,5} = 1$$

$$A_{18,7} = -1$$

$$P_{18} = 0$$

Link 5 (Rear Seat Hanger Member) Equilibrium Equations per the FBD

Moment equation:  $\sum M_A = 0$

$$d_{hanghole} \cdot F_{hangscrew} - F_{seatx} \cdot d_{5seaty} - F_{seaty} \cdot d_{5seatx} + L_5 \cos(\theta_5) \cdot F_{cy} + L_5 \sin(\theta_5) \cdot F_{cx} = 0$$

Rearranging the coefficients for the force matrix yields,

$$A_{19,25} \cdot F_{hangscrew} + A_{19,23} \cdot F_{seatx} + A_{19,24} \cdot F_{seaty} + A_{19,17} \cdot F_{cy} + A_{19,16} \cdot F_{cx} = P_{19}$$

where the coefficients are as follows:

$$A_{19,25} = d_{hanghole}$$

$$A_{19,23} = -d_{5seaty}$$

$$A_{19,24} = -d_{5seatx}$$

$$A_{19,17} = L_5 \cos(\theta_5)$$

$$A_{19,16} = L_5 \sin(\theta_5)$$

$$P_{19} = 0$$

X force equation:  $\sum F_x = 0$

$$F_{5Ax} + F_{hangscrew} \cos(\theta_{hanghole}) - F_{seatx} + F_{cx} = 0$$

Rearranging the coefficients for the force matrix yields,

$$A_{20,21} \cdot F_{5Ax} + A_{20,25} \cdot F_{hangscrew} + A_{20,23} \cdot F_{seatx} + A_{20,16} \cdot F_{cx} = P_{20}$$

where the coefficients are as follows:

$$A_{20,21} = A_{20,16} = 1$$

$$A_{20,23} = -1$$

$$A_{20,25} = \cos(\theta_{hanghole})$$

$$P_{20} = 0$$

Y force equation:  $\sum F_y = 0$

$$F_{5Ay} - F_{hangscrew} \sin(\theta_{hanghole}) - F_{seaty} - F_{cy} = 0$$

Rearranging the coefficients for the force matrix yields,

$$A_{21,22} \cdot F_{5Ay} + A_{21,25} \cdot F_{hangscrew} + A_{21,24} \cdot F_{seaty} + A_{20,17} \cdot F_{cy} = P_{20}$$

where the coefficients are as follows:

$$A_{21,24} = A_{21,17} = -1$$

$$A_{21,22} = 1$$

$$A_{21,25} = -\sin(\theta_{hanghole})$$

$$P_{21} = 0$$

Link 5 (Upholstered Seat Member) Equilibrium Equations per the FBD

Moment equation:  $\sum M_O = 0$

$$\begin{aligned} & -[L_{seatEff} \cos(\theta_{seat})] \cdot F_{5front} + (d_{LB} + d_{5seatx}) \cdot W_{LB} \\ & + \left[ \frac{chest}{2} \cos(\theta_{seat}) \right] W_{ub} \sin^2(\theta_{78}) \\ & + \left[ \frac{chest}{2} \sin(\theta_{seat}) \right] W_{ub} \sin(\theta_{78}) \cos(\theta_{78}) = 0 \end{aligned}$$

Rearranging the coefficients for the force matrix yields,

$$A_{(22,20)} \cdot F_{5front} = P_{22}$$

where the coefficients are as follows:

$$\begin{aligned} A_{(22,20)} &= L_{seatEff} \cos(\theta_{seat}) \\ P_{22} &= (d_{LB} + d_{5seatx}) \cdot W_{LB} + \left[ \frac{chest}{2} \cos(\theta_{seat}) \right] W_{ub} \sin^2(\theta_{78}) \\ &+ \left[ \frac{chest}{2} \sin(\theta_{seat}) \right] W_{ub} \sin(\theta_{78}) \cos(\theta_{78}) \end{aligned}$$

X force equation:  $\sum F_x = 0$

$$F_{seatx} = W_{ub} \sin(\theta_{78}) \cos(\theta_{78})$$

Rearranging the coefficients for the force matrix yields,

$$A_{(23,23)} \cdot F_{seatx} = P_{23}$$

where the coefficients are as follows:

$$\begin{aligned} A_{(23,23)} &= 1 \\ P_{23} &= W_{ub} \sin(\theta_{78}) \cos(\theta_{78}) \end{aligned}$$

Y force equation:  $\sum F_y = 0$

$$F_{5front} + F_{seaty} = W_{LB} + W_{ub} \sin^2(\theta_{78})$$

Rearranging the coefficients for the force matrix yields,

$$A_{(24,20)} \cdot F_{5front} + A_{(24,24)} \cdot F_{seaty} = P_{24}$$

where the coefficients are as follows:

$$\begin{aligned} A_{(24,20)} &= A_{(24,24)} = 1 \\ P_{24} &= W_{LB} + W_{ub} \sin^2(\theta_{78}) \end{aligned}$$



Link 3 (Pushrod) Equilibrium Equations per the FBD

Moment equation:  $\sum M_A = 0$

$$L_3 \cos(\theta_3) \cdot F_{3y} - L_3 \sin(\theta_3) \cdot F_{3x} = 0$$

Rearranging the coefficients for the force matrix yields,

$$A_{(25,11)} \cdot F_{3y} + A_{(25,10)} \cdot F_{3x} = P_{25}$$

where the coefficients are as follows:

$$A_{(25,10)} = -L_3 \sin(\theta_3)$$

$$A_{(25,11)} = L_3 \cos(\theta_3)$$

$$P_{25} = 0$$

Raise/Lower Motion Static Force Analysis

Link 7 Equilibrium Equations per the FBD

Moment equation:  $\sum M_D = 0$

$$-F_{78L} \cdot L_7 + F_{78U} \cdot (L_7 - L_{BOL}) + W_{uB} \cos(\theta_{78}) \cdot dW_{uB} = 0$$

$$dW_{uB} = d_{uB,Proximal} - L_{head,neck}$$

where  $d_{uB,Proximal}$  is defined as the distance from the top of the head to the center of mass of the upper body, and  $L_{head,neck}$  is the length of the head and neck.

Rearranging the coefficients for the force matrix yields,

$$B_{1,14} \cdot F_{78L} + B_{1,15} \cdot F_{78U} = Q_1$$

where the coefficients are as follows:

$$B_{1,14} = \frac{L_7}{dW_{uB} \cos(\theta_{78})}$$

$$B_{1,15} = \frac{L_{BOL} - L_7}{dW_{uB} \cos(\theta_{78})}$$

$$Q_1 = W_{uB}$$

y' Force equation:  $\sum Fy' = 0$

$$F_{78L} - F_{78u} - W_{uB} \cos(\theta_{78}) + F_D = 0$$

Rearranging the coefficients for the force matrix yields,

$$B_{2,14} \cdot F_{78L} + B_{2,15} \cdot F_{78u} + B_{2,18} \cdot F_{Dx} = Q_2$$

where the coefficients are as follows:

$$B_{2,14} = \frac{1}{\cos(\theta_{78})}$$

$$B_{2,15} = \frac{-1}{\cos(\theta_{78})}$$

$$B_{2,18} = \frac{1}{\cos(\theta_{78}) \sin(\theta_{78})}$$

$$Q_2 = W_{uB}$$

Assuming low friction, there is no x' force equation; due to the slider joint, this member is unable to take an axial load. However, the  $F_D$  force is in the y' direction and the

unknown forces to be solved are in the x and y direction. Therefore, relationships for  $F_{Dx}$  and  $F_{Dy}$  are as follows:

$$F_{Dy} = F_D \cos(\theta_{78})$$

$$F_D = \frac{F_{Dy}}{\cos(\theta_{78})}$$

$$F_{Dx} = F_D \sin(\theta_{78})$$

$$F_D = \frac{F_{Dx}}{\sin(\theta_{78})}$$

$$F_{Dx} = F_{Dy} \cdot \tan(\theta_{78})$$

Rearranging the coefficients for the force matrix yields,

$$B_{3,18} \cdot F_{Dx} + B_{3,19} \cdot F_{Dy} = Q_3$$

where the coefficients are as follows:

$$B_{3,18} = 1$$

$$B_{3,19} = -\tan(\theta_{78})$$

$$Q_3 = 0$$

Link 8 Equilibrium Equations per the FBD

Moment equation:  $\sum M_c = 0$

$$F_{78u} \cdot L_8 - F_{78L}(L_8 - L_{BOL}) = 0$$

Rearranging the coefficients for the force matrix yields,

$$B_{4,14} \cdot F_{78L} + B_{4,15} \cdot F_{78u} = Q_4$$

where the coefficients are as follows:

$$B_{4,14} = L_{BOL} - L_8$$

$$B_{4,15} = L_8$$

$$Q_4 = 0$$

y' Force equation:  $\sum F_{y'} = 0$

$$F_c - F_{78L} + F_{78u} = 0$$

The x and y components of  $F_c$  are:

$$F_{cx} = F_c \sin(\theta_{78})$$

$$F_{cy} = F_c \cos(\theta_{78})$$

Rearranging the coefficients for the force matrix yields,

$$B_{5,16} \cdot F_{cx} + B_{5,14} \cdot F_{78L} + B_{5,15} \cdot F_{78u} = Q_5$$

where the coefficients are as follows:

$$B_{5,16} = \frac{1}{\sin(\theta_{78})}$$

$$B_{5,14} = -1$$

$$B_{5,15} = 1$$

$$Q_5 = 0$$

Similar to the relationships found in link 7, the x and y components of  $F_c$  can be arranged in an additional equation:

$$F_{cx} = F_{cy} \cdot \tan(\theta_{78})$$

Rearranging the coefficients for the force matrix yields,

$$B_{6,16} \cdot F_{cx} + B_{6,17} \cdot F_{cy} = Q_6$$

where the coefficients are as follows:

$$B_{6,16} = 1$$

$$B_{6,17} = -\tan(\theta_{78})$$

$$Q_6 = 0$$

Link 4 Equilibrium Equations per the FBD

Applicable geometric relationships for the *CG* of the backrest are:

$$\alpha_{4CM} = \theta_4 - \frac{\pi}{2}$$

$$d_{4CM} = L_{4CM_1} \cos(\alpha_{4CM}) - L_{4CM_2} \cos(\pi - \theta_4)$$

Moment equation:  $\sum M_3 = 0$

$$\begin{aligned} -W_4 \cdot d_{4CM} - F_{Dx}[L_{41} \sin(\delta_{41} - \theta_4)] - F_{Dy}[L_{41} \cos(\delta_{41} - \theta_4)] \\ + F_{4Ax} \left[ L_4 \cos\left(\theta_4 - \frac{\pi}{2}\right) \right] + F_{4Ay} \left[ L_4 \sin\left(\theta_4 - \frac{\pi}{2}\right) \right] - F_{9x} \cdot d_{9y} - F_{9y} \cdot d_{9x} \\ = 0 \end{aligned}$$

Rearranging the coefficients for the force matrix yields,

$$B_{7,18} \cdot F_{Dx} + B_{7,19} \cdot F_{Dy} + B_{7,12} \cdot F_{4Ax} + B_{7,13} \cdot F_{4Ay} + B_{7,4} \cdot F_{9x} + B_{7,3} \cdot F_{9y} = Q_7$$

where the coefficients are as follows:

$$B_{7,4} = -d_{9y}$$

$$B_{7,3} = -d_{9x}$$

$$B_{7,18} = -L_{41} \sin(\delta_{41} + \theta_4)$$

$$B_{7,19} = -L_{41} \cos(\delta_{41} + \theta_4)$$

$$B_{7,12} = L_4 \cos\left(\theta_4 - \frac{\pi}{2}\right)$$

$$B_{7,13} = L_4 \sin\left(\theta_4 - \frac{\pi}{2}\right)$$

$$Q_7 = W_4 \cdot d_{4CM}$$

X force equation:  $\sum F_x = 0$

$$F_{Dx} - F_{4Ax} - F_{3x} - F_{9x} = 0$$

Rearranging the coefficients for the force matrix yields,

$$B_{8,18} \cdot F_{Dx} + B_{8,12} \cdot F_{4Ax} + B_{8,10} \cdot F_{3x} + B_{8,3} \cdot F_{9x} = Q_8$$

where the coefficients are as follows:

$$B_{8,18} = 1$$

$$B_{8,3} = B_{8,12} = B_{8,10} = -1$$

$$Q_8 = 0$$

Y force equation:  $\sum F_y = 0$

$$-F_{Dy} - F_{4Ay} - F_{3y} - F_{9y} - W_4 = 0$$

Rearranging the coefficients for the force matrix yields,

$$B_{9,19} \cdot F_{Dy} + B_{9,13} \cdot F_{4Ay} + B_{9,11} \cdot F_{3y} + B_{9,4} \cdot F_{9y} = Q_9$$

where the coefficients are as follows:

$$B_{9,4} = B_{9,19} = B_{9,13} = B_{9,11} = -1$$

$$Q_9 = W_4$$

Link 5 (Main Seat Member) Equilibrium Equations per the FBD

Moment equation:  $\sum M_A = 0$

$$\begin{aligned} & (F_{2ay} + F_{5front}) \cdot legsep + W_5 \cdot d_{5CM} - d_{hanghole} \cdot F_{hangscrew} + d_{4stopx} \\ & \cdot F_{9screwYrear} + (d_{4stopx} + Holes4stop) \cdot F_{9screwYfront} + 2 \cdot d_{4stopy} \\ & \cdot F_{9screwX} = 0 \end{aligned}$$

Rearranging the coefficients for the force matrix yields,

$$\begin{aligned} & B_{10,25} \cdot F_{hangscrew} + B_{10,2} \cdot F_{2ay} + B_{10,20} \cdot F_{5front} + B_{10,7} \cdot F_{9screwX} + B_{10,8} \\ & \cdot F_{9screwYfront} + B_{10,9} \cdot F_{9screwYrear} = Q_{10} \end{aligned}$$

where the coefficients are as follows:

$$\begin{aligned} B_{10,7} &= 2 \cdot d_{4stopy} \\ B_{10,8} &= d_{4stopx} + Holes4stop \\ B_{10,9} &= d_{4stopx} \\ B_{10,25} &= -d_{hanghole} \\ B_{10,2} &= B_{10,20} = legsep \\ Q_{10} &= -W_5 \cdot d_{5CM} \end{aligned}$$

X force equation:  $\sum F_x = 0$

$$F_{2ax} + F_{4Ax} + F_{2bx} - F_{5Ax} - F_{hangscrew} \cos(\theta_{hanghole}) + 2F_{9screwX} = 0$$

Rearranging the coefficients for the force matrix yields,

$$\begin{aligned} & B_{11,1} \cdot F_{2ax} + B_{11,12} \cdot F_{4Ax} + B_{11,5} \cdot F_{2bx} + B_{11,25} \cdot F_{hangscrew} + B_{11,21} \cdot F_{5Ax} + B_{11,7} \\ & \cdot F_{9screwX} = Q_{11} \end{aligned}$$

where the coefficients are as follows:

$$\begin{aligned} B_{11,1} &= B_{11,12} = B_{11,5} = 1 \\ B_{11,21} &= -1 \\ B_{11,25} &= -\cos(\theta_{hanghole}) \\ B_{11,7} &= 2 \\ Q_{11} &= 0 \end{aligned}$$

Y force equation:  $\sum F_y = 0$

$$-F_{5front} - F_{2ay} + F_{hangscrew} \sin(\theta_{hanghole}) + F_{4Ay} - F_{5Ay} - F_{2by} - F_{9screwYfront} - F_{9screwYrear} - W_5 = 0$$

Rearranging the coefficients for the force matrix yields,

$$B_{12,20} \cdot F_{5front} + B_{12,2} \cdot F_{2ay} + B_{12,25} \cdot F_{hangscrew} + B_{12,13} \cdot F_{4Ay} + B_{12,22} \cdot F_{5Ay} + B_{12,6} \cdot F_{2by} + B_{12,8} \cdot F_{9screwYfront} + B_{12,9} \cdot F_{9screwYrear} = Q_{12}$$

where the coefficients are as follows:

$$B_{12,20} = B_{12,2} = B_{12,22} = B_{12,6} = B_{12,8} = B_{12,9} = -1$$

$$B_{12,13} = 1$$

$$B_{12,25} = \sin(\theta_{hanghole})$$

$$Q_{12} = W_5$$



Link 2a (Front Leg) Equilibrium Equations per the FBD

Moment equation:  $\sum M_A = 0$

$$F_{2ax} \cdot L_2 \sin(\pi - \theta_2) - F_{2ay} \cdot L_2 \cos(\pi - \theta_2) = 0$$

Rearranging the coefficients for the force matrix yields,

$$B_{13,1} \cdot F_{2ax} + B_{13,2} \cdot F_{2ay} = Q_{13}$$

where the coefficients are as follows:

$$B_{13,1} = L_2 \sin(\pi - \theta_2)$$

$$B_{13,2} = -L_2 \cos(\pi - \theta_2)$$

$$Q_{13} = 0$$

Link 2b (Rear Leg) Equilibrium Equations per the FBD

Moment equation:  $\sum M_A = 0$

$$F_{2bx} \cdot L_2 \sin(\pi - \theta_2) - F_{2by} \cdot L_2 \cos(\pi - \theta_2) = 0$$

Rearranging the coefficients for the force matrix yields,

$$B_{14,5} \cdot F_{2bx} + B_{14,6} \cdot F_{2by} = P_{14}$$

where the coefficients are as follows:

$$B_{14,5} = L_2 \sin(\pi - \theta_2)$$

$$B_{14,6} = -L_2 \cos(\pi - \theta_2)$$

$$Q_{14} = 0$$

Link 9 (Back Tension Bar) Equilibrium Equations per the FBD

Moment equation:  $\sum M_A = 0$

$$-F_{9x} \cdot L_9 \sin(\theta_9) + F_{9y} \cdot L_9 \cos(\theta_9) = 0$$

Rearranging the coefficients for the force matrix yields,

$$B_{15,3} \cdot F_{9x} + B_{15,4} \cdot F_{2by} = Q_{15}$$

where the coefficients are as follows:

$$B_{15,3} = -L_9 \sin(\theta_9)$$

$$B_{15,4} = L_9 \cos(\theta_9)$$

$$Q_{15} = 0$$

Link 4 Stop (Back Stop Bracket) Equilibrium Equations per the FBD

Moment equation:  $\sum M_O = 0$

$$F_{9x} \cdot Ht4Stop - F_{9y} \cdot End4Stop - Holes4Stop \cdot F_{9screwYfront} = 0$$

Rearranging the coefficients for the force matrix yields,

$$B_{16,3} \cdot F_{9x} + B_{16,4} \cdot F_{2by} + B_{16,8} \cdot F_{9screwYfront} = Q_{16}$$

where the coefficients are as follows:

$$B_{16,3} = Ht4Stop$$

$$B_{16,4} = -End4Stop$$

$$B_{16,8} = -Holes4Stop$$

$$Q_{16} = 0$$

X force equation:  $\sum F_x = 0$ , assuming the two screws share the load equally

$$F_{9x} - 2F_{9screwX} = 0$$

Rearranging the coefficients for the force matrix yields,

$$B_{17,3} \cdot F_{9x} + B_{17,7} \cdot F_{9screwX} = Q_{17}$$

where the coefficients are as follows:

$$B_{17,3} = 1$$

$$B_{17,7} = -2$$

$$Q_{17} = 0$$

Y force equation:  $\sum F_y = 0$

$$F_{9y} + F_{9screwYfront} + F_{9screwYrear} = 0$$

Rearranging the coefficients for the force matrix yields,

$$B_{18,4} \cdot F_{9y} + B_{18,8} \cdot F_{9screwYfront} + B_{18,9} \cdot F_{9screwYrear} = Q_{18}$$

where the coefficients are as follows:

$$B_{18,4} = B_{18,8} = B_{18,9} = 1$$

$$Q_{18} = 0$$

Link 5 (Rear Seat Hanger Member) Equilibrium Equations per the FBD

Moment equation:  $\sum M_A = 0$

$$d_{hanghole} \cdot F_{hangscrew} - F_{seatx} \cdot d_{5seaty} - F_{seaty} \cdot d_{5seatx} + L_5 \cos(\theta_5) \cdot F_{cy} + L_5 \sin(\theta_5) \cdot F_{cx} = 0$$

Rearranging the coefficients for the force matrix yields,

$$B_{19,25} \cdot F_{hangscrew} + B_{19,23} \cdot F_{seatx} + B_{19,24} \cdot F_{seaty} + B_{19,17} \cdot F_{cy} + B_{19,16} \cdot F_{cx} = Q_{19}$$

where the coefficients are as follows:

$$B_{19,25} = d_{hanghole}$$

$$B_{19,23} = -d_{5seaty}$$

$$B_{19,24} = -d_{5seatx}$$

$$B_{19,17} = L_5 \cos(\theta_5)$$

$$B_{19,16} = L_5 \sin(\theta_5)$$

$$Q_{19} = 0$$

X force equation:  $\sum F_x = 0$

$$F_{5Ax} + F_{hangscrew} \cos(\theta_{hanghole}) - F_{seatx} + F_{cx} = 0$$

Rearranging the coefficients for the force matrix yields,

$$B_{20,21} \cdot F_{5Ax} + B_{20,25} \cdot F_{hangscrew} - B_{20,23} \cdot F_{seatx} + B_{20,16} \cdot F_{cx} = Q_{20}$$

where the coefficients are as follows:

$$B_{20,21} = B_{20,16} = 1$$

$$B_{20,23} = -1$$

$$B_{20,25} = \cos(\theta_{hanghole})$$

$$Q_{20} = 0$$

Y force equation:  $\sum F_y = 0$

$$F_{5Ay} - F_{hangscrew} \sin(\theta_{hanghole}) - F_{seaty} - F_{cy} = 0$$

Rearranging the coefficients for the force matrix yields,

$$B_{21,22} \cdot F_{5Ay} + B_{21,25} \cdot F_{hangscrew} + B_{21,24} \cdot F_{seaty} + B_{20,17} \cdot F_{cy} = Q_{20}$$

where the coefficients are as follows:

$$B_{21,24} = B_{21,17} = -1$$

$$B_{21,22} = 1$$

$$B_{21,25} = -\sin(\theta_{hanghole})$$

$$Q_{21} = 0$$

Link 5 (Upholstered Seat Member) Equilibrium Equations per the FBD

Moment equation:  $\sum M_O = 0$

$$\begin{aligned} & -[L_{seatEff} \cos(\theta_{seat})] \cdot F_{5front} + (d_{LB} + d_{5seatx}) \cdot W_{LB} \\ & + \left[ \frac{chest}{2} \cos(\theta_{seat}) \right] W_{ub} \sin^2(\theta_{78}) \\ & + \left[ \frac{chest}{2} \sin(\theta_{seat}) \right] W_{ub} \sin(\theta_{78}) \cos(\theta_{78}) = 0 \end{aligned}$$

Rearranging the coefficients for the force matrix yields,

$$B_{22,20} \cdot F_{5front} = Q_{22}$$

where the coefficients are as follows:

$$\begin{aligned} B_{22,20} &= L_{seatEff} \cos(\theta_{seat}) \\ Q_{22} &= (d_{LB} + d_{5seatx}) \cdot W_{LB} + \left[ \frac{chest}{2} \cos(\theta_{seat}) \right] W_{ub} \sin^2(\theta_{78}) \\ &+ \left[ \frac{chest}{2} \sin(\theta_{seat}) \right] W_{ub} \sin(\theta_{78}) \cos(\theta_{78}) \end{aligned}$$

X force equation:  $\sum F_x = 0$

$$F_{seatx} = W_{ub} \sin(\theta_{78}) \cos(\theta_{78})$$

Rearranging the coefficients for the force matrix yields,

$$B_{23,23} \cdot F_{seatx} = Q_{23}$$

where the coefficients are as follows:

$$\begin{aligned} B_{23,23} &= 1 \\ Q_{23} &= W_{ub} \sin(\theta_{78}) \cos(\theta_{78}) \end{aligned}$$

Y force equation:  $\sum F_y = 0$

$$F_{5front} + F_{seaty} = W_{LB} + W_{ub} \sin^2(\theta_{78})$$

Rearranging the coefficients for the force matrix yields,

$$B_{24,20} \cdot F_{5front} + B_{24,24} \cdot F_{seaty} = Q_{24}$$

where the coefficients are as follows:

$$\begin{aligned} B_{24,20} &= B_{24,24} = 1 \\ Q_{24} &= W_{LB} + W_{ub} \sin^2(\theta_{78}) \end{aligned}$$

Link 3 (Pushrod) Equilibrium Equations per the FBD

Moment equation:  $\sum M_A = 0$

$$L_3 \cos(\theta_3) \cdot F_{3y} - L_3 \sin(\theta_3) \cdot F_{3x} = 0$$

Rearranging the coefficients for the force matrix yields,

$$B_{25,11} \cdot F_{3y} + B_{25,10} \cdot F_{3x} = Q_{25}$$

where the coefficients are as follows:

$$B_{25,10} = -L_3 \sin(\theta_3)$$

$$B_{25,11} = L_3 \cos(\theta_3)$$

$$Q_{25} = 0$$



## Chassis &amp; Slider Static Force Analysis

Link 6 (Slider & Slider Caster) Equilibrium Equations per the FBD

Moment equation:  $\sum M_O = 0$

$$[dsc + L_6 \cos(\theta_6)](F_{3y}) - [dsc - (d_{slidefront} - L_{11})](F_{slidefront}) + dsc(F_{sliderear}) - Msc = 0$$

Rearranging the coefficients for the force matrix yields,

$$C_{1,4} \cdot F_{slidefront} + C_{1,5} \cdot F_{sliderear} + C_{1,6} = R_1$$

where the coefficients are as follows:

$$C_{1,4} = dsc - (d_{slidefront} - L_{11})$$

$$C_{1,5} = -dsc$$

$$C_{1,6} = Msc$$

$$R_1 = [dsc + L_6 \cos(\theta_6)](F_{3y})$$

Y force equation:  $\sum F_y = 0$

$$Fsc + F_{3y} - F_{slidefront} + F_{sliderear} = 0$$

Rearranging the coefficients for the force matrix yields,

$$C_{3,1} \cdot Fsc + C_{3,4} \cdot F_{slidefront} + C_{3,5} \cdot F_{sliderear} = R_3$$

where the coefficients are as follows:

$$C_{3,1} = C_{3,5} = 1$$

$$C_{3,4} = -1$$

$$R_3 = F_{3y}$$

Summing the moments on the about the caster post axis, assuming forces act only in the direction parallel to the post axis:

$$d_{casterposst} \cdot Fsc - Msc = 0$$

Rearranging the coefficients for the force matrix yields,

$$C_{4,1} \cdot Fsc + C_{4,6} = R_4$$

where the coefficients are as follows:

$$C_{4,1} = d_{casterpost}$$

$$C_{4,6} = -Msc$$

$$R_4 = 0$$

Link 1 (Chassis) Equilibrium Equations per the FBD

Moment equation:  $\sum M_A = 0$

$$\begin{aligned} -d_{slidefront} \cdot F_{slidefront} - d_{FFC} \cdot FFC + [L_{12} \cos(\theta_{12}) - legsep] \cdot F_{2aCy} \\ + L_{12} \cos(\theta_{12}) \cdot F_{2bCy} + L_{11} \cdot F_{sliderear} - d_{FRC} \cdot FRC + L_{12} \sin(\theta_{12}) \\ \cdot F_{2aCx} + L_{12} \sin(\theta_{12}) \cdot F_{2bCx} = 0 \end{aligned}$$

Rearranging the coefficients for the force matrix yields,

$$C_{5,4} \cdot F_{slidefront} + C_{5,2} \cdot FFC + C_{5,5} \cdot F_{sliderear} + C_{5,3} \cdot FRC = R_5$$

where the coefficients are as follows:

$$C_{5,4} = d_{slidefront}$$

$$C_{5,2} = d_{FFC}$$

$$C_{5,5} = -L_{11}$$

$$C_{5,3} = d_{FRC}$$

$$\begin{aligned} R_5 = [L_{12} \cos(\theta_{12}) - legsep] \cdot F_{2aCy} + L_{12} \cos(\theta_{12}) \cdot F_{2bCy} + L_{12} \sin(\theta_{12}) \cdot F_{2aCx} \\ + L_{12} \sin(\theta_{12}) \cdot F_{2bCx} \end{aligned}$$

Y force equation:  $\sum F_y = 0$

$$FFC + FRC + F_{slidefront} - F_{sliderear} + F_{2aCy} + F_{2bCy} = 0$$

Rearranging the coefficients for the force matrix yields,

$$C_{6,2} \cdot FFC + C_{6,3} \cdot FRC + C_{6,4} \cdot F_{slidefront} + C_{6,5} \cdot F_{sliderear} = R_6$$

where the coefficients are as follows:

$$C_{6,2} = C_{6,3} = C_{6,4} = 1$$

$$C_{6,5} = -1$$

$$R_6 = -(F_{2aCy} + F_{2bCy})$$

The final equation to resolve static indeterminacy has to do with assumed distribution of forces among casters. This is done by the following assumptions:

If the combined user and system weight is between the front and middle casters, then

$$FRC = 0.25W_{TOTAL}$$

If the combined user and system weight is between the middle and rear casters, then

$$FSC = 0.25W_{TOTAL}$$

These unknowns are then solved by inverting the square matrix [C] and multi[plying it by the load vector {R}

$$\begin{Bmatrix} FSC \\ FFC \\ FRC \\ F_{slidefront} \\ F_{sliderear} \\ MSC \end{Bmatrix} = \begin{bmatrix} C_{1,1} & \dots & C_{1,6} \\ \vdots & \ddots & \vdots \\ C_{6,1} & \dots & C_{6,6} \end{bmatrix}^{-1} \{R\}$$

## Appendix E. Kinematics and Static Force Computation Code

### Inputs

#### Side Profile Range for Kinematic Analysis

Motion 1: Incline				
Description	Dimension Description	Value	Units	Notes
Input as Backrest	Backrest sweep angle	80	degrees	None

#### Motion 2: Raise

Description	Dimension Description	Value	Units	Notes
Input as Leg	Leg sweep angle	50	degrees	None

#### Side Profile Reference Position Dimensions for Kinematic Analysis

#### Motion 1

Part Description	Link Number	Dimension Description	Value	Units	Notes
A0 - A01-00001 Chassis & Drive Train (GROUND)	1.2	Linear distance between rear leg pivot hole center to the fixed bearing centered on the screw	13.633	inches	Dropbox\USU - Thesis\CREEPER\ - FINAL MODEL FILES --\-- PACK & GO for ANALYSIS -- \Report Drawing Images
A0 - A01-00001 Chassis & Drive Train (GROUND)	1.2	Angle from horizontal to line from the rear leg pivot hole center to the rear-most point in the chassis rail tube, centered on the screw	172.26	deg	Dropbox\USU - Thesis\CREEPER\ - FINAL MODEL FILES --\-- PACK & GO for ANALYSIS -- \Report Drawing Images

A0 - P04-00008 Leg	2	Straight-line distance between pivot point centers on Leg	26.5	inches	Dropbox\USU - Thesis\CREEPER\ - FINAL MODEL FILES --\-- PACK & GO for ANALYSIS -- \Report Drawing Images
A0 - P04-00008 Leg	2	Angle from horizontal to straight-line between pivot point centers on Leg, when leg is in the incline position (all the way down)	168.875	deg	Dropbox\USU - Thesis\CREEPER\ - FINAL MODEL FILES --\-- PACK & GO for ANALYSIS -- \Report Drawing Images
Push Rod	3	Length of push rod, C-C of holes	27.5	inches	
A0 - A01-00015 Full Backrest Subassembly	4	Distance between pivot points on backrest	5.25	inches	
A0 - A01-00015 Full Backrest Subassembly	4	Angle from horizontal to straight-line between seat/rear leg and push rod pivot centers (lower limit)	80	deg	
A0 - A01-00015 Full Backrest Subassembly	4.1	Linear distance from push rod pivot hole center to upper backrest attachment pivot hole center (L41)	26.839	inches	Dropbox\USU - Thesis\CREEPER\ - FINAL MODEL FILES --\-- PACK & GO for ANALYSIS -- \Report Drawing Images

A0 - A01-00015 Full Backrest Subassembly	4.1	Angle from backrest link to line formed from push rod pivot hole center to upper backrest attachment pivot hole center (delta41)	276.594	deg	Dropbox\USU - Thesis\CREEPER\ - FINAL MODEL FILES --\-- PACK & GO for ANALYSIS -- \Report Drawing Images
Seat/Chassis	5	Leg pivot separation distance	15	inches	
A0 - P03-00026 Rear Seat Hanger	5	Linear distance from bridge pivot center to rear leg pivot hole center (L5)	6.94	inches	Dropbox\USU - Thesis\CREEPER\ - FINAL MODEL FILES --\-- PACK & GO for ANALYSIS -- \Report Drawing Images
A0 - P03-00026 Rear Seat Hanger	5	Angle from horizontal to line from the rear leg pivot hole center to the bridge pivot center	104.521	deg	Dropbox\USU - Thesis\CREEPER\ - FINAL MODEL FILES --\-- PACK & GO for ANALYSIS -- \Report Drawing Images
A0 - A01-00009 Slider Subassembly	6	Length from push rod pivot hole center to the rear-most point centered on the screw	38.093	inches	Dropbox\USU - Thesis\CREEPER\ - FINAL MODEL FILES --\-- PACK & GO for ANALYSIS -- \Report Drawing Images
A0 - A01-00009 Slider Subassembly	6	Angle from horizontal to line from the push rod pivot hole center to the rear-most point centered on the screw	177.322	deg	Dropbox\USU - Thesis\CREEPER\ - FINAL MODEL FILES --\-- PACK & GO for ANALYSIS -- \Report Drawing Images

A0 - P03-00015 Left Back Support	7	Linear distance from upper backrest attachment pivot hole center to opposite end of back support (L7)	23.731	inches	
A0 - A01-00003 Bridge Subassembly	8	Distance from bridge pivot center to top end of bridge (L8)	13.5	inches	L8
A0 - A01-00015 Full Backrest Subassembly	4	Center distance between hip pivot and upper backrest pivot	26.749	inches	
A0 - A05-00004 Upholstered Seat Subassembly	5	Normal distance from seat surface to rear seat/leg pivot	5.38	inches	
A0 - A05-00004 Upholstered Seat Subassembly	5	Angle of seat measured from the negative horizontal	4.74	deg	
A0 - P04-00008 Leg	2a	Effective force location distance on front leg from rear hole	2.25	inches	
A0 - P04-00008 Leg	2b	Effective force location distance on rear leg from front hole	8.75	inches	
A0 - A01-00001 Chassis & Drive Train (GROUND)	1	X distance from center of front slide plates to fixed bearing	36.5	inches	d_slideFront



A0 - A01-00001 Chassis & Drive Train (GROUND)	1	X distance from center of front caster bracket to fixed bearing	35.63	inches	d_FFC
A0 - A01-00001 Chassis & Drive Train (GROUND)	1	X distance from center of rear caster bracket to fixed bearing	5.22	inches	d_FRC
A0 - P00-00013 Caster Assembly	NA	Eccentric distance from wheel contact point to shaft axis	1.175	inches	d_casterPost
A0 - A01-00009 Slider Subassembly	6	X distance from slider caster pivot center to the rear-most point centered on the screw	42.67	inches	d_SC
A0 - A05-00004 Upholstered Seat Subassembly	5	Length of seat	17	inches	L_seat
A0 - P03-00026 Rear Seat Hanger	5	Center distance between main rear hanger hole and clocking screw hole	3.516	inches	d_hangHoles
A0 - P03-00026 Rear Seat Hanger	5	Angle from left horizontal to normal force vector line	81.82	deg	theta_hangHoles
A0 - A05-00004 Upholstered Seat Subassembly	5	Effective seat length at contact points	15.92	inches	L_seatEff

A0 - P03-00026 Rear Seat Hanger	5	X-distance from main rear hanger hole to seat contact center	0.865	inches	d5seatX
A0 - P03-00026 Rear Seat Hanger	5	Y-distance from main rear hanger hole to seat contact center	7.093	inches	d5seatY
A0 - A01-00015 Full Backrest Subassembly	4	X-distance from A-pivot on link 4 to link 9 attachment point oriented with link 4 in the raise configuration	1.117	inches	d9x
A0 - A01-00015 Full Backrest Subassembly	4	Y-distance from A-pivot on link 4 to link 9 attachment point oriented with link 4 in the raise configuration	1.123	inches	d9y
A0 - P02-00006 Back Tension Bar	9	Link 9 Length	5.25	inches	L9
A0 - P03-00004 Back Slider Bracket	NA	Center of base flange thickness to side hole center	0.535	inches	Ht4Stop
A0 - P03-00004 Back Slider Bracket	NA	End screw hole separation	0.05	inches	End4Stop
A0 - P03-00004 Back Slider Bracket	NA	Screw hole separation	1.5	inches	Holes4Stop
A0 - P02-00006 Back Tension Bar	9	Link 9 active angle	4.25	deg	theta9

A0 - A02-00012 Left Welded Seat Bar Subassembly	5	X-distance from rear back stop bracket hole to the seat pivot hole at A	4.068	inches	d4StopX
A0 - A02-00012 Left Welded Seat Bar Subassembly	5	Y-distance from center of the thickness of the back stop slot to the seat pivot hole at A	0.802	inches	d4StopY

Side Profile Reference Position Dimensions for Kinematic Analysis

Motion 1 & 2

Part Description	Link Number	Dimension Description	Value	Units
A0 - A01-00015 Full Backrest Subassembly	4	Backrest Assembly Weight	20.5	lbf
A0 - A01-00015 Full Backrest Subassembly	4	Backrest Assembly center of mass distance measured perpendicular from pivot hole line	15.4	inches
A0 - A01-00015 Full Backrest Subassembly	5	Backrest Assembly pushrod pivot hole measured perpendicular from above measurement line	3.1	inches
A0 - A00-00001 CreepUp Level Assembly	NA	Weight of all components to raise	40	lbf
A0 - A00-00001 CreepUp Level Assembly	NA	X-distance of push rod/backrest joint in stage 2 config. to the CM of the system (components to raise) in the raise configuration	4.5	inches
Seat Assembly, including legs	5	X-distance from CM of seat assembly to the rear seat/leg pivot (measured from Point A)	4.8	inches
A0 - A00-00001 CreepUp Level	NA	Total System Weight	100	lbf

Assembly				
A0 - A01-00009 Slider Subassembly	6	Percentage of Total Weight carried by the slider caster when the CM total is between the FC and RC casters	10%	
Seat Assembly, including legs	5	Seat Assembly weight including legs	19.5	lbf

### System Speed

#### Backrest angular velocity

Incline Transition Time	7	seconds
Angular Velocity	11.42857143	deg/sec

#### Anatomical Data per <http://www.exrx.net/Kinesiology/Segments.html>

Description	Value	Units
Weight	300	lbf
Height	76	inches
Upper body composition of total weight	0.65	
Upper body composition of total height	0.398	
X-distance of push rod/backrest joint in stage 2 config. To the CM of user in sitting position	14	inches
Head & Neck Percent Body Weight	0.068	
Trunk Percent Body Weight	0.43	
Total Arm Percent Body Weight	0.094	
Head & Neck Percent Body Length	0.108	
Trunk Percent Body Length	0.29	
Head & Neck Length	8.208	inches
Trunk Length	22.04	inches
Head & Neck Percent Segment Length of CM from Proximal End	0.5	
Trunk Percent Segment Length of CM from Proximal End	0.4	
X_CM Head & Neck from Proximal End	4.104	inches
X_CM Trunk from Proximal End	17.024	inches
X_CM Arms from Proximal End	15.124	inches
Weight from Head & Neck	20.4	lbf
Weight from Trunk	129	lbf
Weight from Arms	28.2	lbf
CM of Upper Body (From Proximal End)	13.9	
Upper Body Length	30.248	

Hip to CM of Upper Body	16.4	
Lower Body Length	45.752	
Half way to the feet from the hip (CM of LB from hip with legs outstretched)	22.876	
Half the distance from hip to LB CM (CM of LB from hip with legs bent)	11.438	
Chest Thickness	12	inches

Hardware Specs

Description	Value	Units	Reference
Axial load to torque Coefficient	0.035	in-lb/lb	Experimental
Lead screw pitch	0.15748	inches	4mm ball screw
Ball screw efficiency	0.75		Estimated
Pulley Pitch Diameter	1.378	inches	SDP-SI

## Matlab Code

```
% This program is used to compute primarily the position and velocity
% values for the slider that follows the screw on the original
% prototype in
% order to maintain constant angular velocity during the inclination
% stage
% and constant vertical velocity of the seat in the raising phase.
% It also includes static force computations and formatted outputs
% including charts.
```

```
clear all
close all
clc
```

```
d2r = pi/180;
r2d = 180/pi;
```

```
% Write File
fID = fopen('PVF_CreepUp_Output.txt','wt');
fprintf(fID, 'OUTPUTS FOR POSITION, VELOCITY, & FORCES');
fprintf(fID, '\n=====');

```

```
%% Inputs from SolidWorks Motion Analysis
GravityRaise = csvread('Linear Motor Force (gravity only in Raise
Configuration).csv', 2, 0);
time_grx = GravityRaise(:,1)+6;
Fmotor_grx = GravityRaise(:,2);
```

```
FullLoadRaise = csvread('Linear Motor Force (Full Load in Raise
Configuration).csv', 2, 0);
time_flx = FullLoadRaise(:,1)+6;
Fmotor_flx = FullLoadRaise(:,2);
```

```

%% RANGE OF MOTION
input_dim = xlsread('PVF_CreepUp_Inputs.xlsx','Motion Range');
back_sweep = input_dim(1,1);
leg_sweep = input_dim(4,1);

%% LINK DIMENSIONS
part_dim = xlsread('PVF_CreepUp_Inputs.xlsx','Part Dimensions');
% Link 1: Main Ground; Chassis
L12 = part_dim(1,3); %> Linear distance between rear leg
pivot % hole center to rear-most point in
the % chassis rail tube, centered on the
screw
theta12 = part_dim(2,3); %> Angle from horizontal to line from
% the rear leg pivot hole center to
% the rear-most point in the chassis
% rail tube, centered on the screw;
% Converted to radians
d_slideFront = part_dim(22,3); % X distance from center of front
slide % plates to fixed bearing
d_FFC = part_dim(23,3); % X distance from center of front
caster % bracket to fixed bearing
d_FRC = part_dim(24,3); % X distance from center of rear caster
% bracket to fixed bearing

% Link 2: Leg
L2 = part_dim(3,3); %> Leg length (pivot to pivot)
theta2_0 = part_dim(4,3); %> Initial leg link angle (angle of leg
% during incline motion)
L2am = part_dim(20,3); % Effective force location distance on
% front leg from rear hole
L2bm = part_dim(21,3); % Effective force location distance on
rear % leg from front hole

% Link 3: Push Rod
L3 = part_dim(5,3); %> Push rod length

% Link 4: Backrest Frame
L4 = part_dim(6,3); %> Backrest link length (distance
between % pivot holes)
theta4_0 = part_dim(7,3); %> Initial link (at lower limit) angle
of % backrest (link 4)
L41 = part_dim(8,3); %> Linear distance from push rod pivot
hole % center to upper backrest attachment
% pivot hole center

```



```

d4StopY = part_dim(41,3); % Y-distance from center of the thickness
of
                                % the back stop slot to the seat pivot
hole
                                % at A

% Link 6: Slider Subassembly
L6 = part_dim(13,3);           % Length from push rod pivot hole
center
                                % to the rear-most point centered on
the
                                % screw
theta6 = part_dim(14,3);      % Angle from horizontal to line from
the
                                % push rod pivot hole center to the
                                % rear-most point centered on the screw
d_SC = part_dim(26,3);        % X distance from slider caster pivot
centered on
                                % center to the rear-most point
                                % the screw

% Link 7: Upper backrest support
L7 = part_dim(15,3);          % Linear distance from upper backrest
opposite
                                % attachment pivot hole center to
                                % end of back support

% Link 8: Bridge
L8 = part_dim(16,3);          %> Distance from bridge pivot center to
top
                                % end of bridge

% Link 9: Tensile Back Stop Member
L9 = part_dim(16,3);          % Link 9 length
theta9 = part_dim(39,3);      % Link 9 active angle

% Other Parts
d_casterPost = part_dim(25,3); % Eccentric distance from wheel
contact
                                % point to shaft axis
Ht4Stop = part_dim(36,3);     % Back stop slider center of base
flange
                                % thickness to side hole center
End4Stop = part_dim(37,3);    % Back stop slider End screw hole
                                % separation
Holes4Stop = part_dim(38,3);  % Back stop slider Screw hole
separation

%% MASS INPUTS
mass = xlsread('PVF_CreepUp_Inputs.xlsx','CM');
W4 = mass(1,3)/2;             % Set weight of link 4 to half of backrest
                                % assembly weight
L4CM1 = mass(2,3);           % Distance normal from link 4 to the center
of

```



```

L4CM2 = mass(3,3); % mass of the backrest assembly
                    % Distance normal from L4CM1 line to the
                    % pushrod attachment pivot
WsysUP = mass(4,3)/2; % Half the Weight of all parts on the
creeper % that will be raised with the user
dCM_sys = mass(5,3); % X-distance of push rod/backrest joint in
                    % stage 2 config. to the CM of the system
                    % (components to raise)
d5CM = mass(6,3); % X-distance from CM of seat assembly to
the % rear seat/leg pivot (Point A)
W_sys = mass(7,3)/2; % Half of Total system weight
W5 = mass(9,3)/2; % Set weight of seat assembly (link 5) to
half % of seat assembly weight

%% SPEED INPUTS
input_spd = xlsread('PVF_CreepUp_Inputs.xlsx','Speeds');
omega4r = input_spd(2,1)*d2r; % Rotation speed of backrest for
stage 1
inclineTime = input_spd(1,1); % Approximate time to incline
backrest

%% ANATOMICAL INPUTS
anatomy = xlsread('PVF_CreepUp_Inputs.xlsx','Anatomical Inputs');
Wt = anatomy(1,1); % Max user weight
Ht = anatomy(2,1); % Max user height
pct_wt = anatomy(3,1); % Percentage of user weight is upper
body
pct_ht = anatomy(4,1); % Percentage of user height is upper
body
dWt = anatomy(5,1); % X-distance of push rod/backrest joint
in % stage 2 config. To the CM of user in
                    % sitting position
L_headneck = anatomy(11,1); % Length of the head and neck combined
d_ubProximal = anatomy(21,1); % Distance from proximal end to upper
                    % body CM
dub = anatomy(23,1); % Hip to CM of Upper Body
dlb_max = anatomy(25,1); % Hip to CM of LB from hip with legs
                    % outstretched
dlb_min = anatomy(26,1); % Hip to CM of LB from hip with legs
bent
chest_thk = anatomy (27,1); % Chest Thickness

%% HARDWARE SPECS
hardware = xlsread('PVF_CreepUp_Inputs.xlsx','Hardware Specs');
pitch = hardware(2,1); % Ball screw pitch (inches)
eff = hardware(3,1); % Ball screw efficiency
PulleyPD = hardware(4,1); % Ball screw efficiency
Ax2Tq = pitch/(2*pi*eff); % Axial load to torque conversion factor
                    % according to Nook industries (lb*in/lb)

%% System CM Values

```

```

CM = xlsread('CM Distances as Functions of Input Angles.xlsx');
dCMsys1 = CM(14,2);

%% Additional Prep Calculations
Wt = Wt/2; % Consider only half the weight as we
analyze % only one side of the system
Wub = pct_wt*Wt; % Half the upper body weight
Wlb = (1-pct_wt)*Wt; % Half the lower body weight
Wseat = WsysUP-W4; % Wseat is the weight of the moveable
system % left over after subtracting off the
backrest
theta4_max = theta4_0 + back_sweep;
armWlb = dlb_max; % For now, set the lower body CM distance
from % A to the max since legs are stretched out
for % this portion of the motion
dWub = Hip2Back-dub; % Application distance of Wub on backrest
from % upper backrest pivot

%% Prelim Setup
nSteps_1 = 100; % Set number of steps for each
nSteps_2 = 100; % stage.
totalSteps = nSteps_1+nSteps_2+1; % Compute array size based on
step % quantities.

timeStep_1 = inclineTime/(nSteps_1); % Determine the time step size
from % the prescribed incline time
and % the number of steps for the
% calculation

t = 0; % Initialize time

time = zeros(totalSteps,1); % Array preallocations
theta3r = zeros(totalSteps,1);
theta4r = zeros(totalSteps,1);
theta2r = zeros(totalSteps,1);
theta78r = zeros(totalSteps,1);
omega78r = zeros(totalSteps,1);
LBOLs = zeros(totalSteps,1); % Bridge backrest overlap
length
LBOLDots = zeros(totalSteps,1);
L11 = zeros(totalSteps,1);
L11dot = zeros(totalSteps,1);
omega3r = zeros(totalSteps,1);
V2X = zeros(totalSteps,1);
F3 = zeros(totalSteps,1);

```

```
F3x = zeros(totalSteps,1);
F3y = zeros(totalSteps,1);
F3type = zeros(totalSteps,1);
FvLateral = zeros(totalSteps,1);
F2m = zeros(totalSteps,1);
F2a = zeros(totalSteps,1);
F2ax = zeros(totalSteps,1);
F2ay = zeros(totalSteps,1);
F2aC = zeros(totalSteps,1);
F2aCx = zeros(totalSteps,1);
F2aCy = zeros(totalSteps,1);
F2aS = zeros(totalSteps,1);
F2aSx = zeros(totalSteps,1);
F2aSy = zeros(totalSteps,1);
F2b = zeros(totalSteps,1);
F2bx = zeros(totalSteps,1);
F2by = zeros(totalSteps,1);
F2bC = zeros(totalSteps,1);
F2bCx = zeros(totalSteps,1);
F2bCy = zeros(totalSteps,1);
F2bS = zeros(totalSteps,1);
F2bSx = zeros(totalSteps,1);
F2bSy = zeros(totalSteps,1);
F4A = zeros(totalSteps,1);
F4Ax = zeros(totalSteps,1);
F4Ay = zeros(totalSteps,1);
Fstop = zeros(totalSteps,1);
F78L = zeros(totalSteps,1);
F78U = zeros(totalSteps,1);
FC = zeros(totalSteps,1);
FCx = zeros(totalSteps,1);
FCy = zeros(totalSteps,1);
FD = zeros(totalSteps,1);
FDx = zeros(totalSteps,1);
FDy = zeros(totalSteps,1);
FRC = zeros(totalSteps,1);
FFC = zeros(totalSteps,1);
FSC = zeros(totalSteps,1);
MSC = zeros(totalSteps,1);
Fscrew = zeros(totalSteps,1);
F5Ax = zeros(totalSteps,1);
F5Ay = zeros(totalSteps,1);
FseatX = zeros(totalSteps,1);
FseatY = zeros(totalSteps,1);
FhangScrew = zeros(totalSteps,1);
Fseat_friction = zeros(totalSteps,1);
Fslide_front = zeros(totalSteps,1);
Fslide_rear = zeros(totalSteps,1);
F5_front = zeros(totalSteps,1);
F5_rearX = zeros(totalSteps,1);
F5_rearY = zeros(totalSteps,1);
dCMUB = zeros(totalSteps,1);
dCMLB = zeros(totalSteps,1);
dCMsys = zeros(totalSteps,1);
```

```

dLB = zeros(totalSteps,1);
X_TOT = zeros(totalSteps,1);
F9x = zeros(totalSteps,1);
F9y = zeros(totalSteps,1);
F9 = zeros(totalSteps,1);
F9screwX = zeros(totalSteps,1);
F9screwYfront = zeros(totalSteps,1);
F9screwYrear = zeros(totalSteps,1);
FslideFront = zeros(totalSteps,1);
FslideRear = zeros(totalSteps,1);
A = zeros(25,25);
B = zeros(25,25);
C = zeros(6,6);
P = zeros(25,1);
Q = zeros(25,1);
R = zeros(6,1);
M8 = zeros(totalSteps,1);

%% Stage 1: INCLINE

theta4r(1,1) = theta4_0*d2r;           % Initialize theta 4
theta12r = theta12*d2r;               % Convert to rads
theta6r = theta6*d2r;
theta5r = theta5*d2r;

for i = 1:nSteps_1+1
    time(i,1) = t;
    % Solve for Loop 2 Position Terms (from eqns (i) & (ii) in
analysis)
    theta2r(i,1) = theta2_0*d2r; %pi - asin(PivHt_1/L2);
    theta3r(i,1) = asin((L12*sin(theta12r) + L2*sin(theta2r(i,1)) - ...
        L4*sin(theta4r(i,1)) - L6*sin(theta6r))/L3); % (2.3)
    L11(i,1) = L3*cos(theta3r(i,1)) + L4*cos(theta4r(i,1)) + ...
        L6*cos(theta6r) - L2*cos(theta2r(i,1)) - L12*cos(theta12r); %
(2.4)

    % Newtons Method to solve for Loop 1 Position Unknowns
    e = 1; % Initialize error
    n = 0; % Initialize Cycle Counter
    LBOL = 6; % Initial guess for overlap length
    theta78 = 40*d2r; % Initial guess for back pad/bridge angle

    while abs(e) > 1e-8
        f = L4*cos(theta4r(i,1)) - L5*cos(theta5r) + L8*cos(theta78) +
...
            L7*cos(theta78) - LBOL*cos(theta78) - ...
            L41*cos(theta4r(i,1) + delta41*d2r);
        g = L4*sin(theta4r(i,1)) - L5*sin(theta5r) + L8*sin(theta78) +
...
            L7*sin(theta78) - LBOL*sin(theta78) - ...
            L41*sin(theta4r(i,1) + delta41*d2r);
        f_LBOL = -cos(theta78);
        f_theta78 = (LBOL-L7-L8)*sin(theta78);
    end
end

```

```

g_LBOL = -sin(theta78);
g_theta78 = (-LBOL+L7+L8)*cos(theta78);

dVEC = [f_LBOL f_theta78; g_LBOL g_theta78]\[-f;-g];
dLBOL = dVEC(1);
dtheta78 = dVEC(2);

e = max(abs(dLBOL),abs(dtheta78));

LBOL = LBOL + dLBOL;
theta78 = theta78 + dtheta78;

n = n+1;
end
theta78r(i,1) = theta78;
LBOLs(i,1) = LBOL;

% Solve for Loop 2 Velocity Terms (from eqns (iii) & (iv) in
analysis)
omega3r(i,1) = -L4*omega4r*cos(theta4r(i,1))/...
(L3*cos(theta3r(i,1))); % (vii)
L1ldot(i,1) = -(L3*omega3r(i,1)*sin(theta3r(i,1)) + ...
L4*omega4r*sin(theta4r(i,1))); % (viii)

% Newtons Method to solve for Loop 1 Velocity Unknowns
e = 1; % Initialize error
n = 0; % Initialize Cycle Counter
LBOLdot = 1; % Initial guess for overlap length rate of change
omega78 = omega4r; % Initial guess for back pad/bridge angular
vel.

while abs(e) > 1e-8
f2 = L4*omega4r*cos(theta4r(i,1)) + ...
(L7+L8-LBOLs(i,1))*omega78*cos(theta78) - ...
LBOLdot*sin(theta78) - ...
L41*omega4r*cos(theta4r(i,1) + delta41*d2r);
g2 = -L4*omega4r*sin(theta4r(i,1)) - ...
(L7+L8-LBOLs(i,1))*omega78*sin(theta78) - ...
LBOLdot*cos(theta78) + ...
L41*omega4r*sin(theta4r(i,1) + delta41*d2r);
f_LBOLdot = -sin(theta78);
f_omega78 = (-LBOLs(i,1)+L7+L8)*cos(theta78);
g_LBOLdot = -cos(theta78);
g_omega78 = (LBOLs(i,1)-L7-L8)*sin(theta78);

dVEC = [f_LBOLdot f_omega78; g_LBOLdot g_omega78]\[-f2;-g2];
dLBOLdot = dVEC(1);
domega78 = dVEC(2);

e = max(abs(dLBOLdot),abs(domega78));

```



```

A(9,11) = -1;
P(9,1) = W4;

A(10,25) = -d_hangHoles;           % (x)
A(10,20) = legSep;
A(10,4) = legSep;
P(10,1) = -W5*d5CM;

A(11,3) = 1;                       % (xi)
A(11,12) = 1;
A(11,7) = 1;
A(11,21) = -1;
A(11,25) = -cos(theta_hangHoles*d2r);

A(12,4) = -1;                      % (xii)
A(12,13) = 1;
A(12,20) = -1;
A(12,22) = -1;
A(12,8) = -1;
A(12,25) = sin(theta_hangHoles*d2r);
P(12,1) = W5;

A(13,9) = L2am;                    % (xiii)
A(13,3) = L2*sin(pi-theta2r(i,1));
A(13,4) = -L2*cos(pi-theta2r(i,1));

A(14,4) = 1;                       % (xiv)
A(14,9) = -1;
A(14,2) = -1;

A(15,3) = -1;                      % (xv)
A(15,1) = 1;

A(16,9) = L2bm;                   % (xvi)
A(16,5) = L2*sin(pi-theta2r(i,1));
A(16,6) = -L2*cos(pi-theta2r(i,1));

A(17,8) = 1;                      % (xvii)
A(17,9) = 1;
A(17,6) = -1;

A(18,7) = -1;                     % (xviii)
A(18,5) = 1;

A(19,25) = d_hangHoles;           % (xix)
A(19,23) = -d5seatY;
A(19,24) = -d5seatX;
A(19,17) = L5*cos(theta5r);
A(19,16) = L5*sin(theta5r);

A(20,21) = 1;                     % (xx)

```

```

A(20,16) = 1;
A(20,23) = -1;
A(20,25) = cos(theta_hangHoles*d2r);

A(21,22) = 1; % (xxi)
A(21,24) = -1;
A(21,17) = -1;
A(21,25) = -sin(theta_hangHoles*d2r);

dCMsys(i,1) = dCMsys1;
dLB(i,1) = dlb_max;
dCMUB(i,1) = chest_thk*sin(theta78) + dWub*cos(theta78) - ...
(L7+L8-LBOL)*cos(theta78) + L5*cos(theta5r) - ...
L2*cos(theta2r(i,1)) - L12*cos(theta12r);
dCMLB(i,1) = dLB(i,1) - L2*cos(theta2r(i,1)) -
L12*cos(theta12r);
X_TOT(i,1) = (Wlb*dCMLB(i,1) + Wub*dCMUB(i,1) + ...
W_sys*dCMsys(i,1))/(W_sys+Wt);
if (dLB(i,1)+d5seatX)>L_seatEff*cos(thetaSeat*d2r)
dLBplusd5seatX = L_seatEff*cos(thetaSeat*d2r);
else
dLBplusd5seatX = (dLB(i,1)+d5seatX);
end

A(22,20) = L_seatEff*cos(thetaSeat*d2r); % (xxii)
P(22,1) = dLBplusd5seatX*Wlb + ...
chest_thk/2*cos(thetaSeat*d2r)*Wub*(sin(theta78))^2 + ...
chest_thk/2*sin(thetaSeat*d2r)*Wub*sin(theta78)*cos(theta78);

A(23,23) = 1; % (xxiii)
P(23,1) = Wub*sin(theta78)*cos(theta78);

A(24,20) = 1; % (xxiv)
A(24,24) = 1;
P(24,1) = Wlb + Wub*(sin(theta78))^2;

A(25,11) = L3*cos(theta3r(i,1)); % (xxv)
A(25,10) = -L3*sin(theta3r(i,1));

res = A\P;

% Store variables in corresponding arrays
F2aCx(i,1) = res(1);
F2aCy(i,1) = res(2);
F2aSx(i,1) = res(3);
F2aSy(i,1) = res(4);
F2bCx(i,1) = res(5);
F2bCy(i,1) = res(6);
F2bSx(i,1) = res(7);
F2bSy(i,1) = res(8);
F2m(i,1) = res(9);
F3x(i,1) = res(10);
F3y(i,1) = res(11);

```



```

F4Ax(i,1) = res(12);
F4Ay(i,1) = res(13);
F78L(i,1) = res(14);
F78U(i,1) = res(15);
FCx(i,1) = res(16);
FCy(i,1) = res(17);
FDx(i,1) = res(18);
FDy(i,1) = res(19);
F5_front(i,1) = res(20);
F5Ax(i,1) = res(21);
F5Ay(i,1) = res(22);
FseatX(i,1) = res(23);
FseatY(i,1) = res(24);
FhangScrew(i,1) = res(25);
F9x(i,1) = 0;
F9y(i,1) = 0;
F9screwX(i,1) = 0;
F9screwYfront(i,1) = 0;
F9screwYrear(i,1) = 0;

% Force components for Z and Y for Femap analysis
beta1 = theta4r(i,1)-theta4_0*d2r;
F3Zfem = F3x(i,1)*cos(beta1)+F3y(i,1)*sin(beta1);
F3Yfem = F3x(i,1)*sin(beta1)-F3y(i,1)*cos(beta1);
F3fem(i,1) = F3Zfem;
F3fem(i,2) = F3Yfem;

% Force Set 2 (chassis forces)
C(1,4) = d_SC-(d_slideFront-L11(i,1));
C(1,5) = -d_SC;
C(1,6) = 1;
R(1,1) = (d_SC + L6*cos(theta6r))*F3y(i,1);

R(2,1) = 0.25*(Wt+W_sys);

C(3,1) = 1;
C(3,4) = -1;
C(3,5) = 1;
R(3,1) = -F3y(i,1);

C(4,1) = d_casterPost;
C(4,6) = -1;

C(5,4) = d_slideFront;
C(5,2) = d_FFC;
C(5,5) = -L11(i,1);
C(5,3) = d_FRC;
R(5,1) = (L12*cos(theta12r) - legSep)*F2aCy(i,1) + ...
        L12*cos(theta12r)*F2bCy(i,1) + L12*sin(theta12r)*F2aCx(i,1) +
...
        L12*sin(theta12r)*F2bCx(i,1);

C(6,2) = 1;

```

```

C(6,3) = 1;
C(6,4) = 1;
C(6,5) = -1;
R(6,1) = -(F2aCy(i,1) + F2bCy(i,1));

if X_TOT(i,1)>=d_FFC
    C(2,1) = 0;
    C(2,3) = 1;
else
    C(2,1) = 1;
    C(2,3) = 0;
end

res2 = C\R;

FSC(i,1) = res2(1);
FFC(i,1) = res2(2);
FRC(i,1) = res2(3);
FslideFront(i,1) = res2(4);
FslideRear(i,1) = res2(5);
MSC(i,1) = res2(6);

% Additional Incline Value Processing
F3(i,1) = sqrt(F3x(i,1)^2+F3y(i,1)^2);
if F3x(i,1)<=0 || F3y(i,1)<=0
    F3(i,1) = F3(i,1);
%     F3type(i,1) = {'Compression'};
% else
%     F3type(i,1) = {'Tension'};
end

F2aC(i,1) = sqrt(F2aCx(i,1)^2+F2aCy(i,1)^2);
F2bC(i,1) = sqrt(F2bCx(i,1)^2+F2bCy(i,1)^2);
F2aS(i,1) = sqrt(F2aSx(i,1)^2+F2aSy(i,1)^2);
F2bS(i,1) = sqrt(F2bSx(i,1)^2+F2bSy(i,1)^2);

F9(i,1) = sqrt(F9x(i,1)^2+F9y(i,1)^2);
if F9x(i,1)<0 || F9y(i,1)<0
    F9(i,1) = -F9(i,1);
%     F9type(i,1) = {'Compression'};
% else
%     F9type(i,1) = {'Tension'};
end

FC(i,1) = sqrt(FCx(i,1)^2+FCy(i,1)^2);
FD(i,1) = sqrt(FDx(i,1)^2+FDy(i,1)^2);
F4A(i,1) = sqrt(F4Ax(i,1)^2+F4Ay(i,1)^2);
F5A(i,1) = sqrt(F5Ax(i,1)^2+F5Ay(i,1)^2);
M8(i,1) = FC(i,1)*(L8-LBOL);

FslideMax(i,:) = ...

```

```

        [(d_FFC-L11(i,1)) 0
         1 -1]\...
        [-L6*cos(theta6r)*F3y(i,1) + L6*sin(theta6r)*F3x(i,1)
         F3y(i,1)];
    FslideFrontMax(i,1) = FslideMax(i,1);
    FslideRearMax(i,1) = FslideMax(i,2);
    M6MAX(i,1) = FslideRearMax(i,1)*(d_FFC-L11(i,1));

    t = t+timeStep_1;
    % The angle of the backrest (input) is increased to the next step
    theta4r(i+1,1) = theta4r(i,1) + omega4r*timeStep_1;
end

% Set the rest of the theta4 values in the second stage of the motions
to
% be fixed as the ending value of stage 1
theta4r(nSteps_1+2:totalSteps,1) = theta4r(nSteps_1+1,1);

%% Transition Analysis
% The purpose of the transition section is to compute the rate at
whiche
% the system would rise at the very start of stage 2 if the slider
velocity
% is the same as it was at the very end of stage 1

theta3_trans = theta3r(nSteps_1+1,1);
theta2_trans = theta2r(nSteps_1+1,1);
L11_trans = L11(nSteps_1+1,1);
L11dot_trans = L11dot(nSteps_1+1,1);
% Compute the angular velocity of link 2 (rear leg)
omega2_trans = L11dot_trans/(L2*(sin(theta2_trans)-...
    tan(theta3_trans)*cos(theta2_trans)));
raiseRate = omega2_trans*L2*cos(theta2_trans); % (xiii)

%% Stage 2: RAISE
% Compute total vertical movement
dSeatHt = L2*sin(theta2_0*d2r-leg_sweep*d2r)-L2*sin(theta2_0*d2r);
raiseTime = dSeatHt/raiseRate; % Compute total time for stage
2
timeStep_2 = raiseTime/(nSteps_2); % Compute time step size
hStep = dSeatHt/nSteps_2; % seat height raise step
h = L2*sin(theta2_0*d2r); % Set initial height at lower
limit
% leg pivot height
t = t-timeStep_1+timeStep_2; % Account for time step
increase
% at the end of stage 1 and
begin
% stage 2 with appropriate time
% step.
CMLBstep = (dlb_max-dlb_min)/(nSteps_2); % Determine the movement
interval
% for the lower body CM

```

```

% Fres = [Wt*dWt + WsysUP*dCMsys
%         0
%         Wt + WsysUP]; % Known Forces from eqn. (xiii)
beta = 0;
for j=nSteps_1+2:nSteps_1+nSteps_2+1
    time(j,1) = t;
    h = h + hStep;
    dh = h-L2*sin(theta2_0*d2r); %> Compute change in height of
                                % upper leg pivot since its
                                % initial position (7.2)

    % Position Terms
    theta2r(j,1) = pi-asin(dh/L2+sin(theta2_0*d2r)); % (7.1)
    theta3r(j,1) = asin((L12*sin(theta12r) + L2*sin(theta2r(j,1)) - ...
        L4*sin(theta4r(j,1)) - L6*sin(theta6r))/L3); % (2.3)
    L11(j,1) = L3*cos(theta3r(j,1)) + L4*cos(theta4r(j,1)) + ...
        L6*cos(theta6r) - L2*cos(theta2r(j,1)) - L12*cos(theta12r); %
(2.4)
    theta78r(j,1) = theta78;
    LBOLs(j,1) = LBOL;

    % Velocity Terms
    omega2r = raiseRate/(L2*cos(theta2r(j,1))); % (xiv)
    omega3r(j,1) = L2*omega2r*cos(theta2r(j,1))/...
        (L3*cos(theta3r(j,1))); % (vii)
    L11dot(j,1) = L2*omega2r*sin(theta2r(j,1)) - ...
        L3*omega3r(j,1)*sin(theta3r(j,1)); % (viii)
    omega78r(i,1) = omega78;
    LBOLdots(i,1) = LBOLdot;

    % Static Force Calculations
    B(1,14) = L7/(dWub*cos(theta78)); % (i)
    B(1,15) = (LBOL - L7)/(dWub*cos(theta78));
    Q(1,1) = Wub;

    B(2,14) = 1/cos(theta78); % (ii)
    B(2,15) = -1/cos(theta78);
    B(2,18) = 1/(cos(theta78)*sin(theta78));
    Q(2,1) = Wub;

    B(3,18) = 1; % (iii)
    B(3,19) = -tan(theta78);

    B(4,14) = LBOL-L8; % (iv)
    B(4,15) = L8;

    B(5,16) = 1/sin(theta78); % (v)
    B(5,14) = -1;
    B(5,15) = 1;

    B(6,16) = 1; % (vi)
    B(6,17) = -tan(theta78);

```

```

alpha4CM = theta4r(j,1) - pi/2;
d4CM = L4CM1 *cos(alpha4CM) - L4CM2*sin(alpha4CM);

B(7,18) = -L41*sin(delta41*d2r + theta4r(j,1));    % (vii)
B(7,19) = -L41*cos(delta41*d2r + theta4r(j,1));
B(7,12) = L4*cos(theta4r(j,1)-pi/2);
B(7,13) = L4*sin(theta4r(j,1)-pi/2);
B(7,3) = -d9x;
B(7,4) = -d9y;
Q(7,1) = W4*d4CM;

B(8,18) = 1;    % (viii)
B(8,12) = -1;
B(8,10) = -1;
B(8,3) = -1;

B(9,19) = -1;    % (ix)
B(9,13) = -1;
B(9,11) = -1;
B(9,4) = -1;
Q(9,1) = W4;

B(10,25) = -d_hangHoles;    % (x)
B(10,20) = legSep;
B(10,2) = legSep;
B(10,9) = d4StopX;
B(10,7) = 2*d4StopY;
B(10,8) = d4StopX + Holes4Stop;
Q(10,1) = -W5*d5CM;

B(11,1) = 1;    % (xi)
B(11,12) = 1;
B(11,5) = 1;
B(11,21) = -1;
B(11,7) = 2;
B(11,25) = -cos(theta_hangHoles*d2r);

B(12,2) = -1;    % (xii)
B(12,20) = -1;
B(12,22) = -1;
B(12,6) = -1;
B(12,8) = -1;
B(12,9) = -1;
B(12,13) = 1;
B(12,25) = sin(theta_hangHoles*d2r);
Q(12,1) = W5;

B(13,1) = L2*sin(pi-theta2r(j,1));    % (xiii)
B(13,2) = -L2*cos(pi-theta2r(j,1));

B(14,5) = L2*sin(pi-theta2r(j,1));    % (xiv)

```

```

B(14,6) = -L2*cos(pi-theta2r(j,1));

B(15,4) = L9*cos(theta9*d2r);           % (xv)
B(15,3) = -L9*sin(theta9*d2r);

B(16,3) = Ht4Stop;
B(16,4) = -End4Stop;
B(16,8) = -Holes4Stop;

B(17,3) = 1;
B(17,7) = -2;

B(18,4) = 1;
B(18,8) = 1;
B(18,9) = 1;

B(19,25) = d_hangHoles;                 % (xix)
B(19,23) = -d5seatY;
B(19,24) = -d5seatX;
B(19,17) = L5*cos(theta5r);
B(19,16) = L5*sin(theta5r);

B(20,21) = 1;                           % (xx)
B(20,16) = 1;
B(20,23) = -1;
B(20,25) = cos(theta_hangHoles*d2r);

B(21,22) = 1;                             % (xxi)
B(21,24) = -1;
B(21,17) = -1;
B(21,25) = -sin(theta_hangHoles*d2r);

    P1X = CM(5,1); % X and Y values of 2 points used for the
equation
    P1Y = CM(5,2); % for the linear changing system center of mass
    P2X = CM(1,1);
    P2Y = CM(1,2);
    m1 = (P2Y-P1Y)/(P2X-P1X);
    dCMsys2 = m1*(theta2r(j,1)*r2d-P1X) + P1Y;
    dCMsys(j,1) = dCMsys2;

    m2 = (dlb_min-dlb_max)/(nSteps_2-1);
    dLB(j,1) = dlb_min + (dlb_max-dlb_min)*cos(beta);
    beta = beta + pi/(2*nSteps_2);

    dCMUB(j,1) = chest_thk*sin(theta78) + dWub*cos(theta78) - ...
        (L7+L8-LBOL)*cos(theta78) + L5*cos(theta5r) - ...
        L2*cos(theta2r(j,1)) - L12*cos(theta12r);
    dCMLB(j,1) = dLB(j,1) - L2*cos(theta2r(j,1)) -
L12*cos(theta12r);
    X_TOT(j,1) = (Wlb*dCMLB(j,1) + Wub*dCMUB(j,1) + ...
        W_sys*dCMsys(j,1))/(W_sys+Wt);

```

```

if (dLB(j,1)+d5seatX)>L_seatEff*cos(thetaSeat*d2r)
    dLBplusd5seatX = L_seatEff*cos(thetaSeat*d2r);
else
    dLBplusd5seatX = (dLB(j,1)+d5seatX);
end

B(22,20) = L_seatEff*cos(thetaSeat*d2r);           % (xxii)
Q(22,1) = dLBplusd5seatX*Wlb + ...
    chest_thk/2*cos(thetaSeat*d2r)*Wub*(sin(theta78))^2 + ...
    chest_thk/2*sin(thetaSeat*d2r)*Wub*sin(theta78)*cos(theta78);

B(23,23) = 1;                                     % (xxiii)
Q(23,1) = Wub*sin(theta78)*cos(theta78);

B(24,20) = 1;                                     % (xxiv)
B(24,24) = 1;
Q(24,1) = Wlb + Wub*(sin(theta78))^2;

B(25,11) = L3*cos(theta3r(j,1));                 % (xxv)
B(25,10) = -L3*sin(theta3r(j,1));

res = B\Q;

F2aCx(j,1) = res(1);
F2aCy(j,1) = res(2);
F2aSx(j,1) = res(1);
F2aSy(j,1) = res(2);
F2bCx(j,1) = res(5);
F2bCy(j,1) = res(6);
F2bSx(j,1) = res(5);
F2bSy(j,1) = res(6);
F9x(j,1) = res(3);
F9y(j,1) = res(4);
F9screwX(j,1) = res(7);
F9screwYfront(j,1) = res(8);
F9screwYrear(j,1) = res(9);
F2m(j,1) = 0;
F3x(j,1) = res(10);
F3y(j,1) = res(11);
F4Ax(j,1) = res(12);
F4Ay(j,1) = res(13);
F78L(j,1) = res(14);
F78U(j,1) = res(15);
FCx(j,1) = res(16);
FCy(j,1) = res(17);
FDx(j,1) = res(18);
FDy(j,1) = res(19);
F5_front(j,1) = res(20);
F5Ax(j,1) = res(21);
F5Ay(j,1) = res(22);
FseatX(j,1) = res(23);
FseatY(j,1) = res(24);
FhangScrew(j,1) = res(25);

```

```

% Force components for Z and Y for Femap analysis
beta1 = theta4r(j,1)-theta4_0*d2r;
F3Zfem = F3x(j,1)*cos(beta1)+F3y(j,1)*sin(beta1);
F3Yfem = F3x(j,1)*sin(beta1)-F3y(j,1)*cos(beta1);
F3fem(j,1) = F3Zfem;
F3fem(j,2) = F3Yfem;

% Force Set 2 (chassis forces)
C(1,4) = d_SC-(d_slideFront-L11(j,1));
C(1,5) = -d_SC;
C(1,6) = 1;
R(1,1) = (d_SC + L6*cos(theta6r))*F3y(j,1);

R(2,1) = 0.25*(Wt+W_sys);

C(3,1) = 1;
C(3,4) = -1;
C(3,5) = 1;
R(3,1) = -F3y(j,1);

C(4,1) = d_casterPost;
C(4,6) = -1;

C(5,4) = d_slideFront;
C(5,2) = d_FFC;
C(5,5) = -L11(j,1);
C(5,3) = d_FRC;
R(5,1) = (L12*cos(theta12r) - legSep)*F2aCy(j,1) + ...
        L12*cos(theta12r)*F2bCy(j,1) + L12*sin(theta12r)*F2aCx(j,1) +
...
        L12*sin(theta12r)*F2bCx(j,1);

C(6,2) = 1;
C(6,3) = 1;
C(6,4) = 1;
C(6,5) = -1;
R(6,1) = -(F2aCy(j,1) + F2bCy(j,1));

if X_TOT(j,1)>=d_FFC
    C(2,1) = 0;
    C(2,3) = 1;
else
    C(2,1) = 1;
    C(2,3) = 0;
end

res2 = C\R;

FSC(j,1) = res2(1);
FFC(j,1) = res2(2);
FRC(j,1) = res2(3);

```



```

FslideFront(j,1) = res2(4);
FslideRear(j,1) = res2(5);
MSC(j,1) = res2(6);

% Additional Incline Value Processing
F3(j,1) = sqrt(F3x(j,1)^2+F3y(j,1)^2);
if F3x(j,1)<=0 || F3y(j,1)<=0
    F3(j,1) = F3(j,1);
%     F3type(j,1) = {'Compression'};
% else
%     F3type(j,1) = {'Tension'};
end

F2aC(j,1) = sqrt(F2aCx(j,1)^2+F2aCy(j,1)^2);
F2bC(j,1) = sqrt(F2bCx(j,1)^2+F2bCy(j,1)^2);
F2aS(j,1) = sqrt(F2aSx(j,1)^2+F2aSy(j,1)^2);
F2bS(j,1) = sqrt(F2bSx(j,1)^2+F2bSy(j,1)^2);

F9(j,1) = sqrt(F9x(j,1)^2+F9y(j,1)^2);
if F9x(j,1)<0 || F9y(j,1)<0
    F9(j,1) = -F9(j,1);
end

FC(j,1) = sqrt(FCx(j,1)^2+FCy(j,1)^2);
FD(j,1) = sqrt(FDx(j,1)^2+FDy(j,1)^2);
F4A(j,1) = sqrt(F4Ax(j,1)^2+F4Ay(j,1)^2);
F5A(j,1) = sqrt(F5Ax(j,1)^2+F5Ay(j,1)^2);
M8(j,1) = FC(j,1)*(L8-LBOL);

FslideMax(j,:) = ...
    [(d_FFC-L11(j,1)) 0
    1 -1]\...
    [-L6*cos(theta6r)*F3y(j,1) + L6*sin(theta6r)*F3x(j,1)
    F3y(j,1)];
FslideFrontMax(j,1) = FslideMax(j,1);
FslideRearMax(j,1) = FslideMax(j,2);
M6MAX(j,1) = FslideRearMax(j,1)*(d_FFC-L11(j,1));

t = t + timeStep_2;
end

slideLen = max(L11) - min(L11); % Total lead screw travel
distance
omegaShaftMax = max(abs(L11dot)/pitch)*60; % RPMs
Torq = abs(F3x*2*Ax2Tq); % Torque of both lead screws combined (in-
lbf)
Torq_inoz = 16*Torq; % Torque converted to in-oz
units
RPS = abs(L11dot)/pitch; % Revs per second of
screws
RPM = 60*abs(L11dot)/pitch; % Revs per minute of
screws
RPS2Torq(:,1) = RPS; % Matrix column 1 is RPS

```

```

RPS2Torq(:,2) = Torq; % Matrix column 2 is torque
RPS2Torq = sortrows(RPS2Torq,1); % Sort the matrix by RPS
T_belt = Torq/(PulleyPD/2); % Belt Tension
REVS = slideLen/pitch;

xval = zeros(20);
yval = zeros(20);
HP = zeros(totalSteps,1);

% Create matrix of values for showing max torque seen at any given RPS
for i=1:20
    xval(i) = max(RPS2Torq(10*i-9:10*i,2)); % Max combined torque of
screws
    yval(i) = max(RPS2Torq(10*i-9:10*i,1)); % Max RPS of screws
end

% Compute Max Horsepower
for i = 1:size(Torq,1)
    HP(i,1) = RPM(i)*Torq(i)/63025.0;
end

Watts = HP*745.7; % Convert HP to W
Amps = Watts/18; % Compute Amps
Eff_max = 0.7; % Maximum DC motor efficiency
Torq_Eff_max = 26.25; % Torque where the DC motor has th max
efficiency
T_max_Drill = 135; % Drill stall torque

for i=1:totalSteps
    if Torq(i) <= Torq_Eff_max;
        DC_Eff(i) = (Eff_max)/(Torq_Eff_max)*Torq(i);
    else Torq(i) > Torq_Eff_max;
        DC_Eff(i) = -Eff_max/(T_max_Drill-Torq_Eff_max)*...
            (Torq(i)-Torq_Eff_max)+Eff_max;
        % Eqn on pg. 58 of Engr Notebook
    end
end

for i=1:totalSteps
    Amps_Eff(i) = Amps(i)/DC_Eff(i);
end

Amp_hr = trapz(time/3600,Amps_Eff); % Amount of Amp-hr to raise all
% the way up
N_cyc_Charge = 1.5/Amp_hr; % Number of cycles on a single
% charge of a 1.5 Ah Battery

fprintf(fID,'\nSlider Stroke: %6.2f Inches %6.2f
mm',slideLen,slideLen*25.4);
fprintf(fID,'\nMax Shaft Speed: %6.0f
RPM',omegaShaftMax);
fprintf(fID,'\nMax Torque: %6.0f in-lb %6.0f
in-oz %6.1f Nm',max(Torq),max(Torq_inoz),max(Torq_inoz)/141.6);

```

```

fprintf(fID, '\nMax Belt Tension:                %6.1f
lbf', max(Torq)/PulleyPD/2);
fprintf(fID, '\nTot. Transition Time:           %6.1f  s', max(time));
fprintf(fID, '\nMaximum Horsepower of Shaft:     %6.1f  HP', max(HP));

fprintf(fID, '\n\nMax Forces:');
fprintf(fID, '\n  Push Rod (Axial):                %6.0f  lbf
[Compression]', max(abs(F3)));
fprintf(fID, '\n  Lead Screw (Axial):                %6.0f  lbf
[Tension]', max(abs(F3x)));
fprintf(fID, '\n  Y-load on Telescopic Slide Pivot:%6.0f
lbf', max(abs(F3y)));
fprintf(fID, '\n  Front Leg (Minimum Axial):           %6.0f
lbf', min(F2a));
fprintf(fID, '\n  Front Leg (Maximum Axial):            %6.0f
lbf', max(F2a));
fprintf(fID, '\n  Rear Leg (Minimum Axial):             %6.0f
lbf', min(F2b));
fprintf(fID, '\n  Rear Leg (Maximum Axial):             %6.0f
lbf', max(F2b));
fclose(fID);

% figure(1)
% hold on
% plot(time, FSC, '--')
% plot(time, FFC, '-')
% plot(time, FRC, ':')
% title('Caster Loads')
% legend('Slider Caster', 'Front (Middle) Caster', 'Rear Caster')

% figure(2)
% hold on
% plot(time, FslideFront, '-')
% plot(time, FslideRear, '--')
% title('Slide Forces')
% legend('Front Slide Force', 'Rear Slide Force')

% plot(time, F3)
% title('F3')
% figure(2)
% plot(time, F9)
% title('F9')
% figure(3)
% plot(time, FC)
% title('FC')
% figure(4)
% plot(time, FD)
% title('FD')
% figure(5)
% plot(time, F4A)
% title('F4A')
% figure(6)
% plot(time, F5A)

```

```

% title('F5A')
% figure(7)
% plot(time,F78U)
% title('F78U')
% figure(8)
% plot(time,F78L)
% title('F78L')
% figure(9)
% plot(time,FhangScrew)
% title('FhangScrew')

% figure(10)
% hold on
% plot(time_grx,Fmotor_grx)
% plot(time(102:201),-F3x(102:201)*2,'--')
% title({'Analysis Method Comparison';'(Gravity Only in Raise
Coffiguration)'})
% legend('SolidWorks','Hand Calculations')
% xlabel('Time at Position (sec)')
% ylabel('Motor Force (lbf)')
%
% figure(11)
% hold on
% plot(time_flx,Fmotor_flx)
% plot(time(102:201),-F3x(102:201)*2,'--')
% title({'Analysis Method Comparison';'(Full Load in Raise
Coffiguration)'})
% legend('SolidWorks','Hand Calculations')
% xlabel('Time at Position (sec)')
% ylabel('Motor Force (lbf)')

    F3(j,1) = sqrt(F3x(j,1)^2+F3y(j,1)^2);
    F9(j,1) = sqrt(F9x(j,1)^2+F9y(j,1)^2);
    FC(j,1) = sqrt(FCx(j,1)^2+FCy(j,1)^2);
    FD(j,1) = sqrt(FDx(j,1)^2+FDy(j,1)^2);
    F4A(j,1) = sqrt(F4Ax(j,1)^2+F4Ay(j,1)^2);
    F5A(j,1) = sqrt(F5Ax(j,1)^2+F5Ay(j,1)^2);

% figure(1)
% plot(xval,yval,'k','linewidth',2)
% xlabel('RPS')
% ylabel('Torque, in-oz')
%
%
% figure(2)
% plot(RPS2Torq(:,1),RPS2Torq(:,2))
% plot(time,abs(L1dot))
%
% figure(3)
% plot(time,-F2a,'k-')
% hold on
% plot(time,-F2b,'k--')
% hold off

```

```

figure(4)
plot(xval,yval*60,'k','linewidth',2)
title('Max Torque Required at Given Shaft Speed');
ylabel('RPM')
xlabel('Torque, (in-lb)')
hold on
plot([135 0],[0 1500],'--k')

figure(5)
[haxes,hRPM,heff] = plotyy(xval,yval*60,[0 Torq_Eff_max T_max_Drill],[0
Eff_max 0]);
grid on
title('RPM and Motor Efficiency vs Torque');
xlabel(haxes(1),'Torque (in-lb)')
ylabel(haxes(2),'DC Motor Efficiency')
ylabel(haxes(1),'RPM')
set(hRPM,'LineWidth',1.5);
set(heff,'LineStyle','--','LineWidth',1.5);
legend('RPM','Efficiency','location','northwest')

% figure(5)
% [haxes,hTorq,hRPM] = plotyy(time,Torq,time,RPM);
% grid on
% title('Torque and Shaft Speed vs Run Time');
% xlabel(haxes(1),'time (s)')
% ylabel(haxes(2),'RPM')
% ylabel(haxes(1),'Torque (in-lb)')
% set(hTorq,'LineWidth',1.5);
% set(hRPM,'LineStyle','--','LineWidth',1.5);
% legend('Torque','RPM','location','northwest')
%
figure(6)
plot(time,Torq,'k')
title('Max Torque Required at Given Time');
xlabel('time (s)')
ylabel('Torque, (in-lb)')
% %
% figure(7)
% plot(time,RPM,'k')
% title('Max Shaft Speed Required at Given Time');
% xlabel('time (s)')
% ylabel('\omega, (RPM)')
% %
% figure(8)
% plot(RPM,HP,'k')
% title('Horse Power at Given Time');
% xlabel('time (s)')
% ylabel('Horse Power')
%
figure(9)
plot(time(1:101),F2m(1:101),'k')
title('Leg Interference Force, & Push Rod Axial Load');
xlabel('time (s)')

```

```

ylabel('Force, (lbf)')
hold on
plot(time(1:101),F3(1:101),'--k')
axis([0,7,150,320])
legend('F_{2m}: Leg Interference','F_3: Push Rod','location','west')

figure(10)
[haxes,hF2m,hF3] =
plotyy(time(1:101),F2m(1:101),time(1:101),F3(1:101),'plot');
% grid on
title('Leg Interference Force & Push Rod Axial Load');
xlabel(haxes(1),'time (s)')
ylabel(haxes(2),'F_3(lbf)')
ylabel(haxes(1),'F_{2m}(lbf)')
% set(hF2m,'LineWidth',1.5);
% set(hF3,'LineStyle','--','LineWidth',1.5);
set(haxes,{'LineStyle'},{'-';'--'})
set(haxes,{'ycolor'},{'r';'b'})
legend('Torque','RPM','location','northwest')

figure(11)
plot(time,F3,'k')
title('Push Rod Axial Load');
xlabel('time (s)')
ylabel('F_3 (lbf)')
axis([0,19,50,550])
hold on
plot([time(1),time(201)],[F3(101),F3(101)],':k')

figure(12)
plot(time(1:101),F2m(1:101),'k')
title('Leg Interference Force (Incline)');
xlabel('time (s)')
ylabel('F_{2m} (lbf)')
axis([0,7,150,200])

```

## Appendix F. Finite Element Analysis Reports

The following is the order of the FEA reports contained in the document:

**Table 9: Numbered list of FEA reports including the part number and description of the analyzed part**

<b>Report No.</b>	<b>Part No. &amp; Description</b>
<b>1</b>	A02-00008 Chassis Welded Subassembly
<b>2</b>	A02-00002 Caster Bracket
<b>3</b>	A02-00016 Welded Backrest Frame Subassembly
<b>4</b>	P03-00027 Sheet Metal Push Rod
<b>5</b>	P04-00008 Leg
<b>6</b>	A02-00008 Chassis Welded Subassembly
<b>7</b>	A02-00012 Left Welded Seat Bar
<b>8</b>	P02-00002 Back Lock Bar
<b>9</b>	P02-00006 Back Tension Bar
<b>10</b>	P02-00009 Ball Nut Mounting Plate
<b>11</b>	P02-00010 Belt Safety Pawl
<b>12</b>	A01-00003 Bridge Subassembly
<b>13</b>	P03-00003 Back Rest Limit Actuator
<b>14</b>	P03-00004 Back Slider Bracket
<b>15</b>	P03-00005 Brake Bracket
<b>16</b>	P03-00013 Front Seat Support
<b>17</b>	P03-00015 Left Back Support
<b>18</b>	A02-00015 Slider Welded Subassembly
<b>19</b>	P03-00017 Left Footrest Pivot Bracket
<b>20</b>	P03-00019 Left Footrest Caster Bracket
<b>21</b>	P03-00021 Left Footrest Latch Bracket
<b>22</b>	P03-00026 Rear Seat Hanger
<b>23</b>	P02-00022 Grooved Idler Pulley Shaft
<b>24</b>	P02-00027 Main Drive Pulley Axle

**Table 10: FEA information table for all completed finite element analyses, including part names, assumptions, and FEA setup information**

<b>FEA Analysis Info Table</b>			
<b>FEA No.</b>	<b>Femap File Name</b>	<b>Targeted Analysis in Part/Assembly</b>	<b>Notes and Assumptions</b>
1	MA0 - A02-00008 Chassis Welded Subassembly (STEP 102).modfem	Basic welds and structure of the chassis under highest loads (Step 102 in force analysis) applied by lead screw and legs	Symmetry chosen with most conservative side in mind; caster brackets loaded up in worst case (caster rotated outward)
2	MA0 - A02-00002 Caster Bracket.modfem	Yield stress in caster bracket	Used spider elements to allow as realistic load/constraint relationships as possible
3	MA0(Part) - Welded Backrest Subassembly (Revision 2).modfem	Welds and structure of the backrest assembly	First analysis did not produce satisfactory results, design was adjusted, welds applied
		Looking for excessive deflections in backrest at full recline	Max Deflection: 0.04" which translates to about 0.08" at the head.
		Structural integrity at highest load in Link 3	None
4	MA0 - P03-00027 Sheet Metal Push Rod (Symmetry).modfem	Find critical buckling loads	Buckling
		Find stress integrity	Stress
5	A0 - P04-00008 Leg (Beefed Up 2).modfem	Yield stress in leg	Highest stress comes during the start of the raise phase
6	A0 - A02-00005 Bridge Bracket Welded Subassembly.X_T	Stress Yielding	None
	A1 - A02-00005 Bridge Bracket Welded Subassembly.modfem	Stress Yielding	Did not include screw head constraint
7	A0 - A02-00012 Left Welded Seat Bar Subassembly.modfem	Stress Yielding	fixed pivot A to reduce free body motion and measured the constraint loads to see if they are reasonable
	A1 - A02-00012 Left Welded Seat Bar Subassembly.modfem	Stress Yielding	Added reinforcement
	A1 - A02-00012 Left Welded Seat Bar Subassembly.modfem	Stress Yielding	Max stress in critical areas
8	A0 - P02-00002 Back Lock Bar.modfem	Stress Yielding	Assume max spring load and 2x the max compressive load in link 9
9	P02-00006 Back Tension Bar	Tensile load stress	None
		Buckling at top position	Used 2x the static load to account for user forcing back



10	A0 - P02-00009 Ball Nut Mounting Plate.modfem	Stress Yielding	None
11	A0 - P02-00010 Belt Safety Pawl.modfem	Stress Yielding	Assume that belt failure occurs while moving the system upward or while the screws are being decelerated rapidly when lowering the chair, therefore neglect the need to include kinetic energy as it is near stopped already.
	A1 - P02-00010 Belt Safety Pawl.modfem	Stress Yielding	
12	A0 - A01-00003 Bridge Subassembly.modfem	Bracket stress, and bridge stress and deflection	Analysis done at step 58, where max moment occurs in bridge
13	A3 - P03-00003 Back Rest Limit Actuator.modfem	Max stress at full 0.12" displacement	Bumper can move up to 0.12 inches until backrest rests on side bumpers
		Max force on sensor plungers under full 0.12" displacement	
		Max force actuator bumper under full 0.12" displacement	
14	A0.1 - P03-00004 Back Slider Bracket.modfem	Stress Yielding	None
15	A2 - P03-00005 Brake Bracket.modfem	Stress Yielding	None
16	A0 - P03-00013 Front Seat Support.modfem	Stress Yielding	Assume the seat adds no stiffness, it only constrains it from rotating
17	A1 - P03-00015 Left Back Support.modfem	Bridge Slot	Glued connection between parts in analysis, consider max upper body load at the highest bridge moment point
		Pivot Hole	
		Frame Welds and Structure	
18	A1.2 - A02-00015 Slider Welded Subassembly.modfem	Distal End Stress	Item 1
	A1.3 - A02-00015 Slider Welded Subassembly (Rear).modfem	Proximal End Stress	Item 2
	A1.4 - A02-00015 Slider Welded Subassembly (Beam).modfem	Beam deflection	Item 3
19	A0 - P03-00017 Left Footrest Pivot Bracket.modfem	Stress Yielding	None
20	A0 - P03-00019 Left Footrest Caster Bracket.modfem	Stress Yielding	None
21	A0 - P03-00021 Left Footrest Latch Bracket.modfem	Stress Yielding	Initial Run
		Stress Yielding	Final Design

22	A0 - P03-00026 Rear Seat Hanger (Left Half).modfem	Stress Yielding	Maximum Stress in Final Model
	A1 - P03-00026 Rear Seat Hanger (Left Half).modfem	Stress Yielding	Max stress in Pivot Hole C
23	A0.1 - P02-00022 Grooved Idler Pulley Shaft.modfem	Cyclic fatigue	All cycles at full load on belt
24	A0 - P02-00027 Main Drive Pulley Axle.modfem	Cyclic fatigue	All cycles at full load on belt
25	Screw End 1.modfem	Cyclic fatigue	No account for sandwiched geometry in model that prevents free bending; assume A36 type material; FOS from hand calcs

**Table 11: FEA results table including material properties, stresses, and safety factors**

<b>FEA Analysis Results Table</b>			
<b>FEA No.</b>	<b>Yield Strength</b>	<b>Max Stress</b>	<b>FOS</b>
1	36300	9141	<b>4.0</b>
2	36300	38929	<b>0.9</b>
3	36300	25756	1.4
	NA	NA	NA
	36300	21512	1.7
4	NA	NA	<b>29.0</b>
	36300	3950	<b>9.2</b>
5	23100	7730	<b>3.0</b>
6	36300	22496	1.6
	36300	11706	<b>3.1</b>
7	36300	47000	0.8
	36300	26935	1.3
	36300	14072	<b>2.6</b>
8	40000	15283	<b>2.6</b>
9	40000	13779	<b>2.9</b>
	NA	NA	<b>6.5</b>
10	40000	6133	<b>6.5</b>
11	40000	17579	2.3
	40000	13335	<b>3.0</b>
12	9280	2870	<b>3.2</b>
13	33000	16358	<b>2.0</b>
	NA	3.51	NA

	NA	12.5	NA
14	36300	9074	<b>4.0</b>
15	47100	15000	<b>3.1</b>
16	33000	29878	<b>1.1</b>
17	33000	10000	<b>3.3</b>
	33000	9000	<b>3.7</b>
	33000	17297	<b>1.9</b>
18	36300	18459	<b>2.0</b>
	36300	9439	<b>3.8</b>
	NA	0.23 inch	NA
19	33000	13255	<b>2.5</b>
20	36300	18561	<b>2.0</b>
21	33000	43758	0.8
	33000	22570	<b>1.5</b>
22	36300	21289	1.7
	36300	10221	<b>3.6</b>
23	30100	9872	<b>9.1</b>
24	44950	33360	<b>4.0</b>
25	NA	NA	<b>2.5</b>

## FINITE ELEMENT ANALYSIS REPORT: FEA #1

**Part/Assembly Model File:** MA0 - A02-00008 Chassis Welded Subassembly (STEP 102).x\_t

**Femap Project File:** MA0 - A02-00008 Chassis Welded Subassembly (STEP 102).modfem

**Purpose of Analysis:** Understanding of the overall welds and structure of the chassis components and welds under the highest loads applied by lead screw and legs.

**Material:** A36 Steel

<b>Stiffness</b>		<b>Limit Stress</b>	
Young's Modulus, E	29000000.	Tension	0.
Shear Modulus, G	0.	Compression	0.
Poisson's Ratio, nu	0.26	Shear	0.
<b>Thermal</b>		Mass Density	7.35736E-4
Expansion Coeff, a	6.E-6	Damping, 2C/Co	0.
Conductivity, k	0.00069444	Reference Temp	70.
Specific Heat, Cp	44.8224		
Heat Generation Factor	0.		

**Loads:** Force Analysis Step No. 102

- F2aCx: -446.9195 lbf
- F2aCy: -91.1213 lbf
- F2bCx: -61.6901 lbf
- F2bCy: -12.5778
- FslideFront: -47.837 lbf
- FslideRear: -25.175 lbf

**Constraints:**

- Symmetry at center of chassis: TZ
- Fixed bearing: TX
- Caster Brackets: TZ

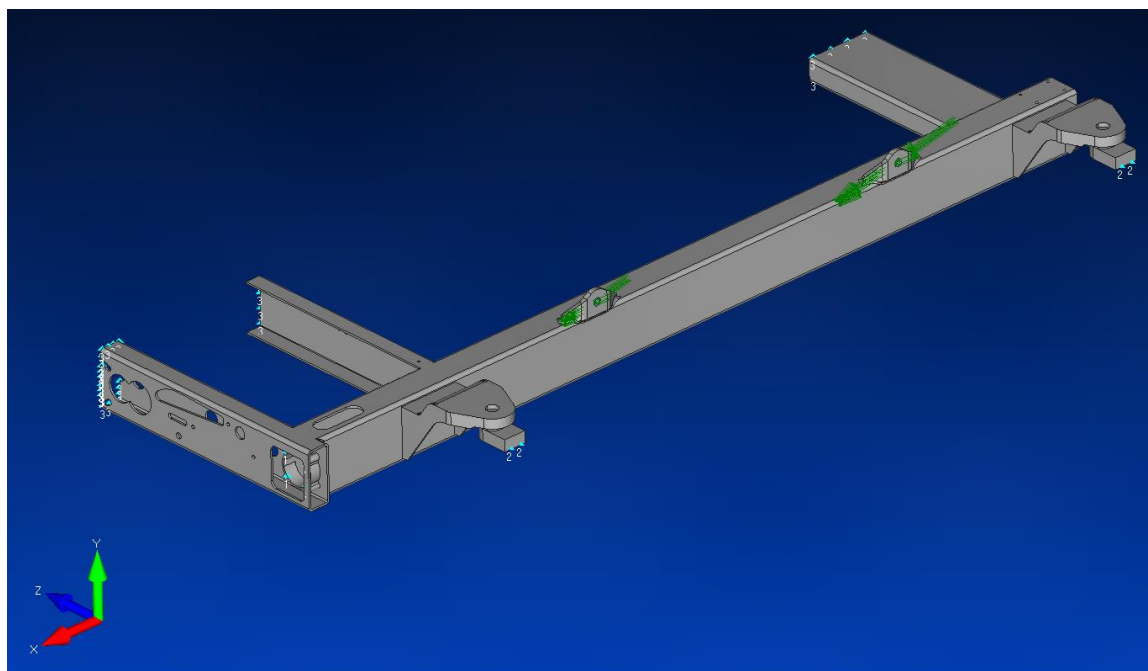
**Mesh:**

- Base Mesh Size: 0.2 inches
- Refined Mesh Size: 0.05 inches

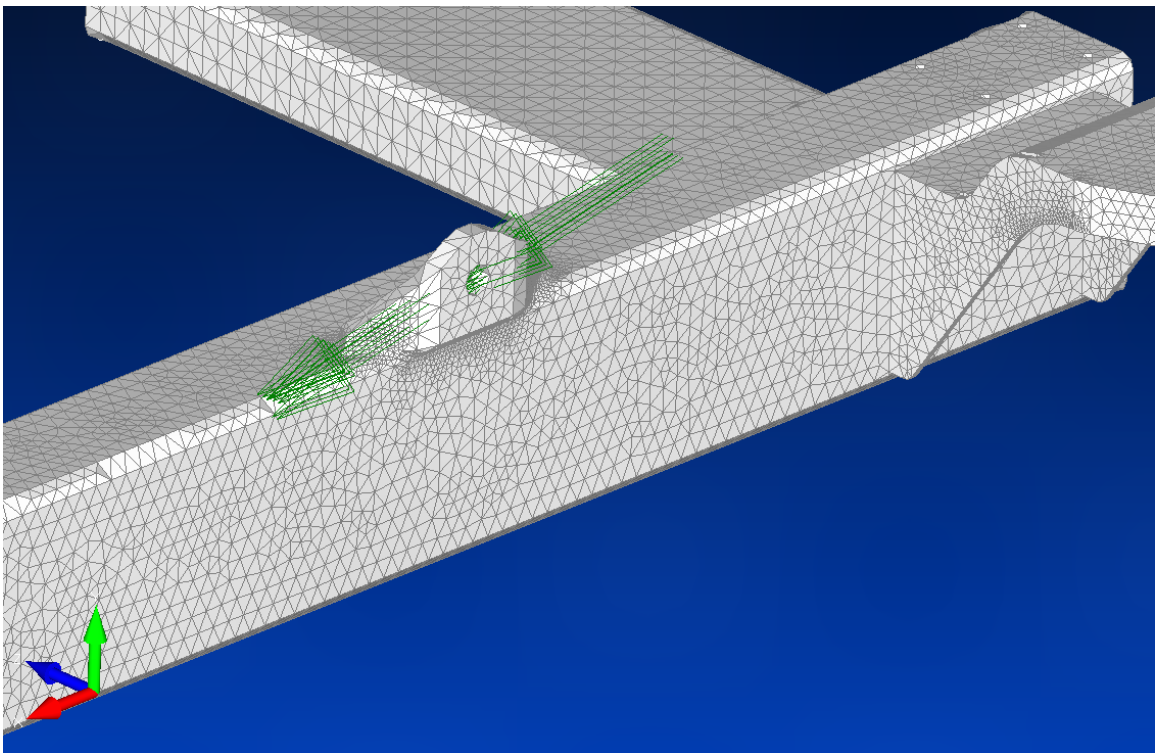
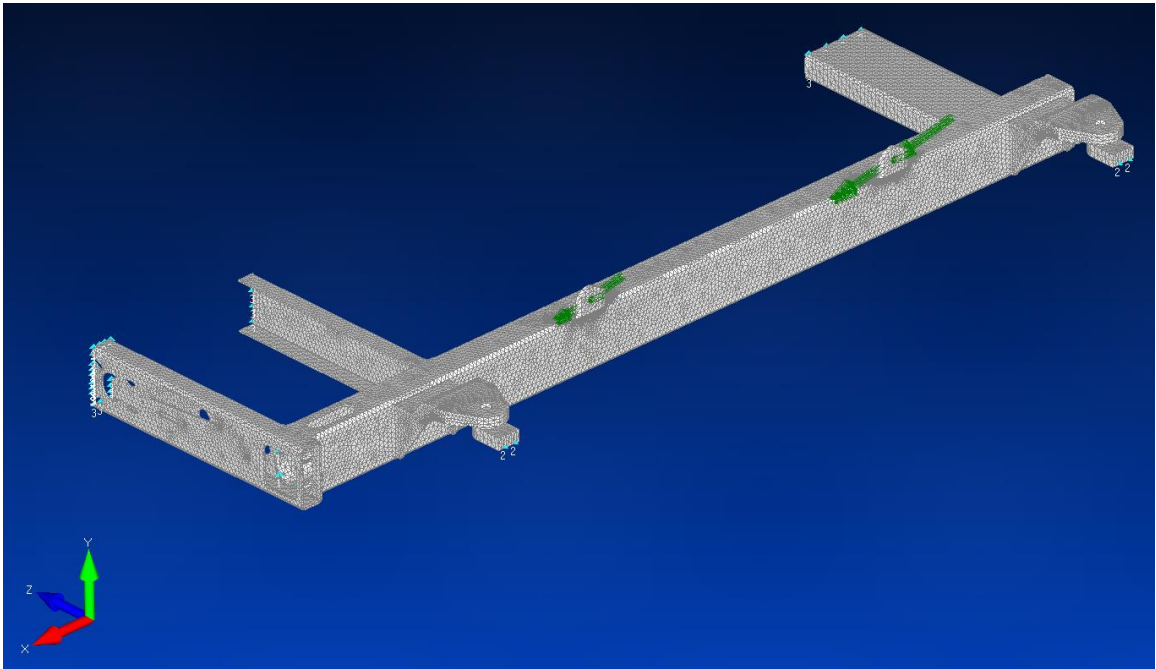


**Pertinent Results:**

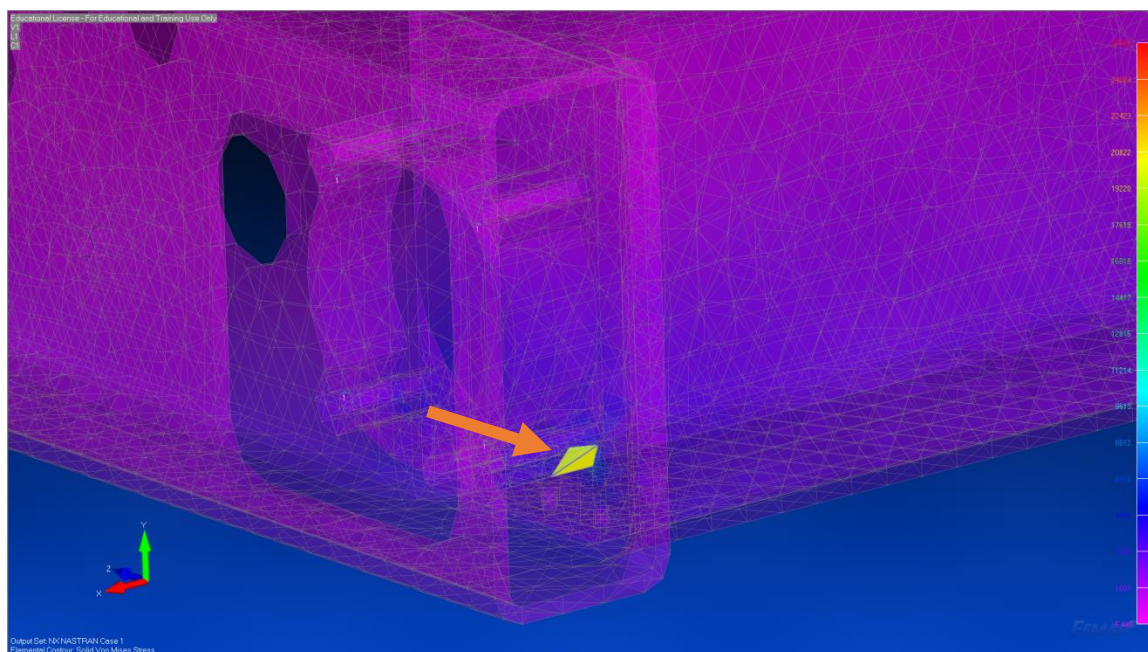
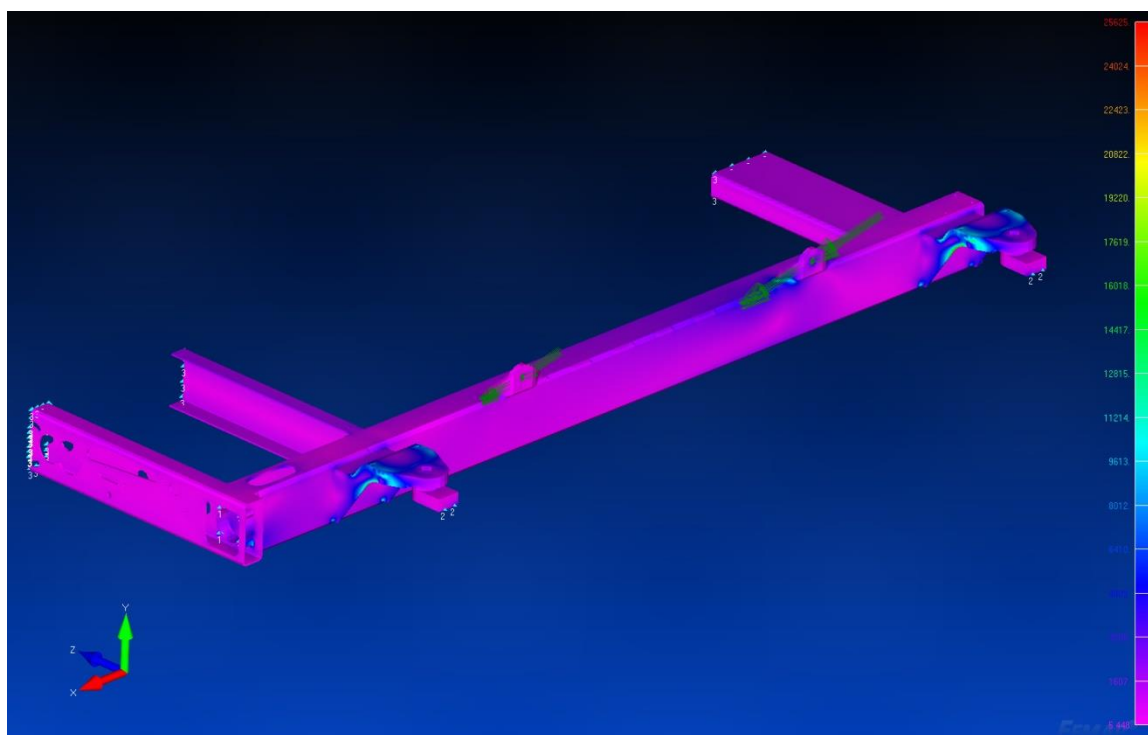
<i>Description</i>	<i>Value</i>
Maximum relative deflection in Y direction from resulting load on caster brackets	0.02 inches
Maximum Local Von-Mises Stress	9,141 psi
Maximum Von-Mises Stress Location	Front leg attachment bracket weld

**MODEL**

# MESH



# RESULTS



**Element 473674**

**Output Set 3 : NX NASTRAN Case 1**

**Value = 9140.9 | Output Vector 60031 : Solid Von Mises Stress**



## FINITE ELEMENT ANALYSIS REPORT: FEA #2

**Part/Assembly Model File:** MA0 - A02-00002 Caster Bracket.x\_t

**Femap Project File:** MA0 - A02-00002 Caster Bracket.modfem

**Purpose of Analysis:** Verification of caster bracket integrity under maximum load

**Material:** A36 Steel

<b>Stiffness</b>		<b>Limit Stress</b>	
Young's Modulus, E	29000000.	Tension	0.
Shear Modulus, G	0.	Compression	0.
Poisson's Ratio, nu	0.26	Shear	0.
<b>Thermal</b>		Mass Density	7.35736E-4
Expansion Coeff, a	6.E-6	Damping, 2C/Co	0.
Conductivity, k	0.00069444	Reference Temp	70.
Specific Heat, Cp	44.8224		
Heat Generation Factor	0.		

**Loads:** Force Analysis Step No. 201

- FFC(201): 100.5 lbf

**Constraints:**

- Attachment surfaces: Fixed

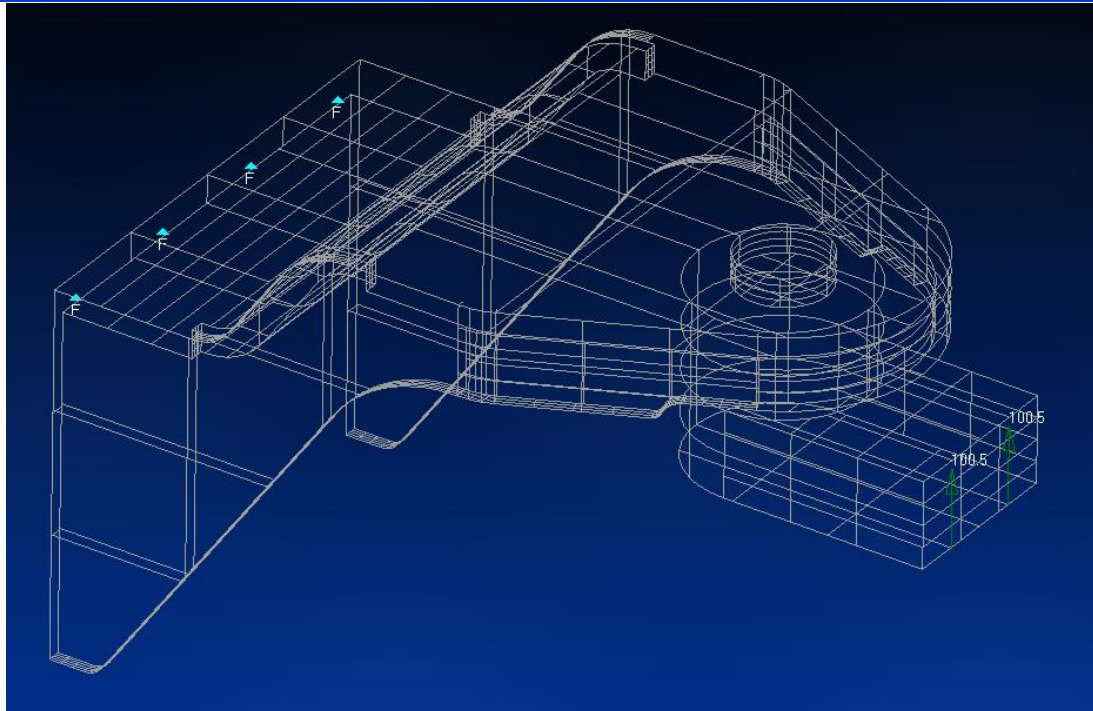
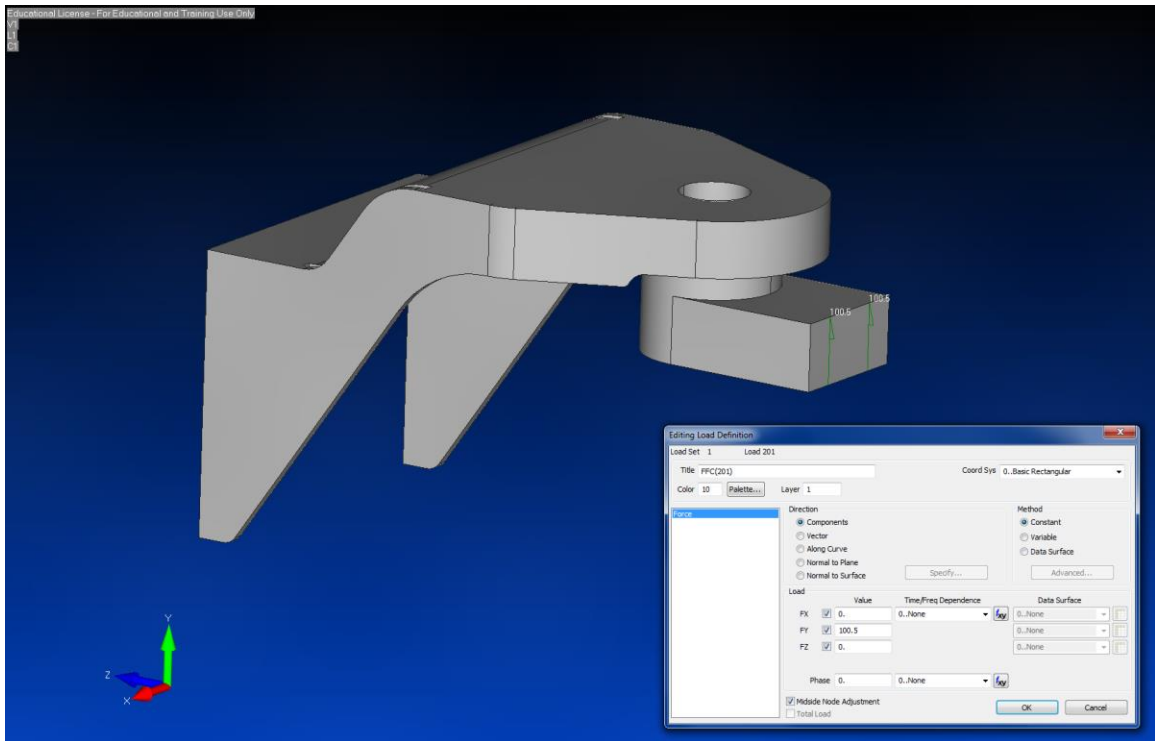
**Mesh:**

- Base Mesh Size: 0.1 inches
- Refined Mesh Size: 0.02 inches

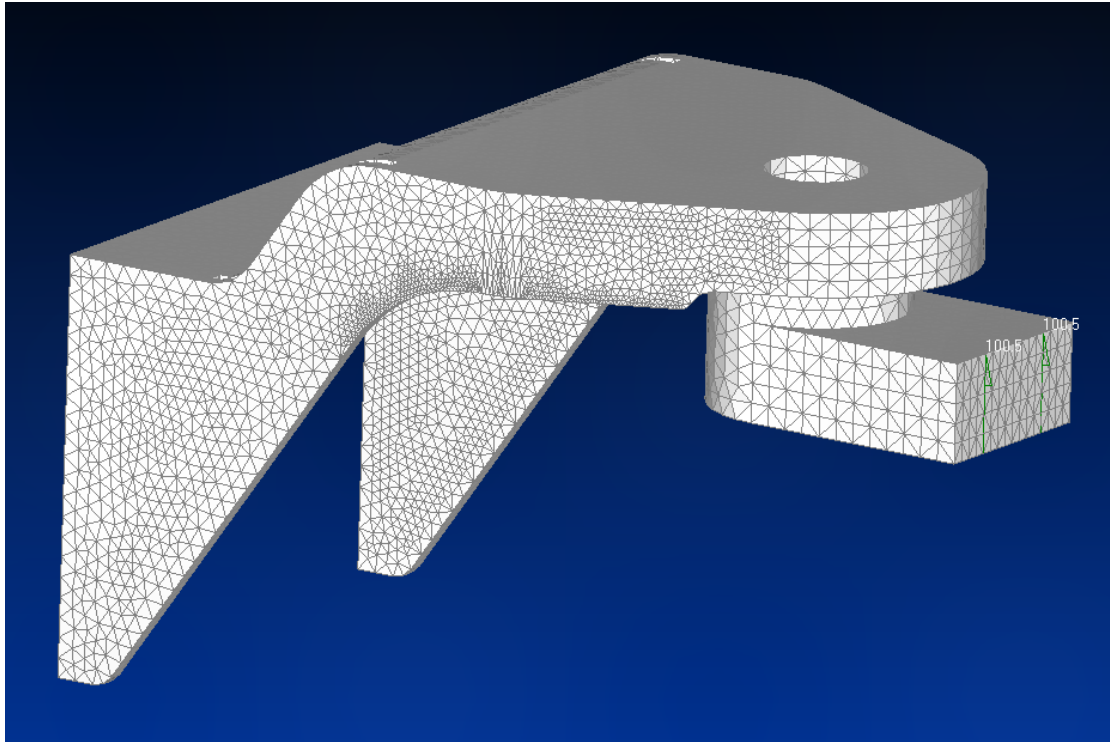
**Pertinent Results:**

<b>Description</b>	<b>Value</b>
Max Von-Mises Stress	38,929 psi
Max Deflection	0.018 inches

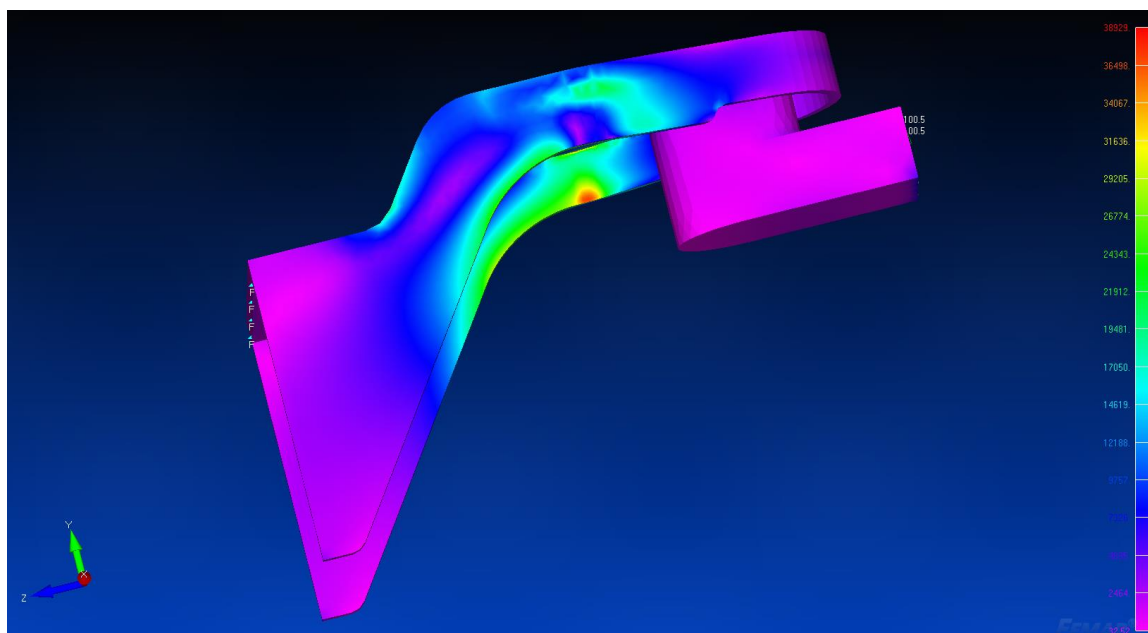
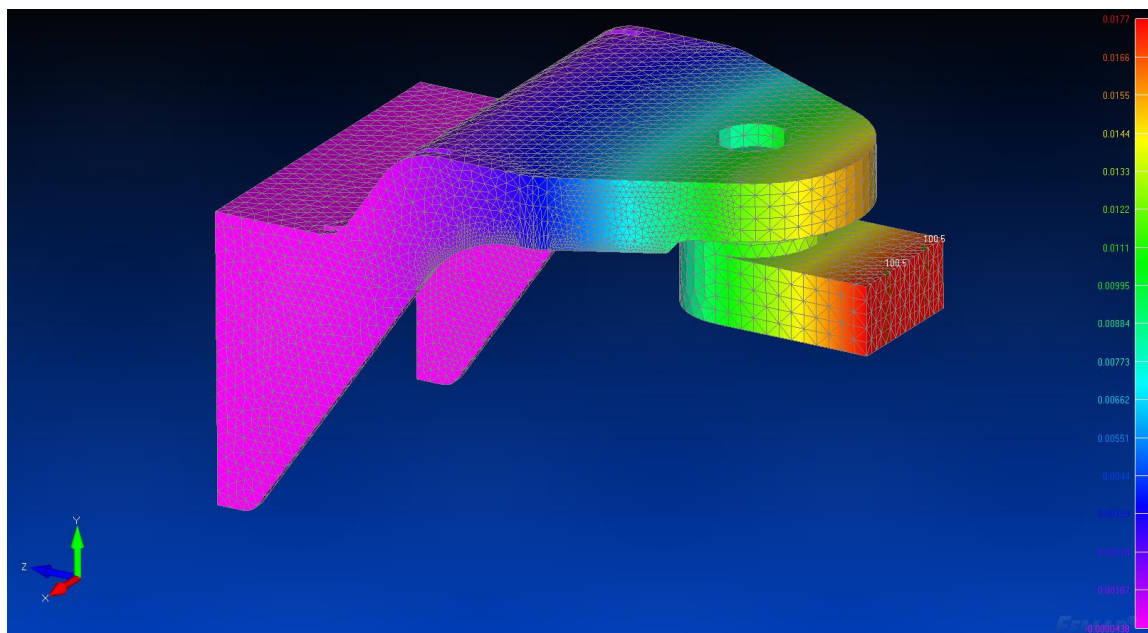
# MODEL



# MESH



# RESULTS



## FINITE ELEMENT ANALYSIS REPORT: FEA #3

**Part/Assembly Model File:** MA0(Part) - Welded Backrest Subassembly (Revision 2).X\_T

**Femap Project File:** MA0(Part) - Welded Backrest Subassembly (Revision 2).modfem

**Purpose of Analysis:** Validate subassembly for stress and deflection in the full recline position

**Material:** A36 Steel

<b>Stiffness</b>		<b>Limit Stress</b>	
Young's Modulus, E	29000000.	Tension	0.
Shear Modulus, G	0.	Compression	0.
Poisson's Ratio, nu	0.26	Shear	0.
<b>Thermal</b>		Mass Density	7.35736E-4
Expansion Coeff, a	6.E-6	Damping, 2C/Co	0.
Conductivity, k	0.00069444	Reference Temp	70.
Specific Heat, Cp	44.8224		
Heat Generation Factor	0.		

### Loads:

- Force Analysis Step No. 1: Greatest bending moment
  - F3x(1): -0.0091 lbf (Femap Y)
  - F3y(1): -307.6601 lbf (Femap Z)
- Force Analysis Step No. 102: Greatest F3 Force
  - F3(102): 512 lbf (Y-489.3697 lbf, Z- 153.6127 lbf)
  - FD(102): 19.25 lbf

### Constraints:

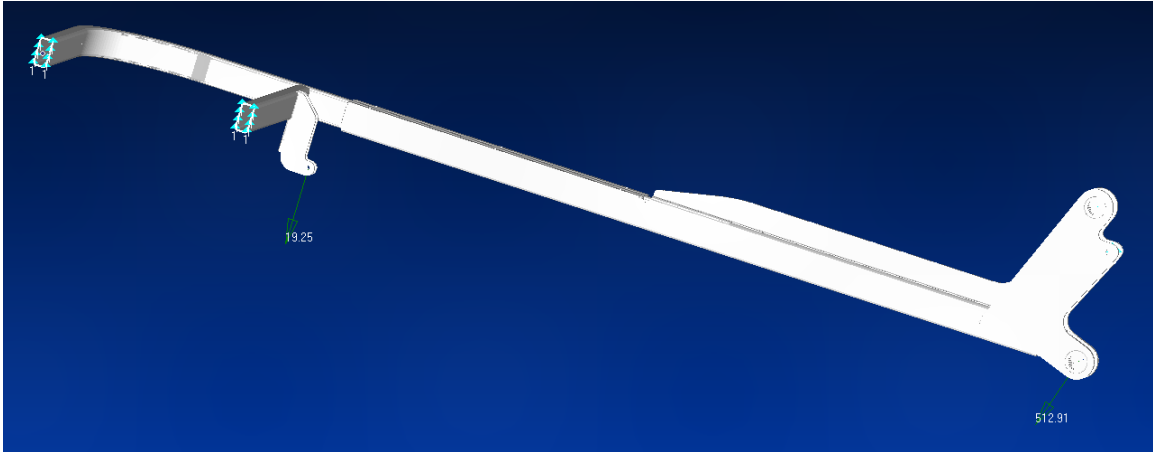
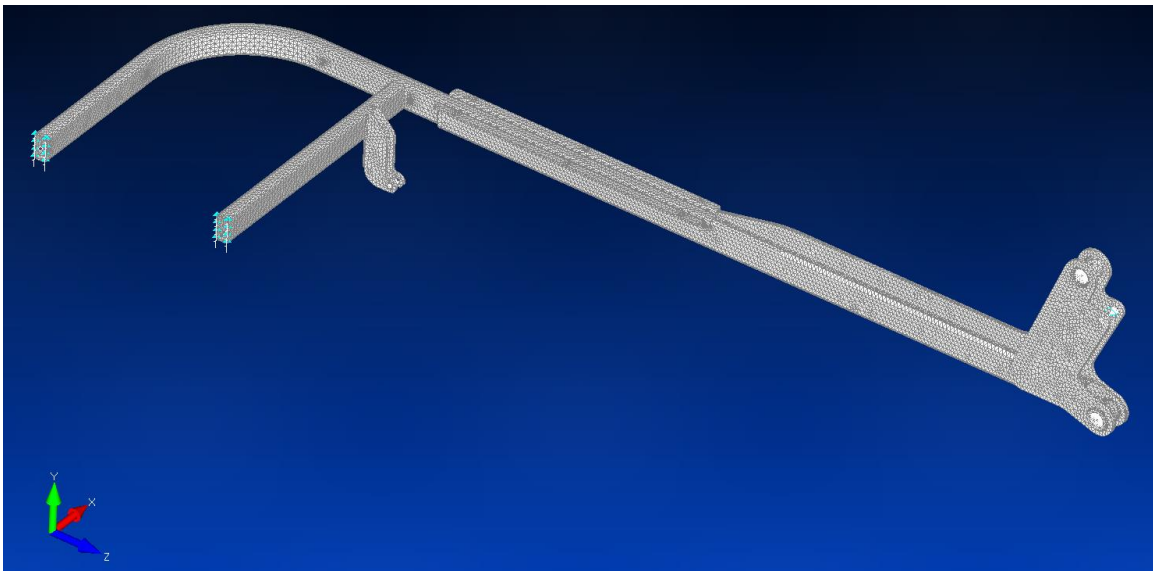
- Symmetry: TX
- Joint A: TX, TY, TZ, RY, RZ
- Force Analysis Step No. 1: Greatest bending moment
  - Joint D: TY
- Force Analysis Step No. 102: Greatest F3 Force
  - Joint 9: TY, TZ

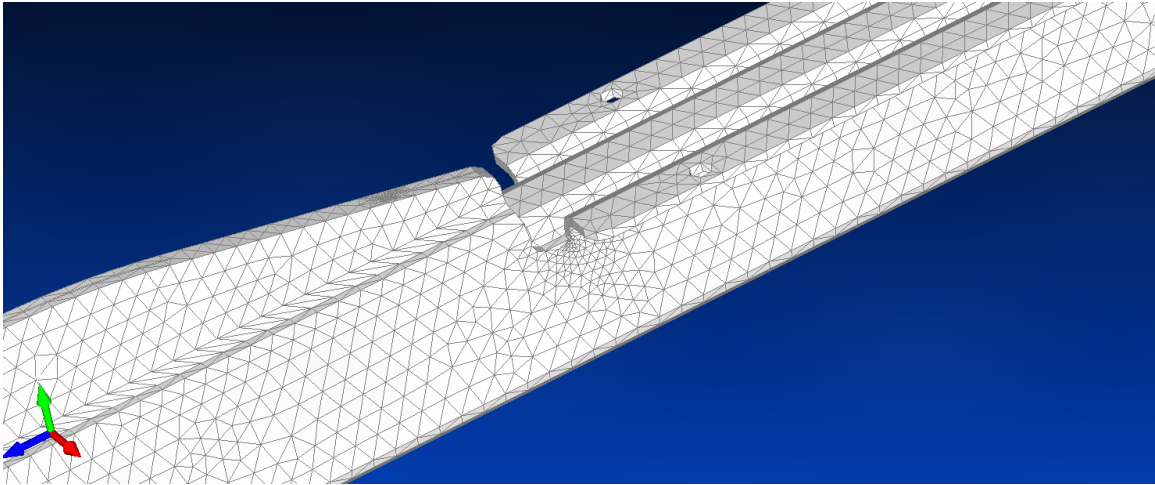
### Mesh:

- Base Mesh Size: 0.15 inches

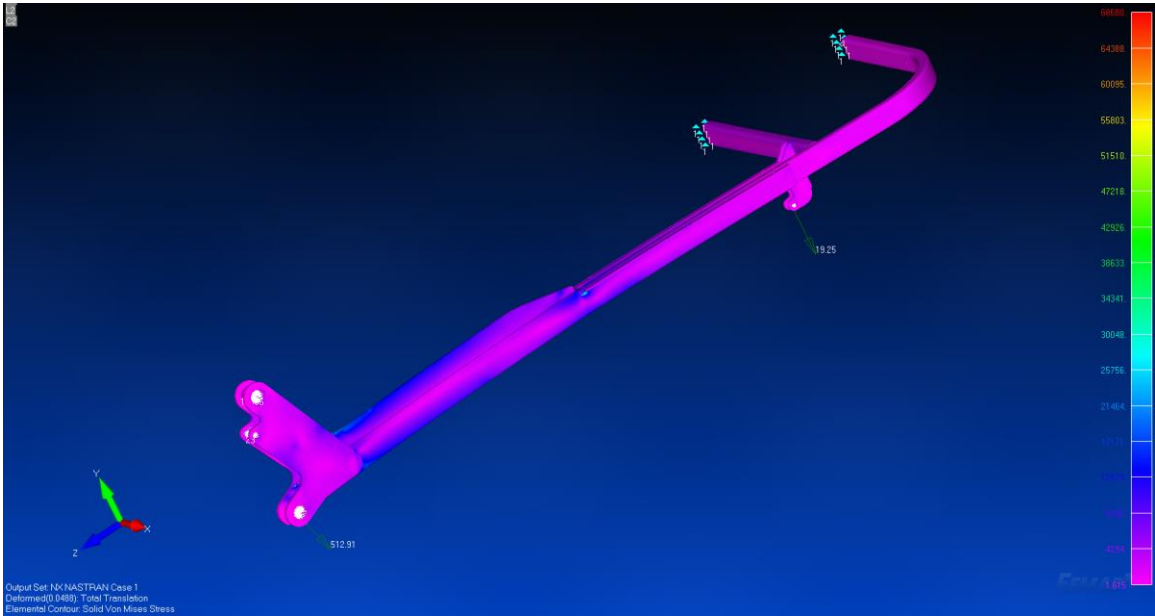
**Pertinent Results:**

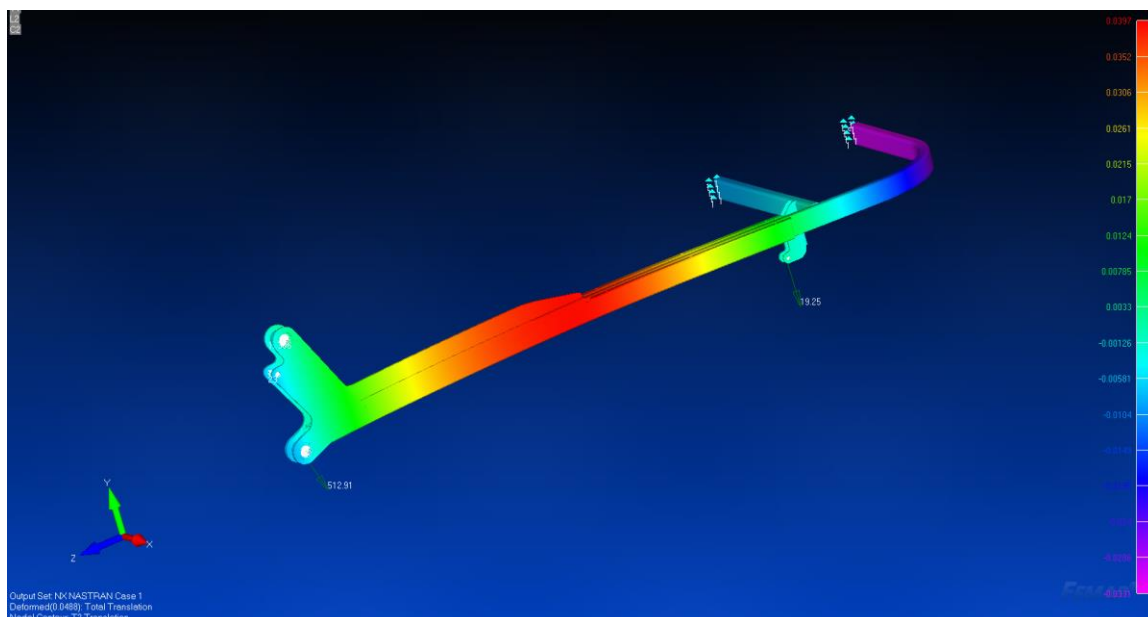
<i>Description</i>	<i>Value</i>
Max Von-Mises Stress (Ignoring localized stress concentration)	25,756 psi
Max Deflection	0.04 inches

**MODEL****MESH**



# RESULTS (1)





## RESULTS (102)





## FINITE ELEMENT ANALYSIS REPORT: FEA #4

**Part/Assembly Model File:** MA0 - P03-00027 Sheet Metal Push Rod (Symmetry).x\_t

**Femap Project File:** MA0 - P03-00027 Sheet Metal Push Rod (Symmetry).modfem

**Purpose of Analysis:** Buckling modes and stress of the push rod under max load (102).

**Material:** A36 Steel

<b>Stiffness</b>		<b>Limit Stress</b>	
Youngs Modulus, E	29000000.	Tension	0.
Shear Modulus, G	0.	Compression	0.
Poisson's Ratio, nu	0.26	Shear	0.
<b>Thermal</b>		<b>Mass Density</b>	
Expansion Coeff, a	6.E-6	Mass Density	7.35736E-4
Conductivity, k	0.00069444	Damping, 2C/Co	0.
Specific Heat, Cp	44.8224	Reference Temp	70.
Heat Generation Factor	0.		

**Loads:** Force Analysis Step No. 102

- F3: 512 lbf (1/2 Load used in Z-direction)

**Constraints:**

- Symmetry at center of chassis: TX
- Pinned End 1: TY, TZ
- Pinned End w/ Load: TY

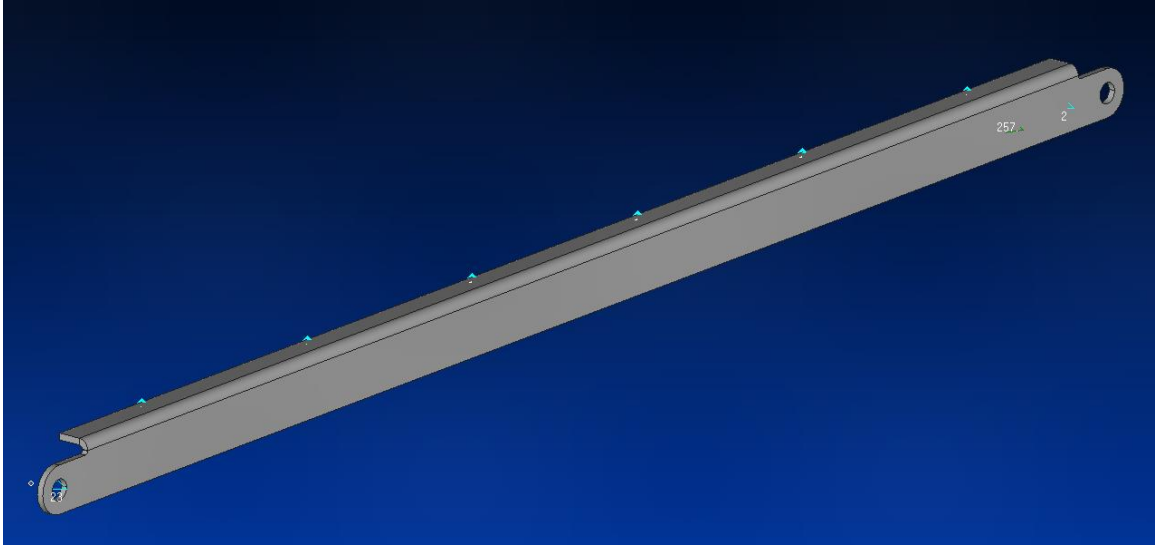
**Mesh:**

- Base Mesh Size: 0.1 inches

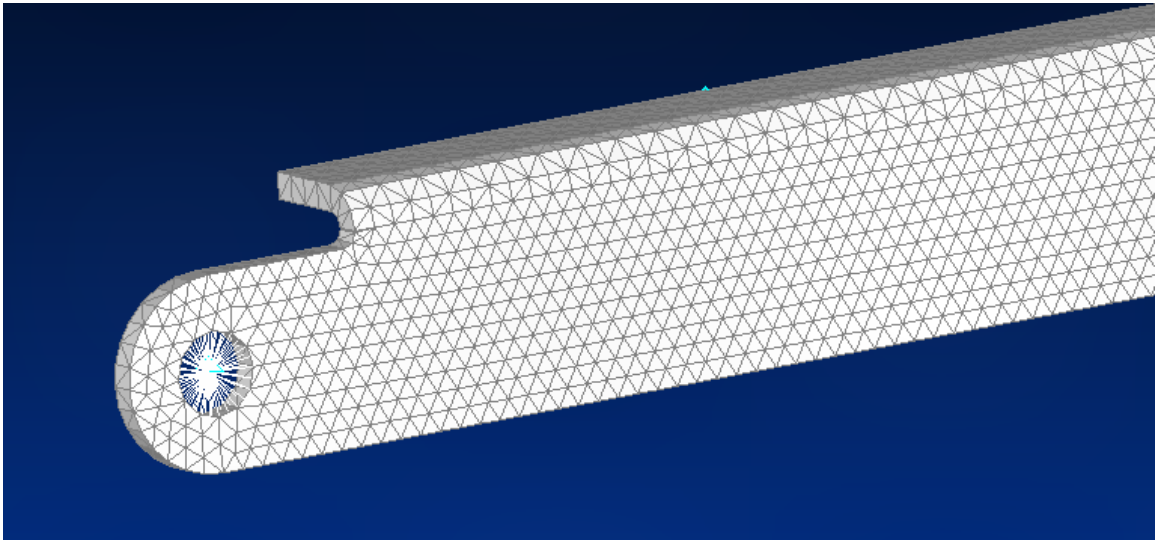
**Pertinent Results:**

<b>Description</b>	<b>Value</b>
First & Second Eigenvalue (buckling multiplier of applied load)	29.0
Maximum Von-Mises Stress	3950 psi

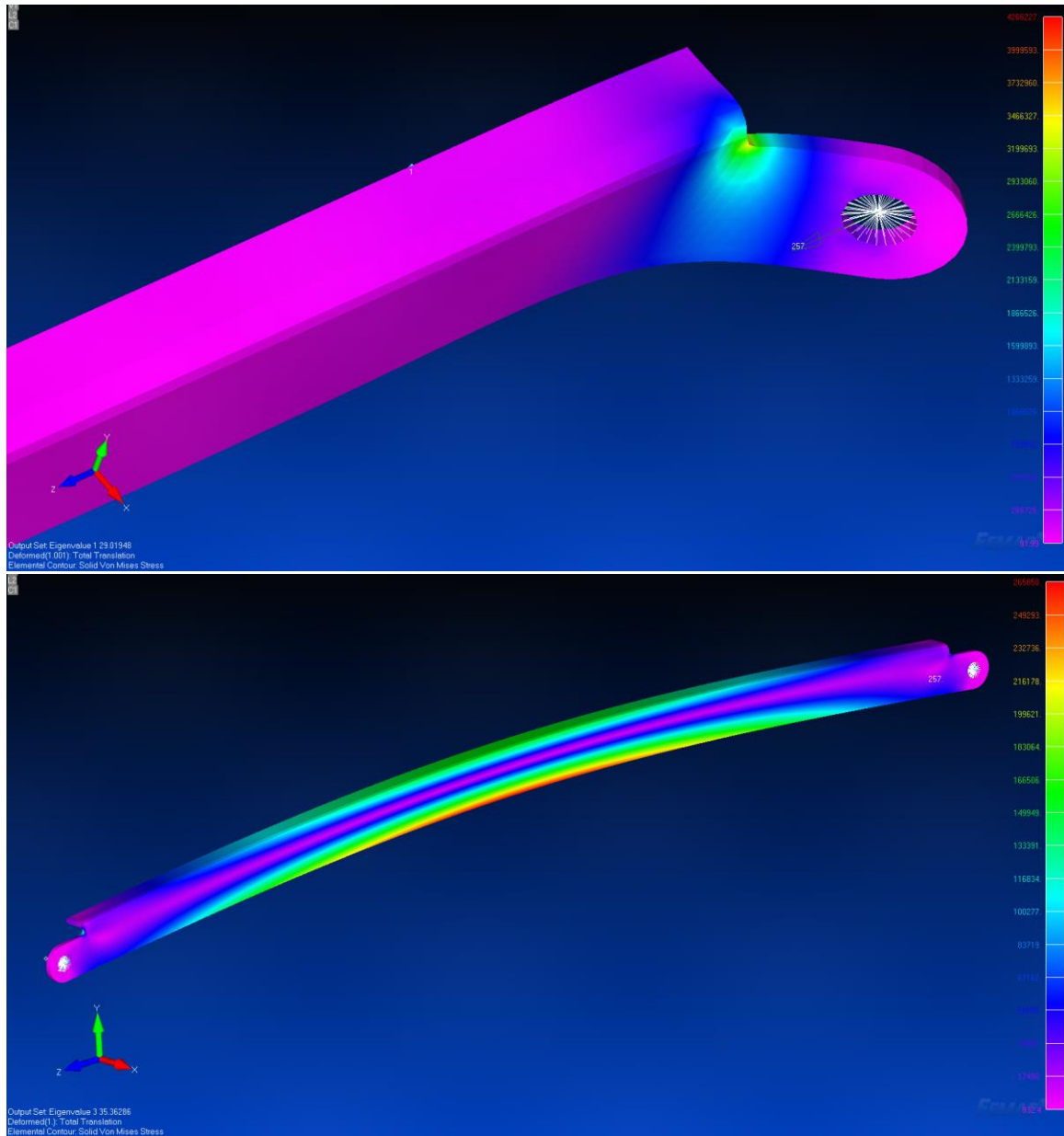
# MODEL



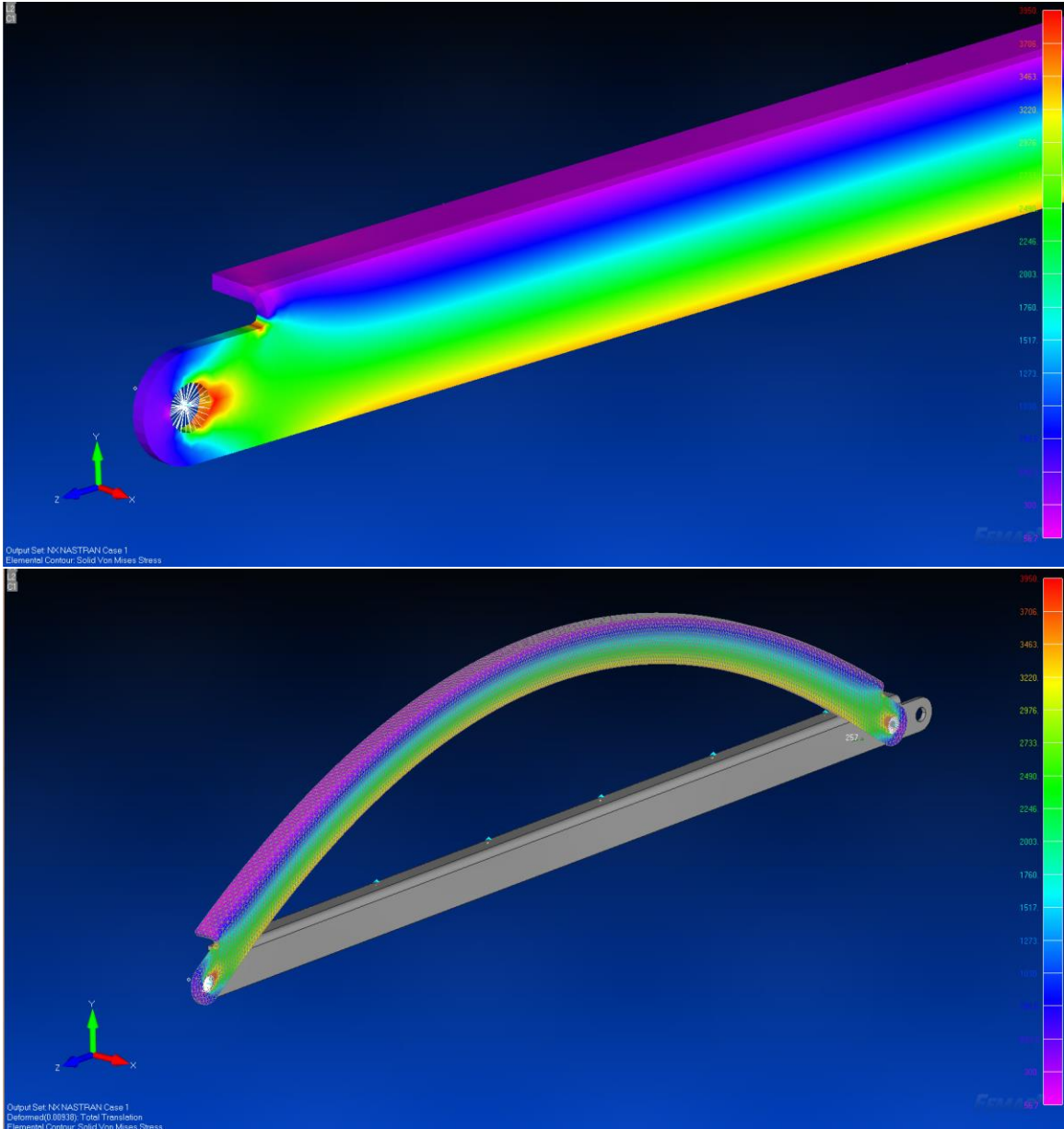
# MESH



# (Buckling) RESULTS



# (Stress) RESULTS



## FINITE ELEMENT ANALYSIS REPORT: FEA #5

### Part/Assembly Model File:

- Initial Model: MA0 - P04-00008 Leg.X\_T
- Final Model: A0 - P04-00008 Leg (Beefed Up 2).X\_T

### Femap Project File:

- Initial Model: MA0 - P04-00008 Leg.modfem
- Final Model: A0 - P04-00008 Leg (Beefed Up 2).modfem

**Purpose of Analysis:** Bending stress under max load (102).

**Material:** Aluminum A380-T5

<b>Stiffness</b>		<b>Limit Stress</b>	
Youngs Modulus, $E$	<input type="text" value="10300000"/>	Tension	<input type="text" value="0."/>
Shear Modulus, $G$	<input type="text" value="0."/>	Compression	<input type="text" value="0."/>
Poisson's Ratio, $\nu$	<input type="text" value=".33"/>	Shear	<input type="text" value="0."/>
<b>Thermal</b>		Mass Density	<input type="text" value="0."/>
Expansion Coeff, $\alpha$	<input type="text" value="0."/>	Damping, $2C/Co$	<input type="text" value="0."/>
Conductivity, $k$	<input type="text" value="0."/>	Reference Temp	<input type="text" value="0."/>
Specific Heat, $C_p$	<input type="text" value="0."/>		
Heat Generation Factor	<input type="text" value="0."/>		

**Loads:** Force Analysis Step No. 102

- F3: 522 lbf (Applied Axially)

**Constraints:**

- Pinned Rear End: TX, TY, TZ, RX, RY
- Pinned End w/ Load: TY', TZ'

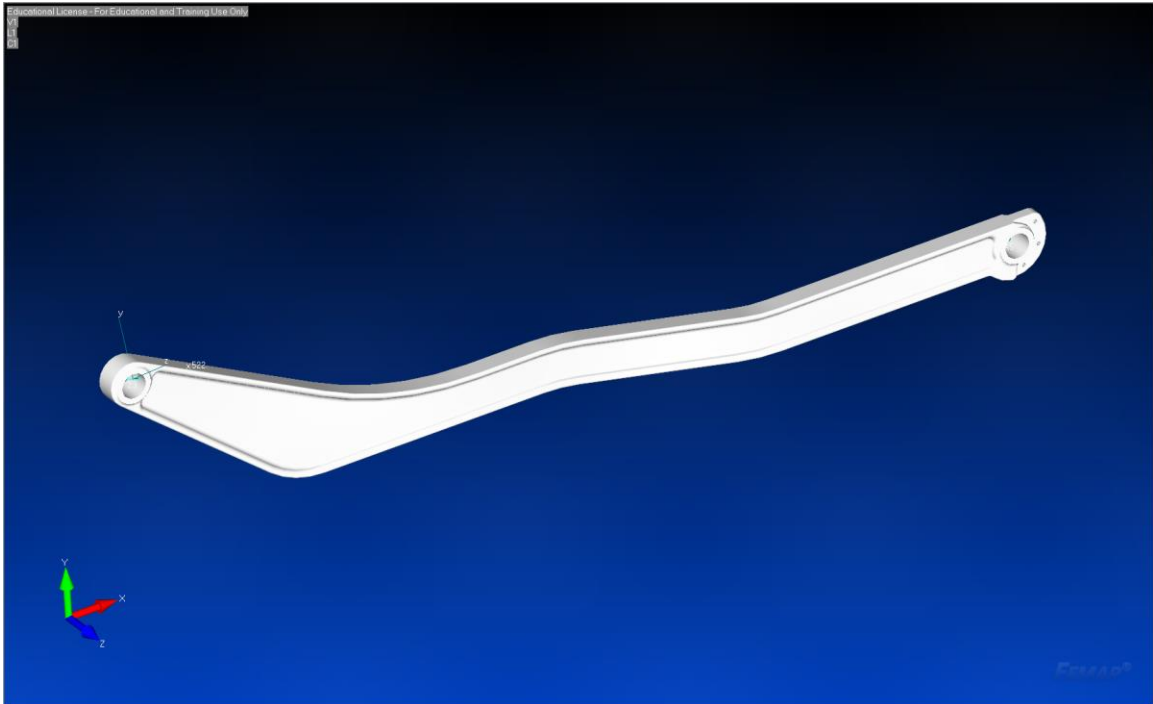
**Mesh:**

- Base Mesh Size: 0.1 inches

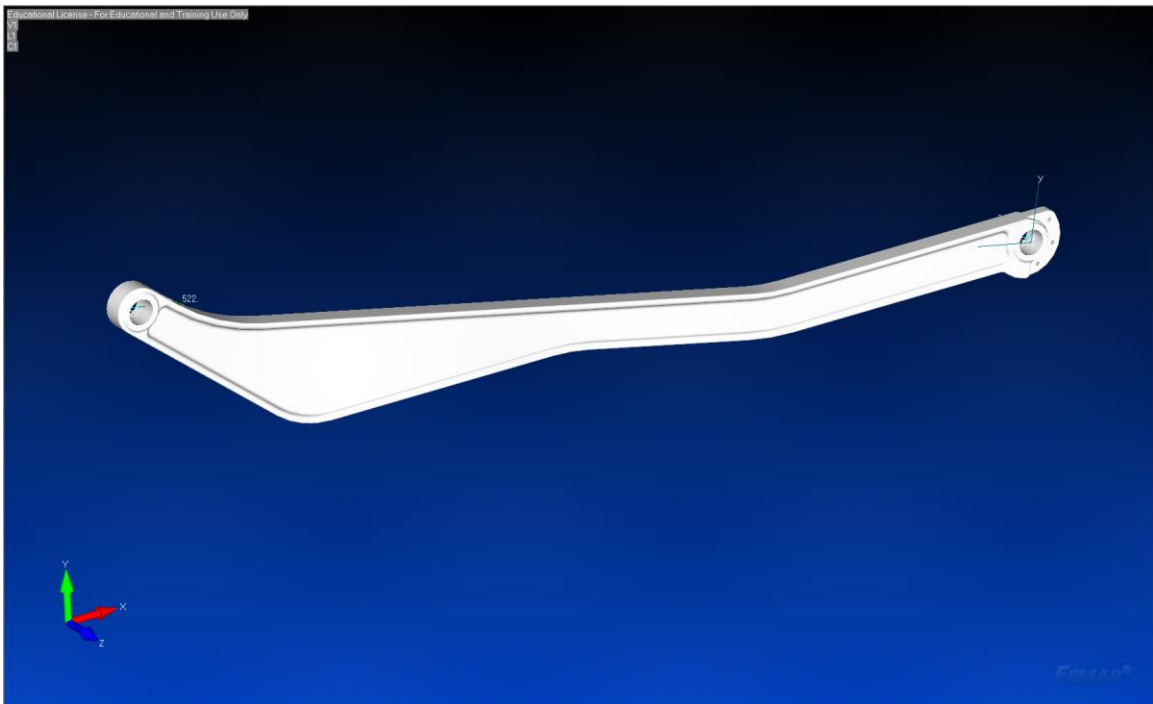
**Pertinent Results:**

<i>Description</i>	<i>Value</i>
Maximum Von-Mises Stress	7,730 psi

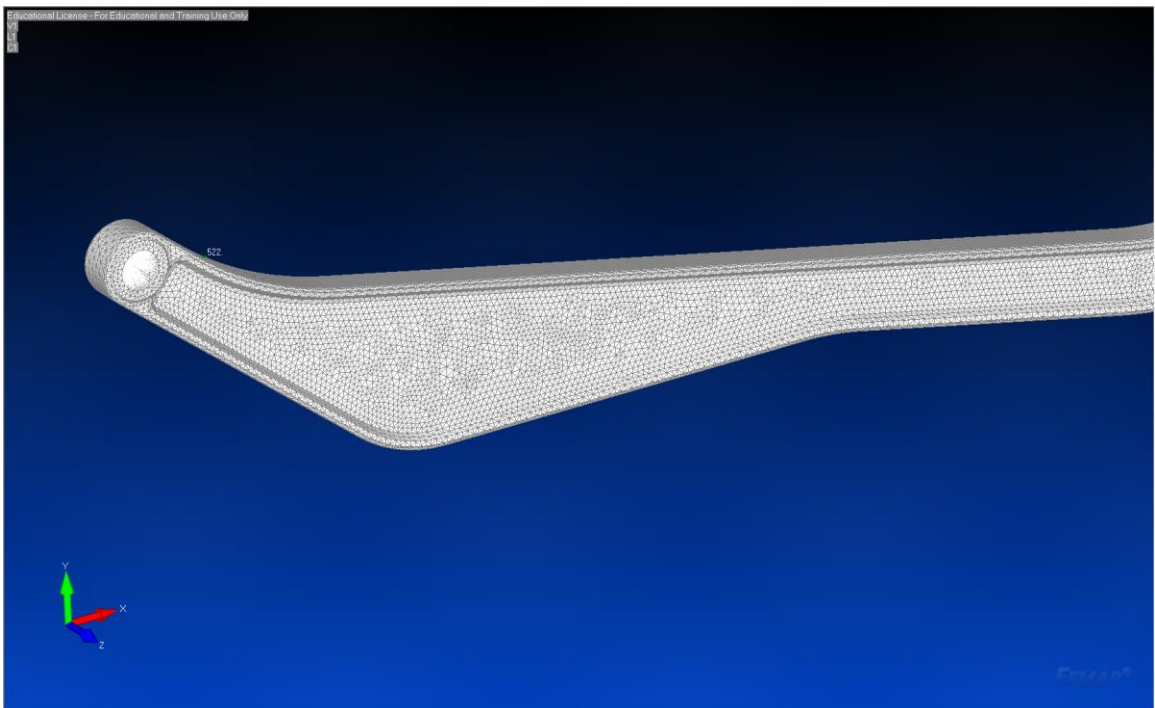
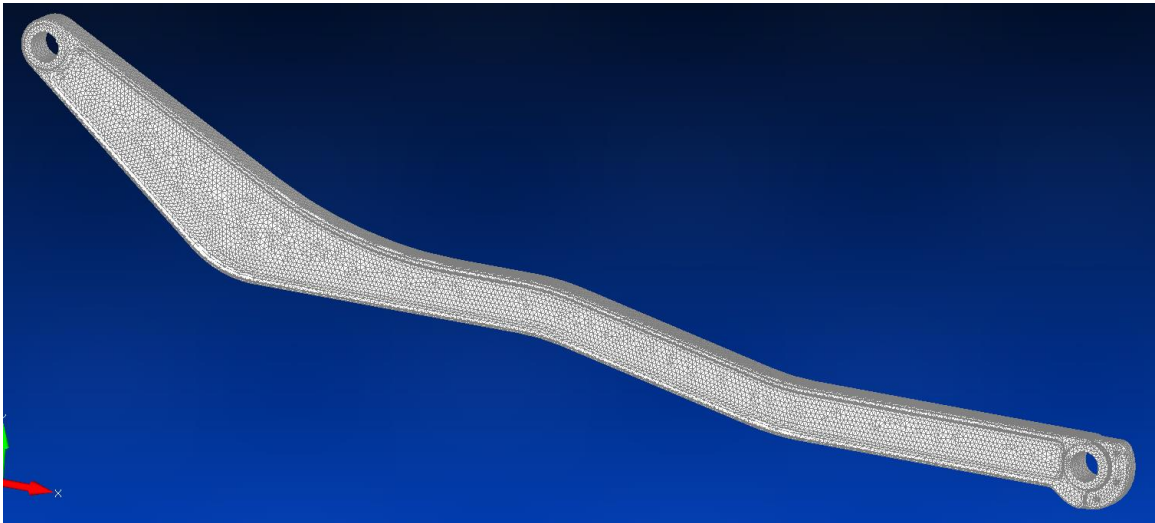
## Initial MODEL



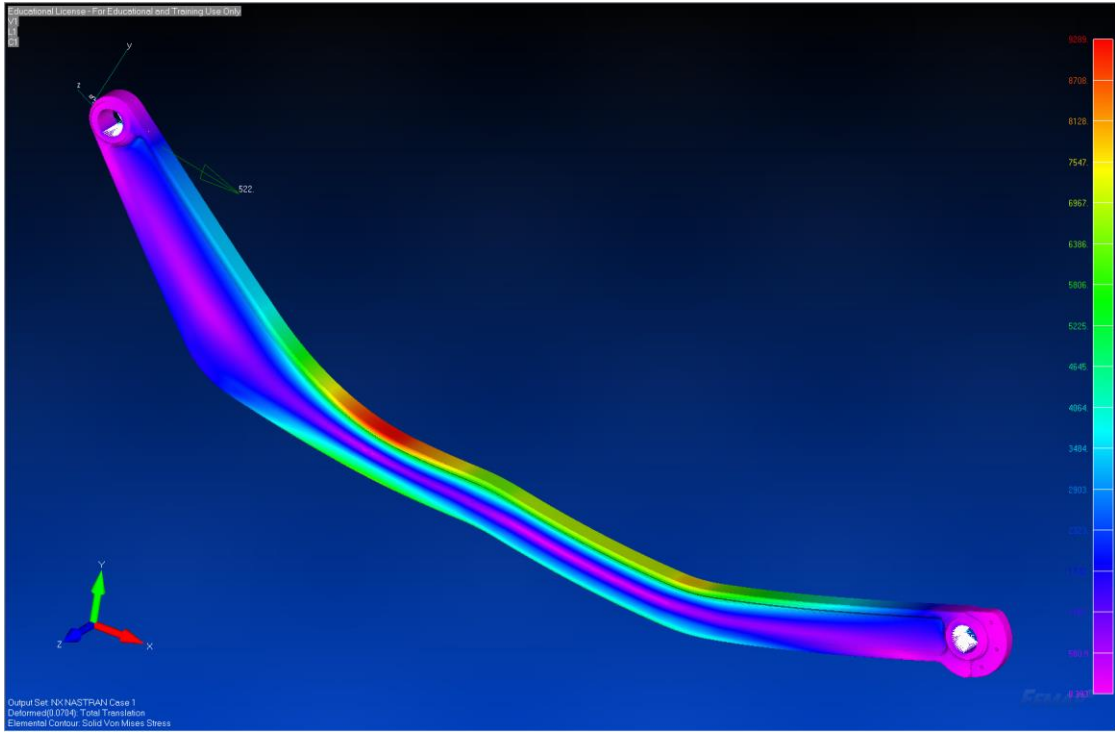
## Final MODEL



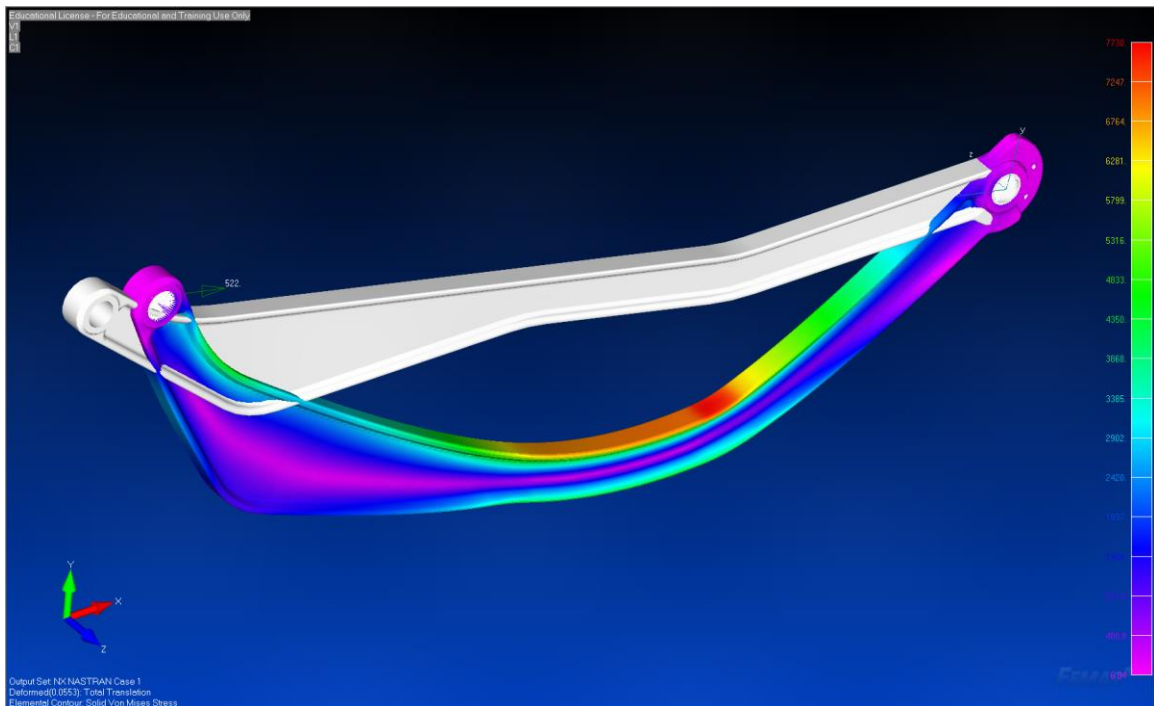
# MESH



# Initial RESULTS (Rev 0)



# Final RESULTS (Rev 1)





## FINITE ELEMENT ANALYSIS REPORT: FEA #6

**Part/Assembly Model File:** MA0 - A02-00008 Chassis Welded Subassembly (STEP 102).x\_t

**Femap Project File:** MA0 - A02-00008 Chassis Welded Subassembly (STEP 102).modfem

**Purpose of Analysis:** Understanding of the overall welds and structure of the chassis components and welds under the highest loads applied by lead screw and legs.

**Material:** A36 Steel

<b>Stiffness</b>		<b>Limit Stress</b>	
Youngs Modulus, E	29000000.	Tension	0.
Shear Modulus, G	0.	Compression	0.
Poisson's Ratio, nu	0.26	Shear	0.
<b>Thermal</b>		Mass Density	7.35736E-4
Expansion Coeff, a	6.E-6	Damping, 2C/Co	0.
Conductivity, k	0.00069444	Reference Temp	70.
Specific Heat, Cp	44.8224		
Heat Generation Factor	0.		

**Loads:** Force Analysis Max Value

- FC: 42 lbf

**Constraints:**

- Rear Hole: TX, TY, TZ, RX, RY
- Front Hole: TX, TY, TZ, RX, RY

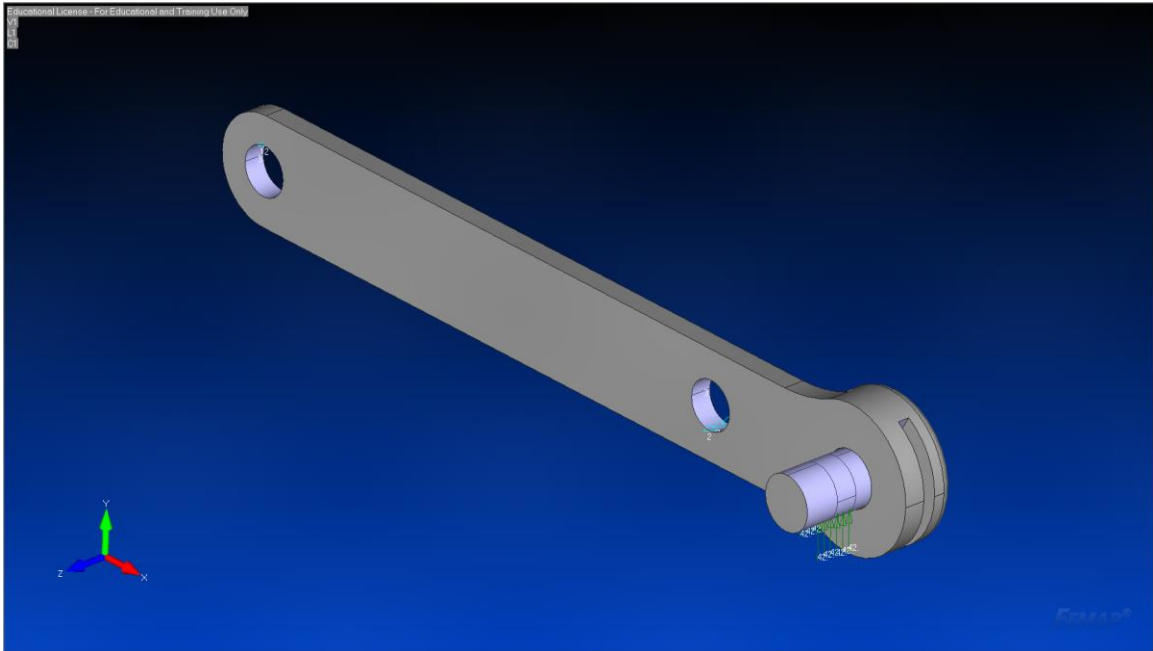
**Mesh:**

- Base Mesh Size: 0.03 inches

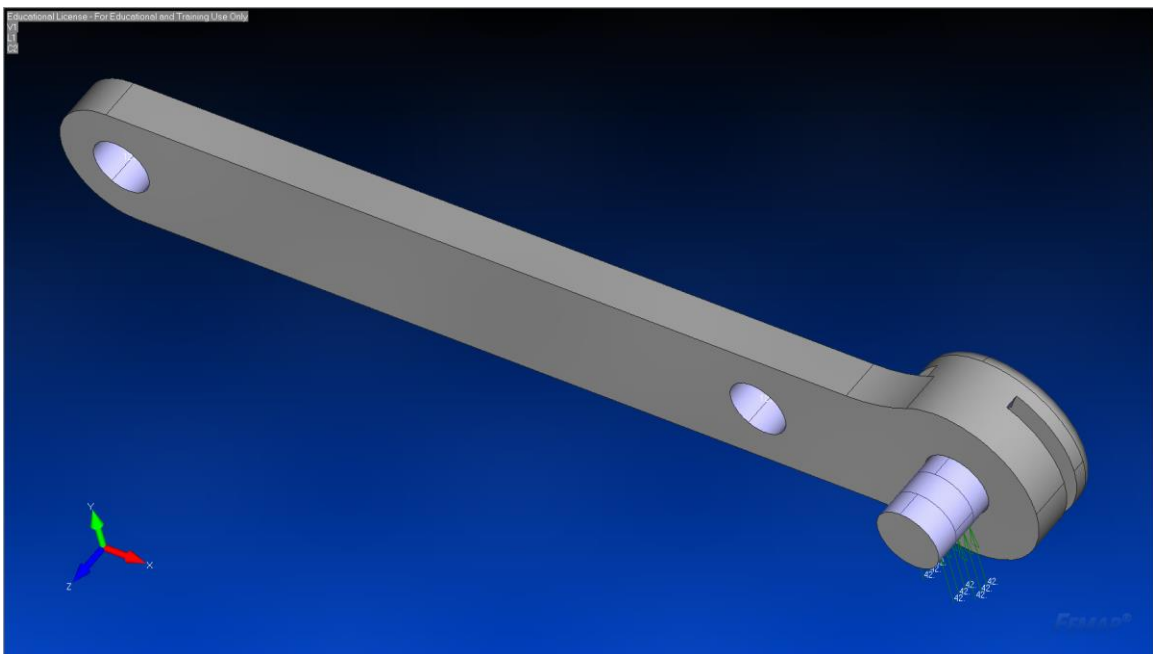
**Pertinent Results:**

<i>Description</i>	<i>Value</i>
Maximum Local Von-Mises Stress	11,706 psi

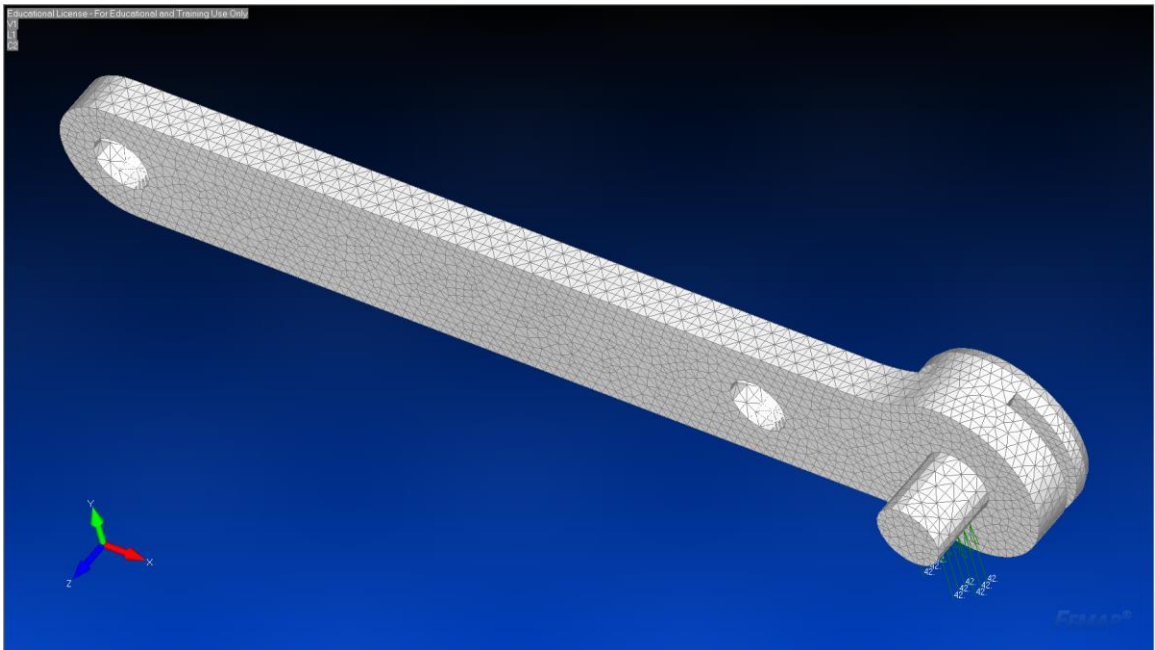
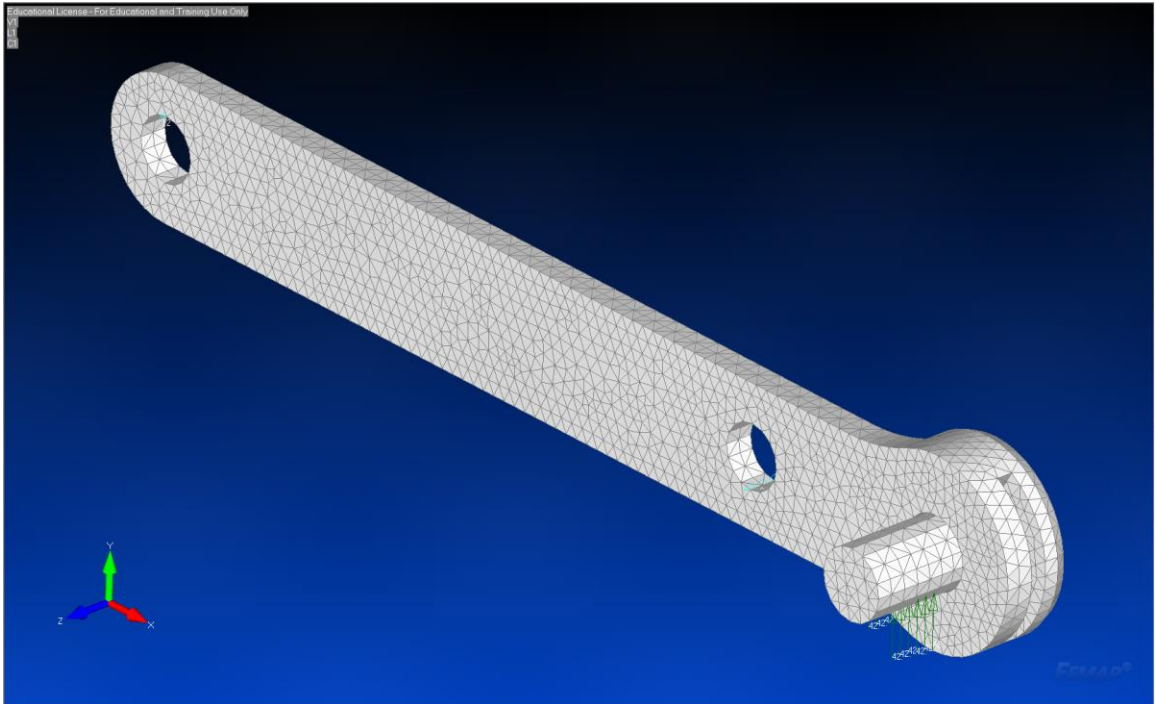
# Initial MODEL



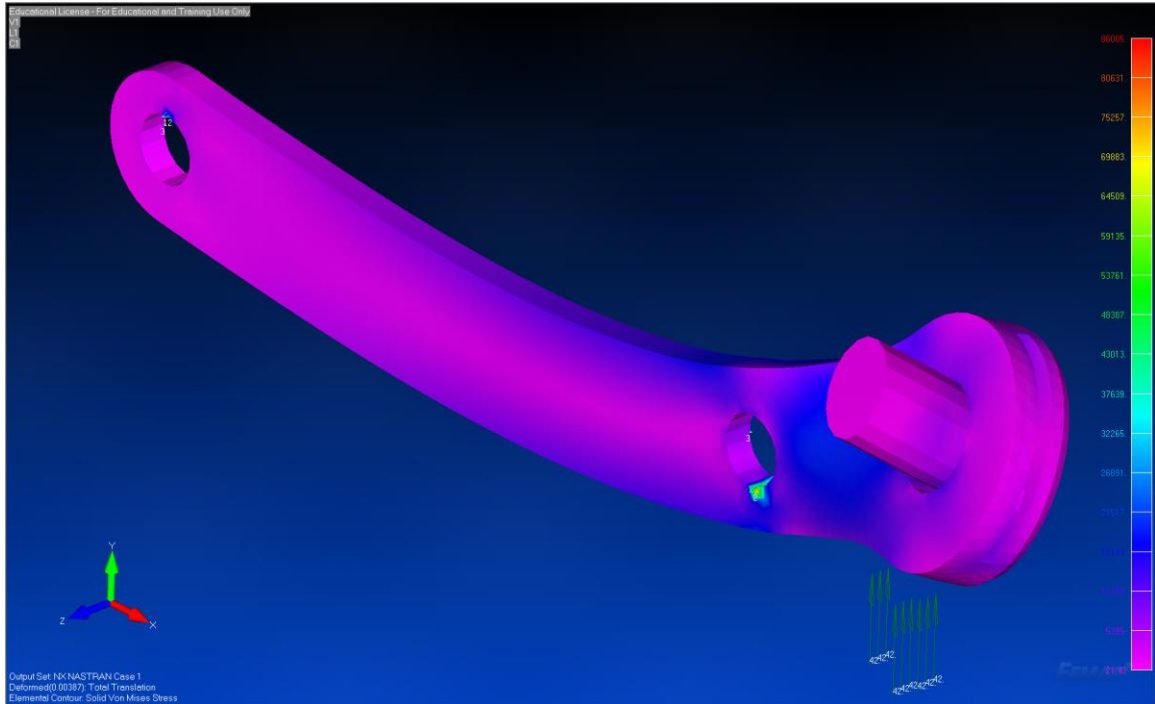
# Final MODEL



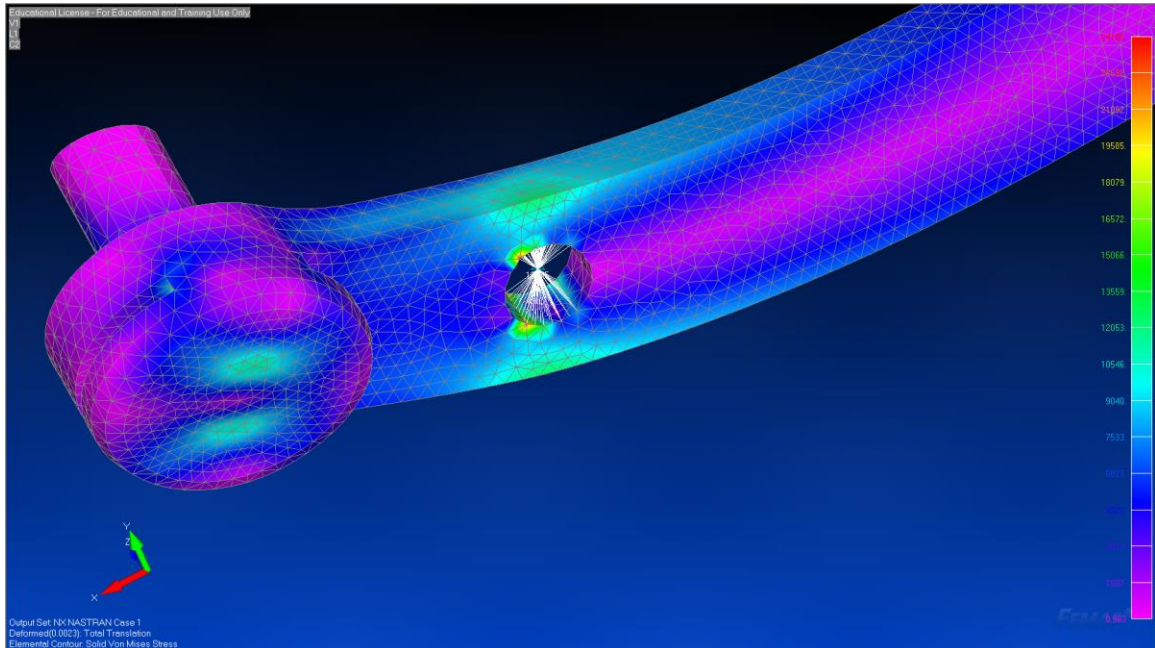
# MESH



# Initial RESULTS (Rev 0)



# Final RESULTS (Rev 1)



## FINITE ELEMENT ANALYSIS REPORT: FEA #7

### Part/Assembly Model File:

- Initial Model: A0 - A02-00012 Left Welded Seat Bar Subassembly.SLDPRT
- Final Model: A1 - A02-00012 Left Welded Seat Bar Subassembly.SLDPRT

### Femap Project File:

- Initial Project: A0 - A02-00012 Left Welded Seat Bar Subassembly.modfem
- Final Project: A1 - A02-00012 Left Welded Seat Bar Subassembly.modfem

**Purpose of Analysis:** Response under max load (102).

**Material:** A36

<b>Stiffness</b>		<b>Limit Stress</b>	
Youngs Modulus, E	29000000.	Tension	0.
Shear Modulus, G	0.	Compression	0.
Poisson's Ratio, nu	0.26	Shear	0.
<b>Thermal</b>		Mass Density	
Expansion Coeff, a	6.E-6	7.35736E-4	
Conductivity, k	0.00069444	Damping, 2C/Co	0.
Specific Heat, Cp	44.8224	Reference Temp	70.
Heat Generation Factor	0.		

### Loads: Force Analysis Step No. 102

- F5A: (Z-58.4, Y-207.9) lbf
- F2aS1: (Z+519.0, Y+105.8) lbf
- F2aS2: (Z-72.0, Y-14.7) lbf
- F2bS1: (Z+83.7, Y+17.1) lbf
- F2bS2: (Z-22.0, Y-4.5) lbf
- F4A: (Z-332.1, Y+35.0) lbf
- F9screwX\*2: Z-195.0 lbf
- F9screwYfront: Y-69.0 lbf
- F9screwYrear: Y+83.5 lbf
- FhangScrew: (Z+76.8, Y+150.5) lbf

### Constraints:

- Front Seat Holes: Fixed

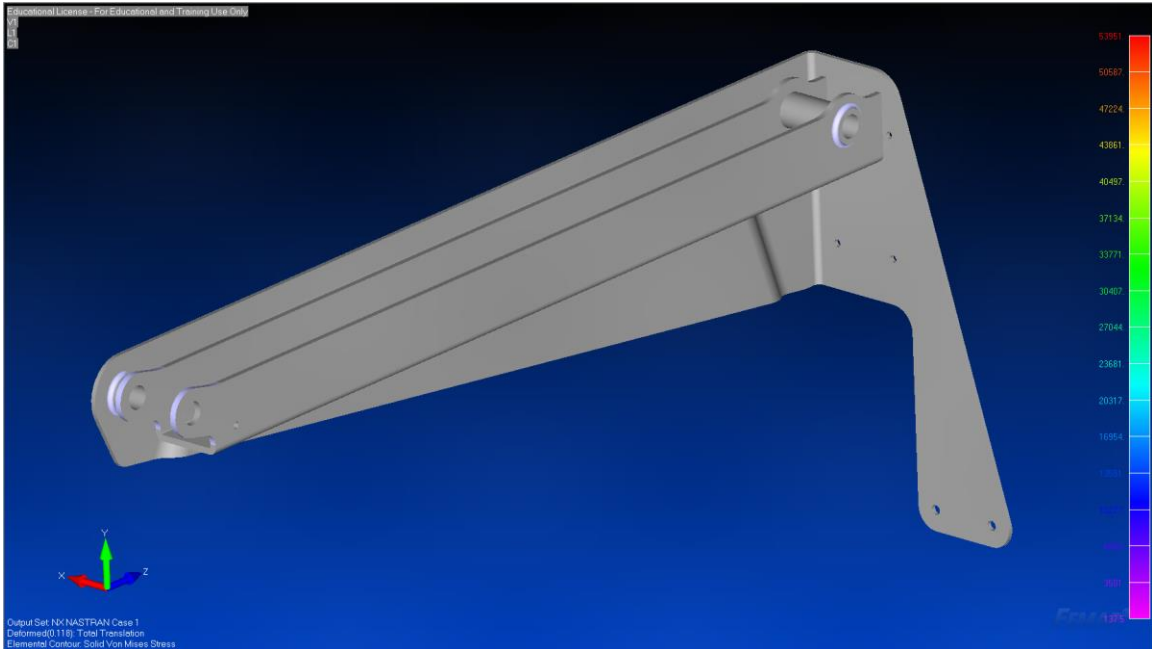
### Mesh:

- Base Mesh Size: 0.1 inches

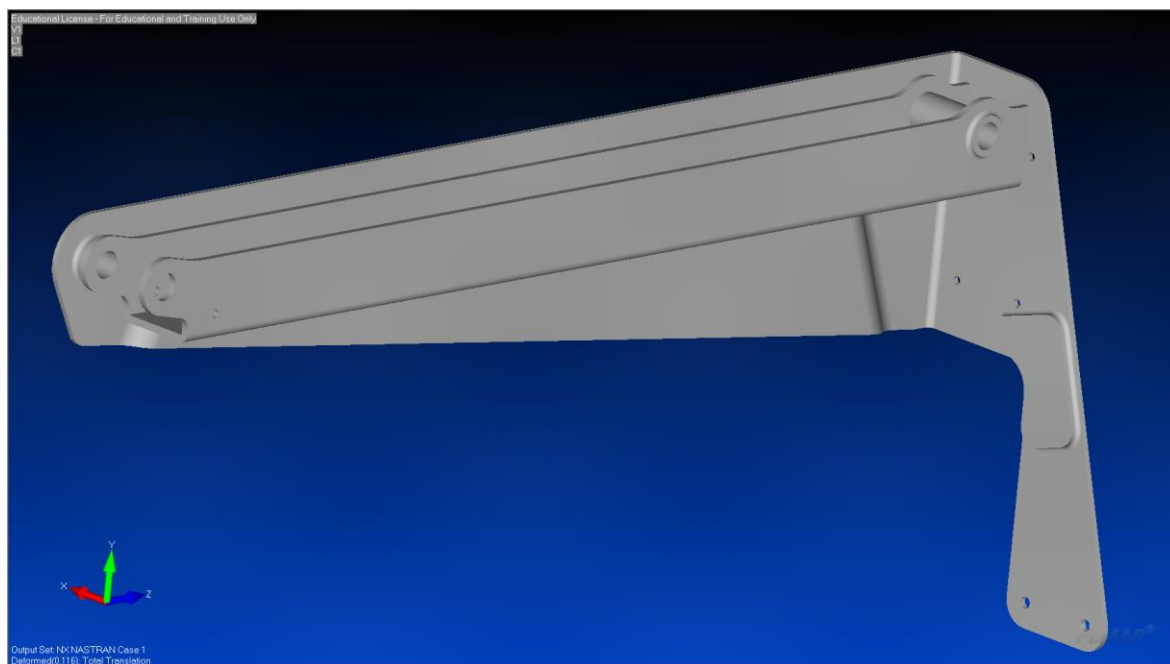
**Pertinent Results:**

<i>Description</i>	<i>Value</i>
Maximum Von-Mises Stress (Non-localized yield)	26,935 psi

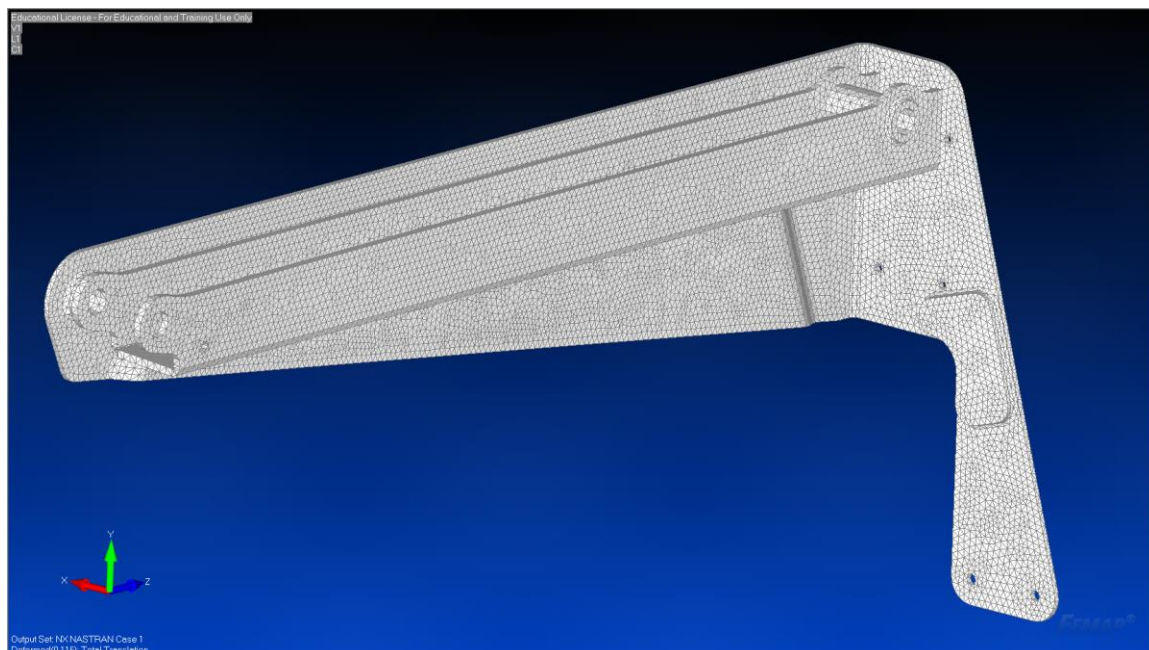
## Initial MODEL



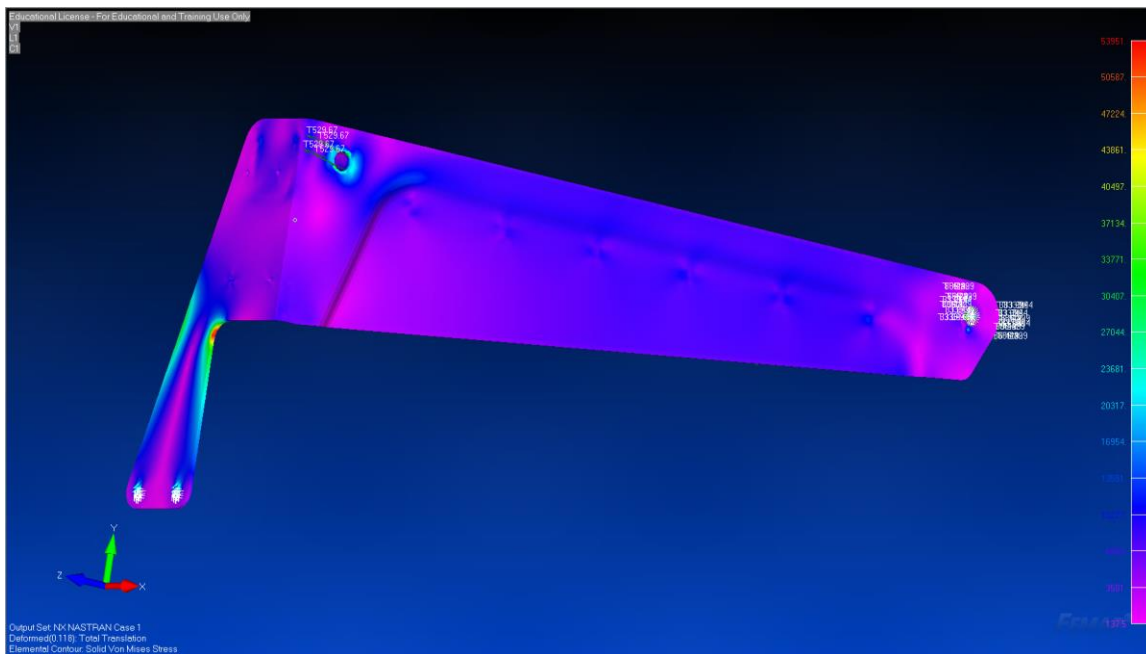
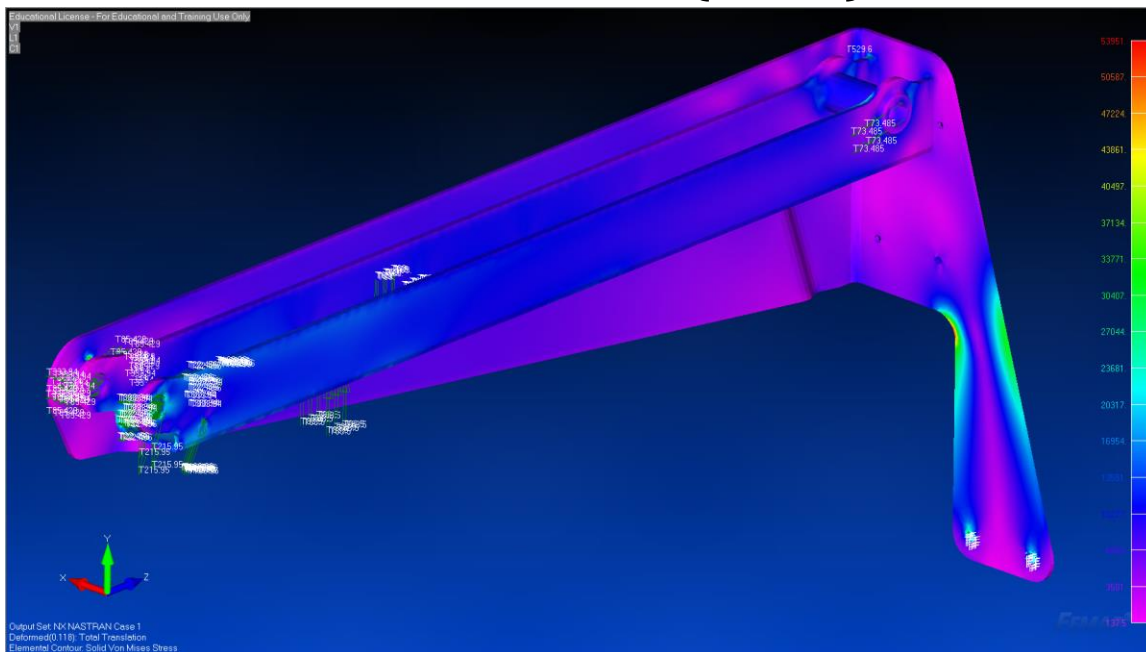
## Final MODEL



## MESH

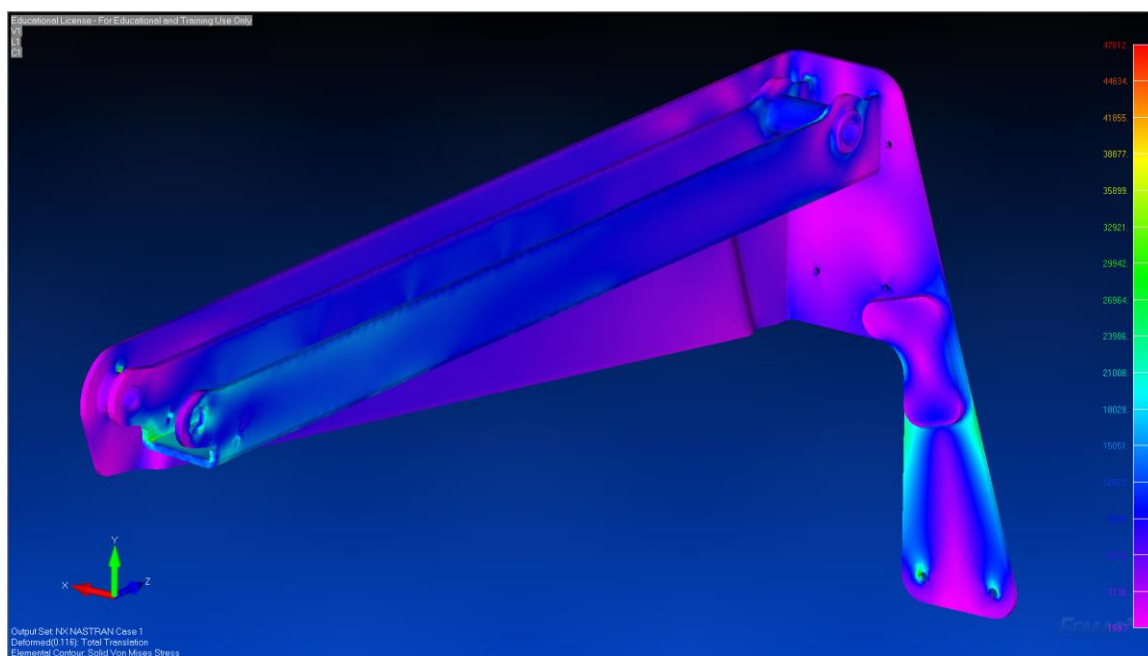
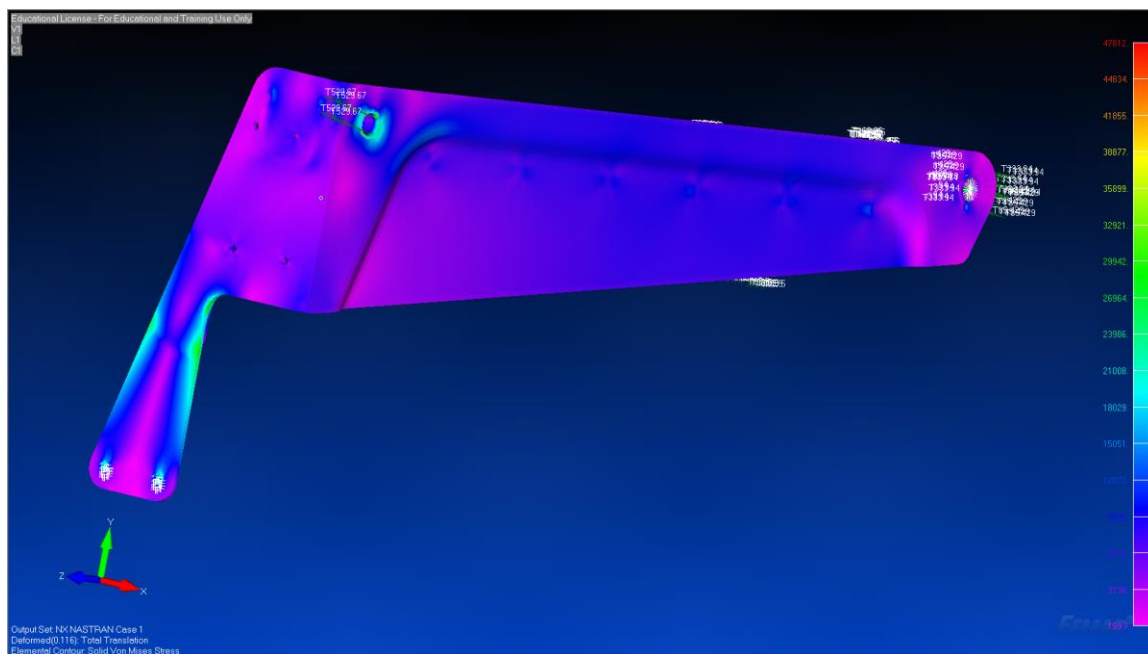


## Initial RESULTS (Rev 0)





# Final RESULTS (Rev 1)



## FINITE ELEMENT ANALYSIS REPORT: FEA #8

**Part/Assembly Model File:** A0 - P02-00002 Back Lock Bar.x\_t

**Femap Project File:** A0 - P02-00002 Back Lock Bar.modfem

**Purpose of Analysis:** Verification of stress and deflection management

**Material:** Aluminum 6061-T6

<b>Stiffness</b>		<b>Limit Stress</b>	
Youngs Modulus, E	9900000.	Tension	35000.
Shear Modulus, G	0.	Compression	35000.
Poisson's Ratio, nu	0.33	Shear	27000.
<b>Thermal</b>		<b>Mass Density</b>	
Expansion Coeff, a	1.265E-5	Damping, 2C/Co	0.
Conductivity, k	0.00206019	Reference Temp	70.
Specific Heat, Cp	81.144		
Heat Generation Factor	0.		

**Loads:** Force Analysis Step No. 201 (maximum F9 compressive value)

- F9: X'-82.0 lbf
- Fspring: Z+9.0 lbf

**Constraints:**

- Bracket Pivot: TX, TY, TZ, RY, RZ
- Contact Line: TX' (X' forms a line between the contact point and the center of the bracket pivot)

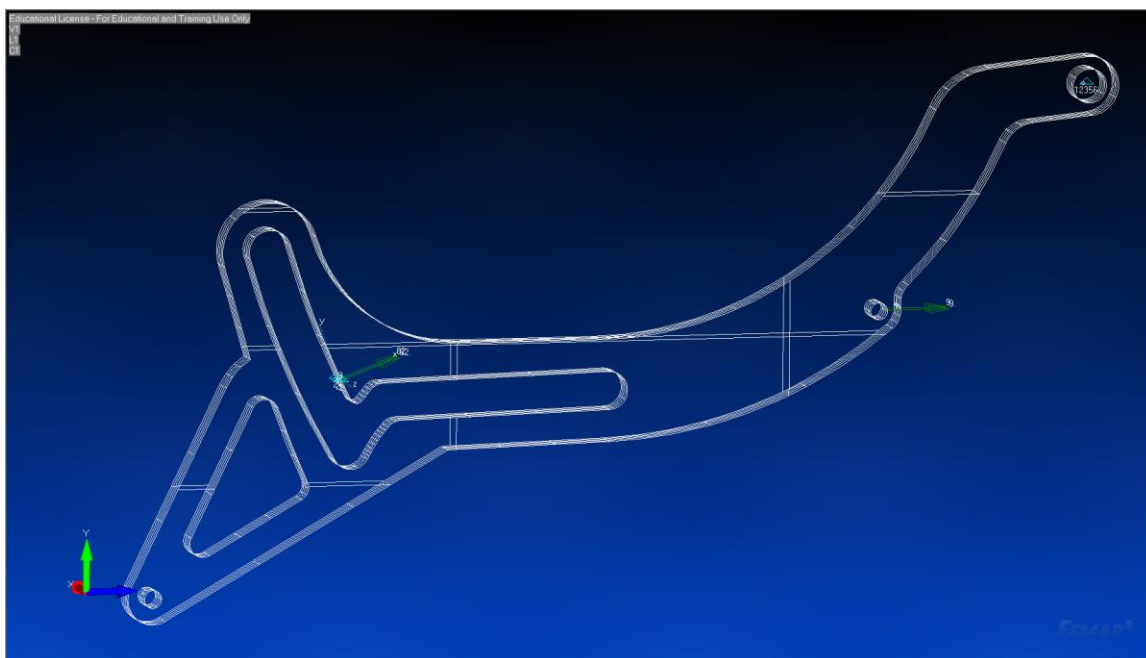
**Mesh:**

- Base Mesh Size: 0.15 inches

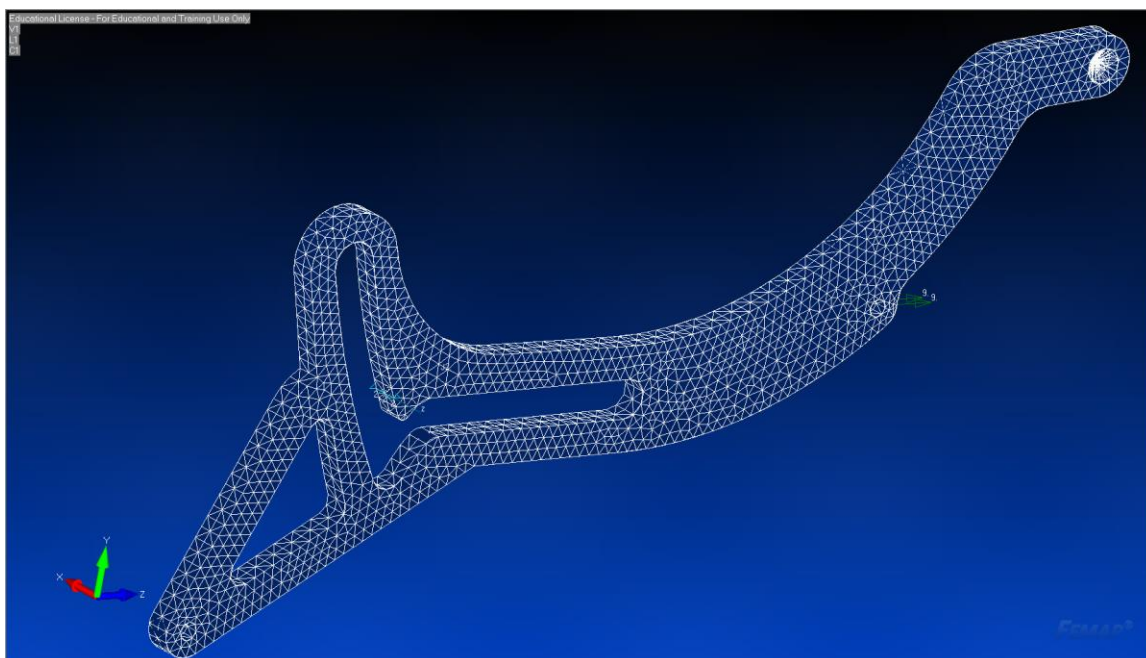
**Pertinent Results:**

<i>Description</i>	<i>Value</i>
Maximum Local Von-Mises Stress	15,283 psi
Maximum Deflection	0.0185 inches

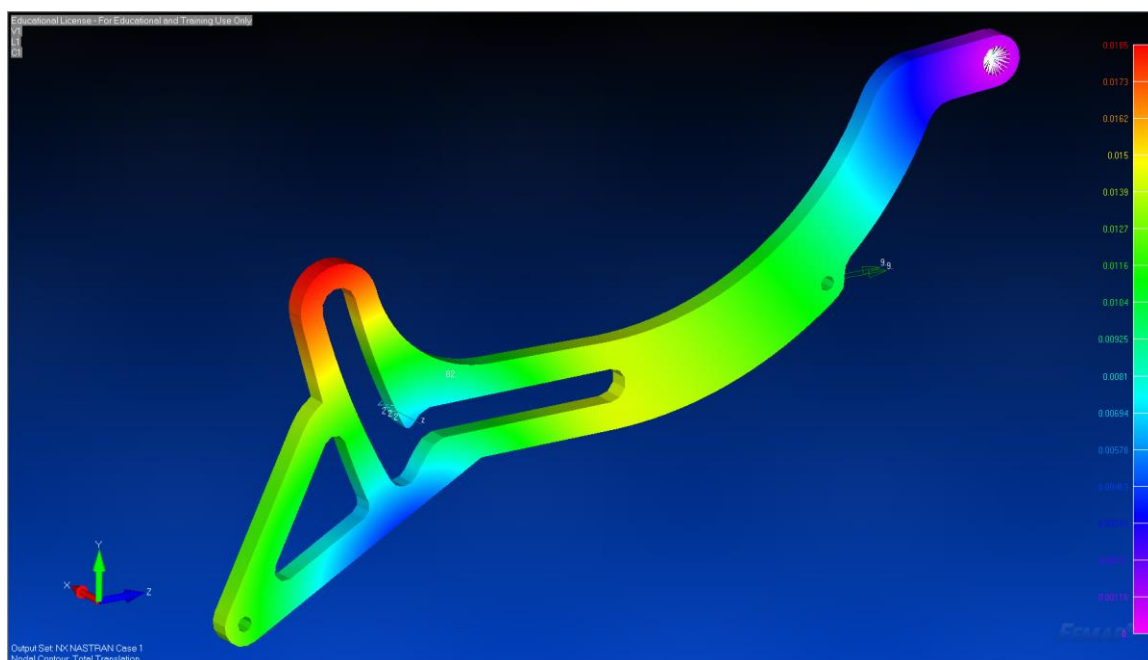
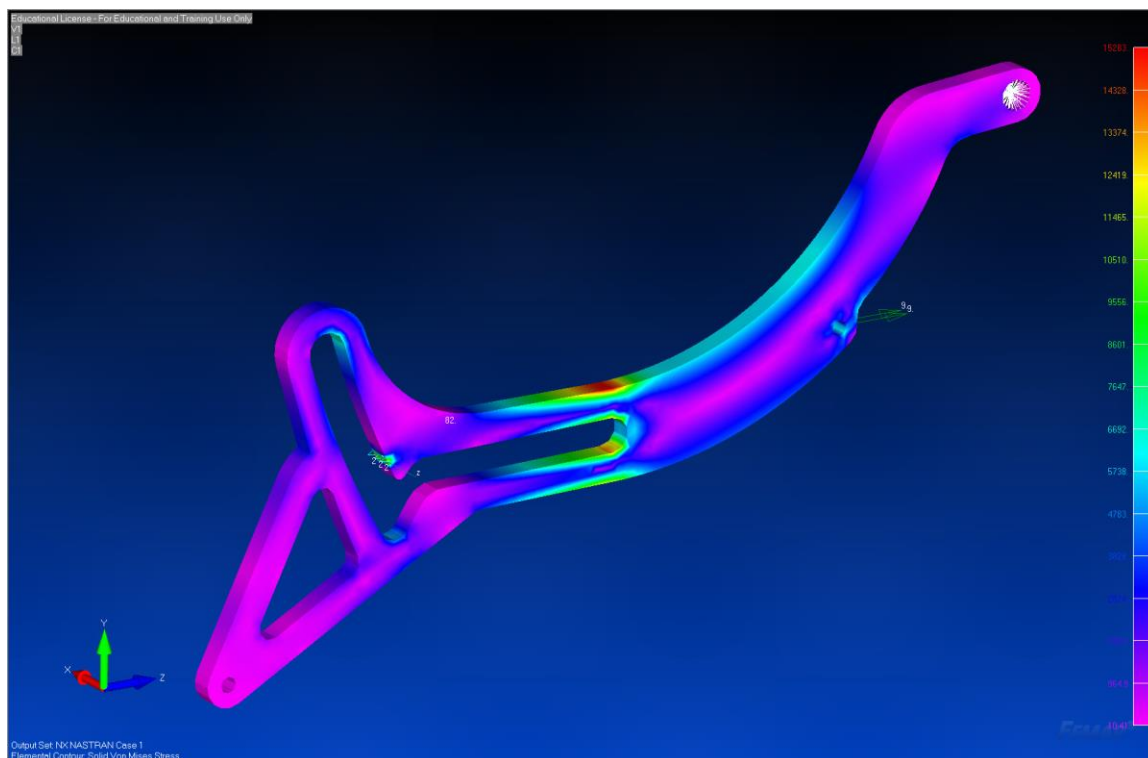
# MODEL



# MESH



# RESULTS



## FINITE ELEMENT ANALYSIS REPORT: FEA #9

**Part/Assembly Model File:** A0 - P02-00006 Back Tension Bar.SLDPRT

**Femap Project File:** A0 - P02-00006 Back Tension Bar.modfem

**Purpose of Analysis:** Validate structural integrity of the back stop.

**Material:** Aluminum 6061-T6

<b>Stiffness</b>		<b>Limit Stress</b>	
Youngs Modulus, E	9900000.	Tension	35000.
Shear Modulus, G	0.	Compression	35000.
Poisson's Ratio, nu	0.33	Shear	27000.
<b>Thermal</b>		<b>Mass Density</b>	
Expansion Coeff, a	1.265E-5	Damping, 2C/Co	0.
Conductivity, k	0.00206019	Reference Temp	70.
Specific Heat, Cp	81.144		
Heat Generation Factor	0.		

**Loads:** Force Analysis Step No. 102

- Tensile - F9:  $195.5 \text{ lbf} / 2 = 97.75 \text{ lbf}$  (because there are two that share the load)
- Compressive – (Buckling): Z-42 lbf (this is 2x the calculated load, which accounts for the user forcibly pushing backward with their back in the full raised position)

**Constraints:**

- Tensile - Fixed: Symmetry Face
- Compressive – Fixed End: TX, TY, TZ, RZ
- Compressive – Free End: TX, TY

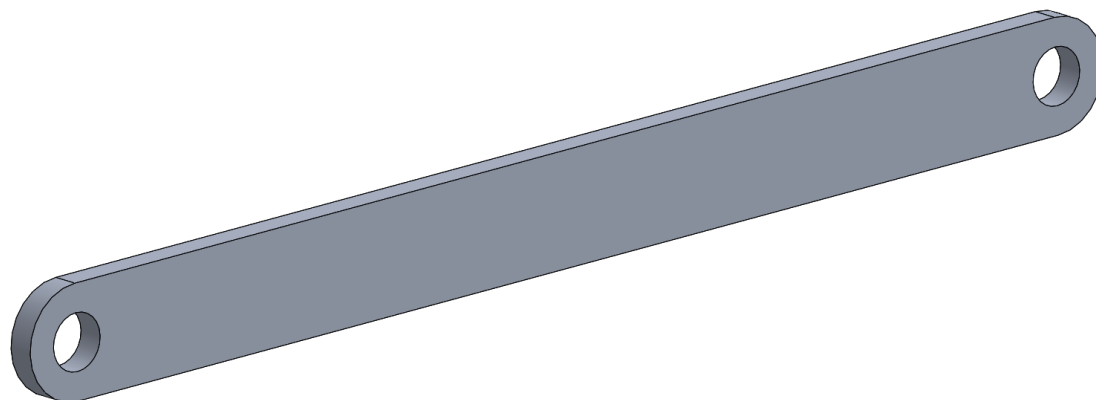
**Mesh:**

- Base Mesh: 0.05 inches
- Refined Mesh: (Inside of hole) 0.015 inches

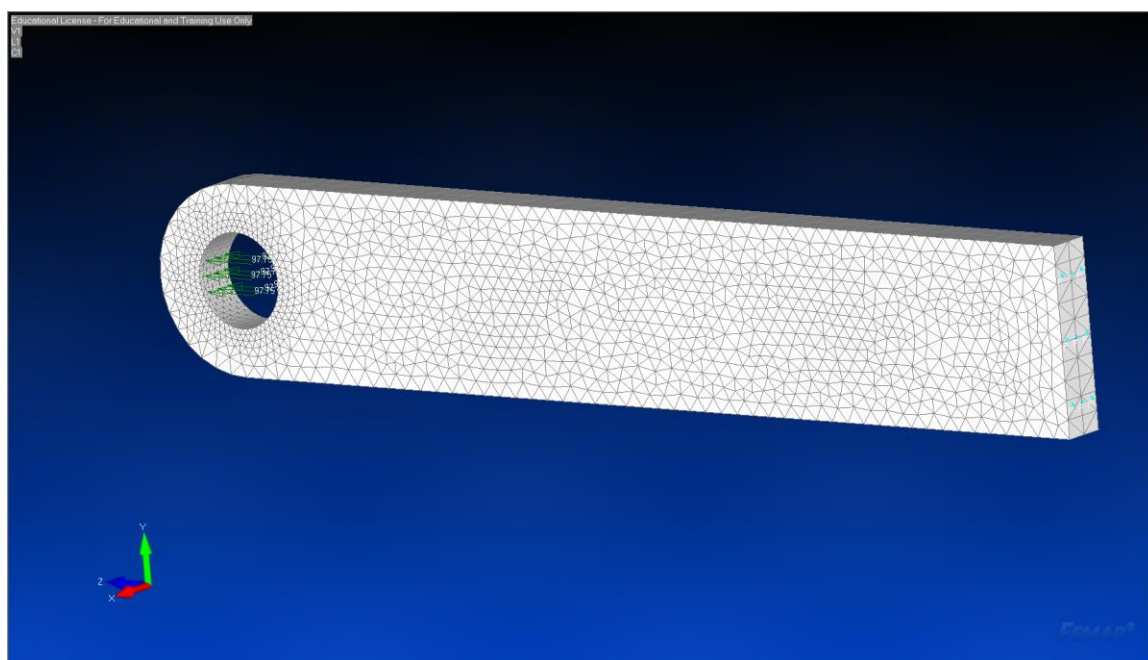
**Pertinent Results:**

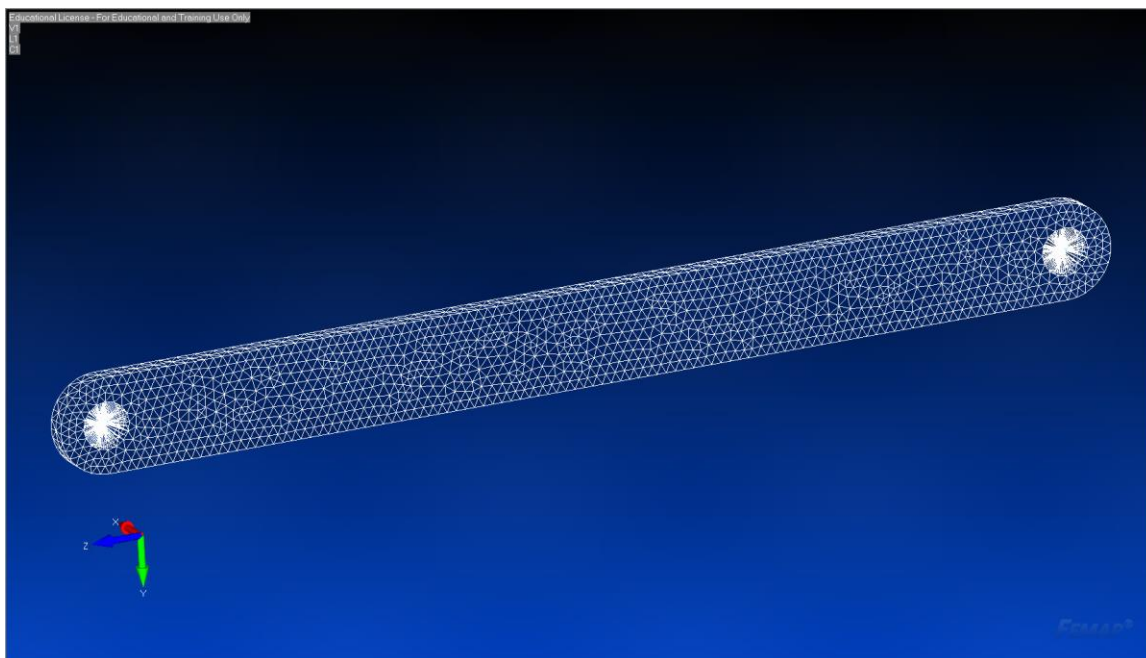
<i>Description</i>	<i>Value</i>
Max Von-Mises Stress in hole	13,779 psi
Max Total Deflection (2x)	0.0016 inches
Buckling Safety Factor (1 <sup>st</sup> Eigenvalue: mode 1)	6.54

# MODEL

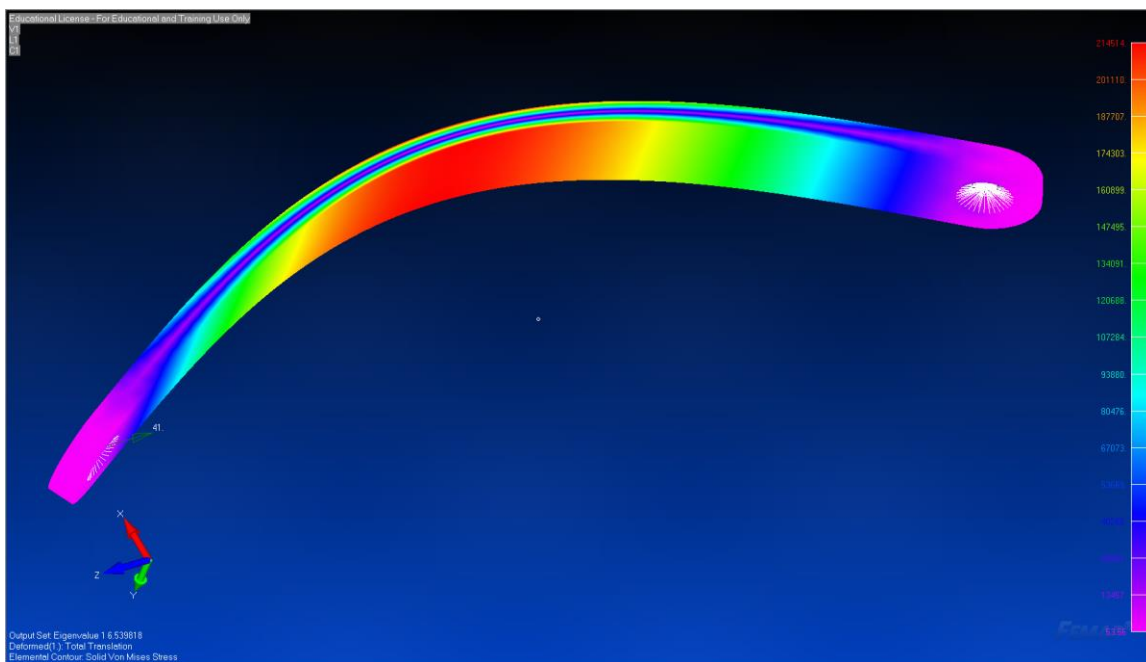


# MESH

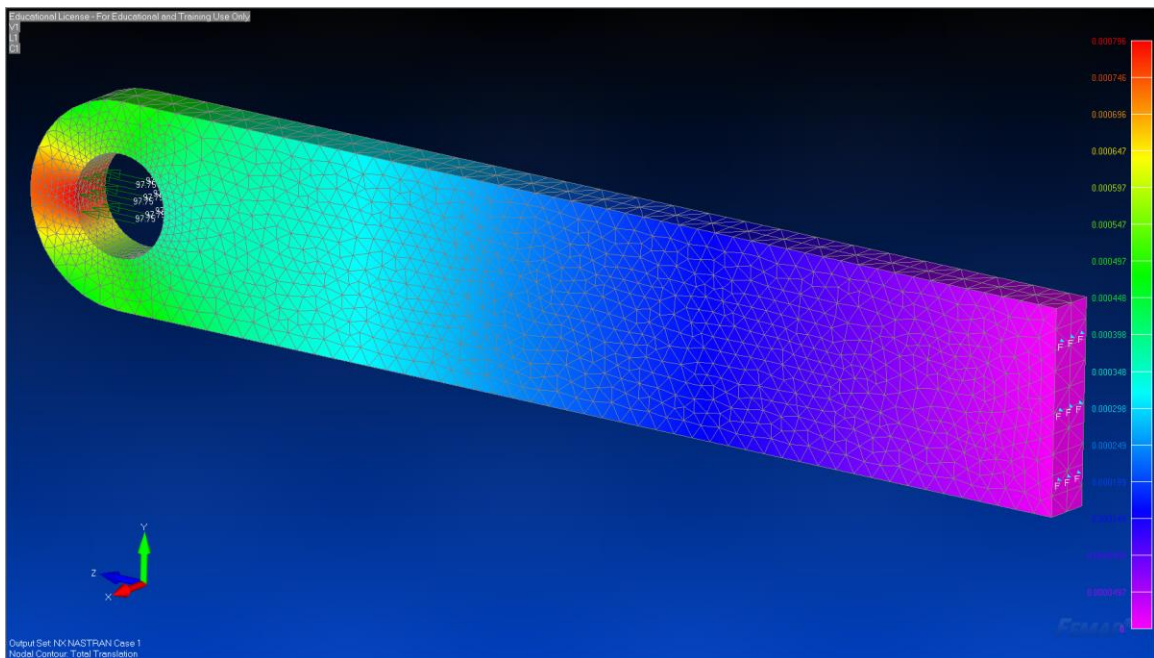
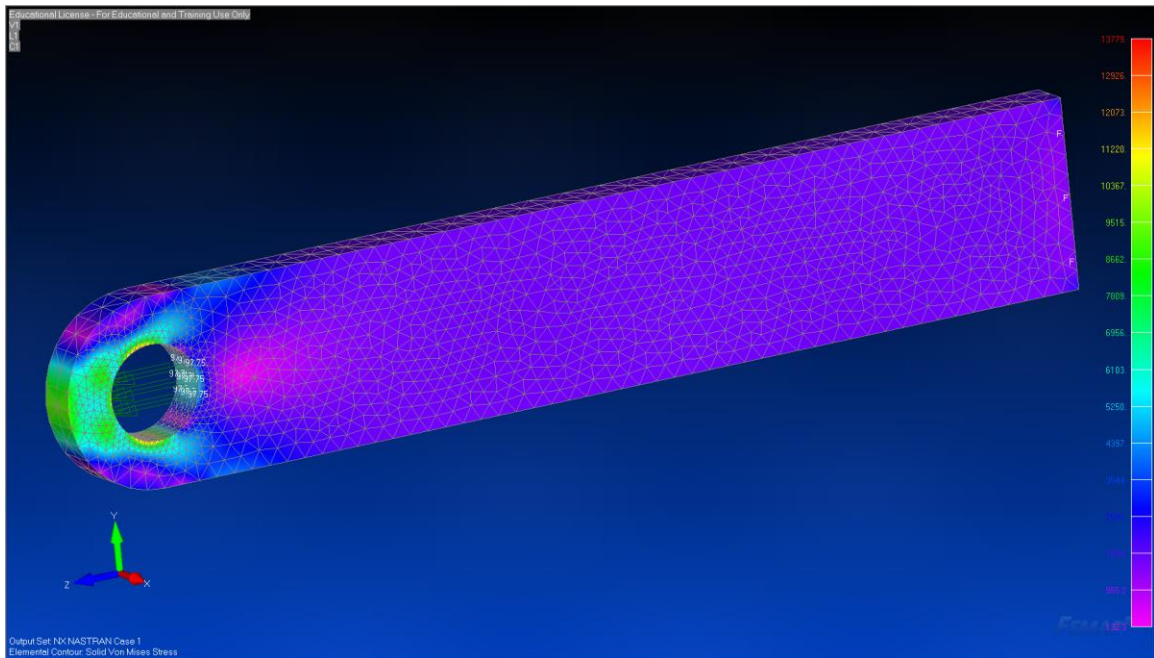




## RESULTS (Buckling)



## RESULTS (Tensile)





## FINITE ELEMENT ANALYSIS REPORT: FEA #10

**Part/Assembly Model File:** A0 - P02-00009 Ball Nut Mounting Plate.SLDPRT

**Femap Project File:** A0 - P02-00009 Ball Nut Mounting Plate.modfem

**Purpose of Analysis:** Verification of stresses with contacts and screw locations

**Material:** Aluminum 6061-T6

Stiffness		Limit Stress	
Youngs Modulus, E	9900000.	Tension	35000.
Shear Modulus, G	0.	Compression	35000.
Poisson's Ratio, nu	0.33	Shear	27000.
Thermal		Mass Density	2.53881E-4
Expansion Coeff, a	1.265E-5	Damping, 2C/Co	0.
Conductivity, k	0.00206019	Reference Temp	70.
Specific Heat, Cp	81.144		
Heat Generation Factor	0.		

**Loads:** Force Analysis Step No. 201 (maximum F9 compressive value)

- F3x: Z-520.0 lbf

**Constraints:**

- Glued Contact between Nut ant Plate
- Tops of Pin Holes: Fixed

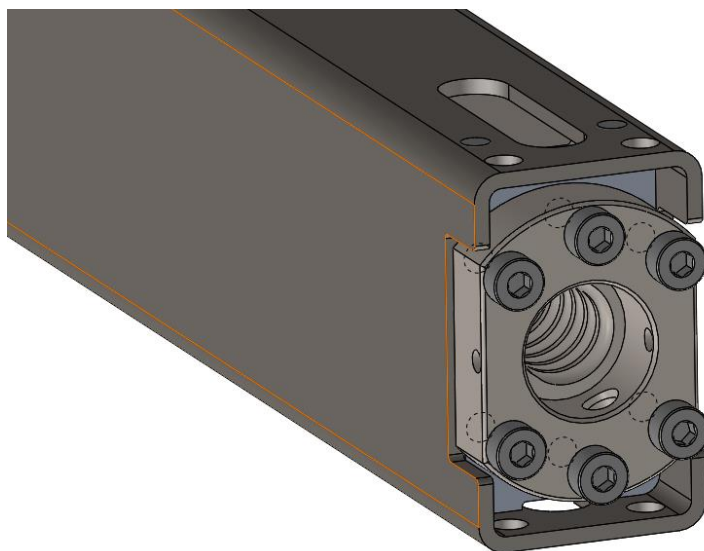
**Mesh:**

- Base Mesh Size: 0.05 inches

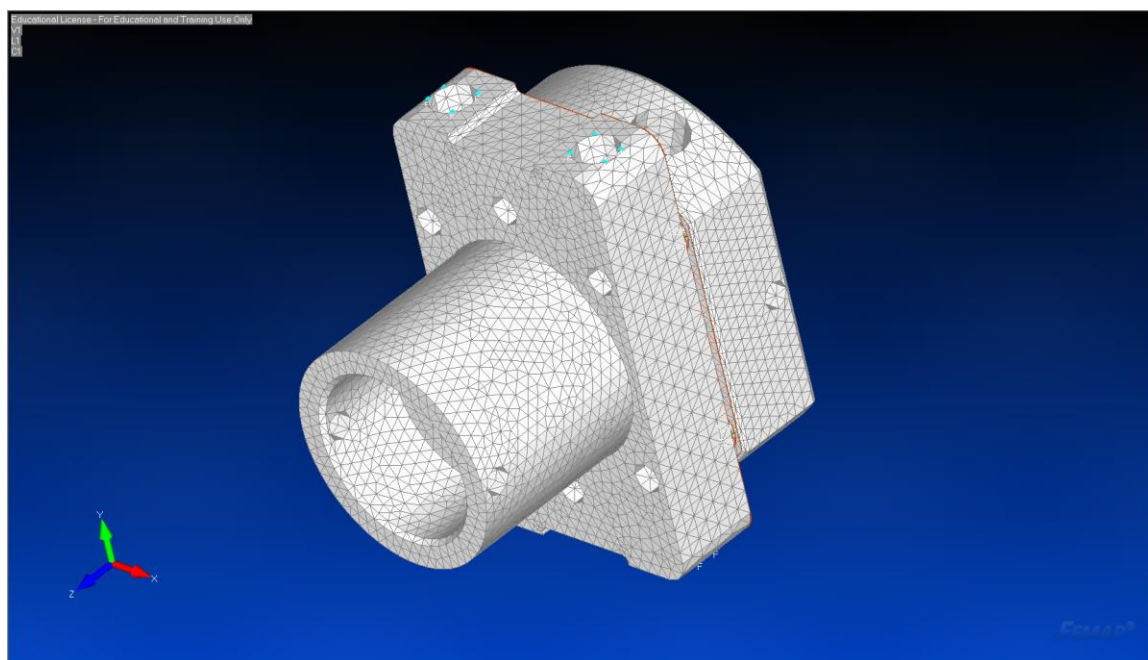
**Pertinent Results:**

<i>Description</i>	<i>Value</i>
Maximum Local Von-Mises Stress	6,133 psi

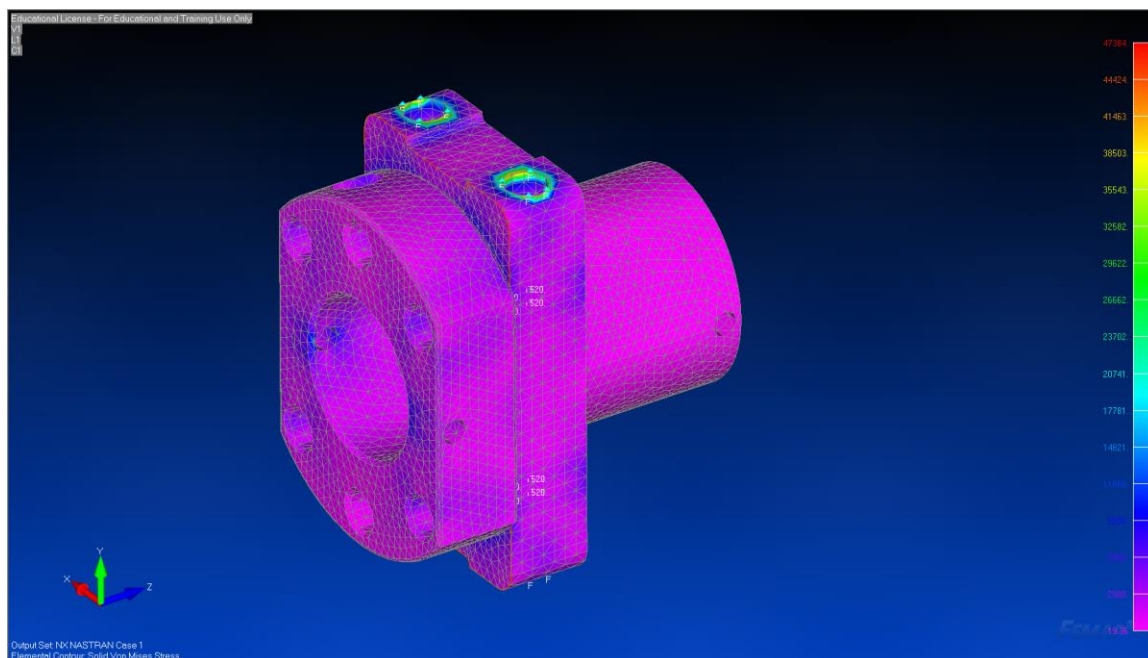
# MODEL



# MESH



# RESULTS



## FINITE ELEMENT ANALYSIS REPORT: FEA #11

### Part/Assembly Model Files:

- Initial: A0 - P02-00010 Belt Safety Pawl.SLDPRT
- Final: A1 - P02-00010 Belt Safety Pawl.SLDPRT

### Femap Project File:

- Initial: A0 - P02-00010 Belt Safety Pawl.modfem
- Final: A1 - P02-00010 Belt Safety Pawl.modfem

**Purpose of Analysis:** Validate structural integrity of the pawl.

**Material:** Aluminum 6061-T6

<b>Stiffness</b>		<b>Limit Stress</b>	
Youngs Modulus, E	9900000.	Tension	35000.
Shear Modulus, G	0.	Compression	35000.
Poisson's Ratio, nu	0.33	Shear	27000.
<b>Thermal</b>		<b>Mass Density</b>	
Expansion Coeff, a	1.265E-5	Mass Density	2.53881E-4
Conductivity, k	0.00206019	Damping, 2C/Co	0.
Specific Heat, Cp	81.144	Reference Temp	70.
Heat Generation Factor	0.		

**Loads:** Both screw torques

- Force from torque: 68 in-lbf = 95.7 lbf combined load on all teeth

**Constraints:**

- Near slot: TX, TY, TZ, RX, RY
- Far slot: TY

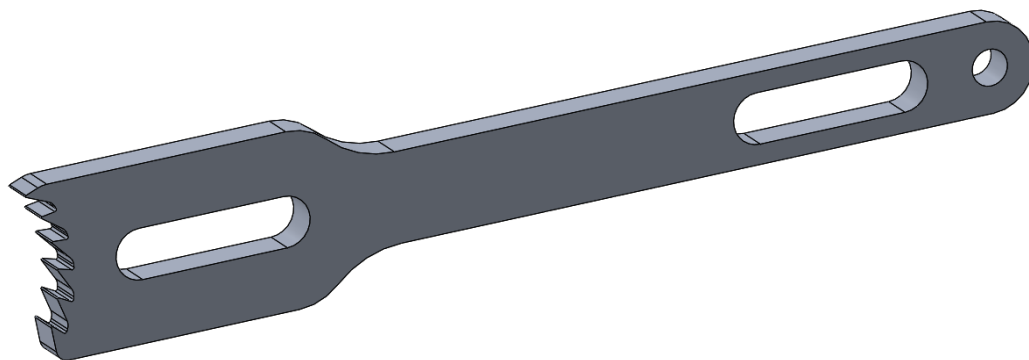
**Mesh:**

- Base Mesh: 0.04 inches

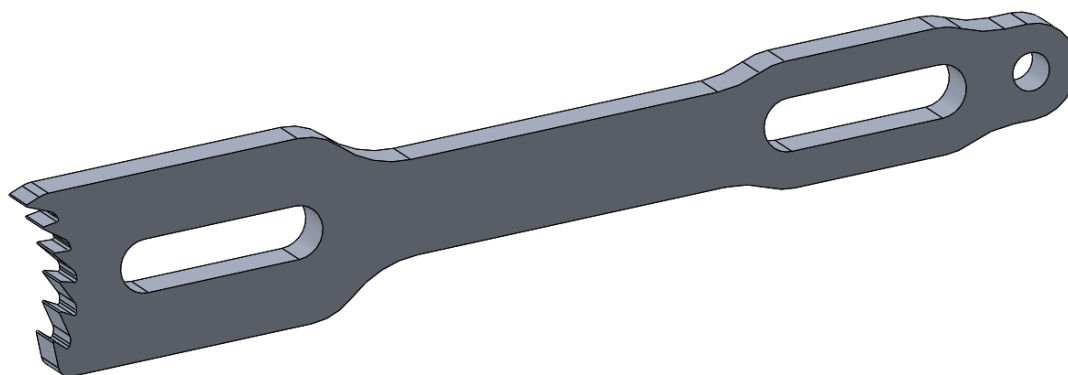
**Pertinent Results:**

<i>Description</i>	<i>Value</i>
Max non-localized Von-Mises Stress (Initial)	17,579 psi
Max non-localized Von-Mises Stress (Final)	13,335 psi

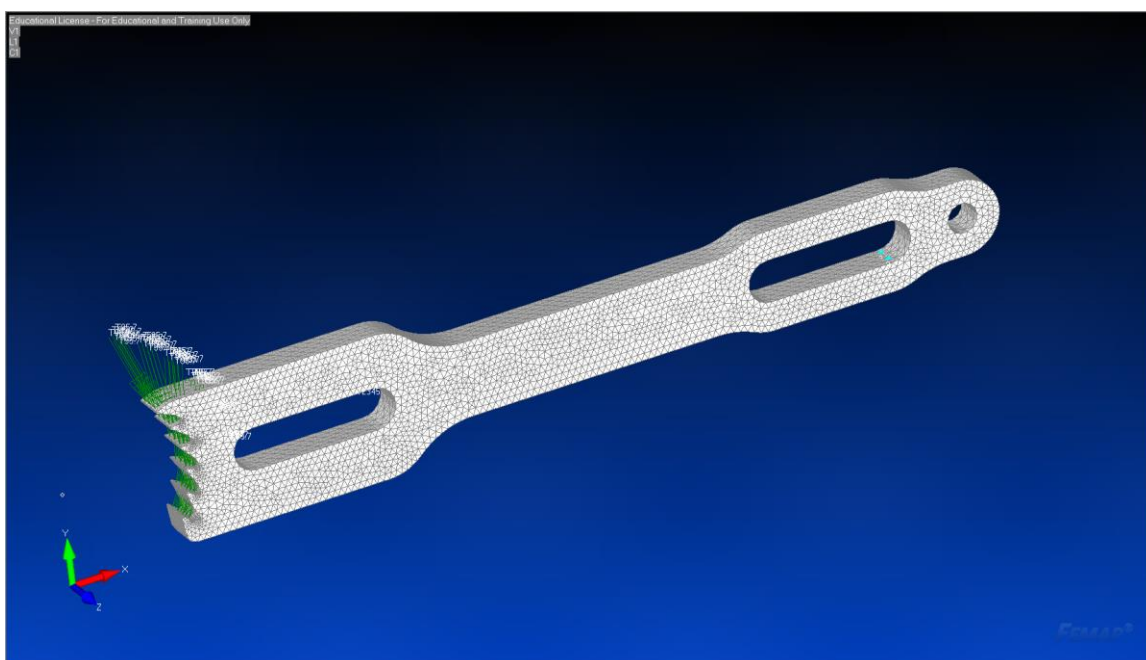
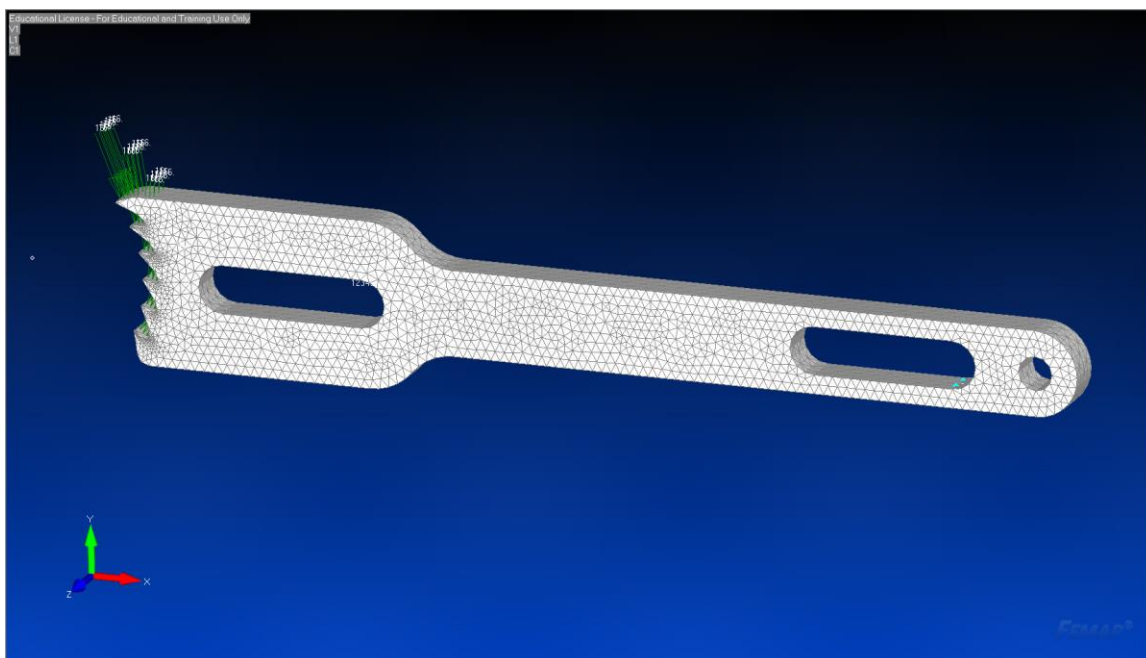
### Initial MODEL



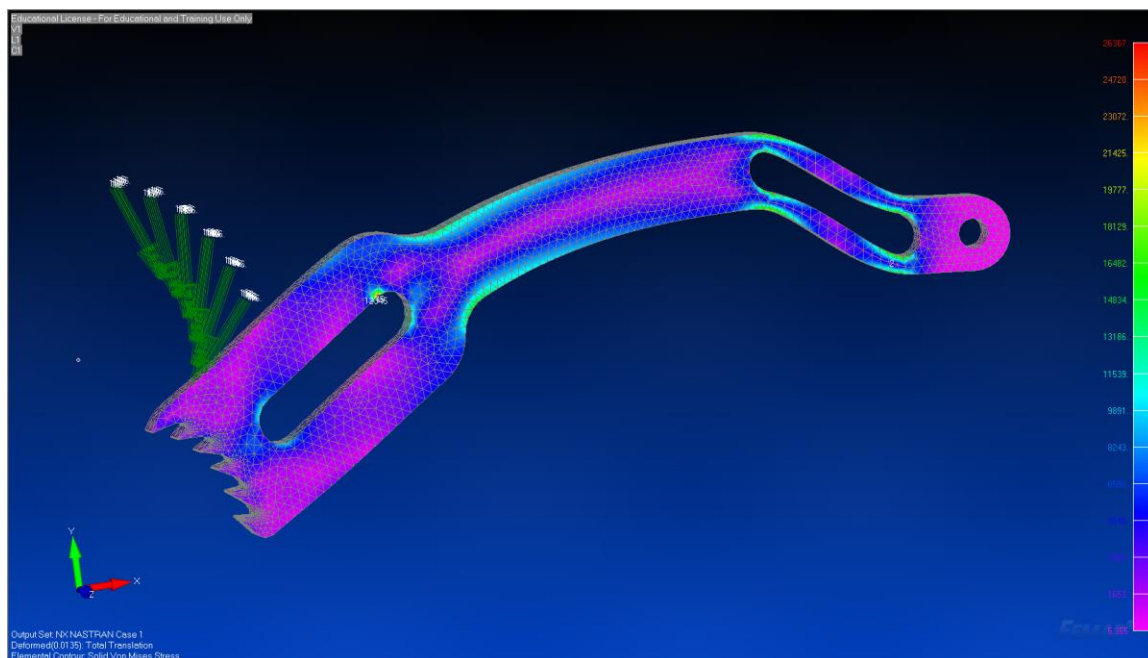
### Final MODEL



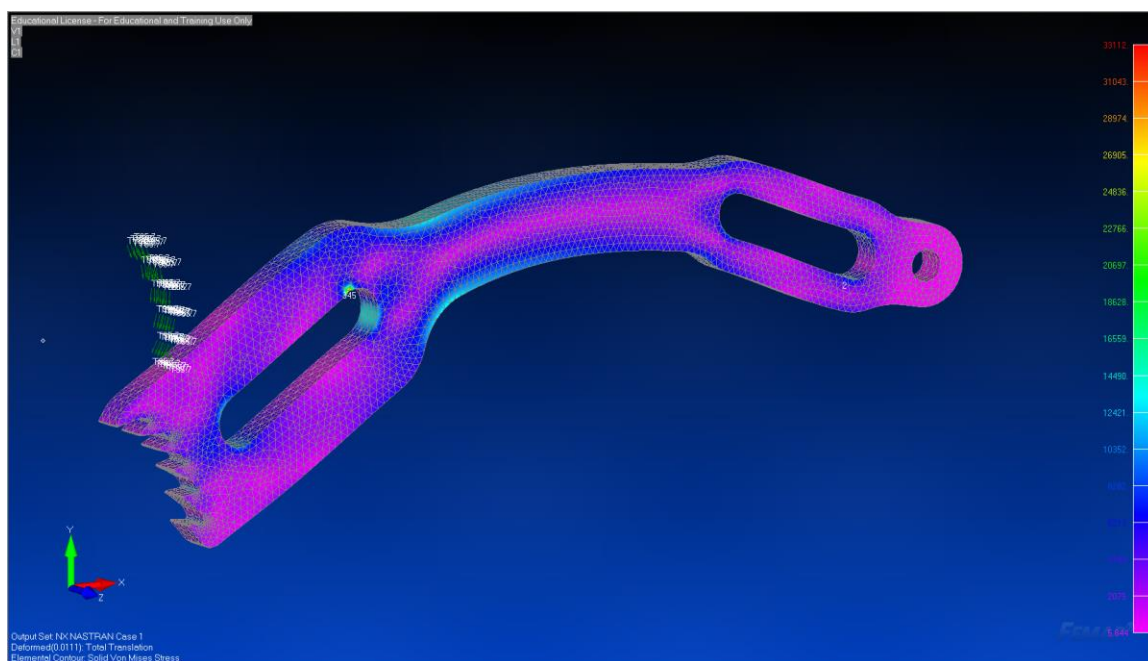
# MESHES



## Initial RESULTS



## Final RESULTS



## FINITE ELEMENT ANALYSIS REPORT: FEA #12

### Part/Assembly Model File:

- A0 - A01-00003 Bridge Subassembly.x\_t

### Femap Project File:

- A0 - A01-00003 Bridge Subassembly.modfem

**Purpose of Analysis:** Validate stresses and deflections to remain well in its guides.

### Material: ABS

<b>Stiffness</b>		<b>Limit Stress</b>	
Youngs Modulus, E	9900000.	Tension	35000.
Shear Modulus, G	0.	Compression	35000.
Poisson's Ratio, nu	0.33	Shear	27000.
<b>Thermal</b>		<b>Mass Density</b>	
Expansion Coeff, a	1.265E-5	Damping, 2C/Co	0.
Conductivity, k	0.00206019	Reference Temp	70.
Specific Heat, Cp	81.144		
Heat Generation Factor	0.		

**Loads:** step 58 gives a max moment in the bridge

- $F78L(58) = Z+44.9 \text{ lbf}$
- $F78U(58) = Z-20.24 \text{ lbf}$

### Constraints:

- Pivot Pin: TY, TZ, RY, RZ
- Symmetry: TX

### Mesh:

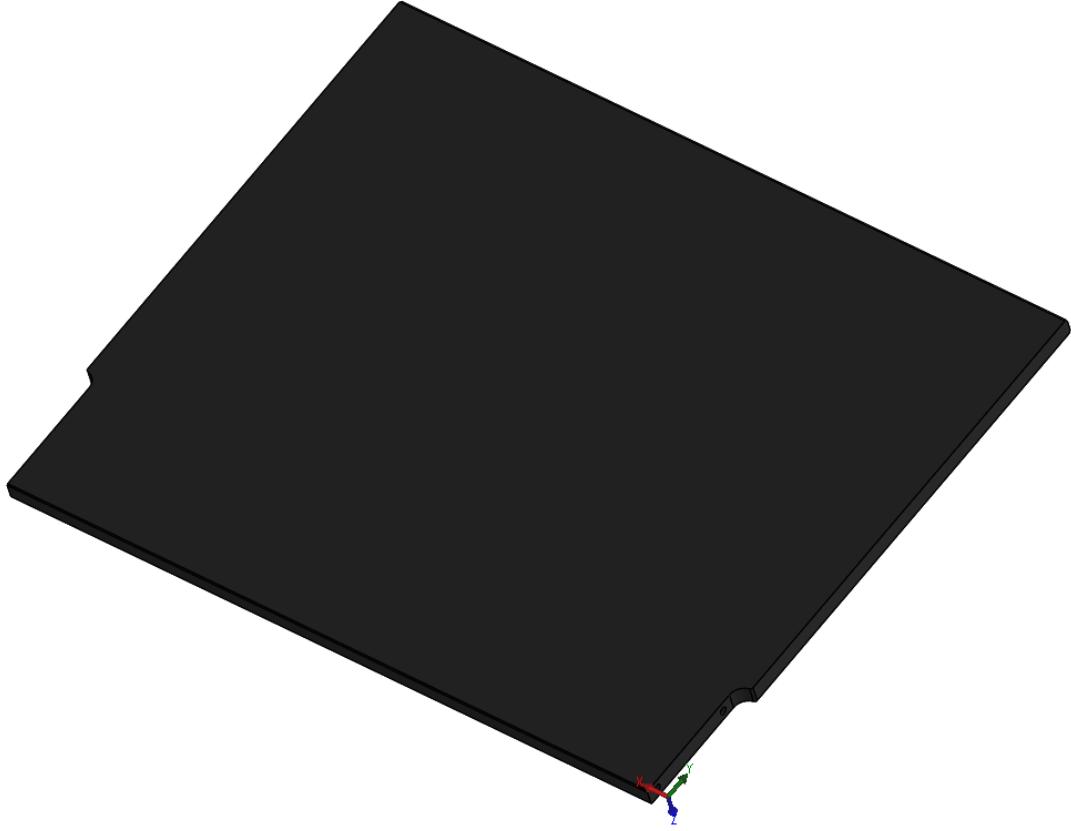
- Base Mesh: 0.25 inches (Bridge)
- Base Mesh: 0.03 inches (Bracket)

### Pertinent Results:

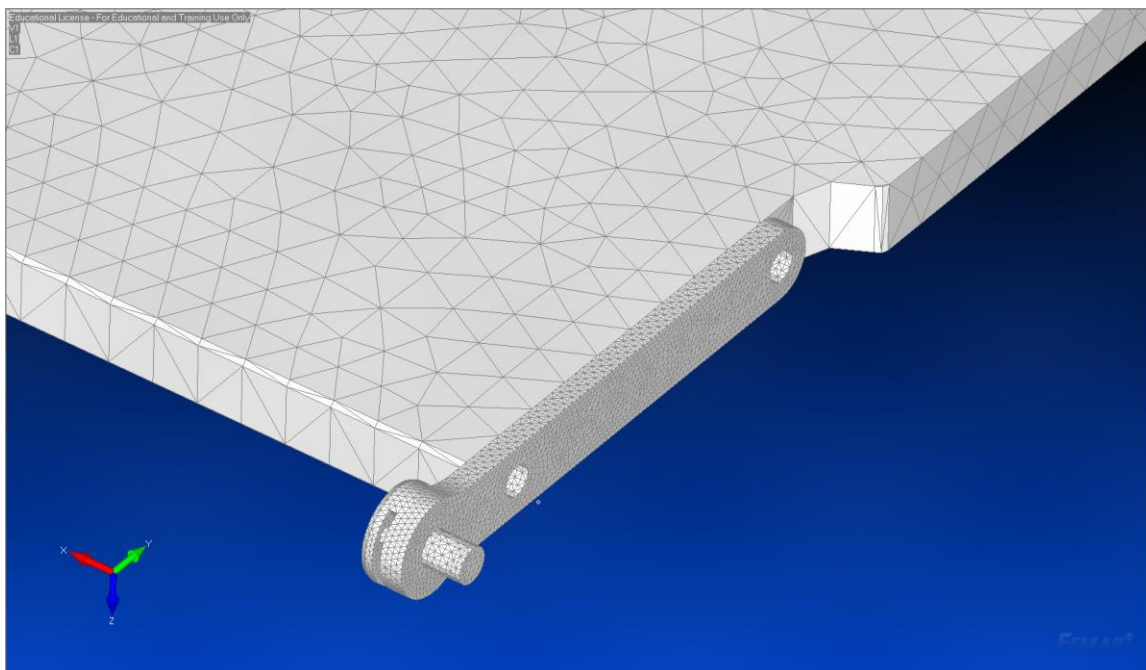
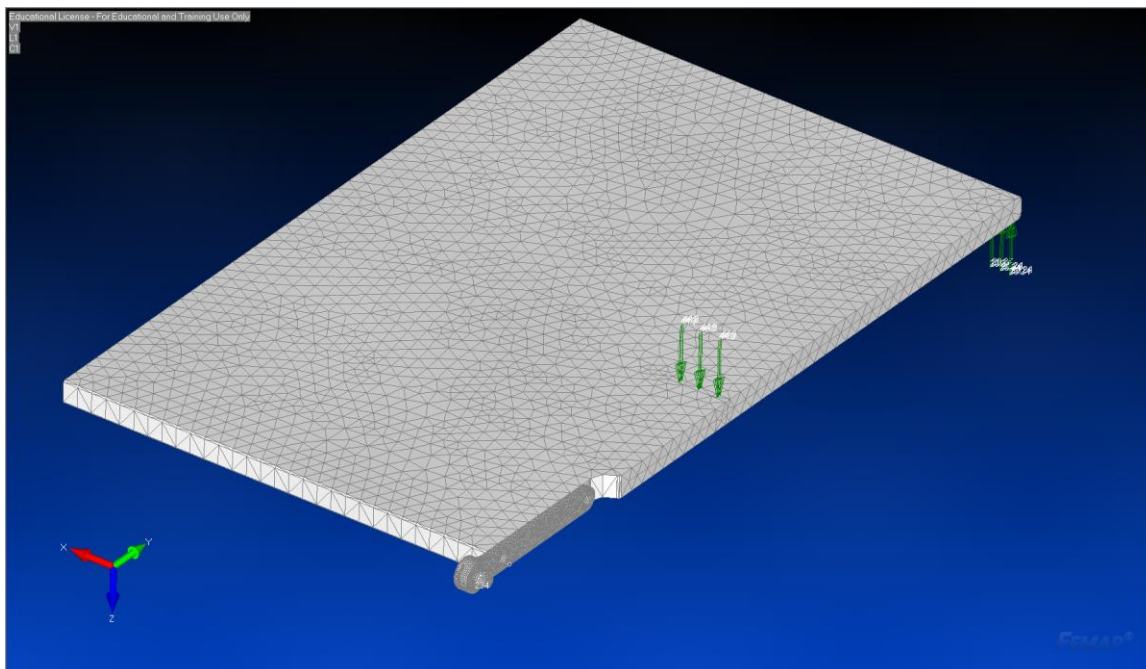
<i>Description</i>	<i>Value</i>
Max localized Von-Mises Stress (Conservative)	2,870 psi
Max lateral deflection	0.003



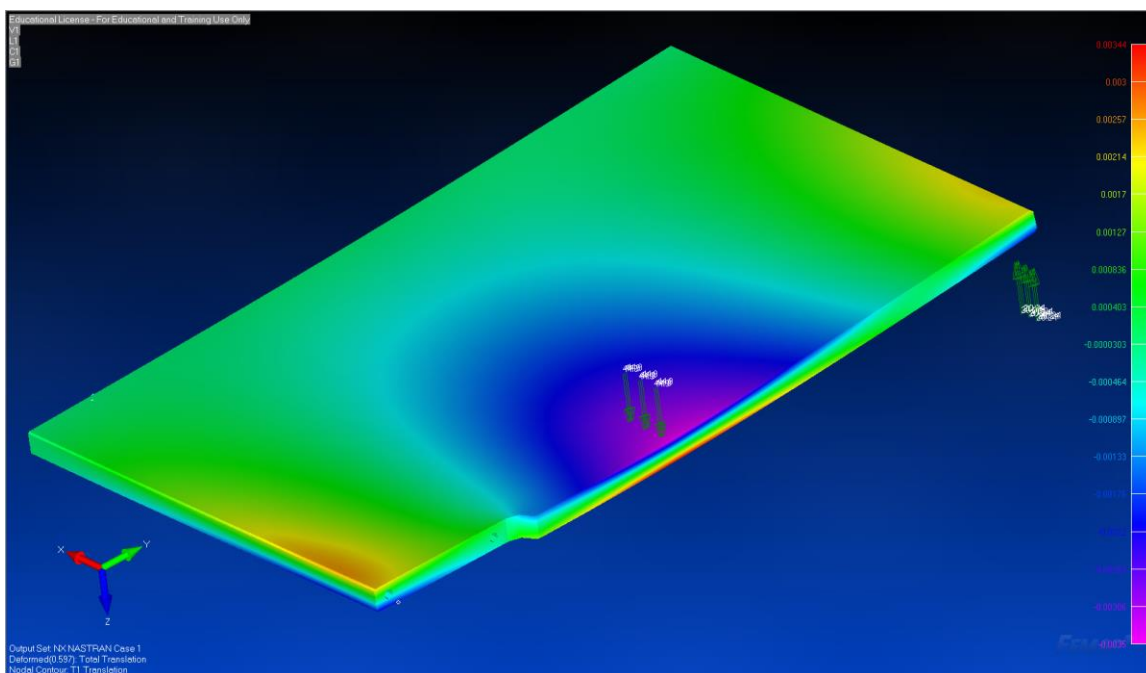
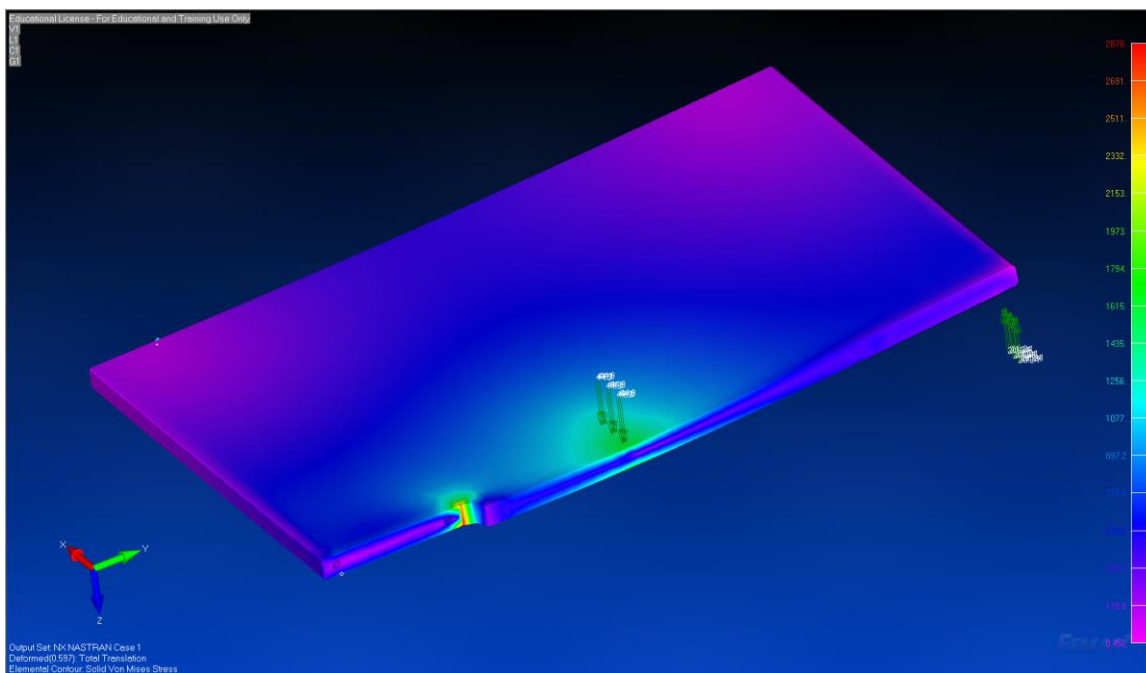
# MODEL



# MESHES



# RESULTS



## FINITE ELEMENT ANALYSIS REPORT: FEA #13

**Part/Assembly Model File:** A3 - P03-00003 Back Rest Limit Actuator.SLDPRT

**Femap Project File:** A3 - P03-00003 Back Rest Limit Actuator.modfem

**Purpose of Analysis:** Validate structural integrity, flexibility, and actuation forces of rear limit actuator.

**Material:** Aluminum 5052-H32

<b>Stiffness</b>		<b>Limit Stress</b>	
Youngs Modulus, E	<input type="text" value="10200000."/>	Tension	<input type="text" value="0."/>
Shear Modulus, G	<input type="text" value="0."/>	Compression	<input type="text" value="0."/>
Poisson's Ratio, nu	<input type="text" value="0.33"/>	Shear	<input type="text" value="0."/>
<b>Thermal</b>		Mass Density	<input type="text" value="0."/>
Expansion Coeff, a	<input type="text" value="0."/>	Damping, 2C/Co	<input type="text" value="0."/>
Conductivity, k	<input type="text" value="0."/>	Reference Temp	<input type="text" value="0."/>
Specific Heat, Cp	<input type="text" value="0."/>		
Heat Generation Factor	<input type="text" value="0."/>		

**Loads:** Displacement

- Enforced displacement: 0.12 inches

**Constraints:**

- Mounting Flange: Fixed
- Bumper Hole: Enforced Displacement TX, TY
- Sensor Contact Surface: TY
- Symmetry Plane: TX

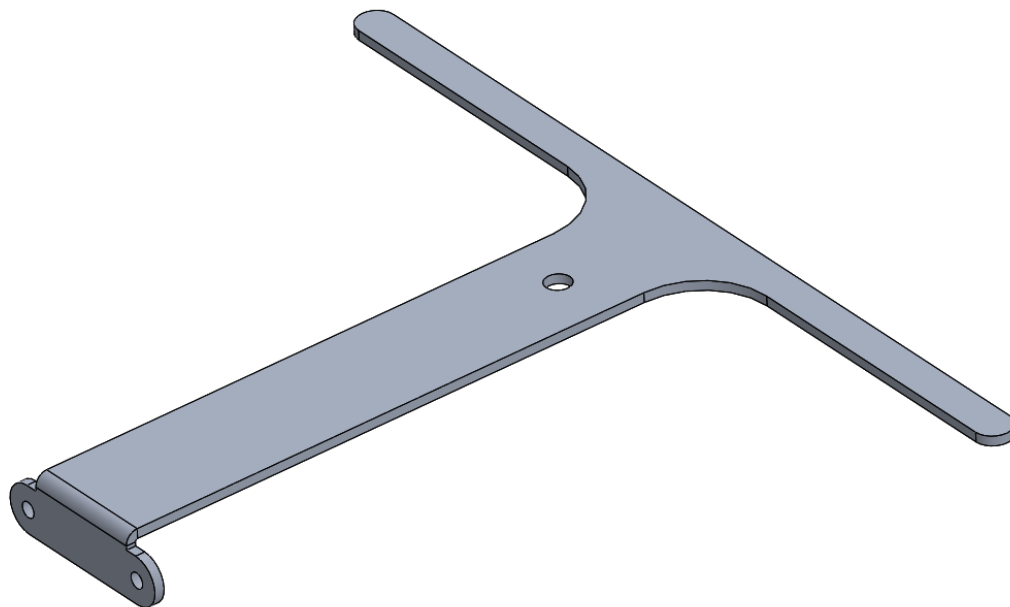
**Mesh:**

- Base Mesh: 0.1 inches

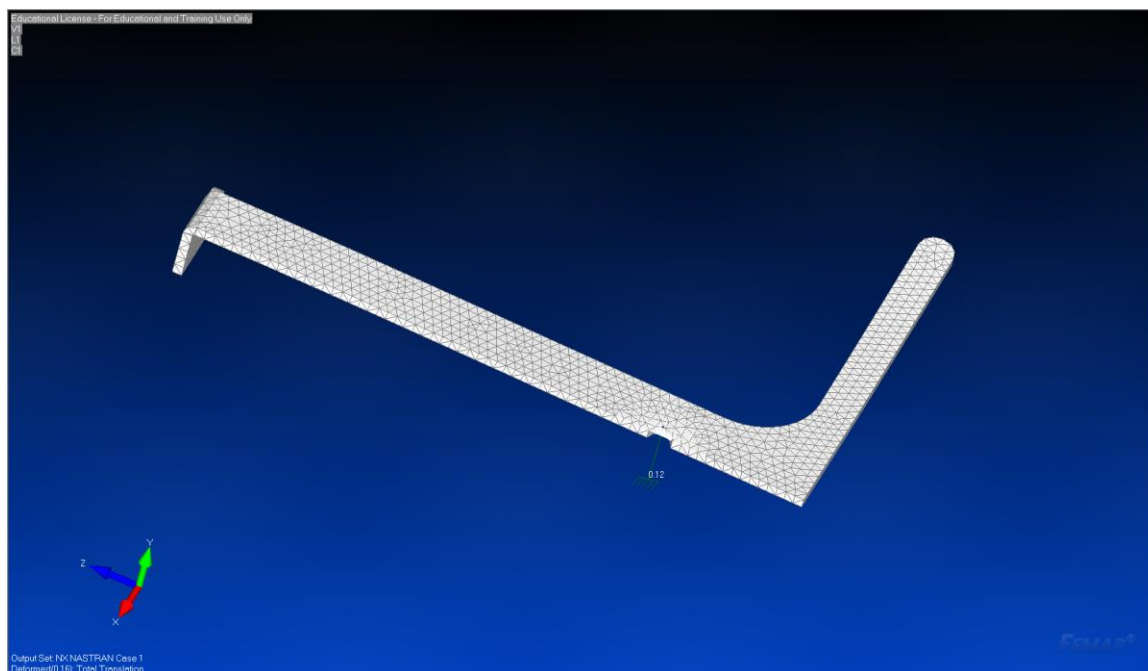
**Pertinent Results:**

<i>Description</i>	<i>Value</i>
Max Von-Mises Stress	29,878 psi
Max Total Deflection	0.047 inches

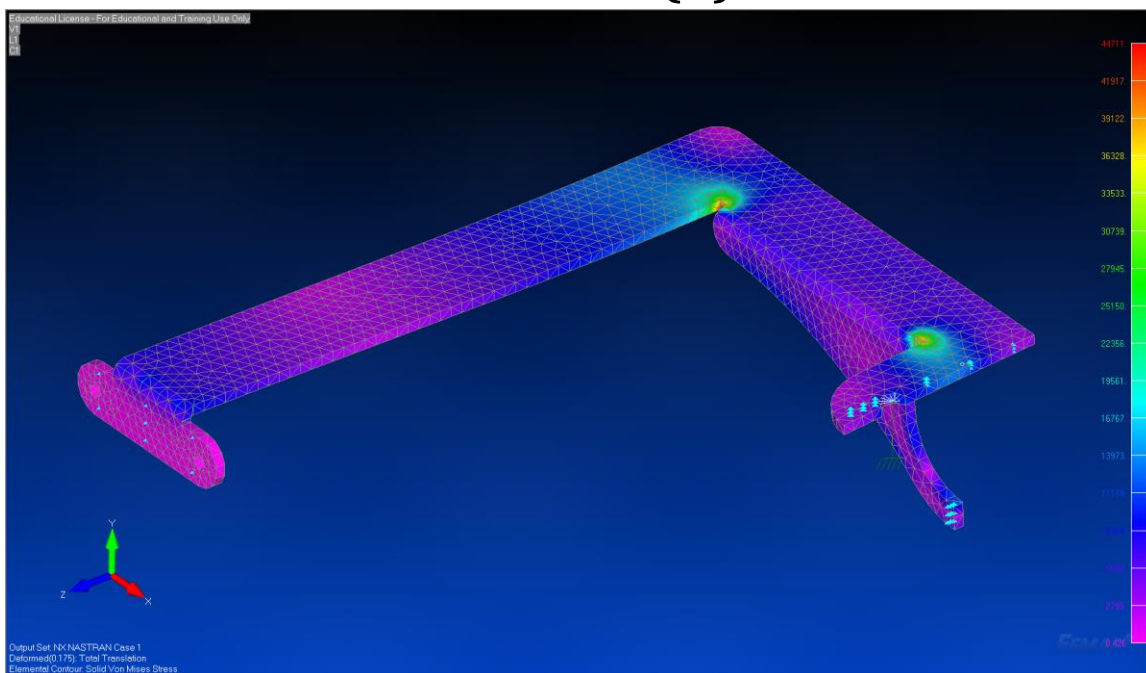
## Final MODEL



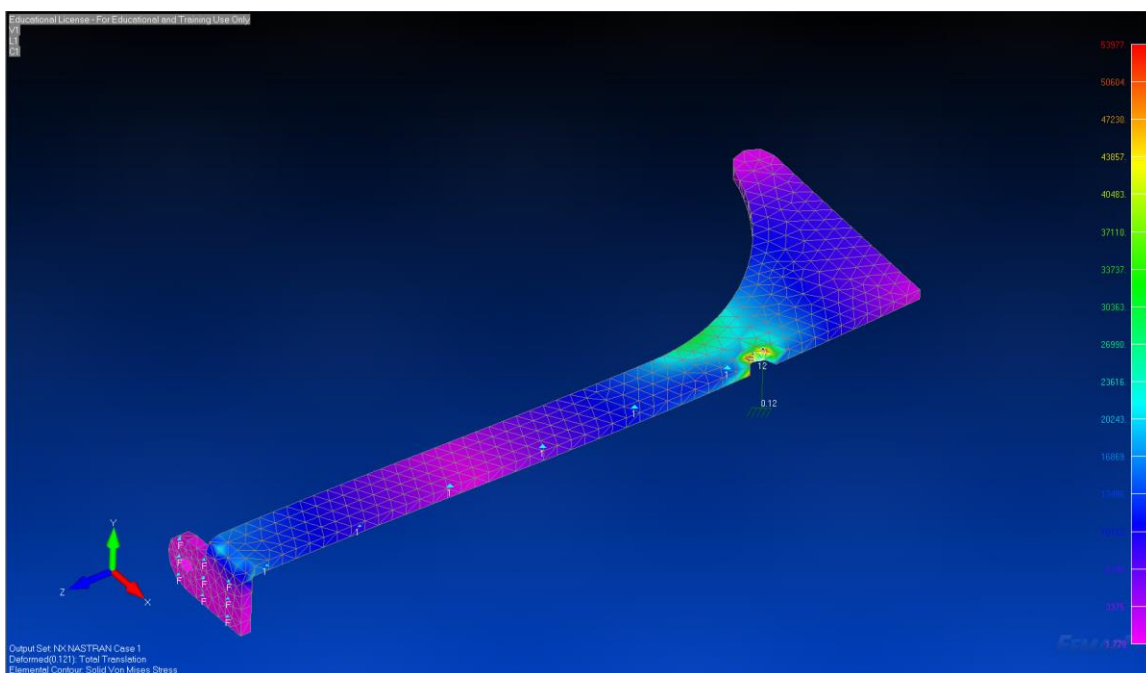
## MESH



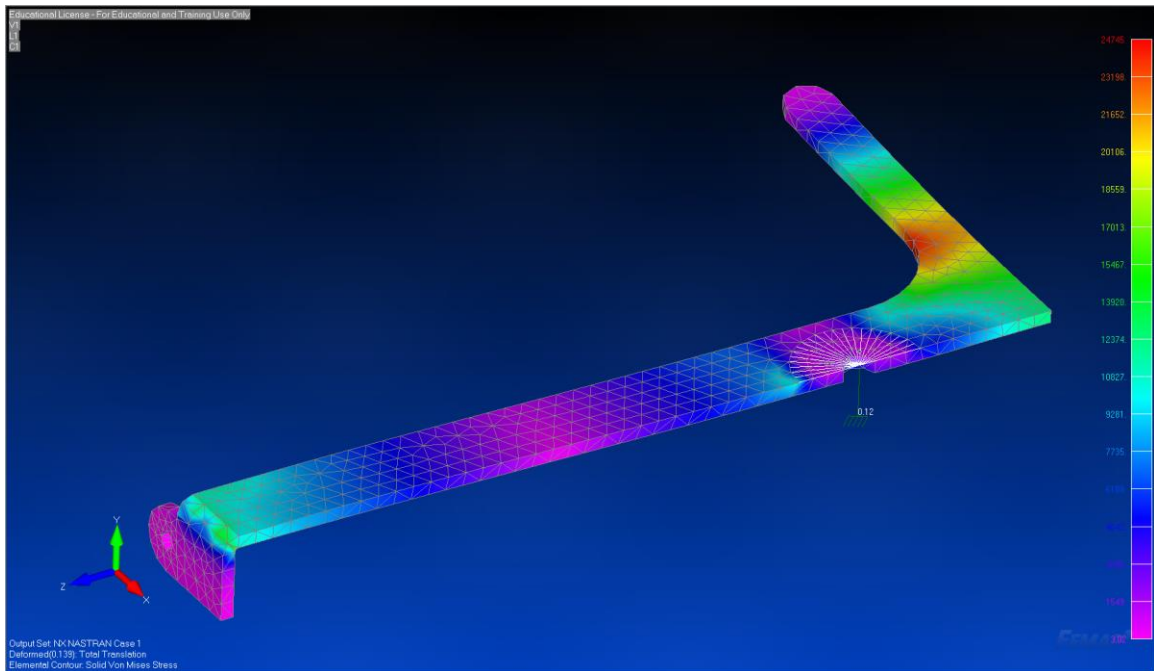
## RESULTS (1)



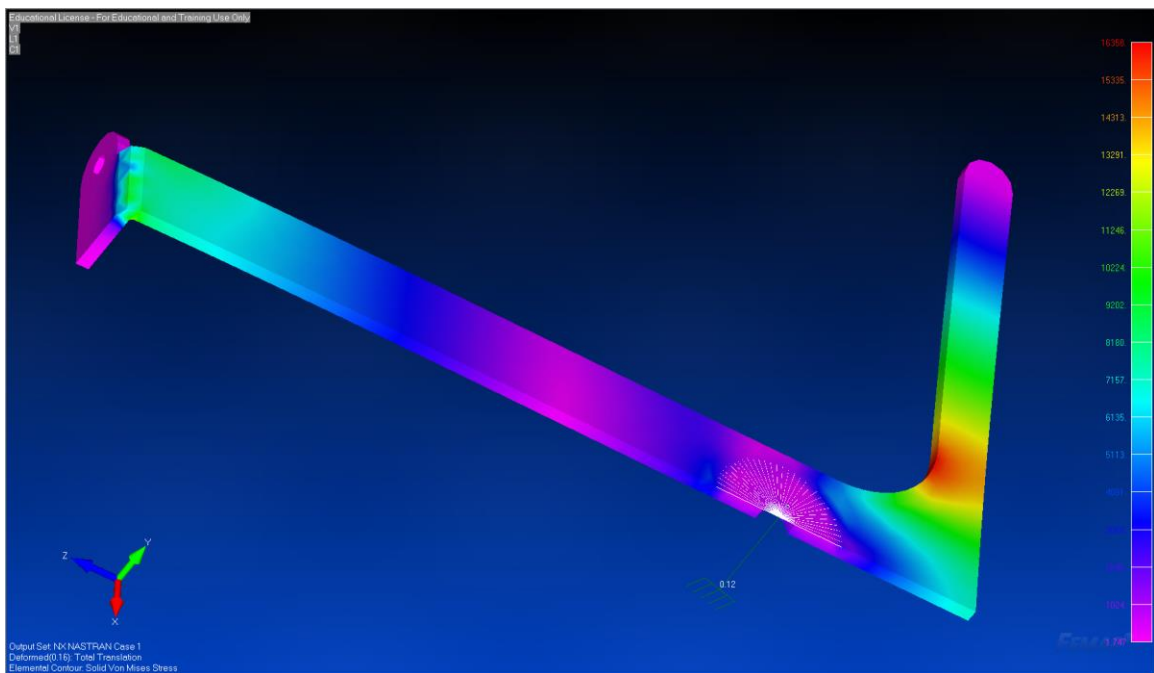
## RESULTS (2)

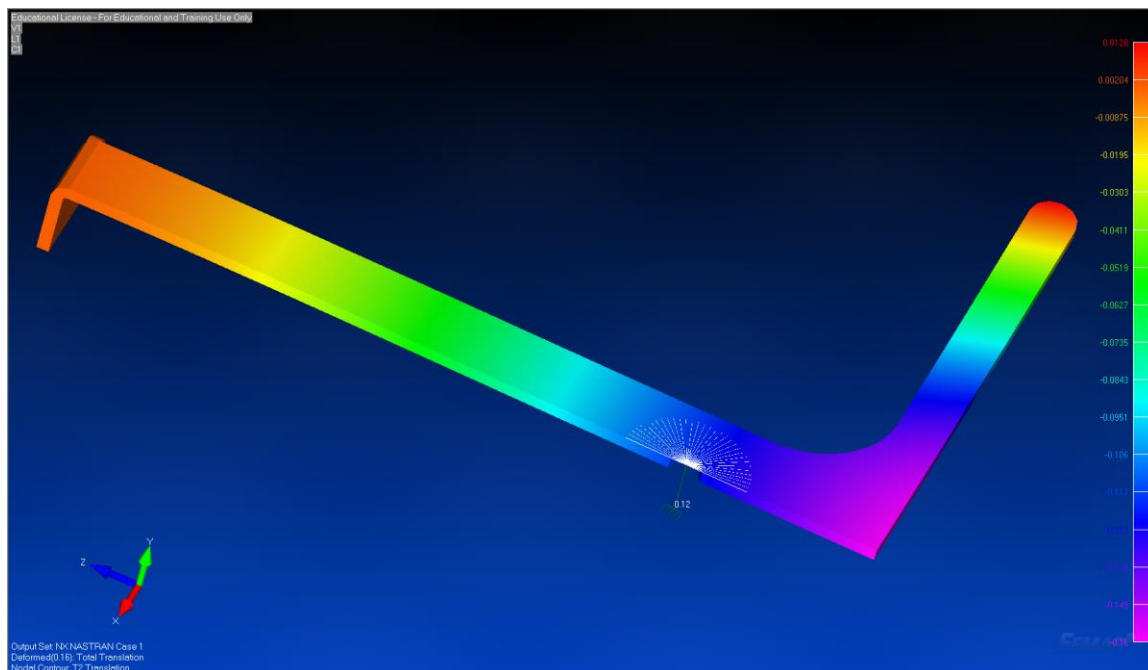


## RESULTS (3)

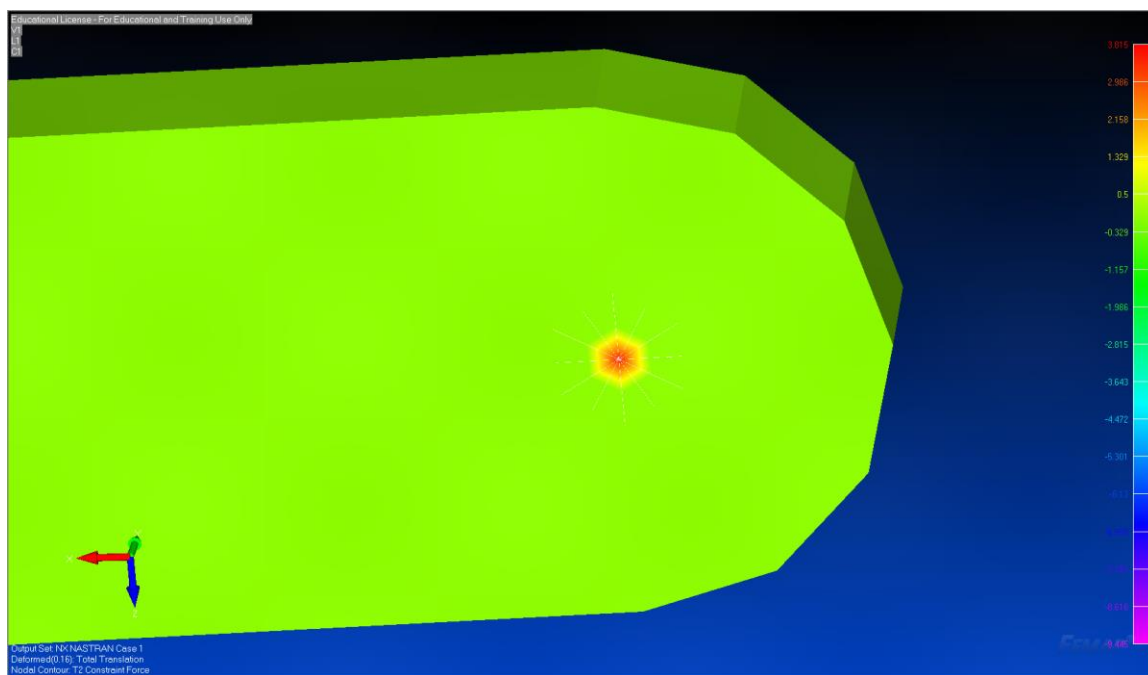


## RESULTS (4) Final





## Sensor Contact Point





## FINITE ELEMENT ANALYSIS REPORT: FEA #14

**Part/Assembly Model File:** A0 - P03-00004 Back Slider Bracket.SLDPRT

**Femap Project File:** A0.1 - P03-00004 Back Slider Bracket.modfem

**Purpose of Analysis:** Verification of material and geometry for stress management in design.

**Material:** A36 Steel

<b>Stiffness</b>		<b>Limit Stress</b>	
Young's Modulus, E	29000000.	Tension	0.
Shear Modulus, G	0.	Compression	0.
Poisson's Ratio, nu	0.26	Shear	0.
<b>Thermal</b>		Mass Density	
Expansion Coeff, a	6.E-6	Damping, 2C/Co	0.
Conductivity, k	0.00069444	Reference Temp	70.
Specific Heat, Cp	44.8224		
Heat Generation Factor	0.		

**Loads:** Force Analysis Max Value

- F9: Y-97.65 lbf, Z-7.25 lbf

**Constraints:**

- Screw Heads: TZ
- Front of Screw Holes: TY
- Symmetry: TX

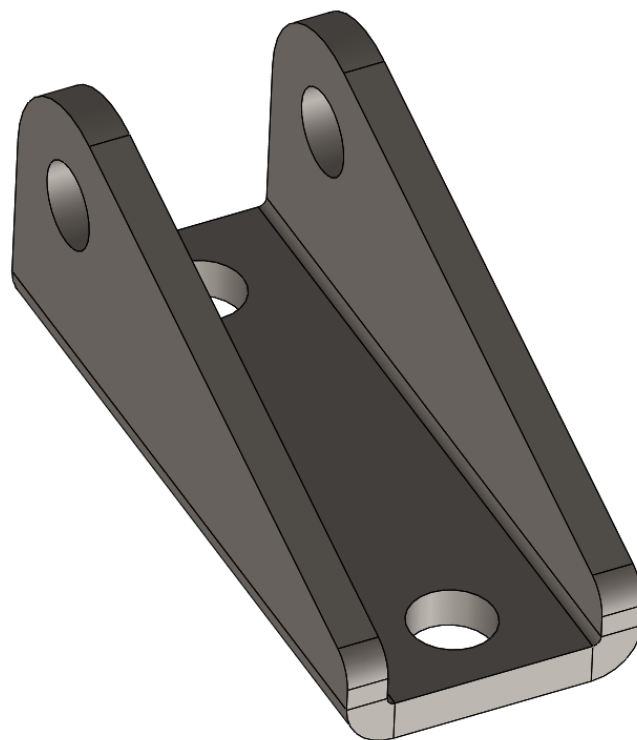
**Mesh:**

- Initial Base Mesh Size: 0.06 inches
- Refined Base Mesh Size: 0.015 inches

**Pertinent Results:**

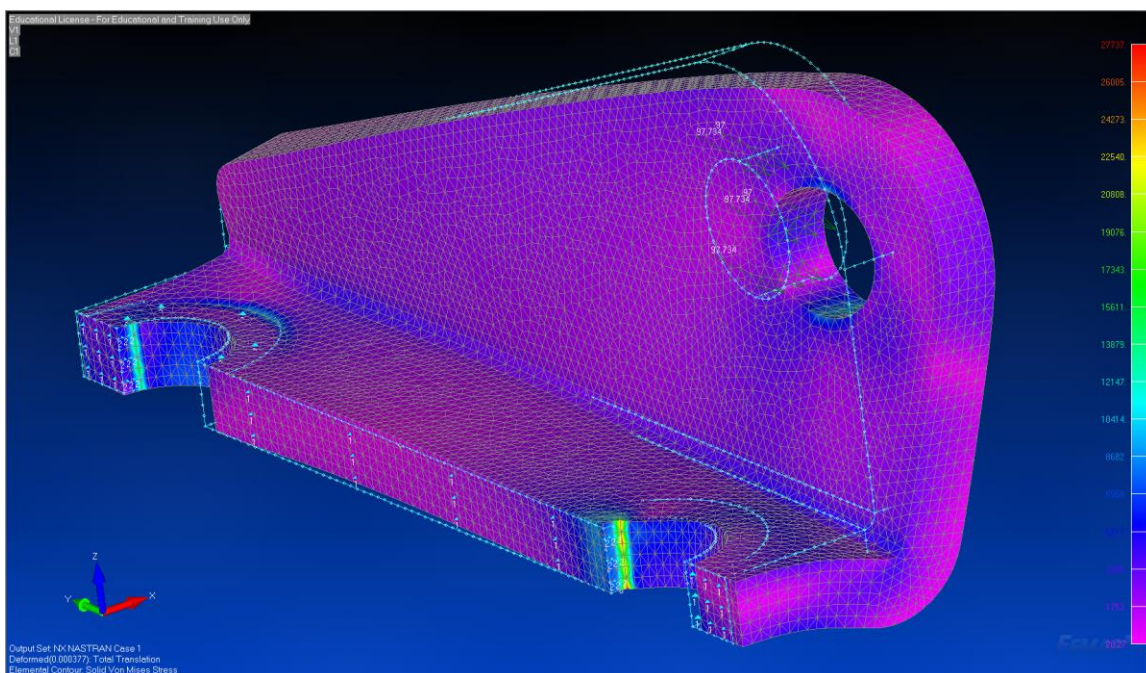
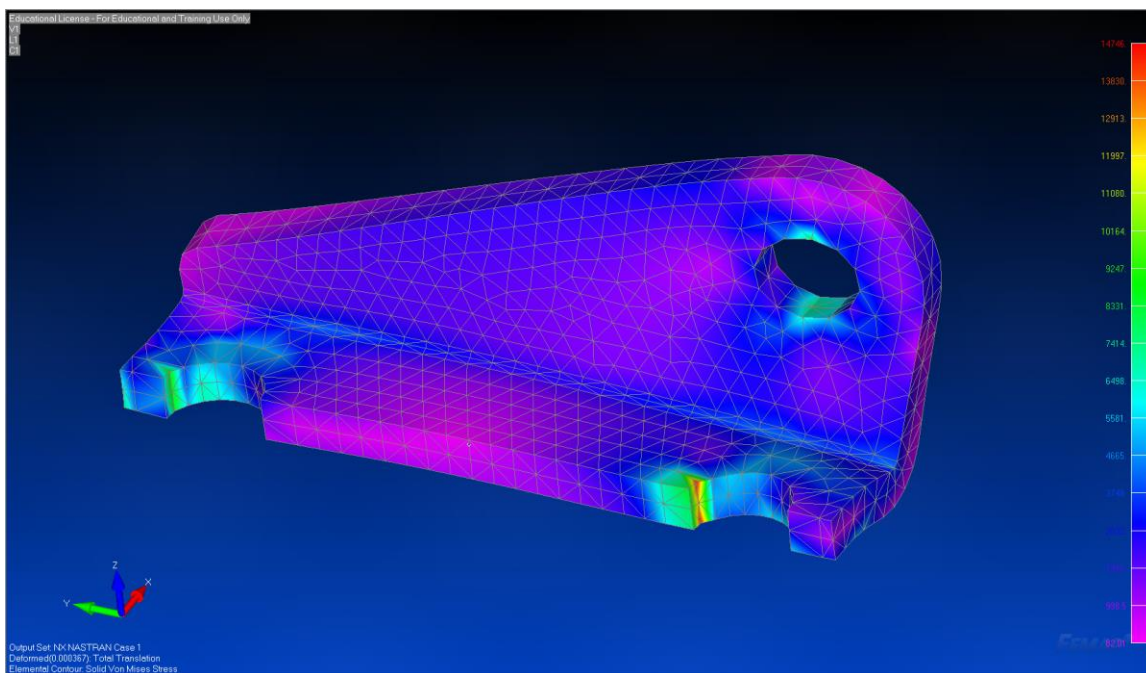
<i>Description</i>	<i>Value</i>
Maximum Local Von-Mises Stress	9,074 psi

# MODEL





# RESULTS



## FINITE ELEMENT ANALYSIS REPORT: FEA #15

**Part/Assembly Model File:** A2 - P03-00005 Brake Bracket.SLDPRT

**Femap Project File:** A2 - P03-00005 Brake Bracket.modfem

**Purpose of Analysis:** Verification of brake bracket integrity.

**Material:** 1015 Steel

<b>Stiffness</b>		<b>Limit Stress</b>	
Young's Modulus, E	<input type="text" value="29700000."/>	Tension	<input type="text" value="0."/>
Shear Modulus, G	<input type="text" value="0."/>	Compression	<input type="text" value="0."/>
Poisson's Ratio, nu	<input type="text" value="0.29"/>	Shear	<input type="text" value="0."/>
<b>Thermal</b>		Mass Density	<input type="text" value="0."/>
Expansion Coeff, a	<input type="text" value="0."/>	Damping, 2C/Co	<input type="text" value="0."/>
Conductivity, k	<input type="text" value="0."/>	Reference Temp	<input type="text" value="0."/>
Specific Heat, Cp	<input type="text" value="0."/>		
Heat Generation Factor	<input type="text" value="0."/>		

**Loads:** X and Z components of 102.8 lbf each direction, simulating the loads the rubber will put on the bracket when a user sits down into the chair

- X+102.8 lbf, Z-102.8 lbf

**Constraints:**

- Screw Heads (only the side in contact with the screw): Fixed

**Mesh:**

- Base Mesh Size: 0.06 inches
- Refined Base Mesh Size: 0.018 inches

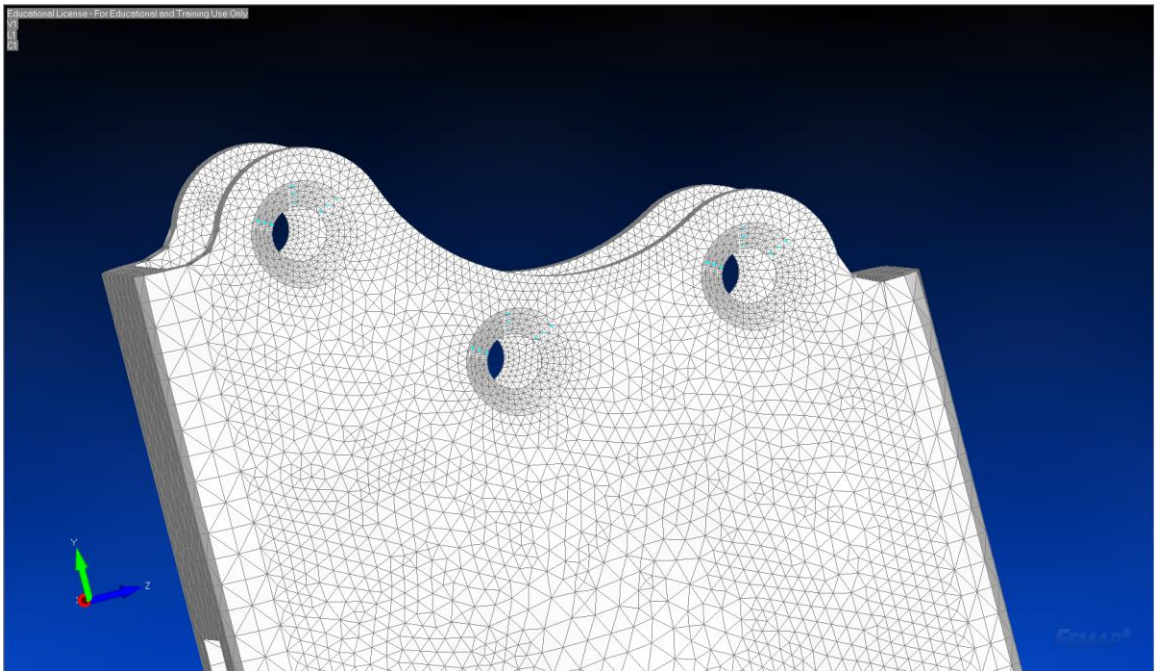
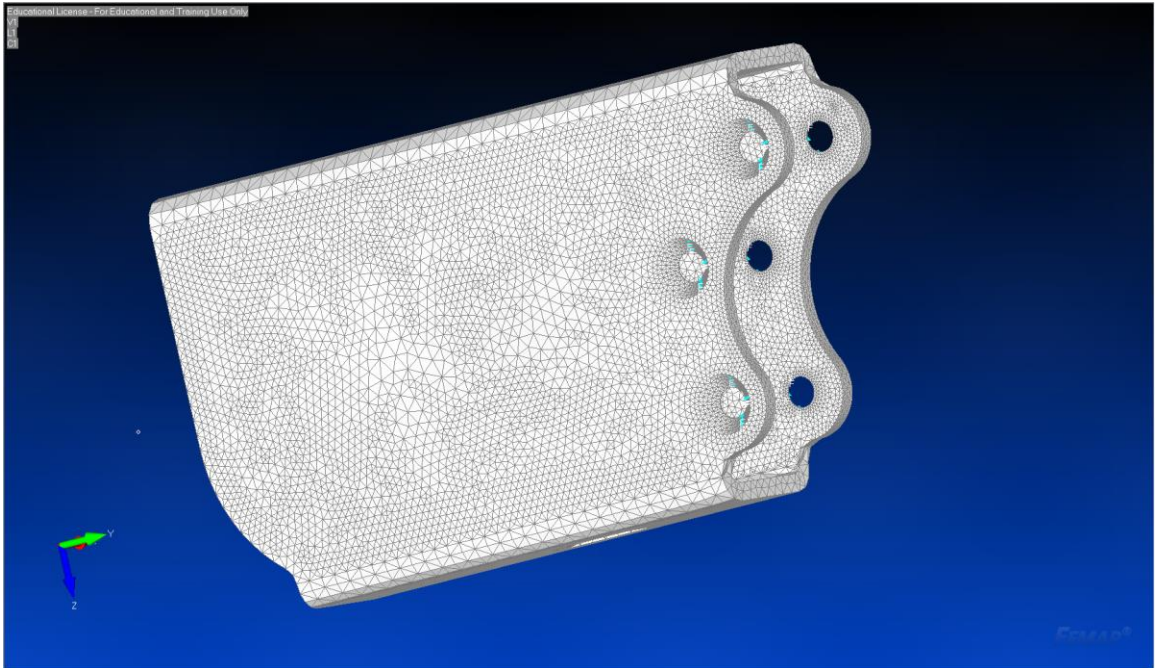
**Pertinent Results:**

<i>Description</i>	<i>Value</i>
Maximum Non-Localized Von-Mises Stress	~15,000 psi

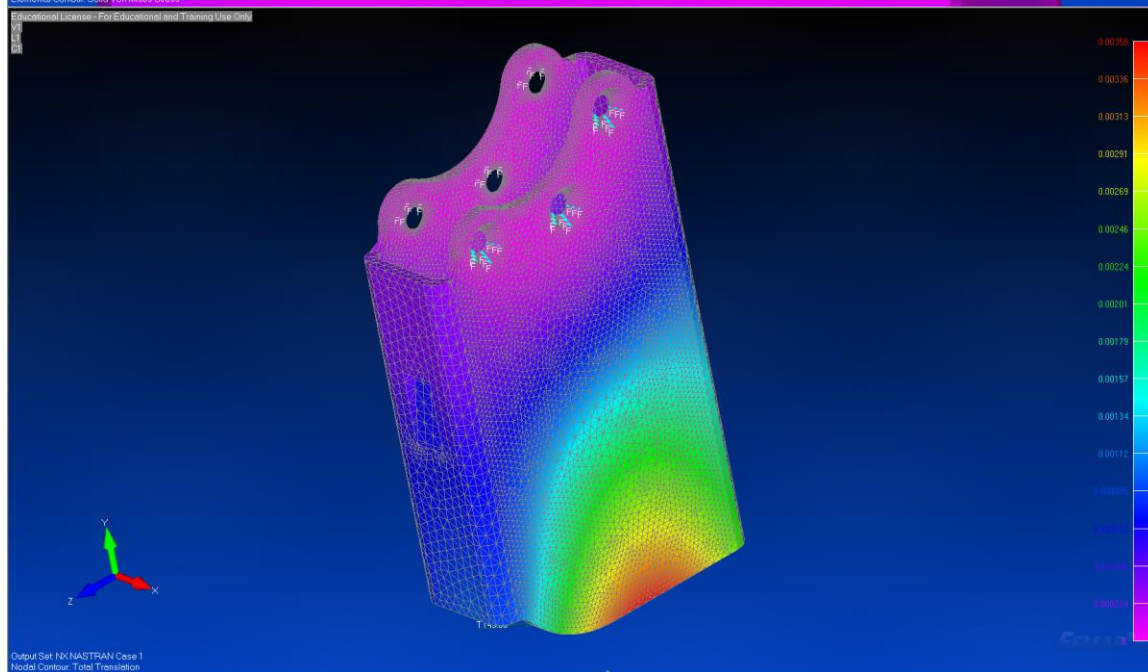
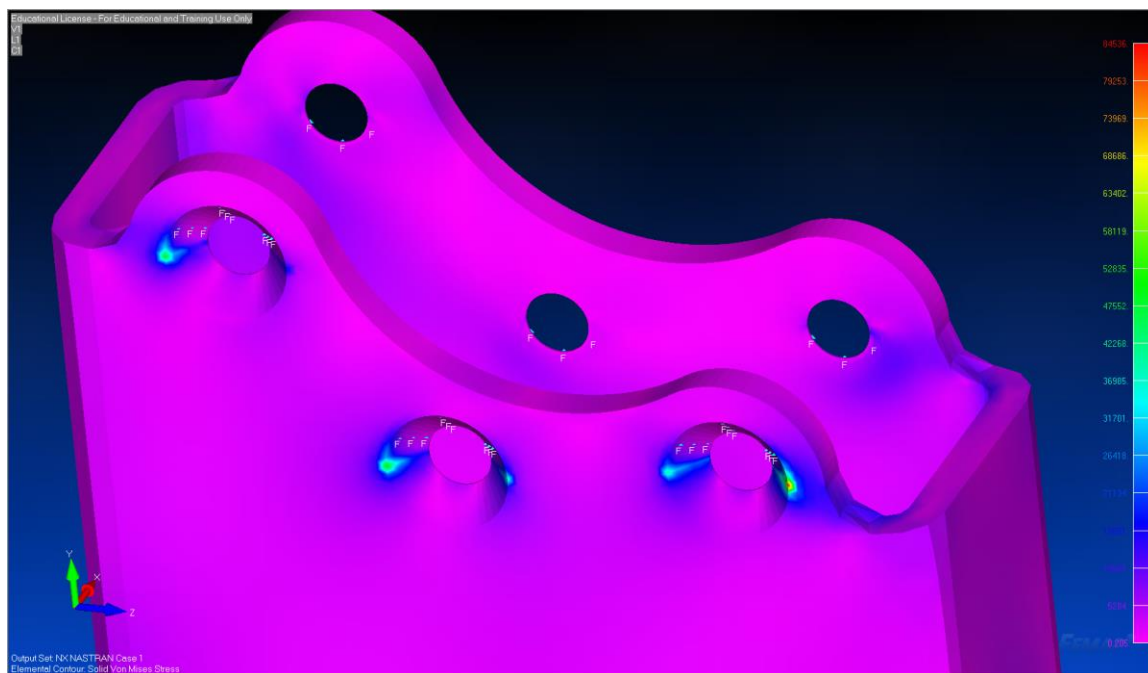
**MODEL**



# MESH



# RESULTS





## FINITE ELEMENT ANALYSIS REPORT: FEA #16

**Part/Assembly Model File:** A0 - P03-00013 Front Seat Support.SLDPRT

**Femap Project File:** A0 - P03-00013 Front Seat Support.modfem

**Purpose of Analysis:** Validate structural integrity of front seat support under full weight of user

**Material:** Aluminum 5052-H32

<b>Stiffness</b>		<b>Limit Stress</b>	
Youngs Modulus, E	<input type="text" value="10200000."/>	Tension	<input type="text" value="0."/>
Shear Modulus, G	<input type="text" value="0."/>	Compression	<input type="text" value="0."/>
Poisson's Ratio, nu	<input type="text" value="0.33"/>	Shear	<input type="text" value="0."/>
<b>Thermal</b>		Mass Density	<input type="text" value="0."/>
Expansion Coeff, a	<input type="text" value="0."/>	Damping, 2C/Co	<input type="text" value="0."/>
Conductivity, k	<input type="text" value="0."/>	Reference Temp	<input type="text" value="0."/>
Specific Heat, Cp	<input type="text" value="0."/>		
Heat Generation Factor	<input type="text" value="0."/>		

**Loads:** 300 lbf (150 lbf half model)

- F: Z+150 lbf

**Constraints:**

- Holes: TY, TZ, RX
- Symmetry: TX
- Seat Contact Surfaces: RX

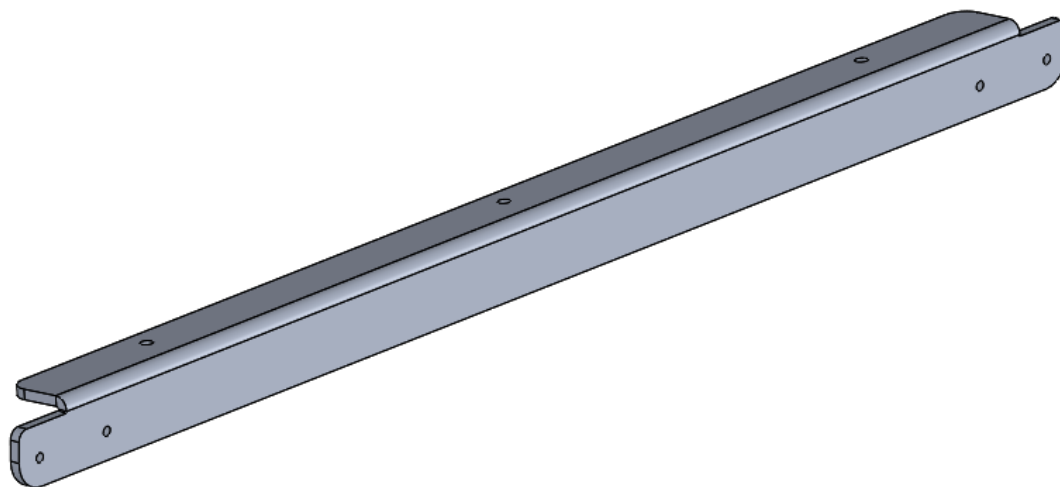
**Mesh:**

- Base Mesh: 0.1 inches

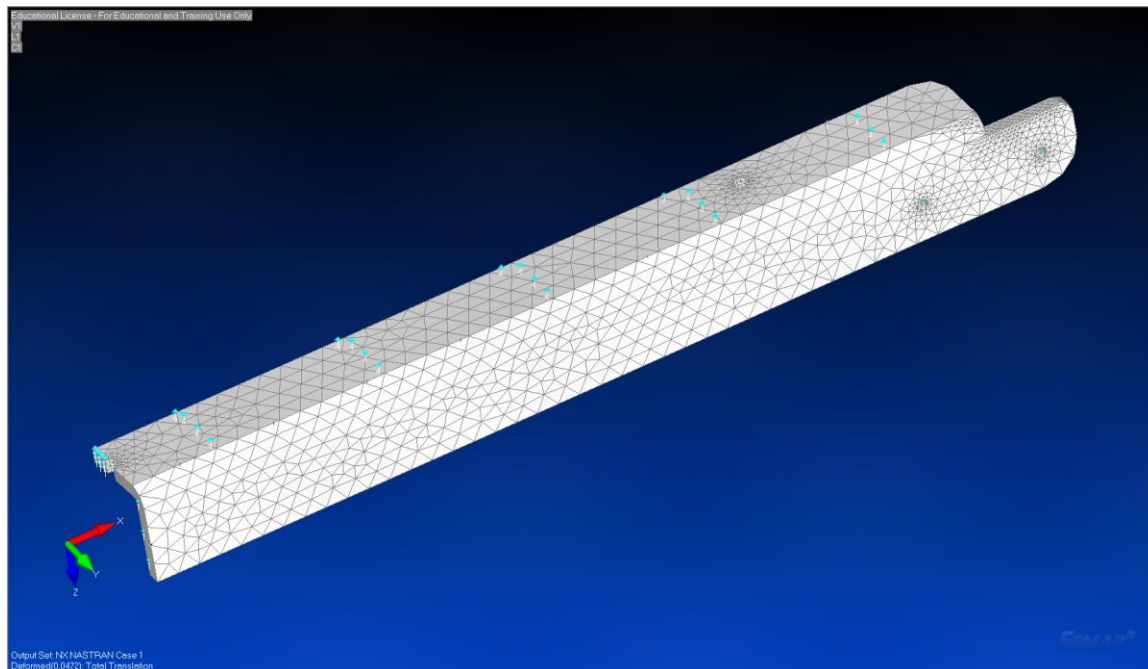
**Pertinent Results:**

<i>Description</i>	<i>Value</i>
Max Von-Mises Stress	29,878 psi
Max Total Deflection	0.047 inches

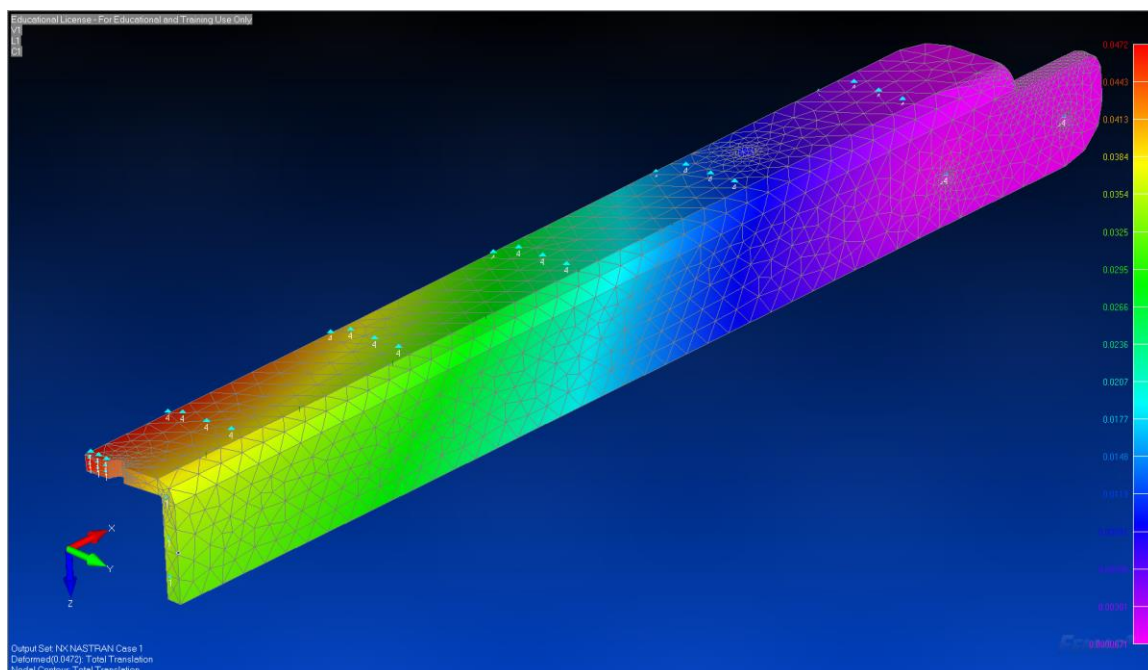
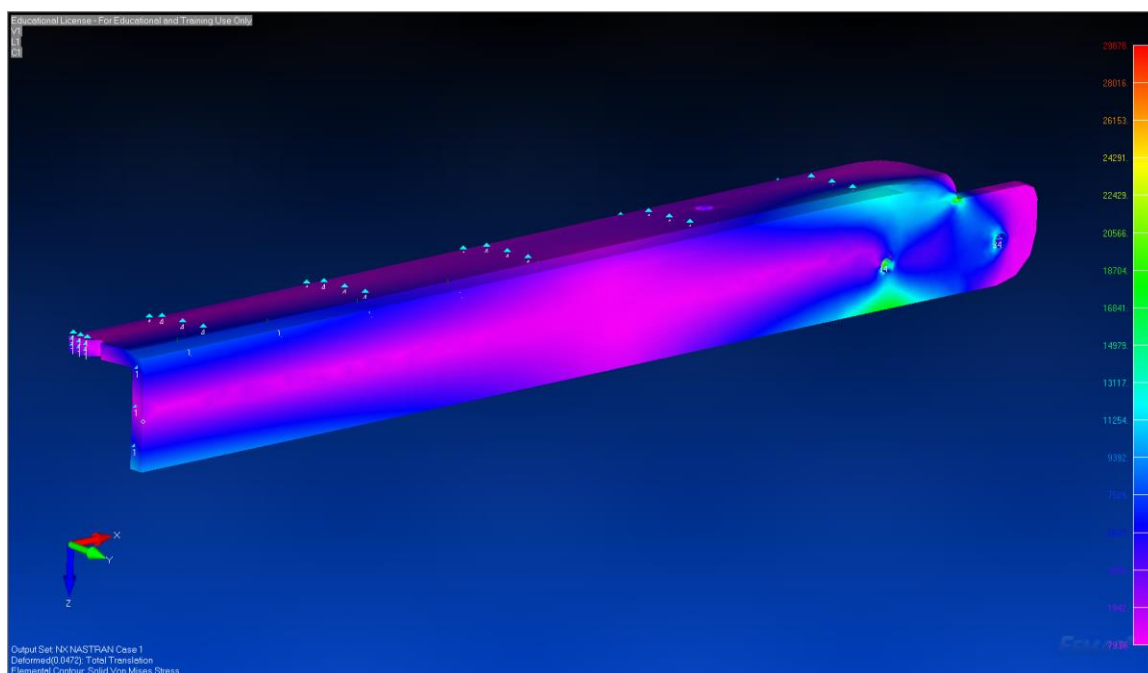
## MODEL



## MESH



# RESULTS



## FINITE ELEMENT ANALYSIS REPORT: FEA #17

### Part/Assembly Model File:

- A0 - P03-00015 Left Back Support.X\_T
- A1 - P03-00015 Left Back Support.SLDPRT

### Femap Project File:

- Initial: A0 - P03-00015 Left Back Support.modfem
- Final: A1 - P03-00015 Left Back Support.modfem

**Purpose of Analysis:** Validate structural integrity of back support members under full weight of user upper body, and verify acceptability of deflection.

**Frame Material:** Aluminum 5052-H32

Stiffness		Limit Stress	
Youngs Modulus, E	10200000.	Tension	0.
Shear Modulus, G	0.	Compression	0.
Poisson's Ratio, nu	0.33	Shear	0.
Thermal		Mass Density	0.
Expansion Coeff, a	0.	Damping, 2C/Co	0.
Conductivity, k	0.	Reference Temp	0.
Specific Heat, Cp	0.		
Heat Generation Factor	0.		

**Backrest Material:** Douglas fir plywood

Stiffness		Limit Stress	
Youngs Modulus, E	1350000.	Tension	0.
Shear Modulus, G	0.	Compression	0.
Poisson's Ratio, nu	0.2	Shear	0.
Thermal		Mass Density	0.
Expansion Coeff, a	0.	Damping, 2C/Co	0.
Conductivity, k	0.	Reference Temp	0.
Specific Heat, Cp	0.		
Heat Generation Factor	0.		

**Loads:** Full portion of upper body weight and load at peak moment of the bridge

- Wub/2: Y-100 lbf
- F78U(58): Y-18.3 lbf

**Constraints:**

- D Pivot Hole: TY, TZ
- Symmetry: TX
- Bridge Contact Surface: TY

**Mesh:**

- Base Mesh (Plywood backrest): 0.375 inches
- Base Mesh (Frame): 0.169 inches
- Refined Mesh (Frame): 0.03 inches

**Pertinent Results:**

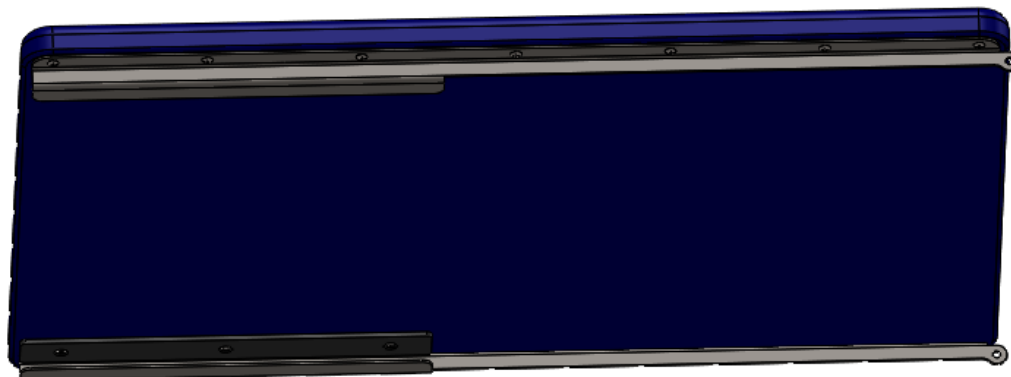
## Initial Results

<i><b>Description</b></i>	<i><b>Value</b></i>
Max Von-Mises Stress in Backrest	1,007 psi
Max Von-Mises Stress in Backrest	64,450 psi
Max Y-Deflection	0.196 inches

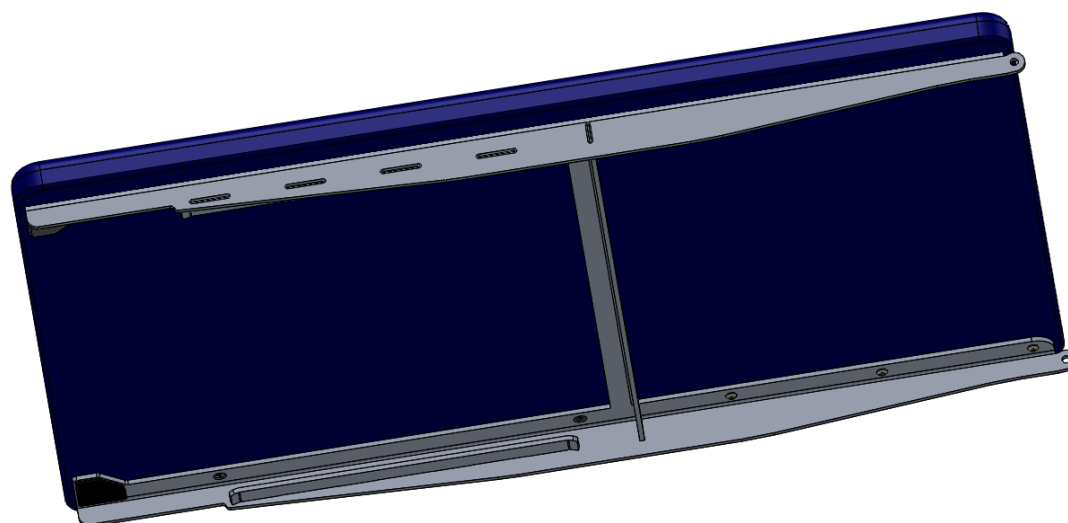
## Final Results

<i><b>Description</b></i>	<i><b>Value</b></i>
Max Von-Mises Stress in Backrest	707 psi
Max Von-Mises Stress in Backrest	17,297 psi
Max Y-Deflection	0.063 inches

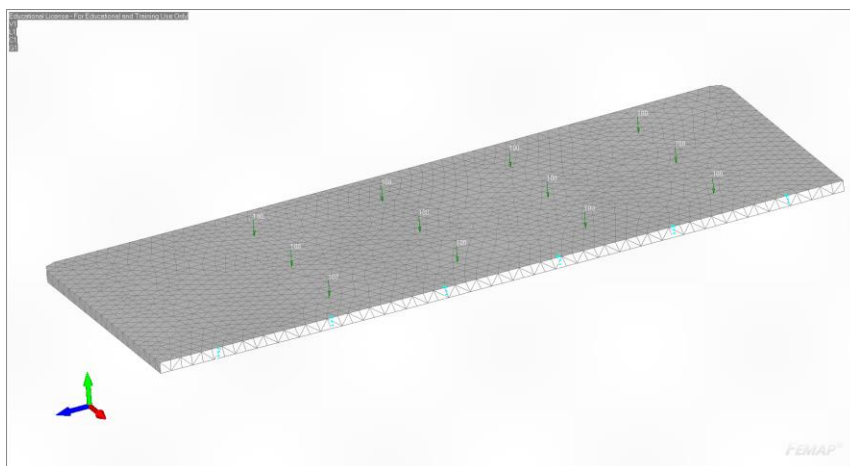
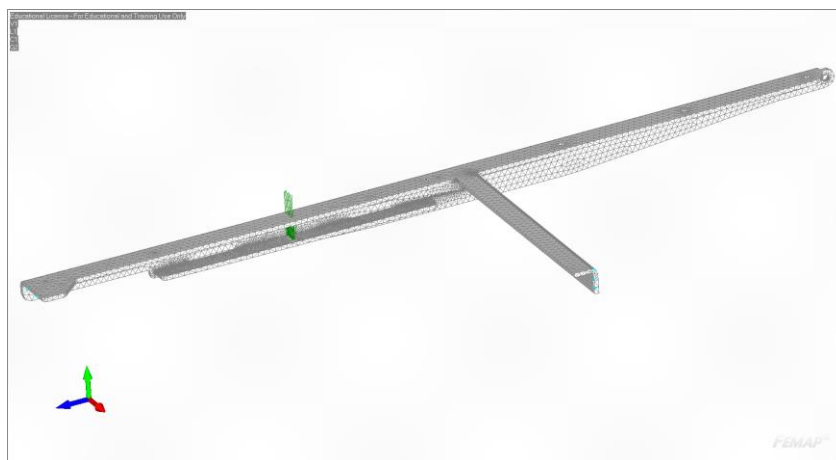
## Initial MODEL

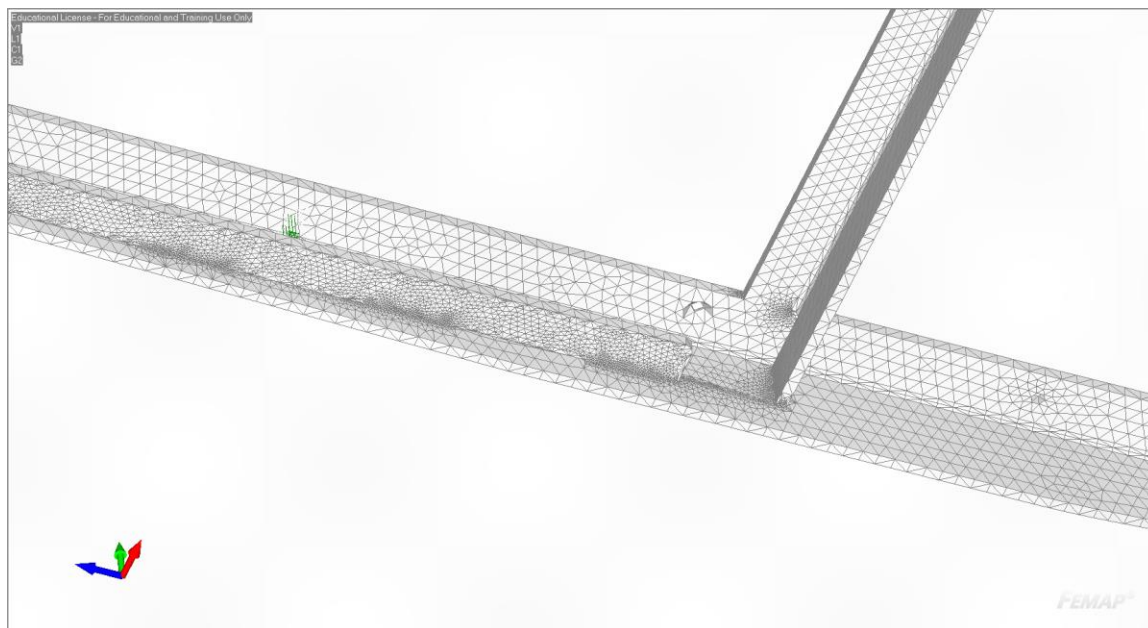


## Final MODEL

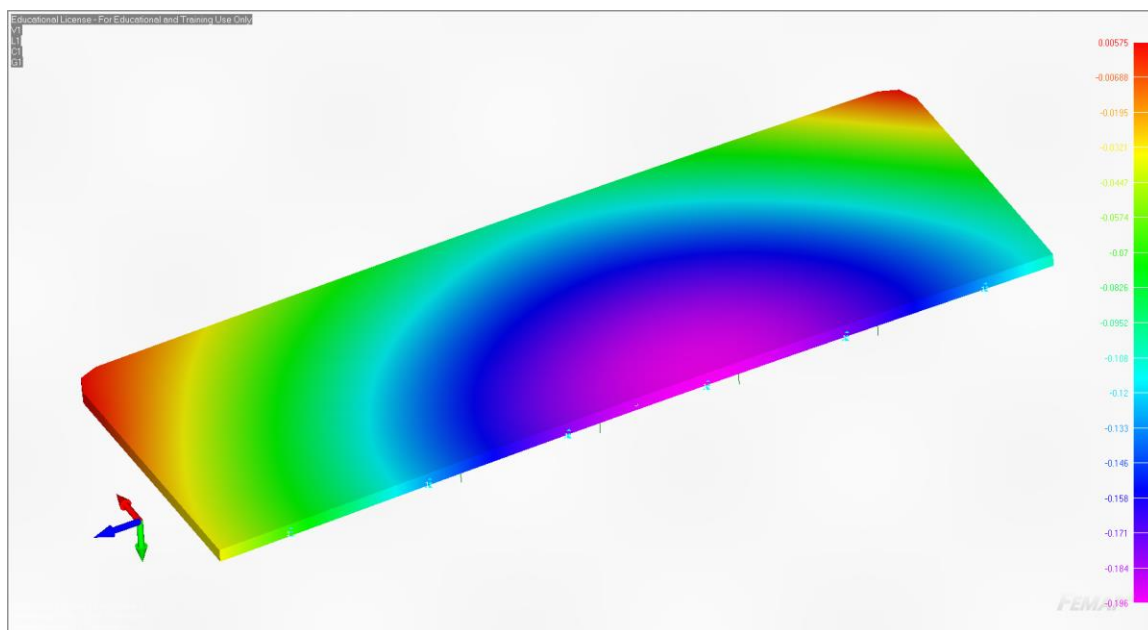


# MESH

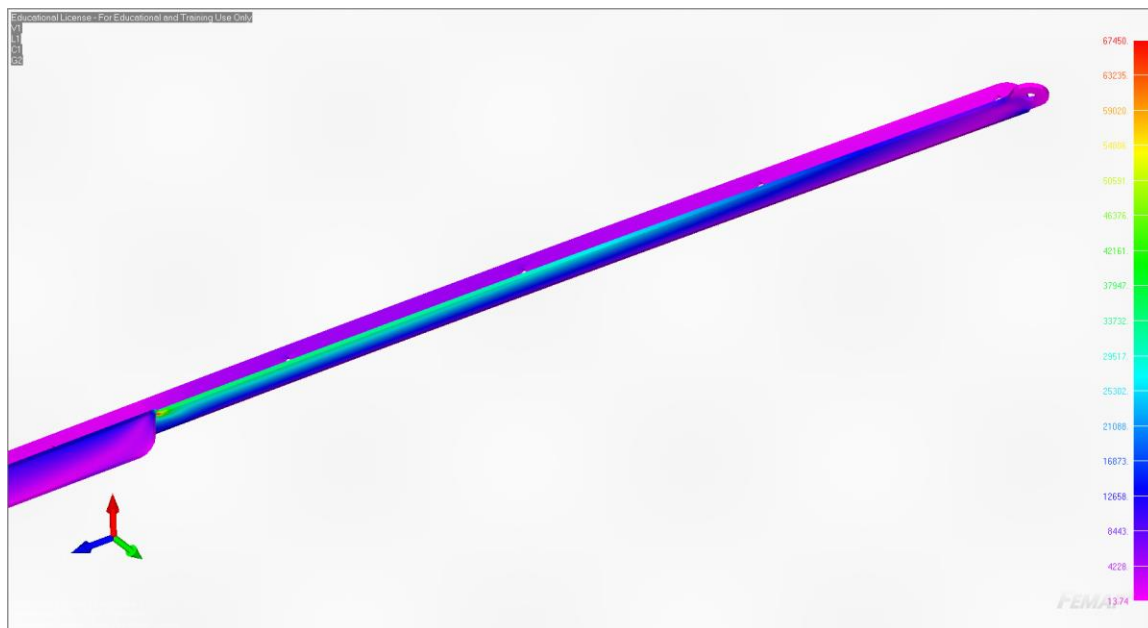




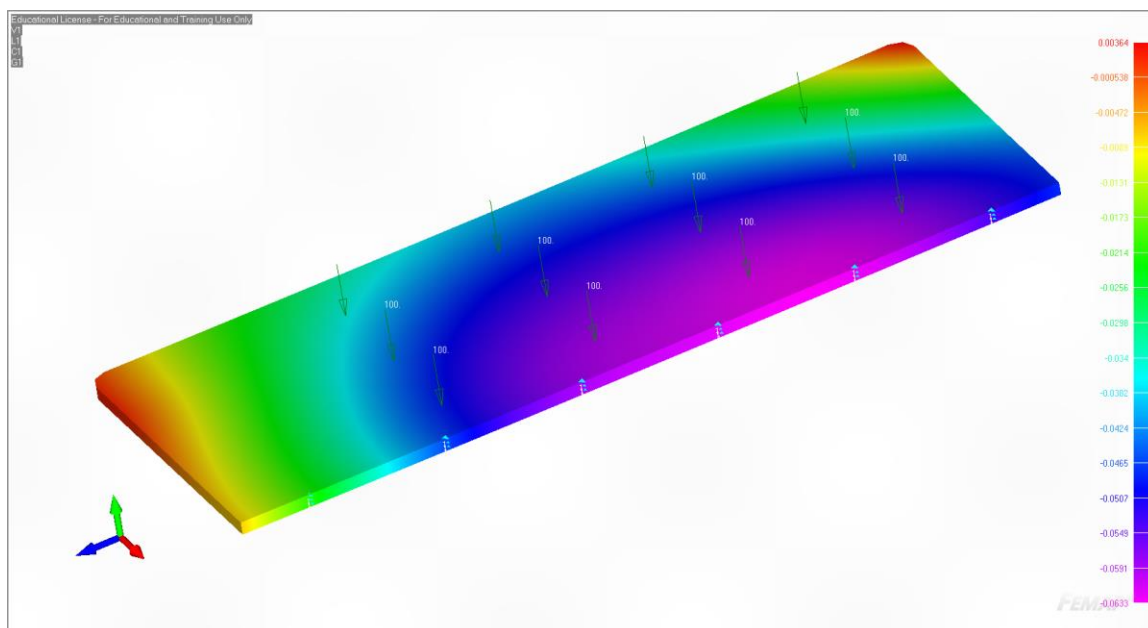
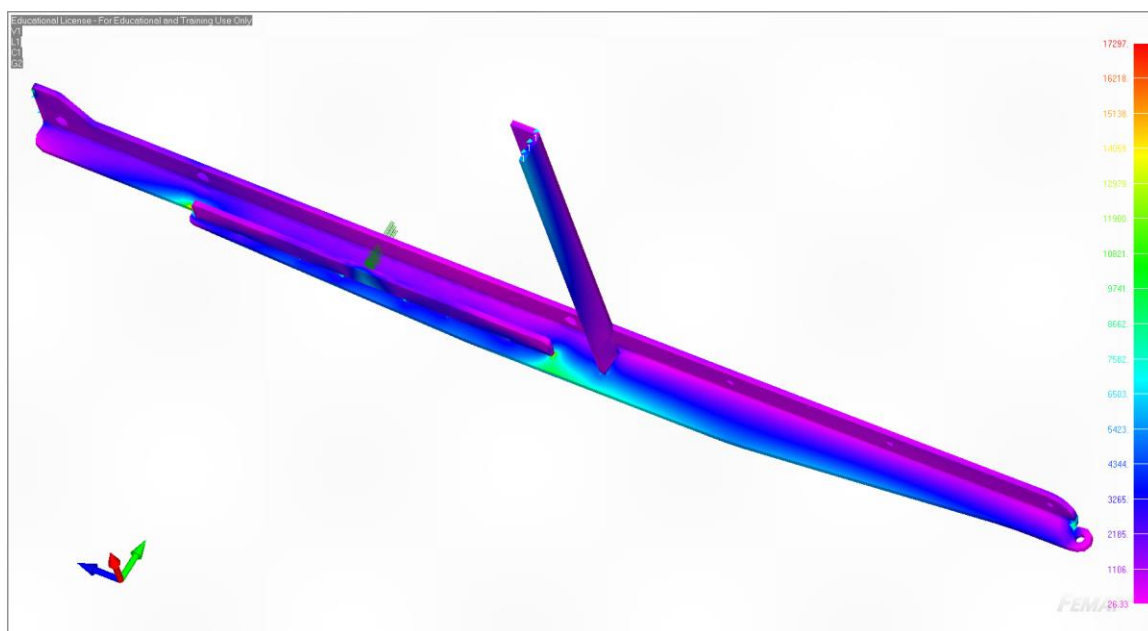
## Initial RESULTS







# Final RESULTS



## FINITE ELEMENT ANALYSIS REPORT: FEA #18

### Part/Assembly Model Files:

- Item 1: A1 - A02-00015 Slider Welded Subassembly (Front Only with Caster).SLDPRT
- Item 2: A1 - A02-00015 Slider Welded Subassembly (Rear).SLDPRT
- Item 3: A1 - P02-00031 Slider.SLDPRT

### Femap Project File:

- Item 1: A1.2 - A02-00015 Slider Welded Subassembly.modfem
- Item 2: A1.3 - A02-00015 Slider Welded Subassembly (Rear).modfem
- Item 3: A1.4 - A02-00015 Slider Welded Subassembly (Beam).modfem

### Purpose of Analysis:

- Item 1: Verify structural integrity at caster end
- Item 2: Verify structural integrity at ball nut end
- Item 3: Identify the deflection in the slider when fully extended

### Material: A36

<b>Stiffness</b>		<b>Limit Stress</b>	
Youngs Modulus, E	29000000.	Tension	0.
Shear Modulus, G	0.	Compression	0.
Poisson's Ratio, nu	0.26	Shear	0.
<b>Thermal</b>		Mass Density	7.35736E-4
Expansion Coeff, a	6.E-6	Damping, 2C/Co	0.
Conductivity, k	0.00069444	Reference Temp	70.
Specific Heat, Cp	44.8224		
Heat Generation Factor	0.		

### Loads: Peak loads on the slider

- Item 1: F3 Max (Half Loads for Symmetry)
  - Caster: Y+36.5 lbf
  - F3(102): Y-33.15, Z+254.3 (lbf)
- Item 2: F3x Max (Half Load for Symmetry)

- Cut Face: Z+255 lbf
- Item 3: Conservative Max Front Caster Load at full extension
  - Distal End: Y+75 lbf

**Constraints:**

- Item 1
  - Symmetry: TX
  - Other DoFs on Cut Face: TY, TZ
- Item 2
  - Symmetry: TX
  - Screw Holes: TY, TZ
- Item 3
  - Proximal End Face: Fixed

**Mesh:**

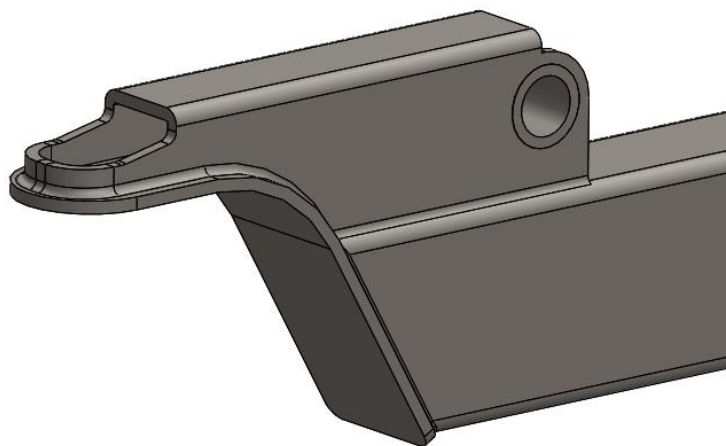
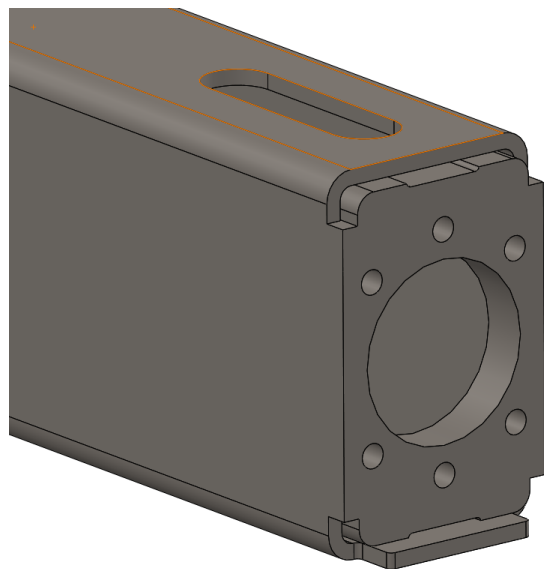
- Base Mesh: 0.06 inches
- Refined Mesh (Frame): 0.02 inches

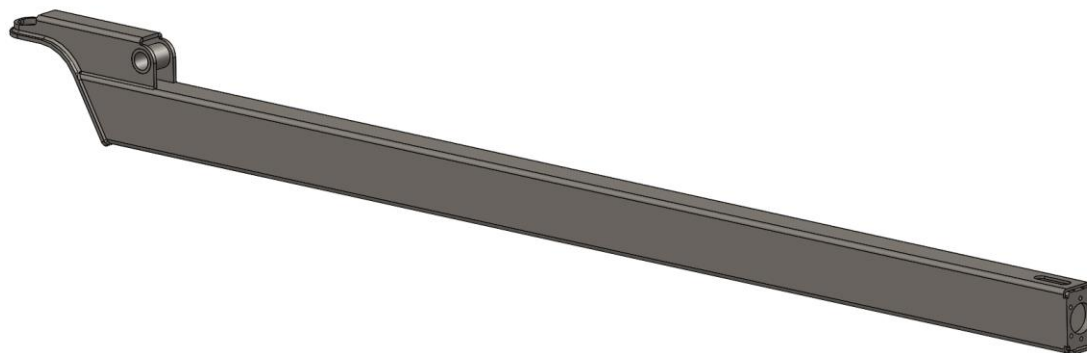
**Pertinent Results:**

Initial Results

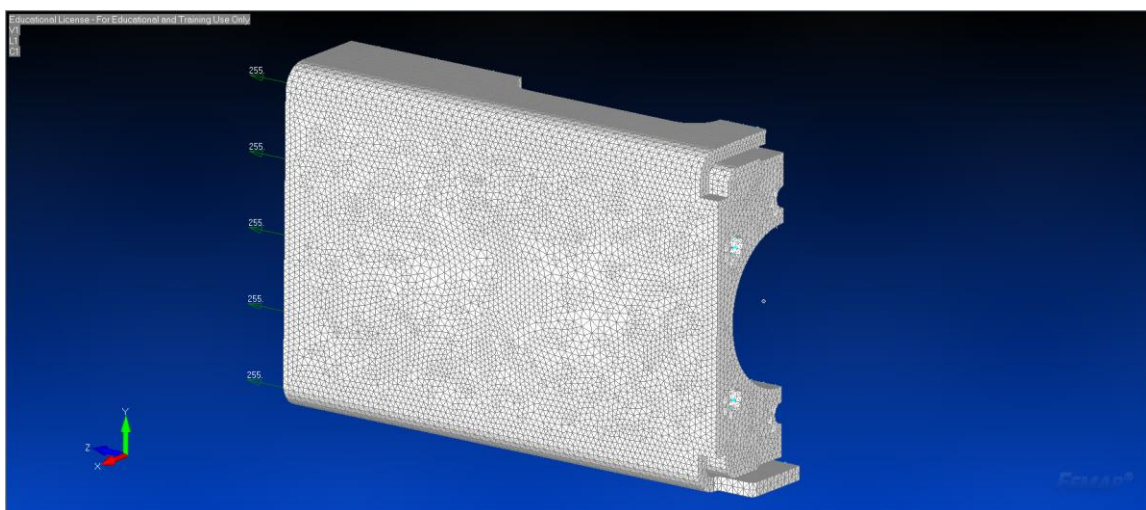
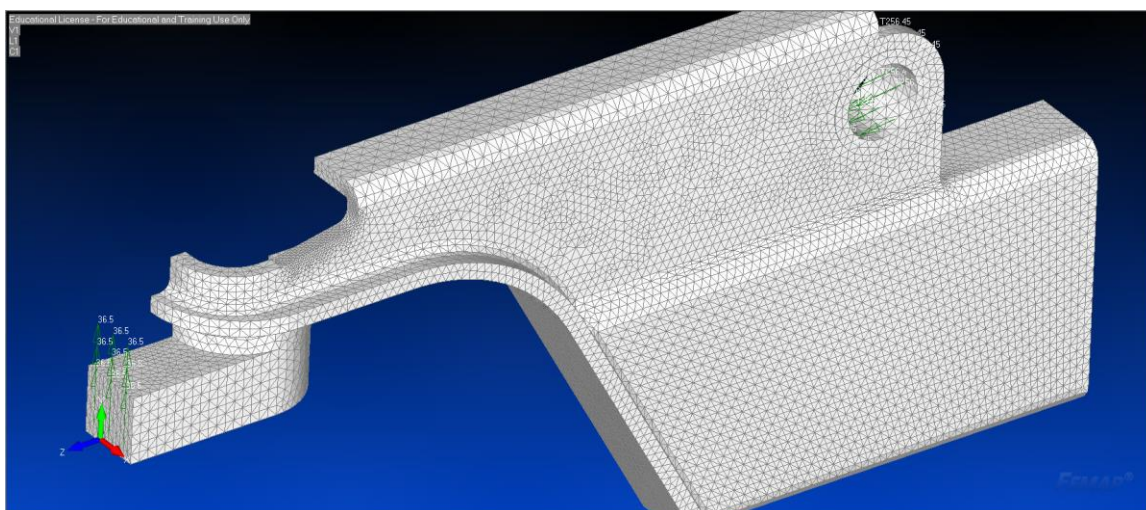
<i>Description</i>	<i>Value</i>
Max Von-Mises Stress (Distal End)	18,459 psi
Max Von-Mises Stress (Proximal End)	9439 psi
Max Y-Deflection of Beam	0.23 inches

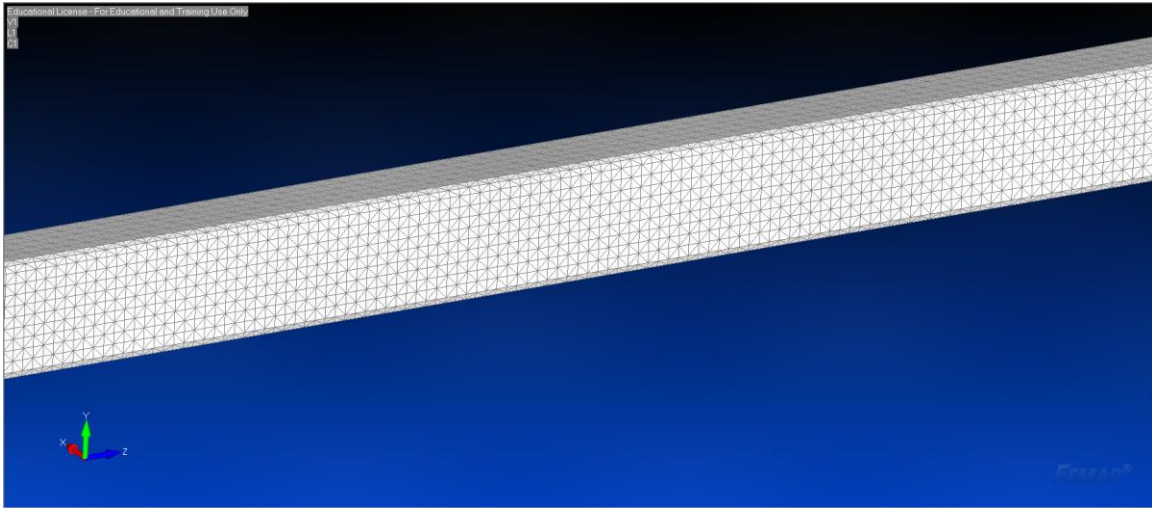
# MODEL



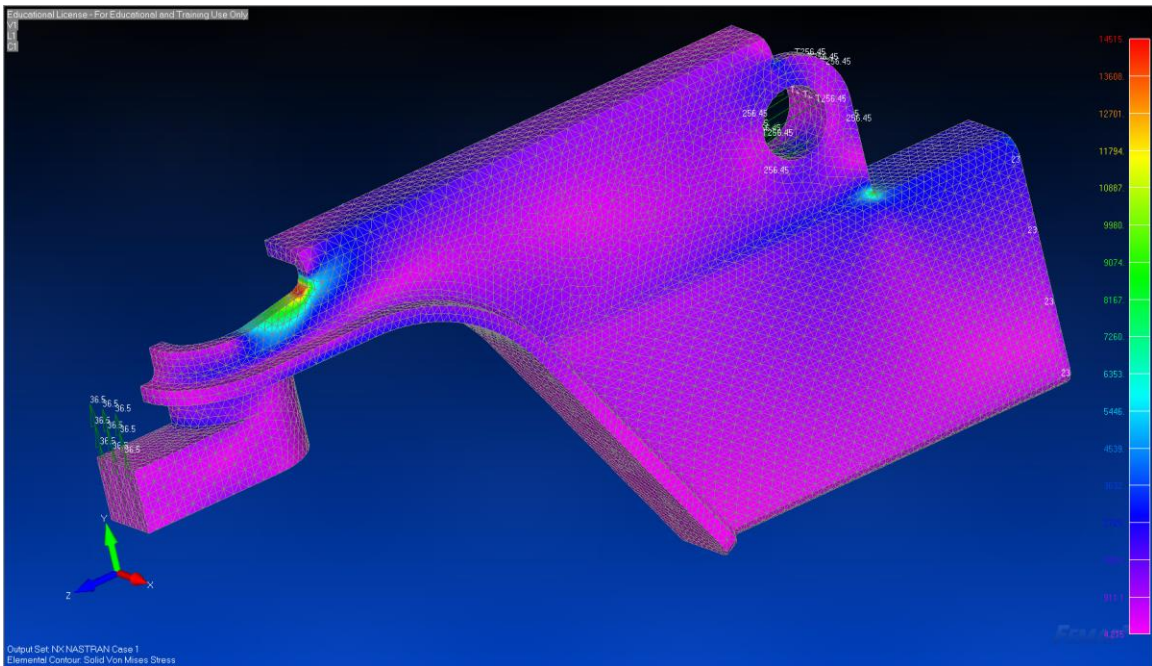


# MESH

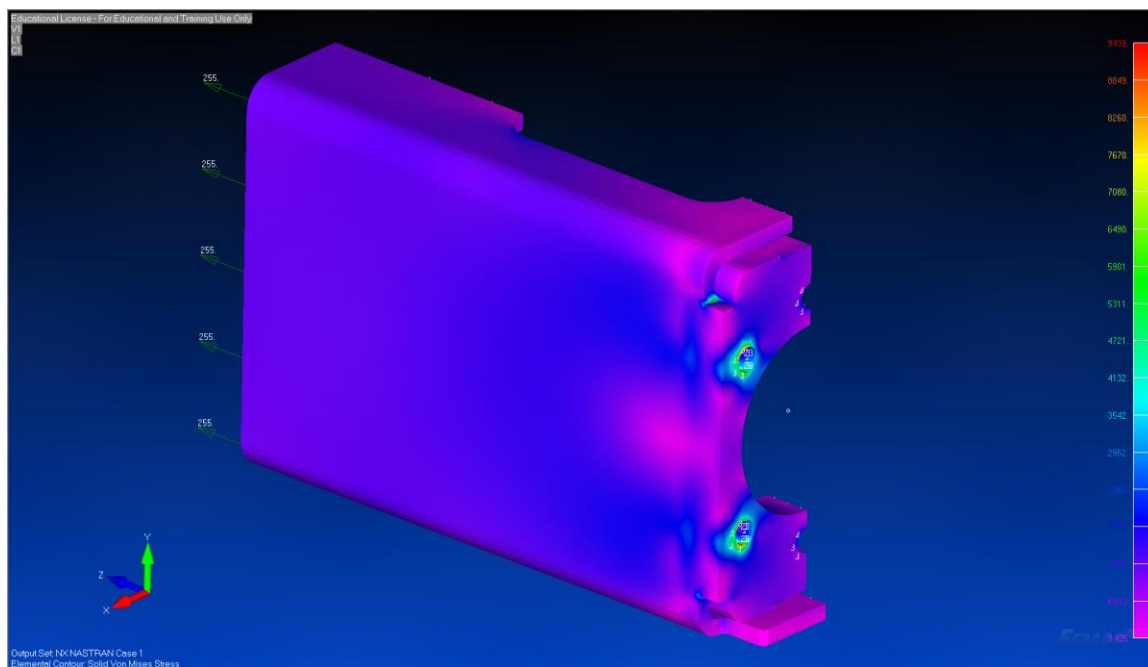
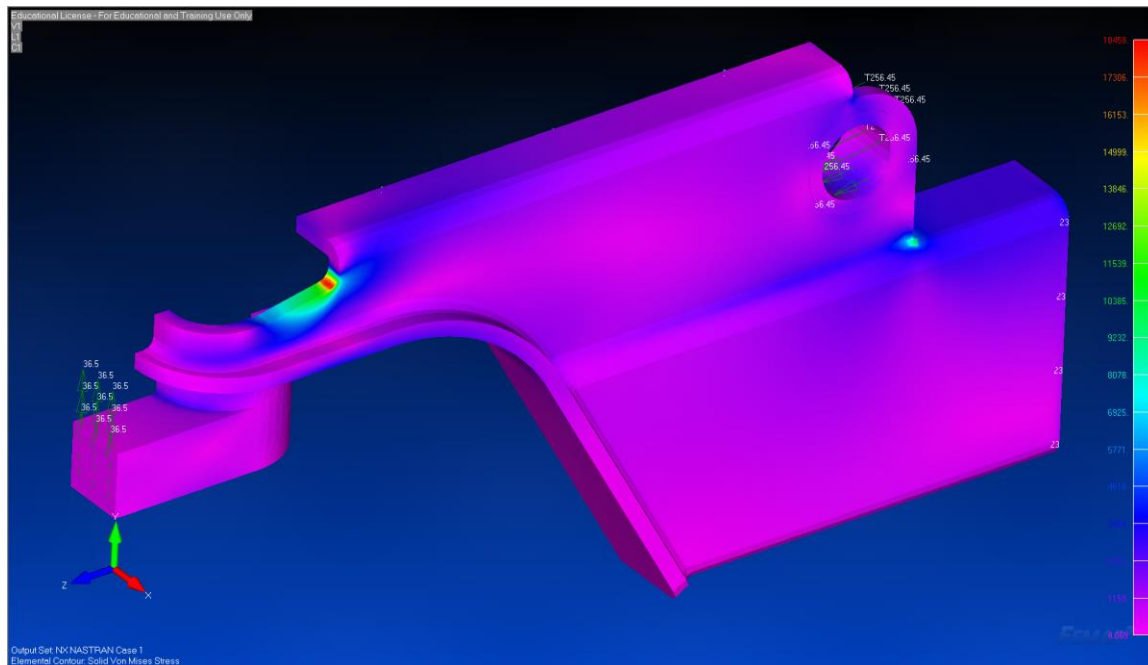




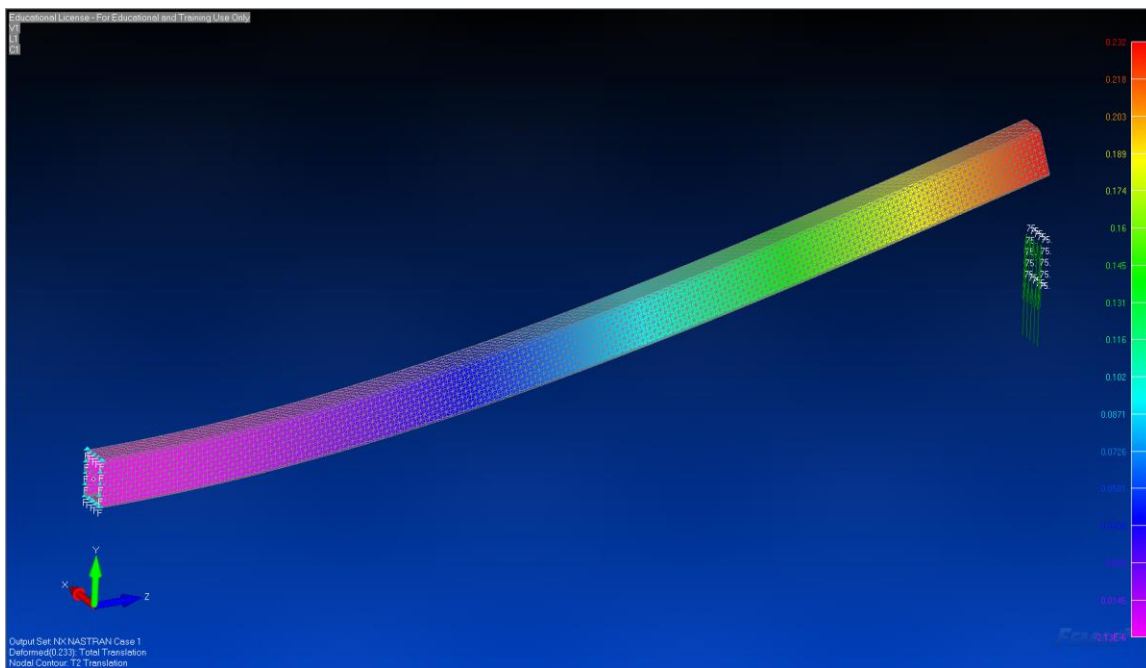
## Initial RESULTS



# Final RESULTS







## FINITE ELEMENT ANALYSIS REPORT: FEA #19

**Part/Assembly Model File:** A0 - P03-00017 Left Footrest Pivot Bracket.SLDPRT

**Femap Project File:** A0 - P03-00017 Left Footrest Pivot Bracket.modfem

**Purpose of Analysis:** Validate structural integrity of footrest pivot bracket

**Material:** Aluminum 5052-H32

<b>Stiffness</b>		<b>Limit Stress</b>	
Young's Modulus, E	<input type="text" value="10200000."/>	Tension	<input type="text" value="0."/>
Shear Modulus, G	<input type="text" value="0."/>	Compression	<input type="text" value="0."/>
Poisson's Ratio, nu	<input type="text" value="0.33"/>	Shear	<input type="text" value="0."/>
<b>Thermal</b>		Mass Density	<input type="text" value="0."/>
Expansion Coeff, a	<input type="text" value="0."/>	Damping, 2C/Co	<input type="text" value="0."/>
Conductivity, k	<input type="text" value="0."/>	Reference Temp	<input type="text" value="0."/>
Specific Heat, Cp	<input type="text" value="0."/>		
Heat Generation Factor	<input type="text" value="0."/>		

**Loads:** 25 lbf (1/4 of the Lower Body)

- F: Y-25.0 lbf

**Constraints:**

- Bottom Pivot Holes: TX, TY, TZ, RX
- Top Pivot Holes: TX, TZ

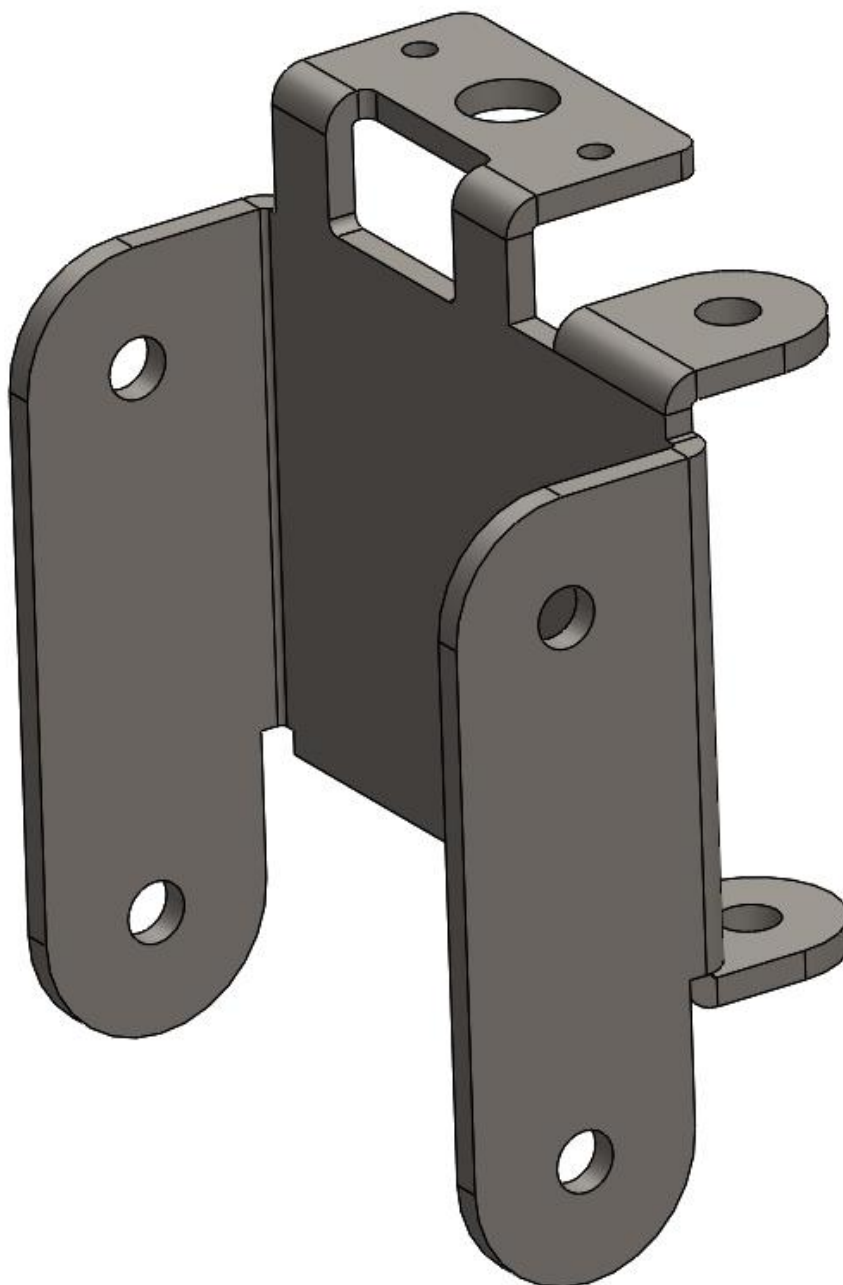
**Mesh:**

- Base Mesh: 0.06 inches

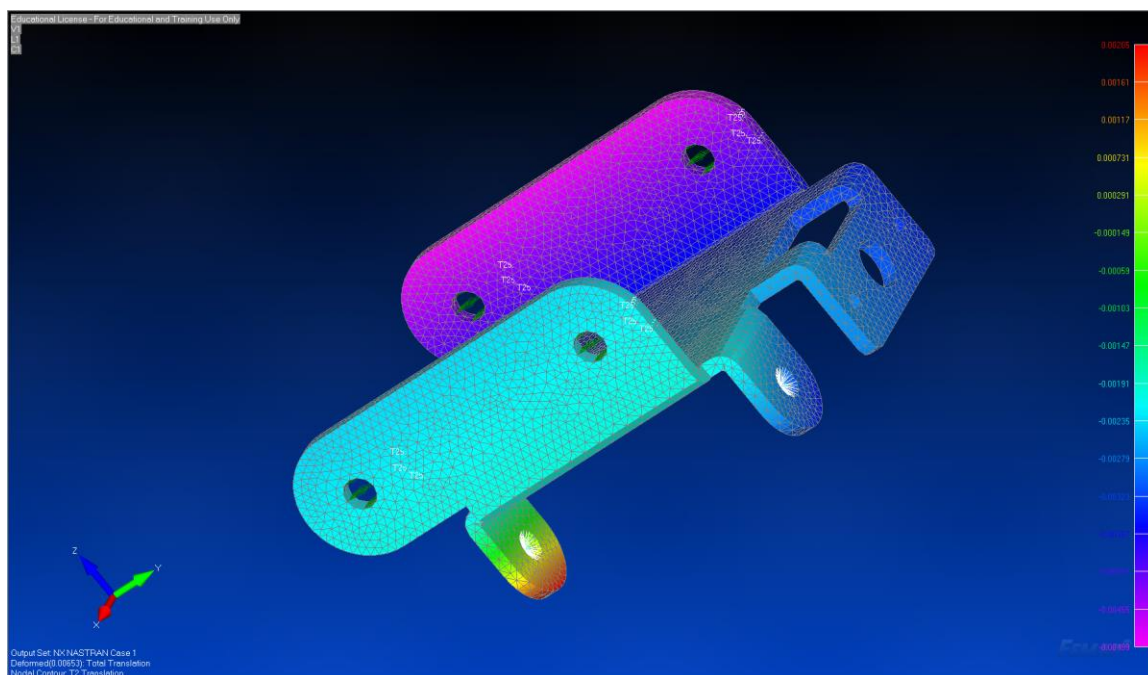
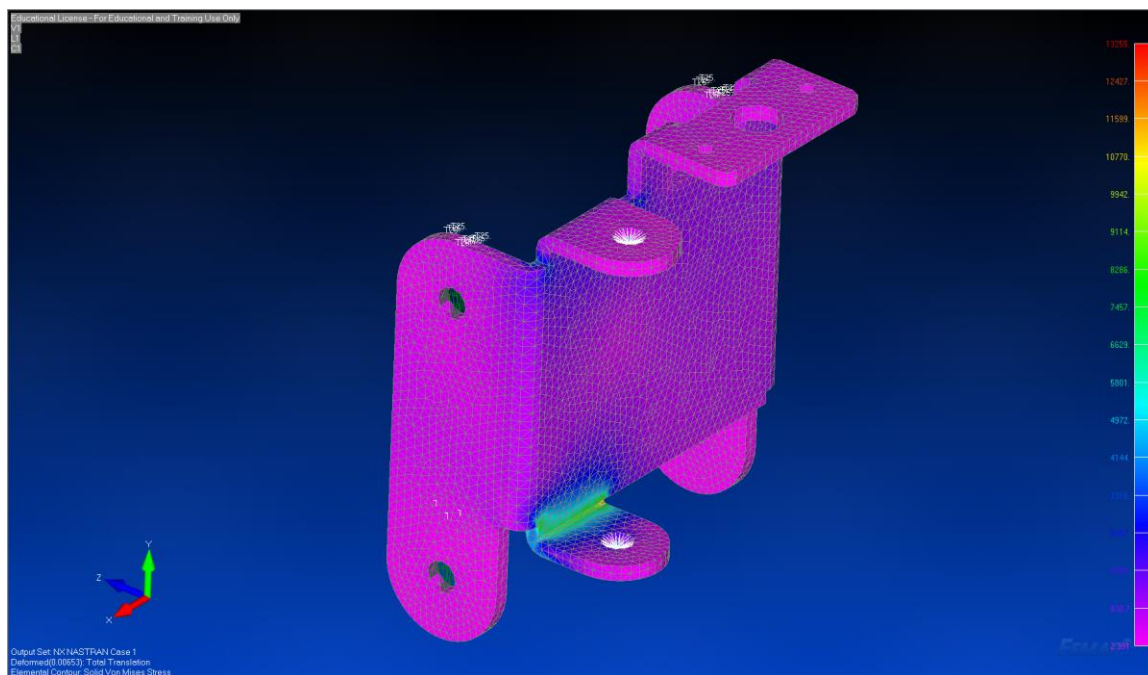
**Pertinent Results:**

<i>Description</i>	<i>Value</i>
Max Von-Mises Stress	13,255 psi
Max Total Deflection	<0.01 inches

# MODEL



# MESH & RESULTS



## FINITE ELEMENT ANALYSIS REPORT: FEA #20

**Part/Assembly Model File:** A0 - P03-00019 Left Footrest Caster Bracket.SLDPRT

**Femap Project File:** A0 - P03-00019 Left Footrest Caster Bracket.modfem

**Purpose of Analysis:** Validate structural integrity of footrest caster bracket under worst case load

**Material:** A36

<b>Stiffness</b>		<b>Limit Stress</b>	
Youngs Modulus, E	29000000.	Tension	0.
Shear Modulus, G	0.	Compression	0.
Poisson's Ratio, nu	0.26	Shear	0.
<b>Thermal</b>		Mass Density	
Expansion Coeff, a	6.E-6	7.35736E-4	
Conductivity, k	0.00069444	Damping, 2C/Co	0.
Specific Heat, Cp	44.8224	Reference Temp	70.
Heat Generation Factor	0.		

**Loads:** 25 lbf (1/4 of the Lower Body) in moment load configuration representing worst case caster load

- F: Y+25.0 lbf

**Constraints:**

- Bottom Pivot Holes: TX, TY, TZ, RY, RZ
- Top Pivot Hole: TY, TZ

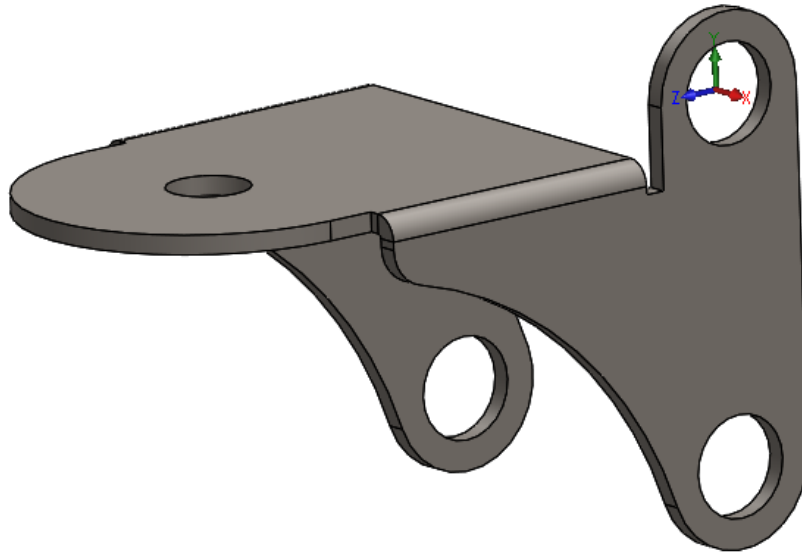
**Mesh:**

- Base Mesh: 0.06 inches

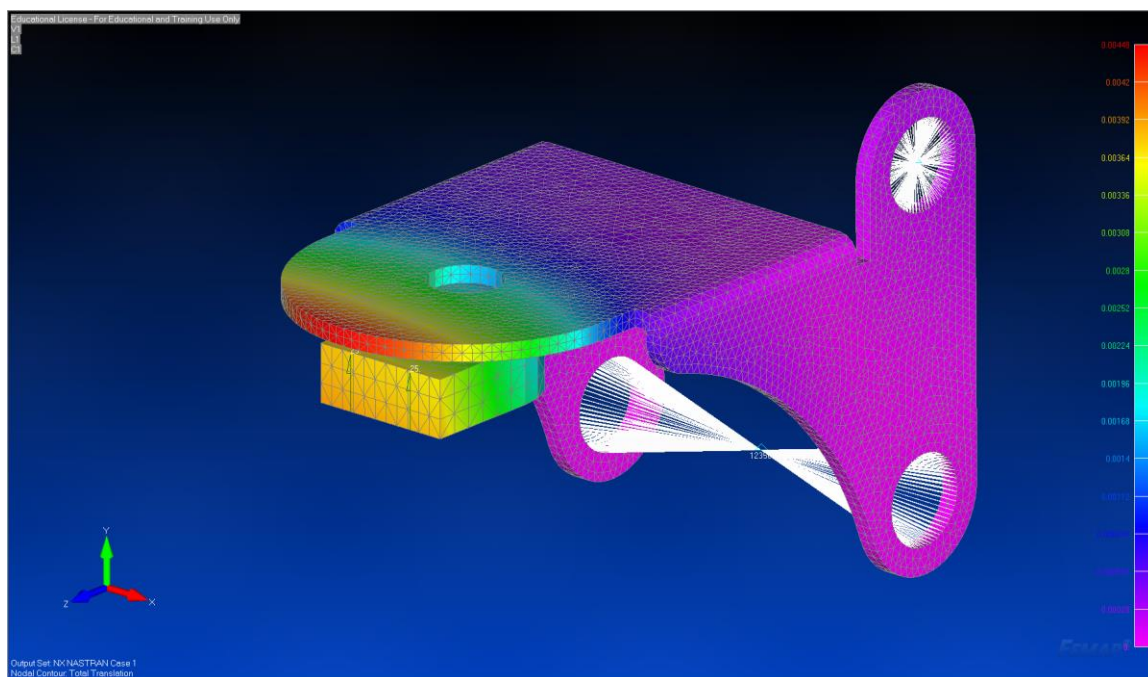
**Pertinent Results:**

<i>Description</i>	<i>Value</i>
Max Von-Mises Stress	18,561 psi
Max Total Deflection	<0.01 inches

# MODEL



# MESH & RESULTS



## FINITE ELEMENT ANALYSIS REPORT: FEA #21

**Part/Assembly Model File:** A0 - P03-00021 Left Footrest Latch Bracket.SLDPRT

**Femap Project File:** A0 - P03-00021 Left Footrest Latch Bracket.modfem

**Purpose of Analysis:** Validate structural integrity of footrest latch bracket

**Material:** Aluminum 5052-H32

<b>Stiffness</b>		<b>Limit Stress</b>	
Young's Modulus, E	10200000.	Tension	0.
Shear Modulus, G	0.	Compression	0.
Poisson's Ratio, nu	0.33	Shear	0.
<b>Thermal</b>		Mass Density	0.
Expansion Coeff, a	0.	Damping, 2C/Co	0.
Conductivity, k	0.	Reference Temp	0.
Specific Heat, Cp	0.		
Heat Generation Factor	0.		

**Loads:** 25 lbf (1/4 of the Lower Body)

- F: Y-25.0 lbf Applied to bottom (and later top) pivot hole(s)

**Constraints:**

- 4 Mounting Holes: Fixed

**Mesh:**

- Base Mesh: 0.03 inches

**Pertinent Results:**

Initial Results

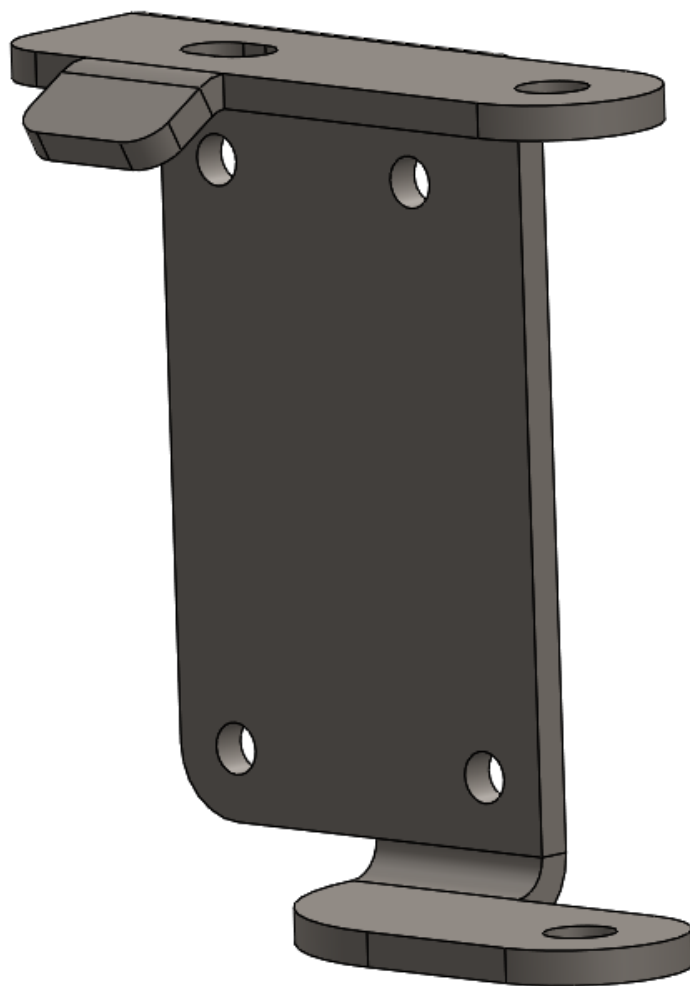
<b>Description</b>	<b>Value</b>
Max Von-Mises Stress	43,758 psi
Max Total Deflection	>0.01 inches

Results after design mod to pivot bracket to share load with top flange

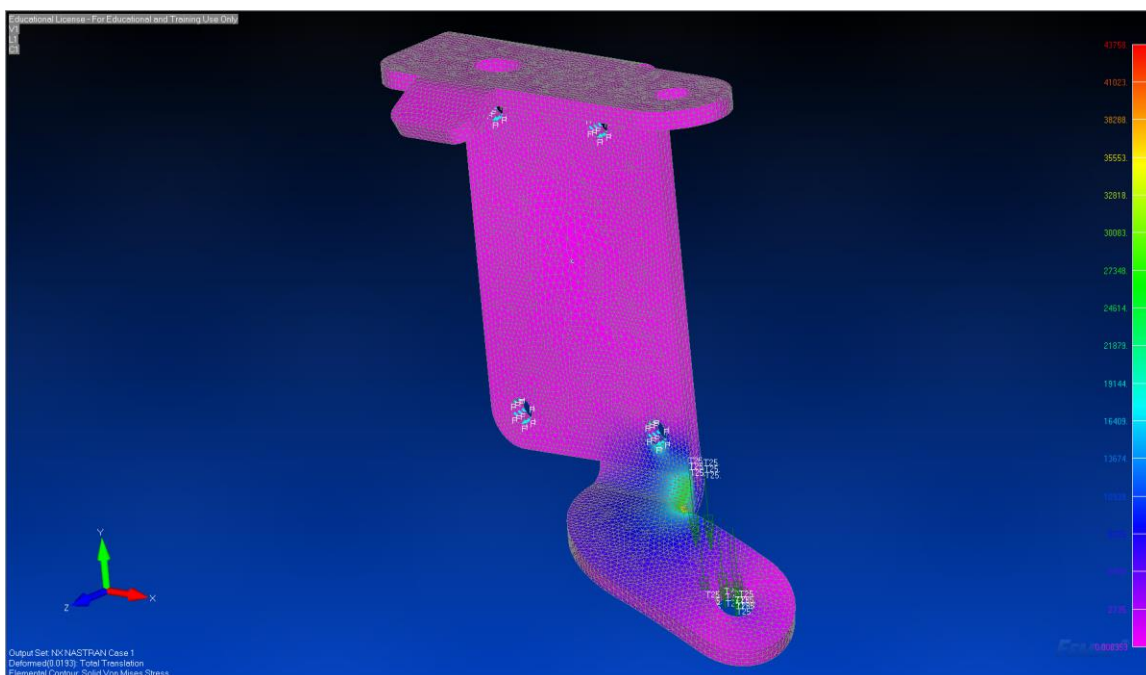
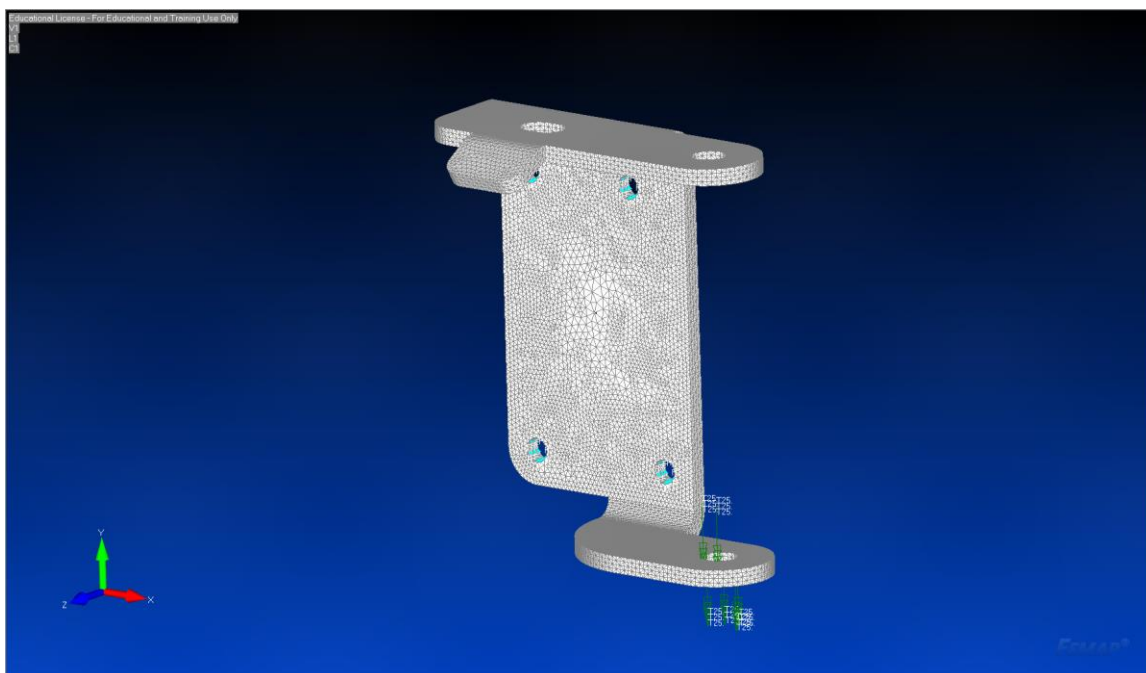
<b>Description</b>	<b>Value</b>
Max Von-Mises Stress	22,570 psi
Max Total Deflection	<0.01 inches

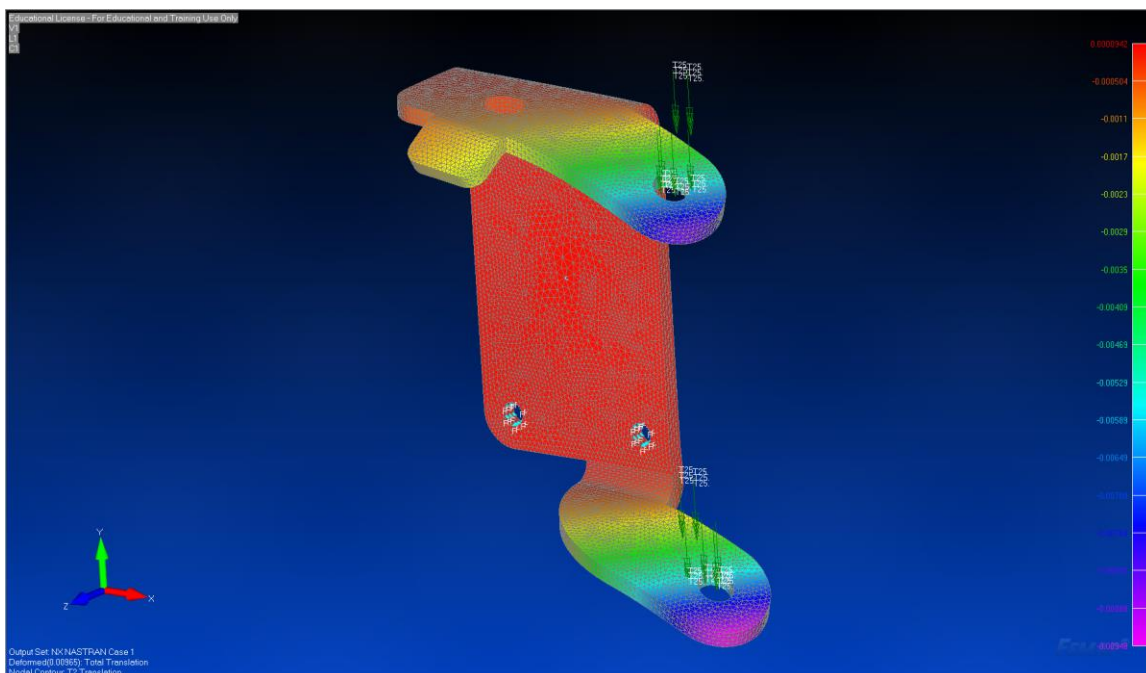
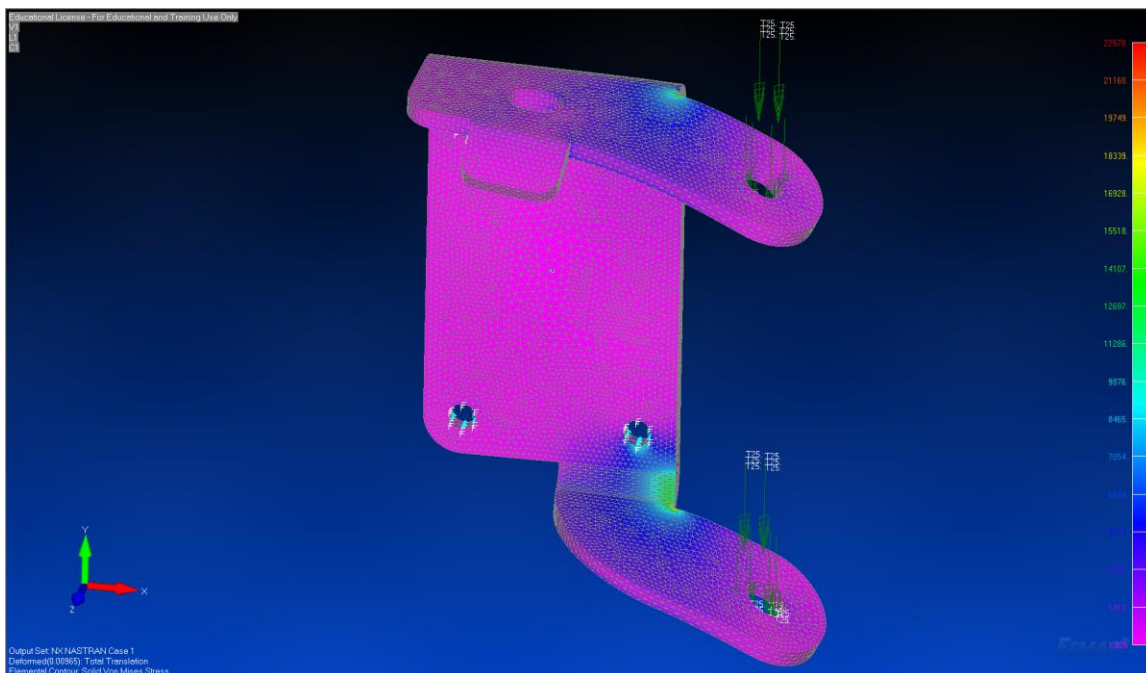


# MODEL



## MESH & RESULTS





## FINITE ELEMENT ANALYSIS REPORT: FEA #22

### Part/Assembly Model File:

- Initial Model: A0 - P03-00026 Rear Seat Hanger (Left Half).SLDPRT
- Final Model: A1 - P03-00026 Rear Seat Hanger (Left Half).SLDPRT

### Femap Project File:

- Initial File: A0 - P03-00026 Rear Seat Hanger (Left Half).modfem
- Final File: A1 - P03-00026 Rear Seat Hanger (Left Half).modfem

**Purpose of Analysis:** Verification of material and geometry for stress management in design.

### Material: A36 Steel

<b>Stiffness</b>		<b>Limit Stress</b>	
Youngs Modulus, E	29000000.	Tension	0.
Shear Modulus, G	0.	Compression	0.
Poisson's Ratio, nu	0.26	Shear	0.
<b>Thermal</b>		<b>Mass Density</b>	
Expansion Coeff, a	6.E-6	Damping, 2C/Co	0.
Conductivity, k	0.00069444	Reference Temp	70.
Specific Heat, Cp	44.8224		
Heat Generation Factor	0.		

### Loads: Force Analysis Max Values

- Initial Analysis (Step 1): Y-42.0 lbf
- Step 201
  - FC: Y-2.63, Z-8.67 (lbf)
  - Fseat: Y-66.0, Z+27.1 (lbf)

### Constraints:

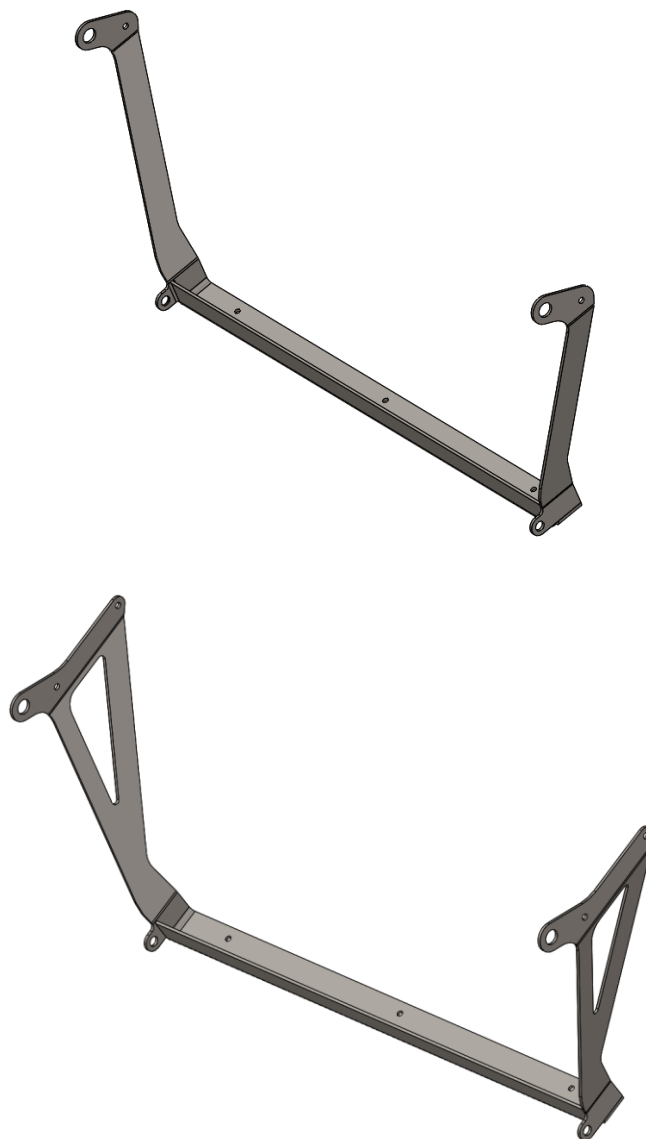
- Attachment Holes: TX, TY, TZ, RY, RZ
- Symmetry: TX

### Mesh:

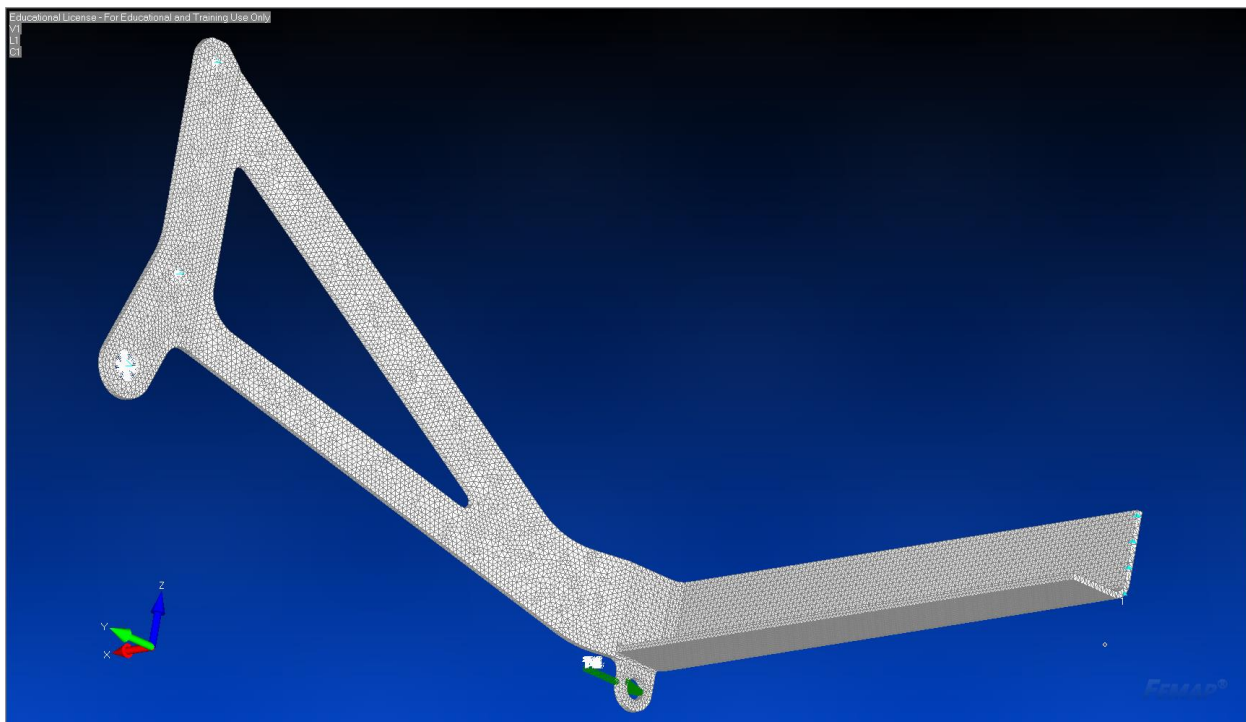
- Base Mesh Size: 0.06 inches

**Pertinent Results:**

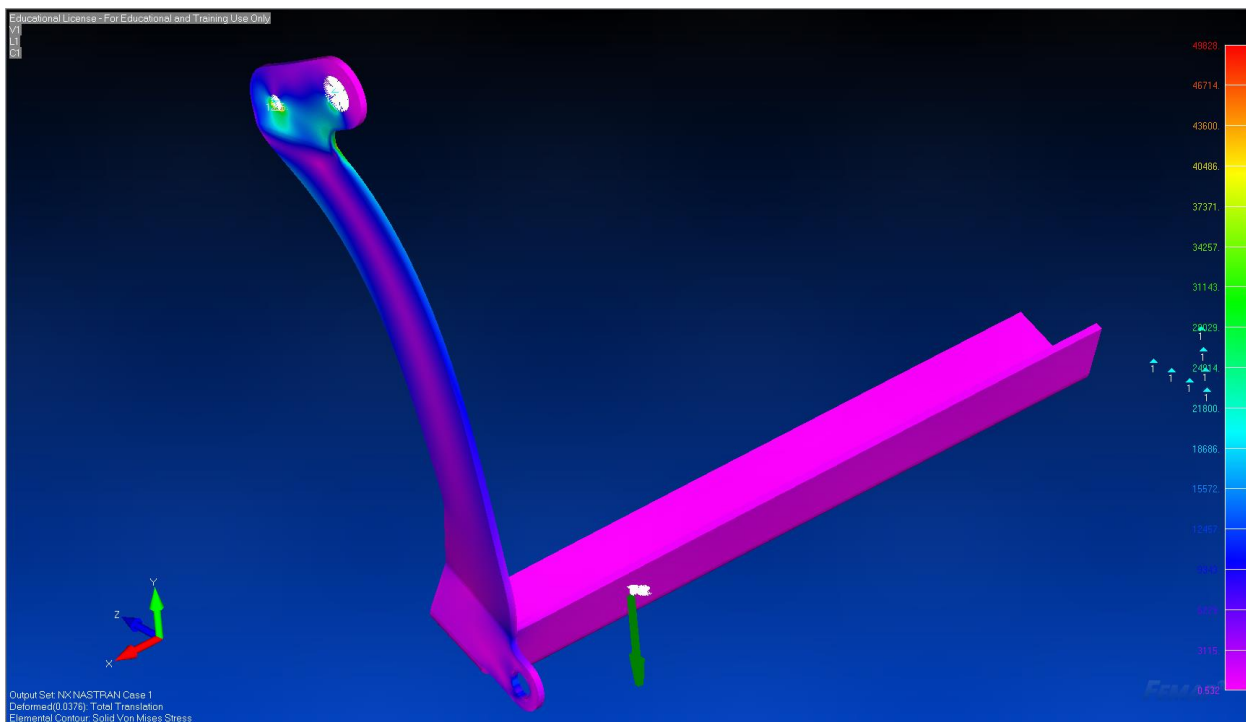
<i>Description</i>	<i>Value</i>
Maximum Von-Mises Stress (Initial Result: Step 1)	49,828 psi
Maximum Non-Local Von-Mises Stress in Final Model (Initial Result: Step 1)	21,289 psi
Maximum Non-Local Von-Mises Stress in Final Model (Initial Result: Step 201)	17,134 psi

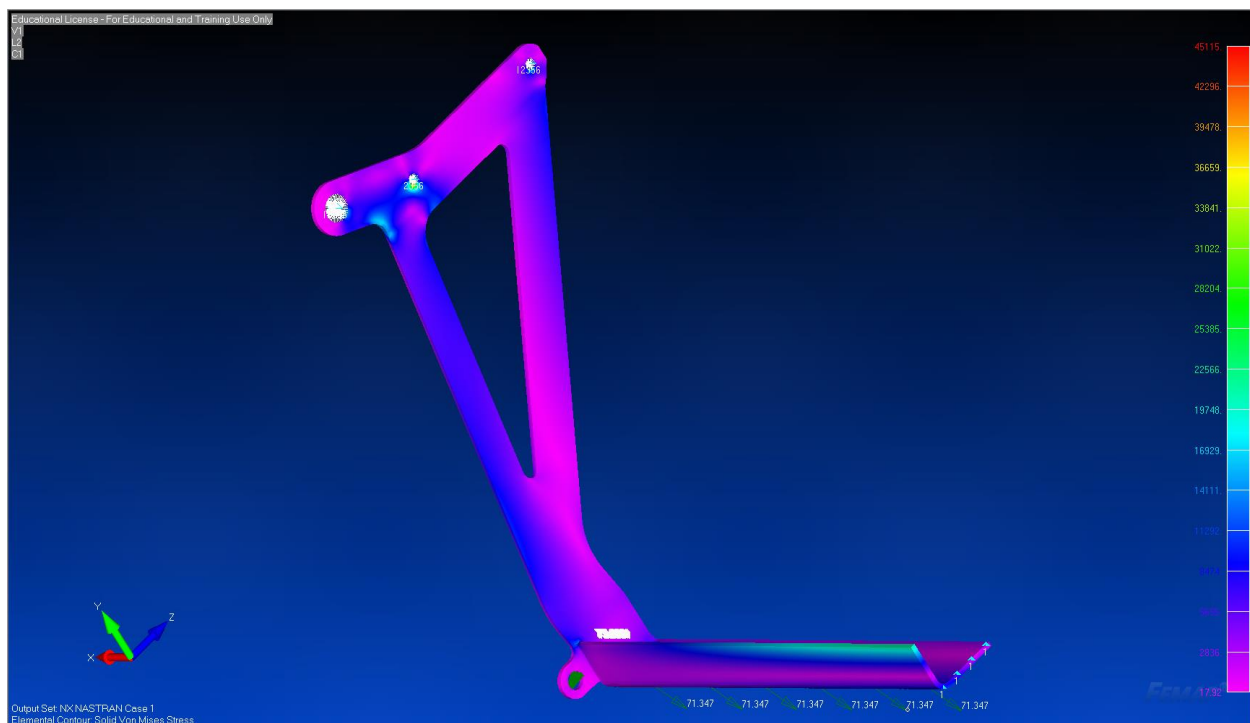
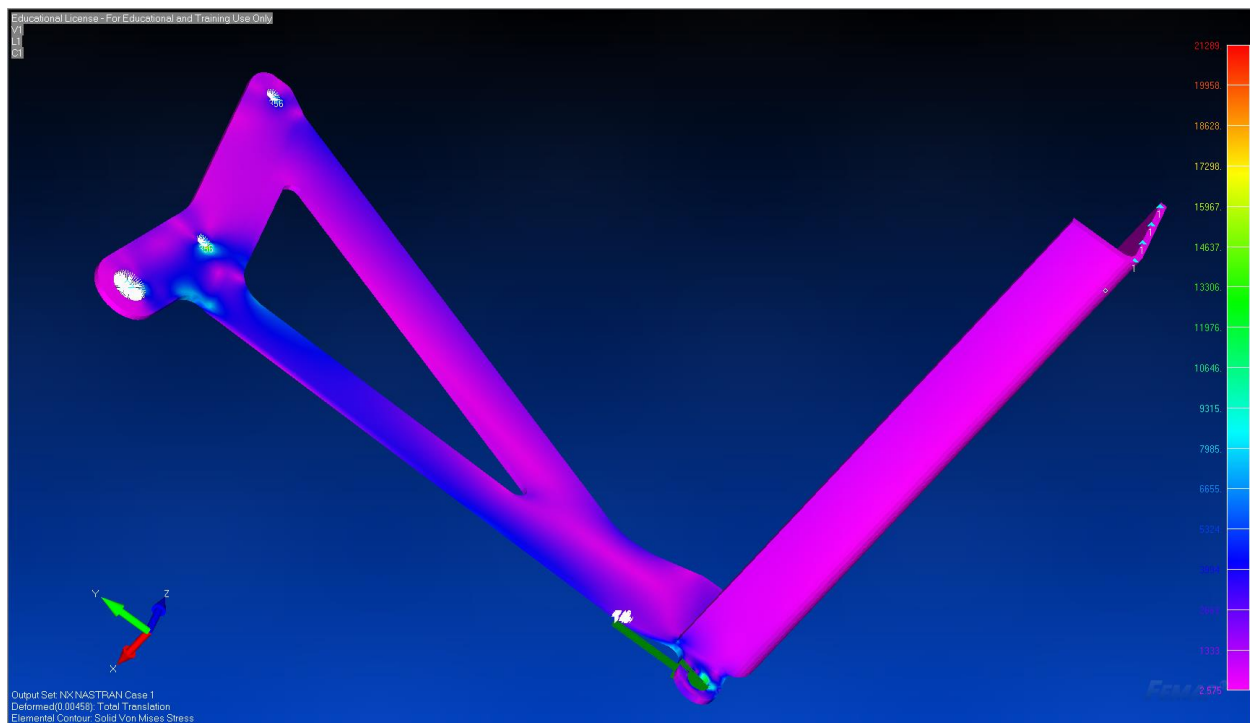
**MODEL (Initial & Final)**

## MESH



## RESULTS





## FINITE ELEMENT ANALYSIS REPORT: FEA #23

**Part/Assembly Model File:** A0 - P02-00022 Grooved Idler Pulley Shaft.SLDPRT

**Femap Project File:** A0.1 - P02-00022 Grooved Idler Pulley Shaft.modfem

**Purpose of Analysis:** Find stress to compare to a cyclic loading chart for fatigue failure

**Material:** 12L14 Steel, Cold Drawn

<b>Stiffness</b>		<b>Limit Stress</b>	
Young's Modulus, $E$	29000000.	Tension	0.
Shear Modulus, $G$	0.	Compression	0.
Poisson's Ratio, $\nu$	0.29	Shear	0.
<b>Thermal</b>		<b>Mass Density</b>	
Expansion Coeff, $\alpha$	6.E-6	Mass Density	7.35736E-4
Conductivity, $k$	0.00069444	Damping, 2C/Co	0.
Specific Heat, $C_p$	44.8224	Reference Temp	70.
Heat Generation Factor	0.		

**Loads:** F\_bend

- F\_bend: Y-7.75 lbf Applied to bottom (and later top) pivot hole(s)

**Constraints:**

- Initial Try: Bearing locations: Fixed
- Second refined model:
  - Front Bearing RE: TX, TY, TZ, RY, RZ
  - Rear Bearing RE: TX, TY

**Mesh:**

- Base Mesh: 0.025 inches
- Refined Mesh: 0.01 inches

**Pertinent Results:**

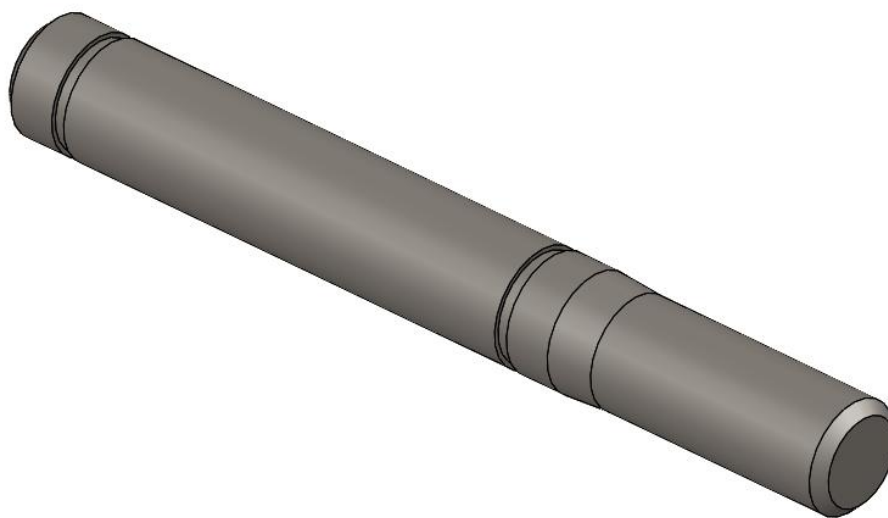


## Fixed Surface Results

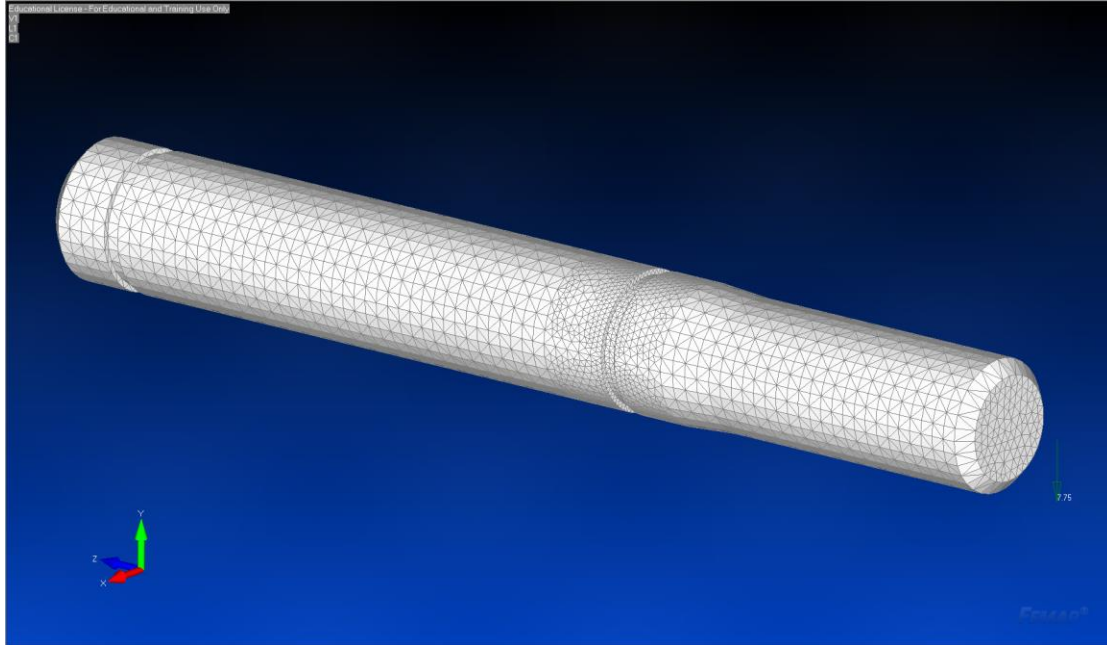
<i>Description</i>	<i>Value</i>
Max Von-Mises Stress	9605 psi

## Rigid Element Model Results

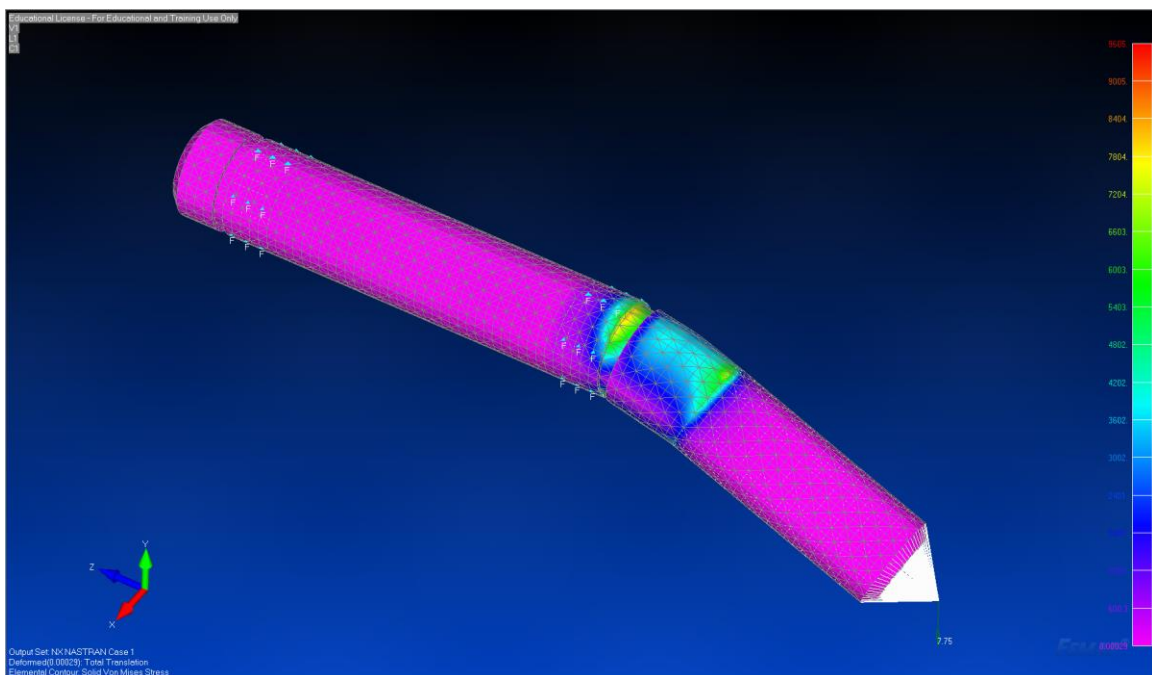
<i>Description</i>	<i>Value</i>
Max Von-Mises Stress	9,872 psi

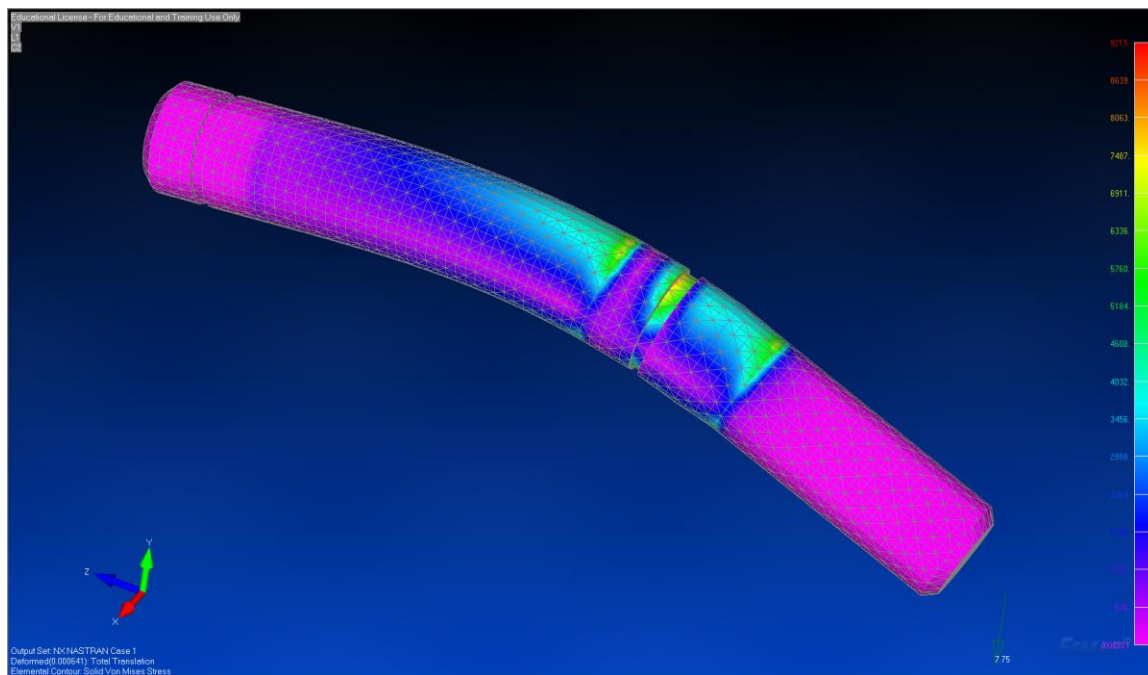
**MODEL**

## Final MESH

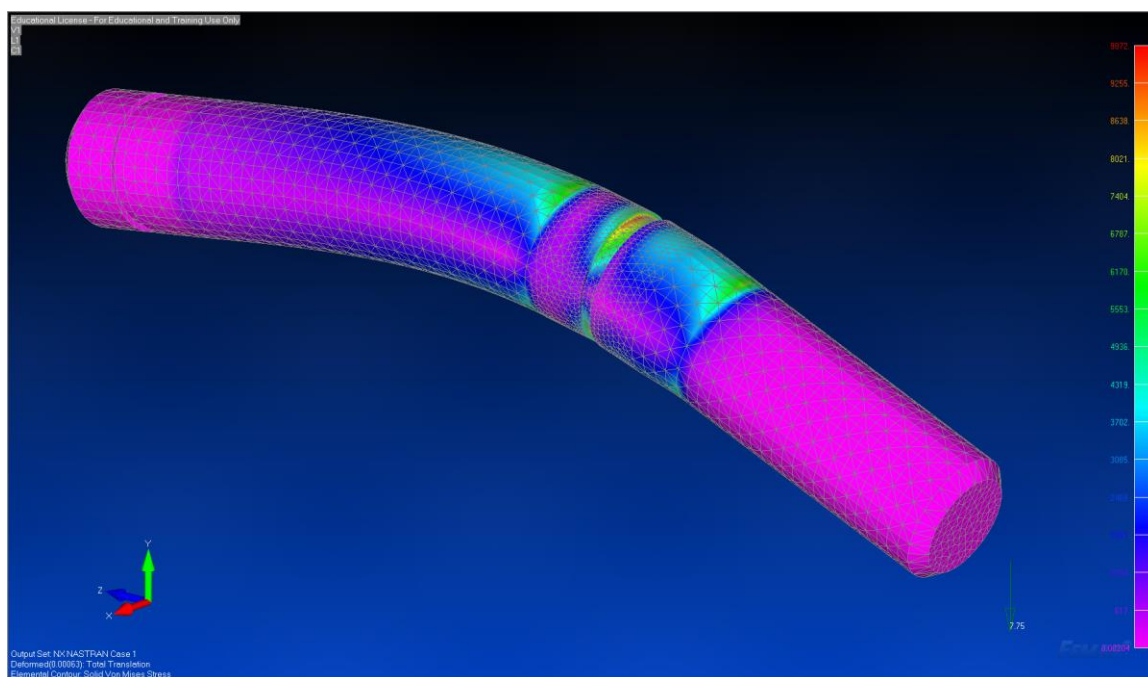


## RESULTS





## Refined Mesh Results



## FINITE ELEMENT ANALYSIS REPORT: FEA #24

**Part/Assembly Model File:** A0 - P02-00027 Main Drive Pulley Axle.SLDPRT

**Femap Project File:** A0 - P02-00027 Main Drive Pulley Axle.modfem

**Purpose of Analysis:** Find stress to compare to a cyclic loading chart for fatigue failure

**Material:** 1144 Cold Drawn High Carbon Steel

<b>Stiffness</b>		<b>Limit Stress</b>	
Young's Modulus, E	<input type="text" value="29700000."/>	Tension	<input type="text" value="0."/>
Shear Modulus, G	<input type="text" value="0."/>	Compression	<input type="text" value="0."/>
Poisson's Ratio, nu	<input type="text" value="0.29"/>	Shear	<input type="text" value="0."/>
<b>Thermal</b>		Mass Density	<input type="text" value="0."/>
Expansion Coeff, a	<input type="text" value="0."/>	Damping, 2C/Co	<input type="text" value="0."/>
Conductivity, k	<input type="text" value="0."/>	Reference Temp	<input type="text" value="0."/>
Specific Heat, Cp	<input type="text" value="0."/>		
Heat Generation Factor	<input type="text" value="0."/>		

**Loads:** Computed loads at bearings, and moment load from belt

- Belt Moment: 34.45 in-lbf, applied at pulley point
- F\_Bearing\_A: X-64.6, Y-108.7 (lbf)
- F\_Bearing\_B: X+47.1, Y+4.4 (lbf)

**Constraints:** Gear and pulley constraints

- Pulley: TX, TY
- Gear: TX, TY, TZ, RZ

**Mesh:**

- Base Mesh: 0.03 inches
- Refined Mesh: 0.015 inches

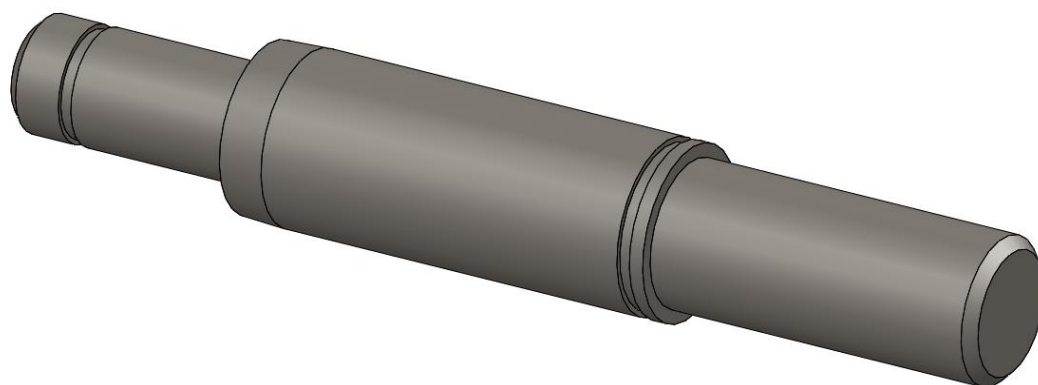
**Pertinent Results:**

Fixed Surface Results

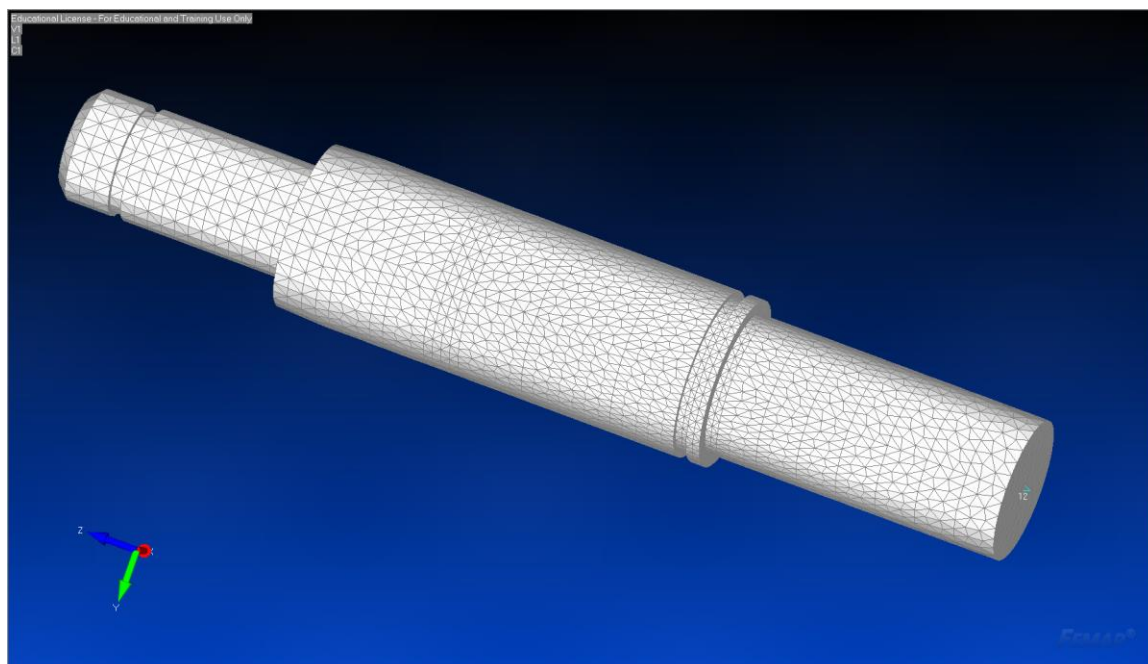
<i>Description</i>	<i>Value</i>
--------------------	--------------

Max Von-Mises Stress	33,360 psi
----------------------	------------

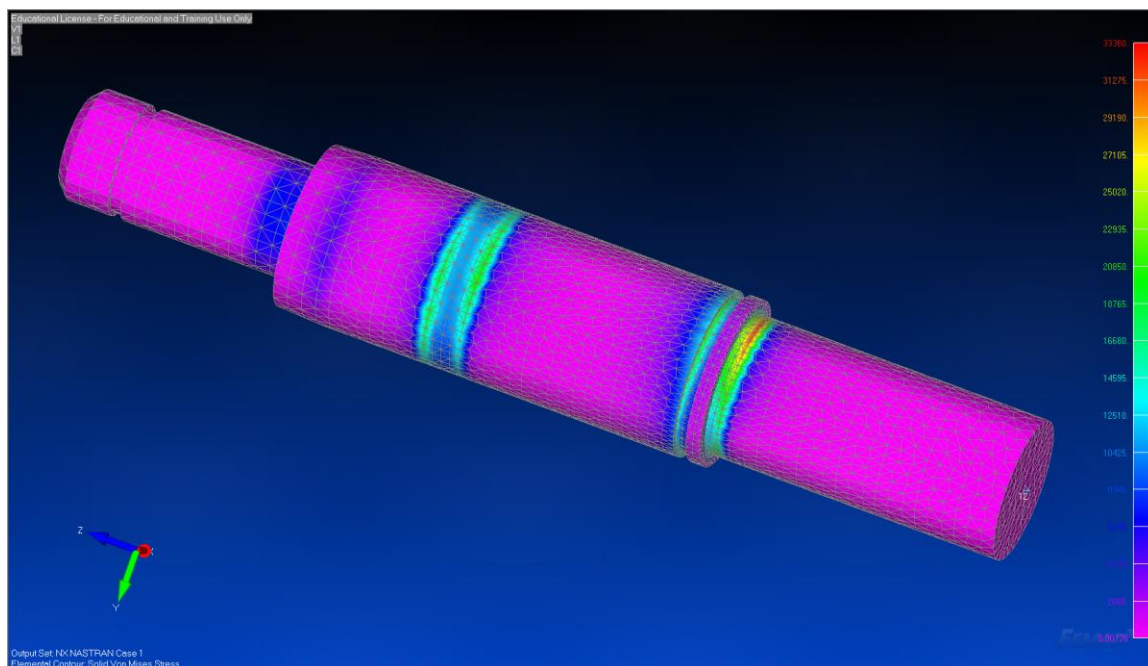
# MODEL



# Final MESH



## RESULTS



### Pulley Constraint Forces

Node 51732

Output Set	1 : NX NASTRAN Case 1		
Value =	-17.7365	Output Vector	52 : T1 Constraint Force
Value =	68.4331	Output Vector	53 : T2 Constraint Force

### Gear Constraint Forces

Node 51730

Output Set	1 : NX NASTRAN Case 1		
Value =	35.2365	Output Vector	52 : T1 Constraint Force
Value =	35.8669	Output Vector	53 : T2 Constraint Force

**Appendix G. Traditional Theoretical Calculations**

The following hand calculations are included in this section:

Weld Analysis on Backrest Support Brackets

Bearing Load Calculations

Caster Calculations

Fixed Bearing and Lead Screw Calculations

Weld Analysis on Fixed Bearing Standoff

Grooved Pulley Shaft Analysis

Leg Attachment Bracket Weld Analysis

Main Bearing Drive Shaft Analysis

Miscellaneous Hardware Calculations

Pins Analysis

Screws & Fasteners Used in Structure

Seat Bar Assembly: Hand Calculations for Applied Forces

Slider Caster & Brake Loads



# Weld Analysis on Backrest Support Brackets

## Resources:

Shigley's Mechanical Engineering Design, Eighth Edition  
Richard G. Budynas, J. Keith Nisbett  
2008 McGraw Hill, New York, NY

Parallel Fillet Welds  
Equation (9-3), (9-5), (9-6),  
Table (9-2), (9-3), (9-4)  
Pgs. 463-465

## Assumptions:

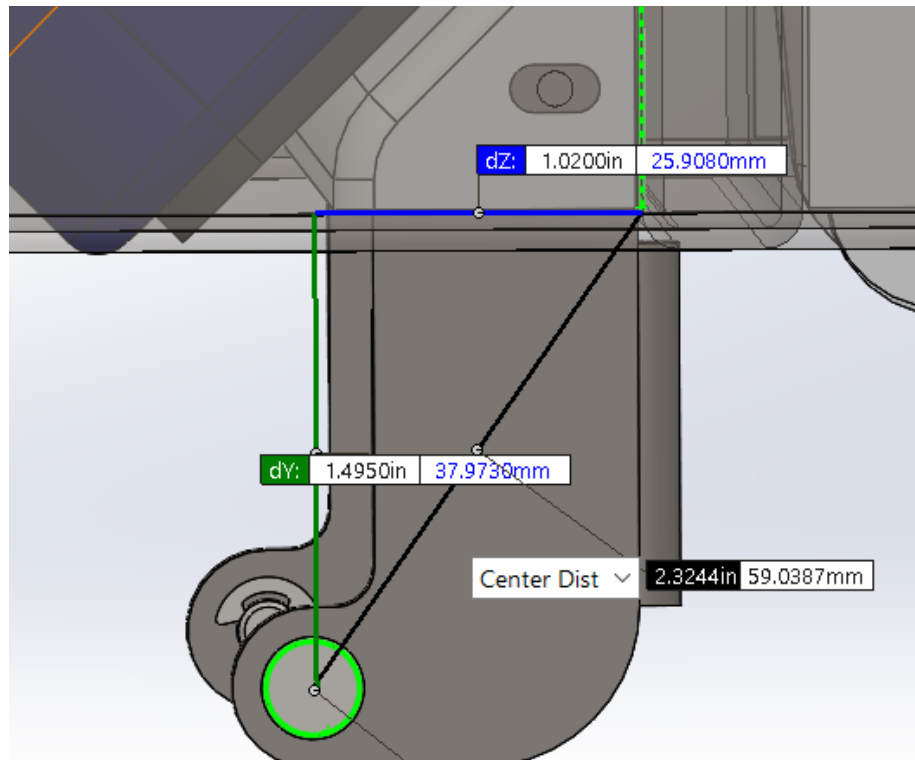
Load applied to pivot D is considered to only act parallel to the welds  
AWS Electrode: E60xx

$$\sigma_{yWeld} := 50ksi$$

Table (9-3)

$$\sigma_{maxWeld} := 0.6\sigma_{yWeld} = 30ksi$$

Bending type loading, Table (9-4)



$$F_{D_{\max}} := 56.6 \text{bf}$$

Max computed load at pivot D

$$F_D := F_{D_{\max}} \cdot 2 = 113.2 \text{bf}$$

Increased load at pivot D

$$h := 0.0625 \text{in}$$

Fillet Size

$$L_1 := 1.0 \text{in}$$

Fillet Length

### *Shear Only*

$$\tau_D := \frac{1.414 F_D}{h \cdot L_1} = 2.561 \text{ksi}$$

Eqn (9-3)

$$\text{FOS} := \frac{\sigma_{\max \text{Weld}}}{\tau_D} = 11.7$$

### *Moment Load*

$$d_{\text{pin}} := 1.02 \text{in}$$

Distance from weld location to pivot pin

$$M_1 := F_D \cdot d_{\text{pin}}$$

Moment created on each bracket

$$A_1 := 1.414 h \cdot L_1$$

Total throat Area, Table (9-2)

$$I_u := \frac{L_1^3}{6}$$

Second Moment of Area, Table (9-2)

$$I := 0.707 h \cdot I_u$$

Eqn (9-6)

$$r := \frac{L_1}{2}$$

Distance to point of interest from weld center

$$\tau_{D1} := \frac{F_D}{A_1} = 1.281 \text{ksi}$$

Primary Shear, Budynas pg. 469

$$\tau_{D2} := \frac{M_1 \cdot r}{I} = 7.839 \text{ksi}$$

Secondary Shear, Budynas pg. 469

$$\tau_{\max} := \sqrt{\tau_{D1}^2 + \tau_{D2}^2} = 7.943 \text{ ksi}$$

$$\text{FOS}_{\text{WeldMetal}} := \frac{\sigma_{\max\text{Weld}}}{\tau_{\max}} = 3.8$$

## Bearing Load Calculations

277

Scale FOS for FMEA, because max dynamic load allowed is considered infinite life load and can be considered to be the load where the FOS in the FMEA = 3.0

$$F_{3\max} := 513\text{bf}$$

$$F_{\text{LegMAX}} := 523\text{bf}$$

### *P00-00005*

$$F_{00005\max} := 1550\text{bf} \quad F_{00005\text{des}} := F_{\text{LegMAX}}$$

$$\text{FOS}_{00005\text{FMEA}} := \frac{F_{00005\max}}{F_{00005\text{des}}} \cdot 3.0 = 8.9$$

### *P00-00030*

$$F_{00030\max} := 1500\text{bf} \quad F_{00030\text{des}} := F_{3\max}$$

$$\text{FOS}_{00030\text{FMEA}} := \frac{F_{00030\max}}{F_{00030\text{des}}} \cdot 3.0 = 8.8$$

### *P00-00031*

$$F_{00031\max} := 1000\text{bf} \quad F_{00031\text{des}} := F_{3\max}$$

$$\text{FOS}_{00031\text{FMEA}} := \frac{F_{00031\max}}{F_{00031\text{des}}} \cdot 3.0 = 5.8$$

### *P00-00037 & 38*

$$F_{3738\max} := 250\text{bf} \quad F_{3738\text{des}} := 250\text{bf}$$

$$\text{FOS}_{3738\text{FMEA}} := \frac{F_{3738\max}}{F_{3738\text{des}}} \cdot 3.0 = 3$$

This requires that the nuts that sandwich these bushings only get torqued to provide an axial force of 250lbf

$$d := 0.375$$

$$d_m := \frac{d + 0.2975}{2} \quad \text{Average of the major and minor diameters}$$

$$\lambda := \operatorname{atan}\left(\frac{1}{\pi \cdot d_m \cdot 16}\right) = 0.059 \quad \text{Thread angle}$$

$$f := 0.15 \quad f_c := 0.15 \quad \text{Pg 423, Budynas}$$

$$\alpha := 30\text{deg} \quad \text{Half the thread angle (60 deg)}$$

$$T_{\max} := \left[ \left( \frac{d_m}{2 \cdot d} \right) \cdot \left( \frac{\tan(\lambda) + f \cdot \sec(\alpha)}{1 - f \cdot \tan(\lambda) \cdot \sec(\alpha)} \right) + 0.625 \cdot f_c \right] \cdot 250 \cdot d \cdot \text{in} \cdot \text{lbf}$$

$$T_{\max} = 18.657 \text{in} \cdot \text{lbf}$$

### *P00-00033 McMaster PN 7804K147*

$$F_{00033\max} := 280\text{lbf}$$

$$F_{00033\text{des}} := \frac{678}{2} \text{gm} \cdot \text{g} \quad \text{Assuming half screw weight}$$

$$\text{FOS}_{00033\text{FMEALoad}} := \frac{F_{00033\max}}{F_{00033\text{des}}} \cdot 3 = 1123.9$$

$$\text{RPM}_{\max\text{Des}} := 2035$$

$$\text{RPM}_{\max33} := 43000$$

$$\text{FOS}_{00033\text{FMEArpm}} := \frac{\text{RPM}_{\max33}}{\text{RPM}_{\max\text{Des}}} \cdot 3 = 63.3$$

*P00-00085 0.25 ID .5 OD Flanged Ball Bearing*

$F_{\text{bearing2}} := 15.915 \text{ lbf}$       From grooved shaft analysis

[http://shop.sdp-si.com/catalog/product/?id=A\\_7Y55-F5025](http://shop.sdp-si.com/catalog/product/?id=A_7Y55-F5025)

## Product Specifications

<b>Bearing Type</b>	Flanged - No Shield
<b>Lubrication</b>	MIL-L-6085A - Oil
<b>Bore Size (B)</b>	0.2500 Inch
<b>Outside Dia. (D)</b>	0.5000 Inch
<b>Material/quality</b>	440C Stainless / ABEC 3
<b>Overall Width (W)</b>	0.1250
<b>Dynamic Load</b>	123 lbs
<b>Static Load</b>	54 lbs
<b>Flange Width (FW)</b>	0.0230 ( 0 = None)
<b>Flange Dia. (F)</b>	0.547 ( 0 = None)
<b>Substitute Part</b>	BBSRIF-814XXX301

$$F_{\text{max85}} := 123 \text{ lbf}$$

Determine Number of Revs

$$\text{teeth}_{\text{Main}} := 22$$

$$\text{teeth}_{\text{Idler}} := 12$$

$$N_{\text{cycCreepUp}} := 20 \cdot 20 \cdot 12 \cdot 10 = 4.8 \times 10^4$$

20 full cycles of creeper per day, 20 days per month,  
12 months per year for 10 years

REVS := 187    Number of revolutions per full stroke of screw (from code)

RPC := 2 · REVS    Number of revolutions of screw per full cycle

$$\text{REV}_{\text{Idler}} := \frac{\text{teeth}_{\text{Main}}}{\text{teeth}_{\text{Idler}}} \cdot \text{RPC}$$

$$\text{REVS}_{\text{total}} := N_{\text{cycCreepUp}} \cdot \text{REV}_{\text{Idler}} = 3.291 \times 10^7$$

a := 3    For ball bearings, Shigley's, pg. 554

$$C_{10} := F_{\text{bearing2}} \cdot \left( \frac{\text{REVS}_{\text{total}}}{10^6} \right)^{\frac{1}{a}} = 51.002 \cdot \text{lbf} \quad \text{Catalog Rating Needed Shigley's Eqn (11-3)}$$

$$\text{FOS}_{85} := \frac{F_{\text{max85}}}{C_{10}} \cdot 3.0 = 7.235$$

## Caster Calculations

281

$$F_{SRFmax} := 110bf$$

$$F_{FCdes} := 100bf$$

$$F_{SCdes} := 73bf$$

$$F_{RCmax} := 53bf$$

$$FOS_{00013FMEA} := \frac{F_{SRFmax}}{F_{FCdes}} \cdot 3.0 = 3.3$$

$$F_{FootCaster} := 52.3bf$$

Wlb from analysis

$$F_{FootCasterMax} := 100bf$$

$$FOS_{00039FMEA} := \frac{F_{FootCasterMax}}{F_{FootCaster}} \cdot 3.0 = 5.7$$



## Fixed Bearing and Lead Screw Calculations

282

$$F_{\text{screw}} := 510\text{bf}$$

$$F_{\text{max}} := 902\text{kgf} \quad \text{Dynamic load rating of bearing and screw}$$

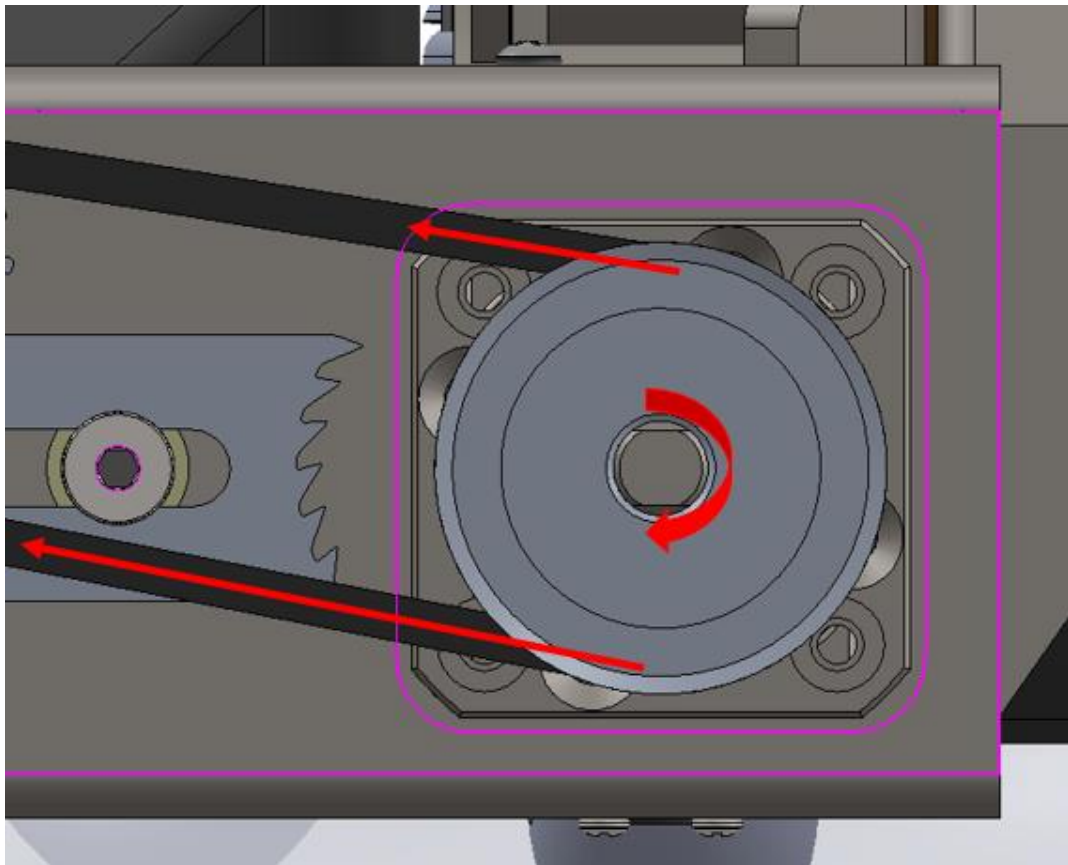
$$\text{FOS}_{\text{Screw}} := \frac{F_{\text{max}}}{F_{\text{screw}}} = 3.899$$

$$d_{\text{Force}} := 0.7\text{lin} \quad \text{Distance from "Fixed constraint" to center of belt force}$$

Right screw is the worst case

$$T_{\text{belt}} := 50\text{bf} \quad \text{Max belt tension}$$

$$\text{PD}_{\text{pulley}} := 1.378\text{n} \quad \text{Pulley pitch diameter}$$



$$M_{\text{Screw}} := \frac{T_{\text{belt}}}{2} \cdot \frac{PD_{\text{pulley}}}{2} = 17.225 \text{ in}\cdot\text{lb}$$

$$PR := \frac{PD_{\text{pulley}}}{2} = 0.689 \text{ in}$$

$$\sigma_{\text{max}} := 21437 \text{ psi}$$

$$\sigma_{yA36} := 36300 \text{ psi} \quad \text{Yield stress of A36}$$

$$S_{eA36} := \frac{\sigma_{yA36}}{2} \quad \text{Endurance limit}$$

$$FOS_{\text{fatigue}} := \frac{S_{eA36}}{\sigma_{\text{max}}} \cdot 3.0 = 2.541$$

# Weld Analysis on Fixed Bearing Standoff

### Resources:

Shigley's Mechanical Engineering Design, Eighth Edition  
Richard G. Budynas, J. Keith Nisbett  
2008 McGraw Hill, New York, NY

Nominal Weld Stress  
Equation (9-1), Tables (9-3), (9-4)  
Pgs. 460, 472

### Assumptions:

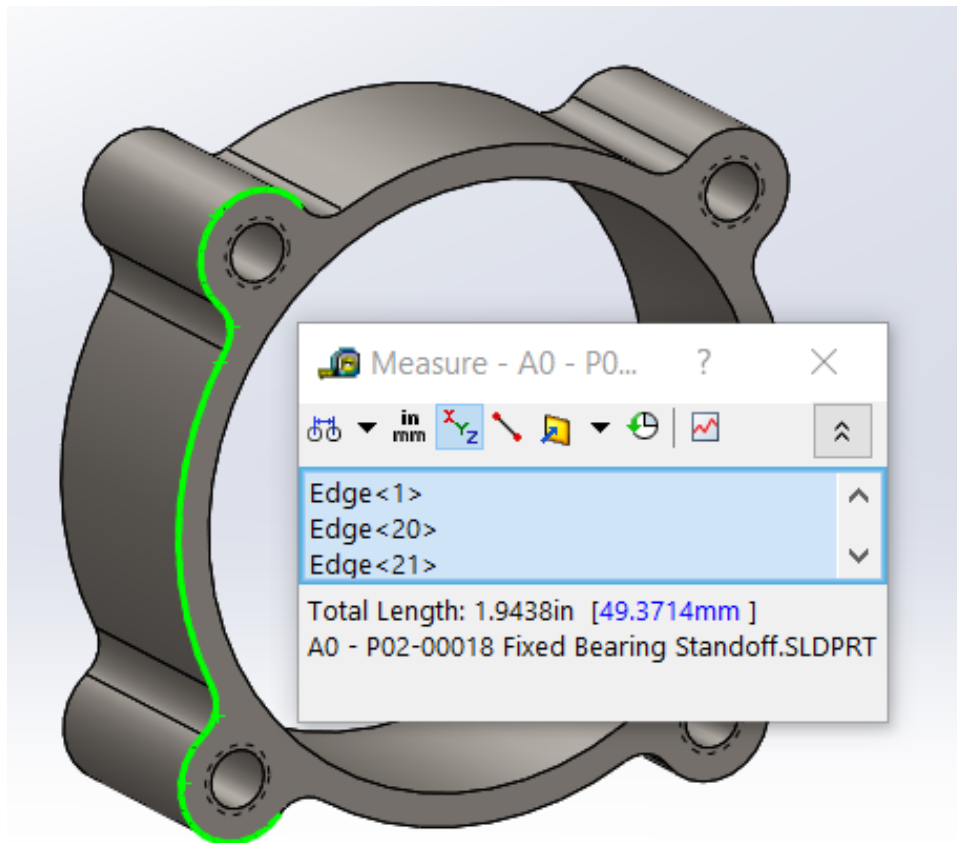
Perfect load transfer from standoff to other chassis components  
Welds only applied to regions under the vertical sides of the chassis side rails  
AWS Electrode: E60xx

$$\sigma_{yWeld} := 50\text{ksi}$$

Table (9-3)

$$\sigma_{maxWeld} := 0.3\sigma_{yWeld} = 15\text{ksi}$$

Shear type loading, Table (9-4)



$$F_{\text{screw}} := 510 \text{bf}$$

Max axial load per screw

$$P := 2 \cdot 1.94 \text{in}$$

Perimeter (total length) of weld

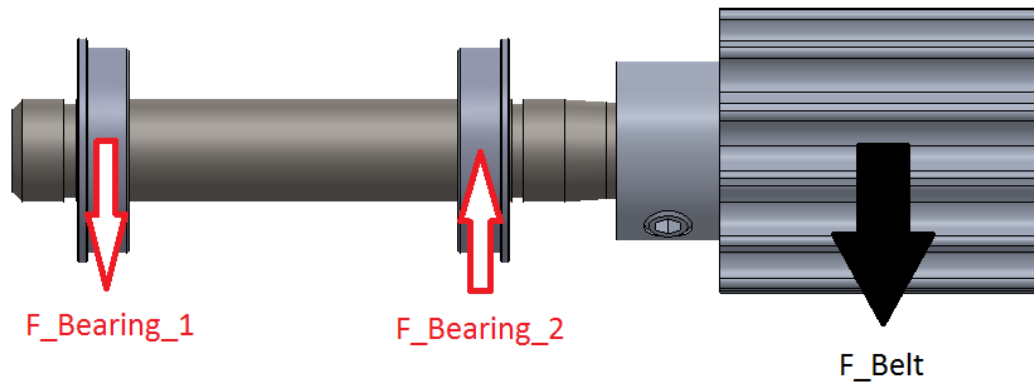
$$h := 0.062 \text{in}$$

$$\sigma := \frac{F_{\text{screw}}}{h \cdot P} = 2.12 \text{ksi}$$

$$\text{FOS} := \frac{\sigma_{\text{maxWeld}}}{\sigma} = 7.075$$

## Grooved Pulley Shaft Analysis

286



$$T_{\text{Belt}} := 50\text{ lbf}$$

$$F_{\text{Belt}} := 2 \cdot T_{\text{Belt}} \cdot \sin(4.5\text{ deg}) = 7.846\text{ lbf}$$

Solve for reaction force  $F_{\text{bearing}_2}$  because it will be the largest

$$F_{\text{Bearing}_2} := \frac{F_{\text{Belt}} \cdot (1.056 - 0.0625 + 0.105 + 0.79)}{(1.056 - 0.125)} = 15.915\text{ lbf}$$

From FEA

$$\sigma_{\text{maxFEA}} := 9872\text{ psi}$$

$$\sigma_{y12L14} := 6020\text{ psi}$$

$$S_e := 0.5 \cdot \sigma_{y12L14}$$

$$FOS_{\text{infiniteLife}} := 3.0 \cdot \frac{S_e}{\sigma_{\text{maxFEA}}} = 9.147$$

# Leg Attachment Bracket Weld Analysis

## Resources:

Shigley's Mechanical Engineering Design, Eighth Edition  
Richard G. Budynas, J. Keith Nisbett  
2008 McGraw Hill, New York, NY

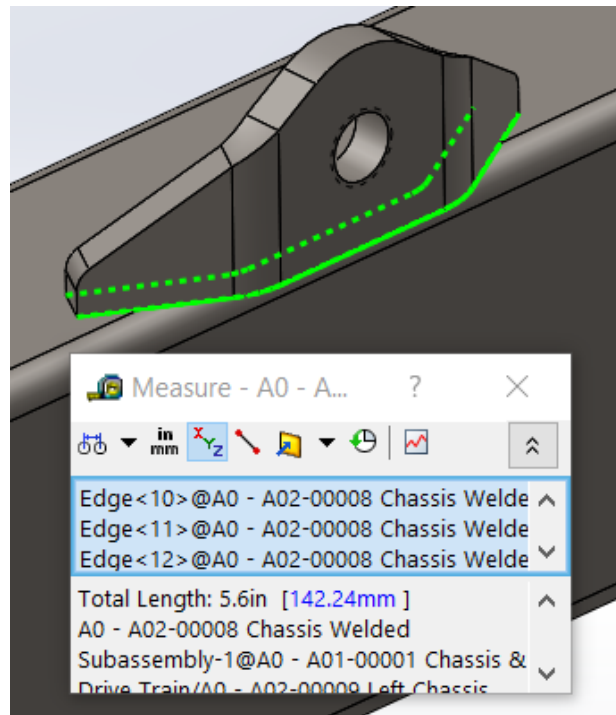
Nominal Weld Stress  
Equation (9-1), Tables (9-3), (9-4)  
Pgs. 460, 472

## Assumptions:

AWS Electrode: E60xx  
Entire load is in worst case type (shear)  
Tubing is SAE1018 CDS (Cold Drawn Seamless)  
Bracket is SAE1018 CD  
Uniform Cyclic Loading  
Loading is in pure shear

$$\sigma_{yWeld} := 50\text{ksi} \quad \text{Table (9-3)}$$

$$\sigma_{maxWeld} := 0.4\sigma_{yWeld} = 20\text{ksi} \quad \text{Shear type loading, Table (9-4)}$$



$$S_{ut1018} := 64 \text{ksi}$$

$$h := 0.062 \text{in}$$

$$L_1 := \frac{5.6 \text{in}}{2} = 2.8 \text{in}$$

$$N_{cyc} := 20 \cdot 250 \cdot 10 = 5 \times 10^4$$

Number of loading cycles: 20x a day for  
250 days a year for 10 years.

$$S'_e := 0.5 \cdot S_{ut1018}$$

Endurance limit, Eqn (6-8)

$$A_1 := 5.6 \text{in} \cdot 0.707 h$$

$$a := 2.7 \quad b := -0.265$$

Table (6-2)

$$k_a := a \cdot \left( S_{ut1018} \cdot \frac{1}{\text{ksi}} \right)^b$$

Eqn (6-19)

$$k_b := 1$$

Eqn (6-21), (Uniform shear stress)

$$k_c := 0.59$$

Eqn (6-26), (Shear)

$$k_d := 1$$

$$k_e := 1$$

$$k_f := 1$$

$$S_e := k_a \cdot k_b \cdot k_c \cdot k_d \cdot k_e \cdot k_f \cdot S'_e = 16.933 \text{ksi}$$

$$F_{max} := 523 \text{lbf}$$

Max of all F2aC, F2bC Loads

$$F_{min} := 0 \text{lbf}$$

$$F_m := \frac{F_{max} + F_{min}}{2} = 261.5 \text{lbf}$$

Pg 292, Budynas

$$F_a := \left| \frac{F_{max} - F_{min}}{2} \right| = 261.5 \text{lbf}$$

$$k_{fs} := 2.0$$

Table (9-5), (T-butt joint)

$$\tau'_a := \frac{k_{fs} \cdot F_a}{A_1} = 2.131 \cdot \text{ksi}$$

Pg 478

$$\tau'_m := \frac{k_{fs} \cdot F_m}{A_1} = 2.131 \cdot \text{ksi}$$

$$n_f := \frac{1}{\frac{\tau'_a}{S_e} + \frac{\tau'_m}{0.4 \cdot S_{ut1018}}} = 4.783$$

Table (6-6), pg. 299, Modified Goodman

Minimum safety factor for infinite life

$$\tau_{\max} := \frac{F_{\max}}{0.707 \cdot h \cdot 2 \cdot L_1} = 2.131 \cdot \text{ksi}$$

$$\text{FOS} := \frac{\sigma_{\max \text{Weld}}}{\tau_{\max}} = 9.387$$

Because  $\text{FOS} > n_f$  we conclude that the design is justified for infinite life.

By normalizing the  $n_f$  value as 3 the FMEA FOS can be looked at as:

$$\text{FOS}_{\text{FMEA}} := \frac{\text{FOS}}{n_f} \cdot 3 = 5.887$$



# Main Bearing Drive Shaft Analysis

$$\alpha := 45\text{deg} \qquad \text{PD}_{\text{gear}} := 1\text{in} \qquad \text{PD}_{\text{pulley}} := 1.378\text{in}$$

$$\text{PA} := 14.5\text{deg} \qquad \text{T}_{\text{belt}} := 50\text{lbf}$$

$$\text{arm}_{\text{gear}} := \frac{\text{PD}_{\text{gear}}}{2} \cdot \cos(\text{PA})$$

$$\text{F}_{\text{gear}} := \frac{\text{T}_{\text{belt}} \cdot \frac{\text{PD}_{\text{pulley}}}{2}}{\frac{\text{PD}_{\text{gear}}}{2} \cdot \cos(\text{PA})} = 71.167\text{lbf}$$

$$a_1 := \left( .6155 - \frac{.3125}{2} \right) \text{in}$$

$$-F_{\text{gear}} \cdot \sin(\text{PA}) = -17.819\text{lbf}$$

$$b_1 := \left( 1.31 - .25 - \frac{.3125}{2} \right) \text{in}$$

$$F_{\text{gear}} \cdot \cos(\text{PA}) = 68.9\text{lbf}$$

$$c_1 := \left( 2.12 - \frac{.3125}{2} - .081 \right) \text{in}$$

$$F_{\text{bearingAx}} := \frac{F_{\text{gear}} \cdot \sin(\text{PA}) \cdot a_1 - \text{T}_{\text{belt}} \cdot \cos(\alpha) \cdot c_1}{b_1} = -64.6\text{lbf}$$

$$F_{\text{bearingBx}} := F_{\text{gear}} \cdot \sin(\text{PA}) - \text{T}_{\text{belt}} \cdot \cos(\alpha) - F_{\text{bearingAx}} = 47.063\text{lbf}$$

$$F_{\text{bearingAy}} := \frac{-(\text{T}_{\text{belt}} \cdot \sin(\alpha) \cdot c_1 + F_{\text{gear}} \cdot \cos(\text{PA}) \cdot a_1)}{b_1} = -108.667\text{lbf}$$

$$F_{\text{bearingBy}} := -(F_{\text{gear}} \cdot \cos(\text{PA}) + \text{T}_{\text{belt}} \cdot \sin(\alpha) + F_{\text{bearingAy}}) = 4.41\text{lbf}$$

$$M_{\text{belt}} := \text{T}_{\text{belt}} \cdot \frac{\text{PD}_{\text{pulley}}}{2} = 34.45\text{in} \cdot \text{lbf}$$

$$F_{\text{bearingA}} := \sqrt{F_{\text{bearingAx}}^2 + F_{\text{bearingAy}}^2} = 126.418\text{lbf}$$

$$F_{\text{bearingB}} := \sqrt{F_{\text{bearingBx}}^2 + F_{\text{bearingBy}}^2} = 47.269 \text{ lbf}$$

$$F_{\text{Amax}} := 633 \text{ lbf} \quad \text{Max dynamic load on bearing A, P00-00035}$$

$$F_{\text{Bmax}} := 330 \text{ lbf} \quad \text{Max dynamic load on bearing B, P00-00036}$$

$$\text{FOS}_A := \frac{F_{\text{Amax}}}{F_{\text{bearingA}}} = 5.023$$

$$\text{FOS}_B := \frac{F_{\text{Bmax}}}{F_{\text{bearingB}}} = 6.981$$

Scale FOS for FMEA, because max dynamic load allowed is considered infinite life load and can be considered to be the load where the FOS in the FMEA = 3.0

$$\text{FOS}_{\text{AFMEA}} := \frac{F_{\text{Amax}}}{F_{\text{bearingA}}} \cdot 3.0 = 15.069$$

$$\text{FOS}_{\text{BFMEA}} := \frac{F_{\text{Bmax}}}{F_{\text{bearingB}}} \cdot 3.0 = 20.944$$

### Sanity Check:

$$-F_{\text{gear}} \cdot \sin(\text{PA}) = -17.819 \text{ lbf}$$

$$F_{\text{gear}} \cdot \cos(\text{PA}) = 68.9 \text{ lbf}$$

Check values with pulley constraint forces in FEA Model

### Femap Output:

```
Node 51732
Output Set      1 : NX NASTRAN Case 1
Value =        -17.7365 | Output Vector      52 : T1 Constraint Force
Value =         68.4331 | Output Vector      53 : T2 Constraint Force
```

$$T_{\text{belt}} \cdot \sin(\alpha) = 35.355 \text{ lbf}$$

$$T_{\text{belt}} \cdot \cos(\alpha) = 35.355 \text{ lbf}$$

Check values with gear constraint forces in FEA Model

Femap Output:

```
Node 51730
Output Set      1 : NX NASTRAN Case 1
Value =        35.2365 | Output Vector      52 : T1 Constraint Force
Value =        35.8669 | Output Vector      53 : T2 Constraint Force
```

### *Endurance Limit*

$$\sigma_{y1144} := 89900 \text{ psi}$$

$$\sigma_{\text{maxFEA}} := 33360 \text{ psi}$$

$$S_e := 0.5 \cdot \sigma_{y1144} = 4.495 \times 10^4 \cdot \text{psi}$$

$$\text{FOS}_{\text{infinteLife}} := 3.0 \cdot \frac{S_e}{\sigma_{\text{maxFEA}}} = 4.042$$

# Miscellaneous Hardware Calculations

## P00-00088 Spring 9654K211

$$L_{\min} := 2.25\text{in}$$

$$L_{\max} := 3.4\text{in}$$

### Steel Extension Spring

Zinc-Plated, 2.25" Length, .375" OD, .048" Wire



Packs of 3

In stock  
\$3.36 per pack of 3  
9654K211

**ADD TO ORDER**

Spring OD	0.375"
Wire Diameter	0.048"
Extended Length	3.4"
Load, lbs.	
Minimum	2.38
Maximum	9.53
Rate	6.22 lbs./inch
Additional Specifications	Zinc Plated with Loop Ends 2.25" Overall Length
RoHS	Compliant

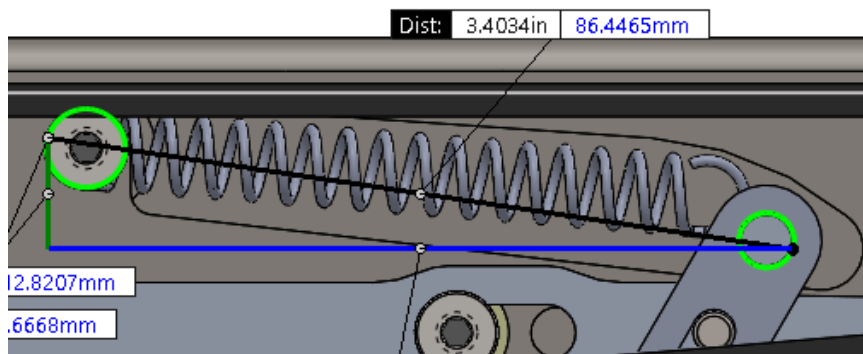
Min stretch (Spec):

$$L_{DT\min} := 2.52\text{in}$$

Max stretch (Spec):

$$L_{DT\max} := 3.4\text{in}$$

## Belt Safety System

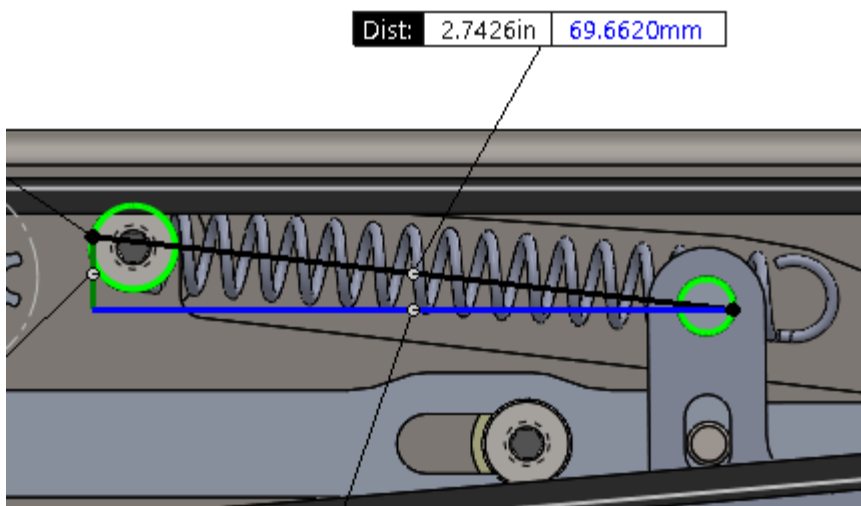


$$\text{Stretch}_{\text{maxBelt}} := 3.403\text{n}$$

Max potential stretch on spring in belt safety system

$$\text{FOS}_{\text{OverStretchBelt}} := 3.0 \frac{L_{\text{DTmax}}}{\text{Stretch}_{\text{maxBelt}}} = 2.997$$

FOS against overstretching spring in belt safety system



$$\text{Stretch}_{\text{minBelt}} := 2.74\text{n}$$

Min potential stretch on spring in belt safety system

$$\text{Stretch}_{\text{minBelt}} > L_{\text{DTmin}} = 1$$

Is the minimum stretched length of the spring at least as long as the spring? Yes

### Back Lock System

$$\text{Stretch}_{\text{maxBack}} := 3.3\text{n}$$

Max potential stretch on spring in back lock system

$$\text{FOS}_{\text{OverStretchBack}} := 3.0 \frac{L_{\text{DTmax}}}{\text{Stretch}_{\text{maxBack}}} = 3.091$$

FOS against overstretching spring in back lock system

$$\text{Stretch}_{\text{minBack}} := 2.74\text{n}$$

Min potential stretch on spring in back lock system

$$\text{Stretch}_{\text{minBack}} > L_{\text{DTmin}} = 1$$

Is the minimum stretched length of the spring in the back lock system at least as long as the spring? Yes

$$\text{Rating}_{\text{Ahr}} := \frac{.12\text{hp}}{18\text{V}} \cdot 16\text{sec} = 0.022 \text{ A}\cdot\text{hr}$$

Approximation of amp-hr needed to raise system, more refined in code.

$$\text{Batt}_{\text{Ahr}} := 1.5\text{A}\cdot\text{hr}$$

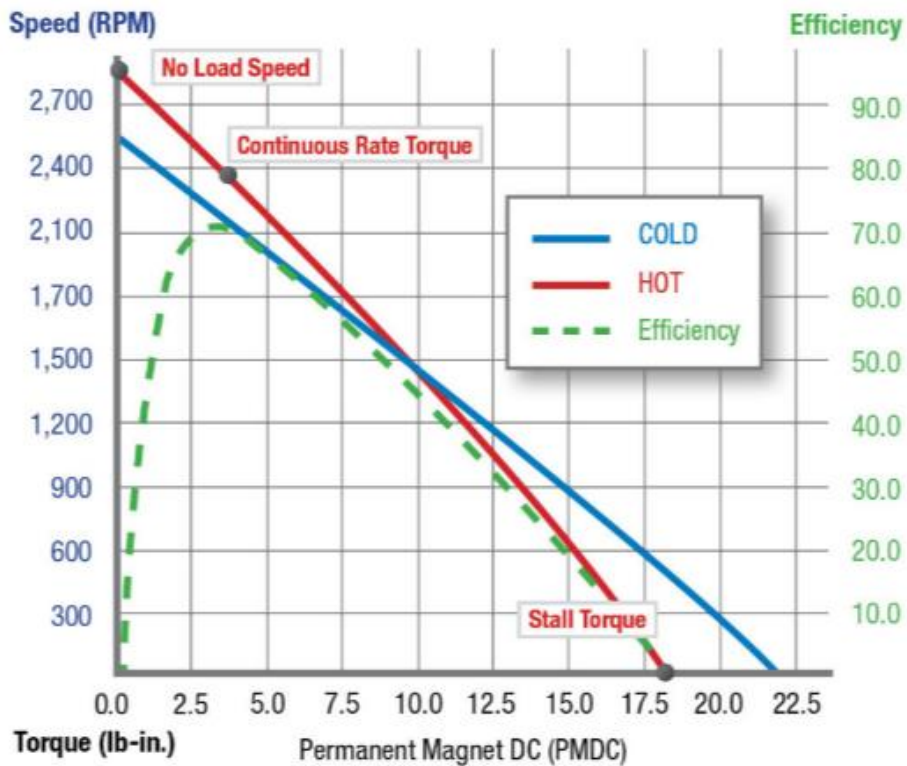
$$1\text{hp} = 745.7\text{W}$$

$$\epsilon_{\text{sys}} := 0.5$$

$$N_{\text{cycONcharge}} := \epsilon_{\text{sys}} \cdot \frac{\text{Batt}_{\text{Ahr}}}{\text{Rating}_{\text{Ahr}}} = 33.945$$

$$T_{\text{maxDrill}} := \frac{450}{1500} \cdot (450\text{in}\cdot\text{lbf}) = 135\text{in}\cdot\text{lbf}$$

Max torque producible by drill when set on the fast setting (1500 RPM). The low gear setting produces a max torque of 450 in-lbf and a no-load speed of 450 RPM.



Peak efficiency approximately what percentage of max torque?

$$T_{\text{maxEffChart}} := 3.5$$

$$T_{\text{maxChart}} := 18$$

$$X_{\text{maxEff}} := \frac{T_{\text{maxEffChart}}}{T_{\text{maxChart}}} = 0.194$$

$$T_{\text{maxEff}} := X_{\text{maxEff}} T_{\text{maxDrill}} = 26.25 \text{ in}\cdot\text{lbf}$$

Use this value in code along with a maximum efficiency of 70%

**Resources:**

Material Properties: [www.matweb.com](http://www.matweb.com)

Shigley's Mechanical Engineering Design, Eighth Edition  
 Richard G. Budynas, J. Keith Nisbett  
 2008 McGraw Hill, New York, NY

Pure Shear  
 Equation (3-23)  
 Pgs. 84

**Assumptions:**

Load line of action passes through the centroid of the pin's cross-section  
 Pin is straight and homogenous  
 Load applied far from the end

*P00-00066: 0.25 Dia x 0.875 L Clevis Pin*

$$D_{66} := 0.25 \text{ in}$$

$$F_{9\text{MAX}} := 195.5 \text{ bf}$$

$$A_{\text{XS}66} := \pi \cdot \left( \frac{D_{66}}{2} \right)^2$$

$$\tau_{66} := \frac{F_{9\text{MAX}}}{2A_{\text{XS}66}} = 1991.3 \text{ psi} \quad \text{Shigley, Eqn (3-23); double shear}$$

Material: 18-8 Stainless Steel  
 Properties used for Carlson 303 Austenitic Stainless Steel

<http://www.matweb.com/search/DataSheet.aspx?MatGUID=ff2edc95955a4d cc9ff1b816da80606a&ckck=1>

$$\sigma_{\text{Y}303} := 35 \text{ ksi}$$

$$\text{FOS}_{66} := \frac{\sigma_{\text{Y}303}}{\tau_{66}} = 17.576$$

*P00-00067: 0.187 Dia x 0.625 L Clevis Pin*

$$D_{67} := 0.187 \text{ in}$$

$$F_{\text{D}\text{MAX}} := 56.6 \text{ bf}$$



$$A_{XS67} := \pi \cdot \left( \frac{D_{67}}{2} \right)^2$$

$$\tau_{67} := \frac{F_{DMAX}}{2A_{XS67}} = 1030.4 \text{ psi} \quad \text{Shigley, Eqn (3-23); double shear}$$

Material: 18-8 Stainless Steel

Properties used for Carlson 303 Austenitic Stainless Steel

<http://www.matweb.com/search/DataSheet.aspx?MatGUID=ff2edc95955a4d cc9ff1b816da80606a&ckck=1>

$$FOS_{67} := \frac{\sigma_{Y303}}{\tau_{67}} = 33.967$$

*P00-00092, P01-00001: 0.375 Dia x 1.31 L Clevis Pin*

$$D_{92} := 0.375 \text{ in} \quad F_{3MAX} := 513 \text{ bf}$$

$$A_{XS92} := \pi \cdot \left( \frac{D_{92}}{2} \right)^2$$

$$\tau_{92} := \frac{F_{3MAX}}{2A_{XS92}} = 2322.4 \text{ psi} \quad \text{Shigley, Eqn (3-23); double shear}$$

Material: 18-8 Stainless Steel

Properties used for Carlson 303 Austenitic Stainless Steel

<http://www.matweb.com/search/DataSheet.aspx?MatGUID=ff2edc95955a4d cc9ff1b816da80606a&ckck=1>

$$FOS_{92} := \frac{\sigma_{Y303}}{\tau_{92}} = 15.071$$



$$D_{17} := 0.375 \text{ in}$$

$$F_{2aCmax} := 523 \text{ lbf}$$

$$F_{2bCmax} := 243 \text{ lbf}$$

$$A_{XS17} := \pi \cdot \left( \frac{D_{92}}{2} \right)^2$$

Cross sectional area of bolt under shear

$$\tau_{17} := \frac{F_{2aCmax}}{A_{XS17}} = 4735.3 \text{ psi}$$

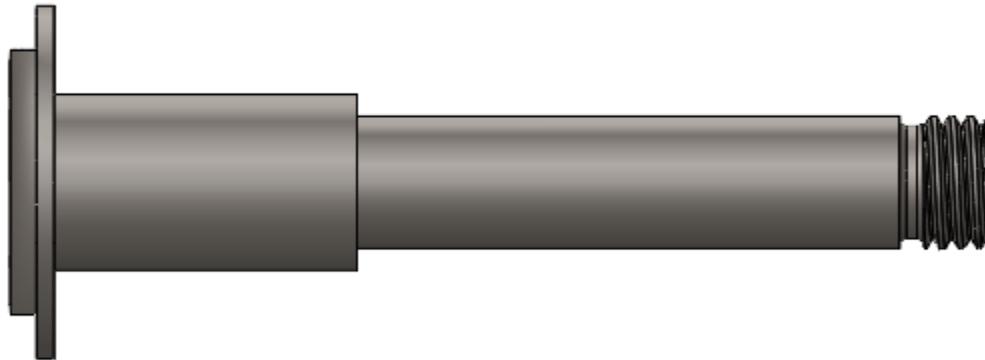
Shigley, Eqn (3-23); single shear

Material: AISI 1340 Steel, normalized at 870°C (1600°F), air cooled, 25 mm (1 in.) round

<http://www.matweb.com/search/DataSheet.aspx?MatGUID=77349059708a4766b1393b2e578b5fba&ckck=1>

$$\sigma_{Y1340} := 80.9 \text{ ksi}$$

$$FOS_{17} := \frac{\sigma_{Y1340}}{\tau_{17}} = 17.084$$



Double Shear Loads

$$F_{4Amax} := 340bf$$

Single Shear Loads

$$F_{2aSmax} := 472bf \quad \text{Largest}$$

$$F_{2bSmax} := 231bf$$

$$F_{5Amax} := 129bf$$

$$D_{25} := 0.375in$$

$$A_{XS25} := \pi \cdot \left( \frac{D_{92}}{2} \right)^2$$

Cross sectional area of bolt section under shear

$$\tau_{25} := \frac{F_{2aSmax}}{A_{XS25}} = 4273.6 \text{ psi}$$

Shigley, Eqn (3-23); single shear

Material: AISI 1340 Steel, normalized at 870°C (1600°F), air cooled, 25 mm (1 in.) round

<http://www.matweb.com/search/DataSheet.aspx?MatGUID=77349059708a4766b1393b2e578b5fba&ckck=1>

$$FOS_{25} := \frac{\sigma_{Y1340}}{\tau_{25}} = 18.93$$

*P00-00057*

$n_{57} := 6$	Number of screws to support the load
$S_{\text{proof12.9}} := 970\text{MPa}$	Proof strength of metric property class 12.9 See pg. A-8 of Fastenal Technical Reference Guide
$A_{M4} := 8.78\text{mm}^2$	Thread Tensile Stress Area of M4-0.7 screw See pg. A-7 of Fastenal Technical Reference Guide
$F_{\text{screw}} := 510\text{bf}$	Max axial load on screw set

$$\sigma_{57} := \frac{F_{\text{screw}}}{n_{57} \cdot A_{M4}}$$

$$\text{FOS}_{57} := \frac{S_{\text{proof12.9}}}{\sigma_{57}} = 22.5$$

*P00-00064*

$n_{64} := 6$	Number of screws to support the load
$S_{\text{proofF835}} := 145\text{ksi}$	Proof strength of an ASTM F835 grade screw See pg. A-1 of Fastenal Technical Reference Guide
$A_{64} := 0.0318\text{in}^2$	Thread Tensile Stress Area of 1/4-20 screw See pg. A-7 of Fastenal Technical Reference Guide
$F_{9\text{screwYfront}} := 69\text{bf}$	Max axial load on screw front screw of back stop slider

$$\sigma_{64} := \frac{F_{9\text{screwYfront}}}{n_{64} \cdot A_{64}}$$

$$\text{FOS}_{64} := \frac{S_{\text{proofF835}}}{\sigma_{64}} = 401$$

*P00-00042 Self Tap 6/32 PH Screw*

Fastenal Technical Reference Guide

Pg. 2, use tensile stress area; shear strength is 60% of ultimate tensile strength

Pg. 3, use minimum tensile strength of low carbon steels at 60,000 psi

Pg. A-7, tensile stress area.

$$S_{1\text{shear}} := 0.6 \cdot 60\text{ksi} = 36\text{ksi}$$

Single shear strength of low carbon screw

$$A_{6.32} := 0.00909\text{in}^2$$

Tensile stress area of a 6-32 screw

$$F_{\text{hangScrew.MAX}} := 81.25\text{bf}$$

$$v_{00042} := \frac{F_{\text{hangScrew.MAX}}}{A_{6.32}} = 8.938 \times 10^3 \cdot \text{psi}$$

$$\text{FOS}_{42} := \frac{S_{1\text{shear}}}{v_{00042}} = 4.03$$

## Seat Bar Assembly: Hand Calcs for Applied Forces

303

$$X \quad \begin{bmatrix} -(.191 + .25) & 1.43 + .25 \\ 1 & -1 \end{bmatrix}^{-1} \cdot \begin{pmatrix} 0 \\ 61.7 \end{pmatrix} = \begin{pmatrix} 83.661 \\ 21.961 \end{pmatrix}$$

$$Y \quad \begin{bmatrix} -(.191 + .25) & 1.43 + .25 \\ 1 & -1 \end{bmatrix}^{-1} \cdot \begin{pmatrix} 0 \\ 12.6 \end{pmatrix} = \begin{pmatrix} 17.085 \\ 4.485 \end{pmatrix}$$

$$\begin{pmatrix} -0.25 & 1.55 + .25 \\ 1 & -1 \end{pmatrix}^{-1} \cdot \begin{pmatrix} 0 \\ 446.9 \end{pmatrix} = \begin{pmatrix} 518.981 \\ 72.081 \end{pmatrix}$$

$$\begin{pmatrix} -0.25 & 1.55 + .25 \\ 1 & -1 \end{pmatrix}^{-1} \cdot \begin{pmatrix} 0 \\ 91.1 \end{pmatrix} = \begin{pmatrix} 105.794 \\ 14.694 \end{pmatrix}$$

Guess for the length of the through hole for the front leg pivot

$$b_2 := .75$$

X Values of F2aS and F2bS joints

$$F_{2aS} := 446.9 \quad F_{2bS} := 61.7$$

$$F_{9x} := 195 \quad F_{4Ax} := 332.1$$

$$\begin{pmatrix} F_{2bS1} \\ F_{2bS2} \end{pmatrix} := \begin{pmatrix} -0.3125 & 1.478 + 0.3125 \\ 1 & -1 \end{pmatrix}^{-1} \cdot \begin{pmatrix} 0 \\ F_{2bS} \end{pmatrix} = \begin{pmatrix} 74.746 \\ 13.046 \end{pmatrix}$$

$$\begin{pmatrix} F_{2aS1} \\ F_{2aS2} \end{pmatrix} := \begin{pmatrix} -0.3125 & b_2 + 0.3125 \\ 1 & -1 \end{pmatrix}^{-1} \cdot \begin{pmatrix} 0 \\ F_{2aS} \end{pmatrix} = \begin{pmatrix} 633.108 \\ 186.208 \end{pmatrix}$$

$$b_1 := \frac{F_{2aS2} \cdot b_2 + (F_{9x} + F_{4Ax}) \cdot 0.603 - F_{2bS1} \cdot 1.478}{F_{2aS1} - F_{2aS2}} = 0.777$$

## Slider Caster & Brake Loads

304

$$X_{TOT} := 30.8' \quad W_t := 150 \quad d_{Brake} := 13.4'$$

$$W_{sys} := 50 \quad d_{SC} := 42.6'$$

$$\begin{pmatrix} F_{Brake} \\ F_{SC} \end{pmatrix} := \begin{pmatrix} d_{Brake} & d_{SC} \\ 1 & 1 \end{pmatrix}^{-1} \cdot \begin{bmatrix} (W_t + W_{sys}) \cdot X_{TOT} \\ W_t + W_{sys} \end{bmatrix}$$

$$F_{Brake} = 81.248$$

$$F_{SC} = 118.752$$

## Appendix H. Failure Mode and Effects Analysis (FMEA) Table

**Table 12: Complete FMEA table, segmented into 3 columnar sections**

Column 1

BACKGROUND				
LINE NUMBER	PART/ASSEMBLY NUMBER	PART/ASSEMBLY DESCRIPTION	CONTEXT USED	FAILURE MODE
1	A01-00001	Chassis & Drive Train	Individual Components and subassemblies analyzed	NA
2	A01-00002	Tension Pulley Arm Subassembly	Individual Components and subassemblies analyzed	NA
3	A01-00003	Bridge Subassembly	Individual Components and subassemblies analyzed	NA
4	A01-00004	Back Rest Frame Tube Welded Subassembly	Main Backrest Structure	Yielding
5	A01-00005	Back Lock Slider Subassembly	Individual Components and subassemblies analyzed	NA
6	A01-00006	Limit Switch Subassembly	Individual Components and subassemblies analyzed	NA
7	A01-00007	Brake Subassembly	Individual Components and subassemblies analyzed	NA
8	A01-00008	Recline Limit Actuator Subassembly	Individual Components and subassemblies analyzed	NA
9	A01-00009	Slider Subassembly	Individual Components and subassemblies analyzed	NA
10	A01-00010	Backrest & Headrest Subassembly	Used just for weld analysis	Weld failure on backrest support bracket
11	A01-00011	Back Rest Subassembly	Individual Components and subassemblies analyzed	NA
12	A01-00012	Ball Screw Subassembly	Individual Components and subassemblies analyzed	NA
13	A01-00014	Footrest Caster Bracket (Bushing, Washer, Screw) Subassembly	Individual Components and subassemblies analyzed	NA
14	A01-00015	Full Backrest Subassembly	Individual Components and subassemblies analyzed	NA
15	A01-00016	Footrest Subassembly	Individual Components and subassemblies analyzed	NA
16	A01-00017	Footrest Strut Subassembly	Individual Components and subassemblies analyzed	NA
17	A01-00018	Back Lock Bar Subassembly	Individual Components and subassemblies	NA



			analyzed	
18	A01-00019	Left Footrest Caster Bracket Subassembly	Individual Components and subassemblies analyzed	NA
19	A01-00020	Right Footrest Caster Bracket Subassembly	Individual Components and subassemblies analyzed	NA
20	A01-00021	Left Footrest Bracket Subassembly	Individual Components and subassemblies analyzed	NA
21	A01-00022	Right Footrest Bracket Subassembly	Individual Components and subassemblies analyzed	NA
22	A01-00023	Left Footrest Attachment Bracket Subassembly	Individual Components and subassemblies analyzed	NA
23	A01-00024	Right Footrest Attachment Bracket Subassembly	Individual Components and subassemblies analyzed	NA
24	A01-00025	Makita Drill Assembly with Gear	Individual Components and subassemblies analyzed	NA
25	A01-00026	Leg & Bearing Subassembly	Individual Components and subassemblies analyzed	NA
26	A01-00027	Push Rod Subassembly	Individual Components and subassemblies analyzed	NA
27	A01-00028	Pulley Wheel Subassembly	Individual Components and subassemblies analyzed	NA
28	A02-00001	Welded Back Bar Subassembly	Main Backrest Structure	Yielding
29	A02-00002	Main Caster Bracket Welded Subassembly	Main casters	Yielding
30	A02-00003	Welded Foot Rest Subassembly	Footrest	Yielding
31	A02-00004	Welded Foot Rest Strut Subassembly	Footrest	Yielding
32	A02-00005	Bridge Bracket Welded Subassembly	Bridge assembly	Yielding
33	A02-00006	Belt Safety Gear Welded Subassembly	Drive train	None Identified
34	A02-00007	Drive Train Rail Welded Subassembly	Welded chassis	Weld failure on fixed bearing standoff
35	A02-00008	Chassis Welded Subassembly	Main frame	Weld failure
36	A02-00009	Left Chassis Rail Welded Subassembly	Main frame	Weld failure
37	A02-00010	Right Chassis Rail Welded Subassembly	Mirror of A02-00009	NA
38	A02-00012	Left Welded Seat Bar Subassembly	Seat member	Weld failure
39	A02-00013	Right Welded Seat Bar Subassembly	Mirror of A02-00012	NA
40	A02-00014	Backrest Frame Welded Subassembly	Backrest Subassembly	Stress Yielding
41	A02-00015	Slider Welded Subassembly	Main Kinematics	Weld failure at rear end of the slider

42				Caster bracket yielding
43	A02-00016	Welded Backrest Frame Subassembly	Main Kinematics	Stress Yielding
44	P00-00001	Grade 5 0.25-20 Hex Nut	On P00-00059 shoulder bolts that hold P02-00010 belt safety pawls	Nut comes off
45			On P00-00059 shoulder bolt that holds P00-00088 tension pulley spring	Nut comes off
46	P00-00002	HTD 25mm WD x 1135mm PL Timing Belt	Main drive train system	Belt breaks
47	P00-00003	#6 x 0.625L Flat Head Wood Screw	Securing of the Delrin slide strips on the backrest	Screw backs out, shears off,
48	P00-00004	FK10 Fixed Bearing Support	Fixed Bearing for Lead Screws	Bearings break or seize
49	P00-00005	Roller Bearing 0.5ID 0.5L	Bearing on leg pivot points	Bearings break or seize
50	P00-00006	Thin 0.5-28 Nut	Nut backing up the gear on the Drill motor shaft	Nut comes loose
51	P00-00007	Leg Spacer 0.686OD 0.513ID 0.25L	Legs next to bearings	None Identified
52	P00-00013	Caster Assembly	Main casters on assembly	Casters bend
53	P00-00021	0.187 ID 0.500 OD 0.062L Nylon Washer	Spacing washers at backrest pivot point	Washer breaks, falls off
54			Spacer washer that laterally contains the back lock	Washer breaks, falls off
55	P00-00022	0.125 ID 0.500 OD 0.125L Nylon Washer	Slider washer for back lock bar	Washer breaks, falls off, or wears down
56	P00-00023	Ball Screw 900 mm	Main drive train system	Ball nut begins to slip
57			Main drive train system	Shaft fatigues at pulley attachment location
58	P00-00024	Ball Nut	Main drive train system	Ball nut begins to slip
59	P00-00025	0.252 ID 0.472 OD 0.059L Nylon Washer	On P00-00059 shoulder bolts that hold P02-00010 belt safety pawls	Washer breaks, falls off, or wears down
60	P00-00026	0.50D 0.257ID 0.375L Nylon Washer	Spacer washer for back tension bars	Washer breaks, falls off
61	P00-00027	0.433OD 0.256ID 0.22L Nylon Washer	Spacer washer for upper hole of back lock bar	Washer breaks, falls off
62	P00-00028	0.19ID 0.25OD 0.156L 0.49FD 0.062FT Nylon Flanged Washer	Bridge pivot pin	Washer breaks, falls off, or wears down
63	P00-00029	0.189ID 0.25OD 0.249L 0.5FD 0.062FT Nylon Flanged Washer	Back lock bar bushing that the track slides on	Washer breaks, falls off, or wears down
64	P00-00030	0.377 ID 0.563 OD 1.0 L Bushing	Main Bushing for push rods (both ends)	Become Sloppy
65	P00-00031	0.377 ID 0.563 OD 0.75 L Bushing	Main Bushing at Seat/backrest Interface	Become Sloppy
66	P00-00032	Snap Action Plunger Limit Switch	Limit for recline motion	Does not deactivate
67	P00-00033	8mm ID Flanged Bearing	Support bearing for lead screws	Bearings break or seize

68	P00-00034	Snap Action Roller Limit Switch	Limit for seat up motion	Does not deactivate
69	P00-00035	Flanged Bearing 0.375 bore	Support bearing for timing pulley drive shaft	Bearings break or seize
70	P00-00036	Flanged Ball Bearing 0.25 bore	Support bearing for timing pulley drive shaft	Bearings break or seize
71	P00-00037	Bronze Thrust Bearing 0.5ID 1.0OD 0.062T	Main leg, footrest and backrest thrust bearing	Wears thin
72	P00-00038	Bronze Thrust Bearing 0.375ID 0.75OD 0.125T	Additional seat/backrest pivot thrust bearing	Wears thin
73	P00-00039	Caster 100# 2in	Main casters on footrest	Casters bend
74	P00-00040	Lock Nut 2-56	Nut that secures all limit switches	Nut comes off
75	P00-00041	Acorn Nut 0.3125-18	Main Caster Nut	Nut comes off
76	P00-00042	Self-Tap PH 6-32 0.375L	Attachment of seat frame to seat support	Screw backs out, shears off,
77			Attachment of footrest bracket to seat frame	Screw backs out, shears off,
78	P00-00043	Black Oxide 18-8 Stainless Steel Flat Washer	Head rest attachments	None Identified
79	P00-00044	No. 8 Washer 0.75 OD	Footrest caster bracket	None Identified
80	P00-00045	Pan head wood screw #6 x 0.5L	Fasten seat to brackets and backrest to brackets	Screws pull out of wood
81	P00-00046	PH Screw 8-32 x 0.375L	Hold the back shroud to the pivot pin	Screw backs out
82	P00-00047	#8 Washer	Brake subassembly	None Identified
83	P00-00048	Studded Knob 10-32 x 0.75L	Head rest attachments	Loosen or fall out
84	P00-00049	Rubber Bumper 0.25 tall	Main Backrest resting pad	Breaks/falls apart under load conditions
85	P00-00050	Drill Bushing	Tension pulley subassembly	Wears out or seizes
86	P00-00051	Spring Pin	Footrest pivot lock	Post doesn't lock
87	P00-00052	Truss Head Screw 8-32 x 0.75L	Brake Pad through screw	Screw and standoff shears
88	P00-00053	Standoff 8-32 x 0.5L	Brake Pad through standoff	Screw and standoff shears
89	P00-00054	Acorn Nut 8-32	Brake Pad nut	Nut falls off
90	P00-00055	8-32 x 0.5L Socket Button Head	Footrest caster bracket	Screw backs out
91	P00-00056	0.25-20 x .3125 Socket Button Head	Recline limit actuator bumper	Screw backs out
92	P00-00057	M4x18 Socket Head	Hold ball nut to slider	Tensile failure, or backing out
93	P00-00058	6-32 x 0.31 Flat Head Screw	Hold spring pin on footrest bracket	Screw backs out
94	P00-00059	0.25DIA 0.25L Shoulder Bolt	Hold belt safety components and tensioner spring	None Identified
95	P00-00060	2-56 x 0.75 L Pan Head Screw	Screw that holds the limit switches	Shearing of screw
96	P00-00061	M5 Fender Washer	Front washer to drive gear	None Identified
97	P00-00062	#8 Fender Washer	Hold the back shroud to the pivot pin	None Identified

98	P00-00063	0.375-16 thin nut	Seat leg axle posts	Nut comes off
99	P00-00064	0.25-28 x 0.625 Socket Button Head	Screws for holding back stop carriage together	Shear or tensile failure
100	P00-00065	Actuator Bumper	Main actuation	Bumper does not actuate limit switches
101	P00-00066	0.25 Dia x 0.875 L Clevis Pin	Connection pin for backrest to back stop tension bars	Pin shears
102				Pin falls out
103	P00-00067	0.1875D x 0.625L Clevis Pin	Connection pin for backrest brackets to backrest support brackets	Pin shears
104				Pin falls out
105	P00-00068	#5 x .31 L Sheet Metal Screw	Hold Backrest bumper pads on	Screw comes out
106	P00-00069	2-56 x .1875 L Standoff	Standoff recline limit switches	None Identified
107	P00-00070	0.375 Shaft Retaining Ring	Retaining of main drive pulley axle in bearing	Gets rubbed away by bearing
108	P00-00071	0.25 ID Retaining Ring	Retaining of idler pulleys and shafts	Gets rubbed away by bearing or other mating surfaces
109	P00-00072	4-40 x 0.1875 Flat Head Undercut	Screws for mounting brakes to rear legs	Shear, or screw backs out
110	P00-00073	3in x 0.25DIA Aluminum Standoff	Pivot shaft for footrest brackets	None Identified
111	P00-00074	#2 Washer	Retention of limit switches	None Identified
112	P00-00075	0.187 Dia Press-on Retaining Ring	Holds washer/bushing on seat sides	Ring falls off
113	P00-00076	0.25DIA x 0.875L Pin	Pivot Pin for upper hole of back lock bar	Pin shears
114	P00-00077	0.1875 DIA x .4375L Pin	Slider pin for tension pulley arm	Pin comes out
115	P00-00078	0.1875 DIA x .375L Pin	Pivot pins for belt safety system components	Pin comes out
116	P00-00079	0.3125 Washer	Washer on caster posts	None Identified
117	P00-00080	19.1mm PD HTD Pulley for 15mm belt	Idler pulleys for ribbed side of belt	Pulley falls off
118	P00-00081	Hubless Spur Gear 1 in PD .375 bore	Main motor shaft to drive pulley axle	Gear slips on pulley shaft
119				Gears wear out, break teeth
120	P00-00082	#10 Tilobular Screw	Fasten bridge bracket to bridge	Screw shears or backs out
121	P00-00083	0.25-28 Square Nut	Holds back lock slider assembly together	Nut comes off
122	P00-00084	0.75 Internal Retaining Ring	Holds bearing in free end support	Ring falls out
123	P00-00085	0.25 ID .5 OD Flanged Ball Bearing	Support bearings for idler timing pulleys	Bearings break or seize
124	P00-00086	Bronze Bushing	Outer bushing of footrest caster bracket	None Identified
125	P00-00087	35mm PD Flanged HTD Pulley for 15mm Belt	Main drive and ball screw timing pulleys	Set screws loosen

126	P00-00088	Spring 9654K211	Back lock bar	Spring breaks or loses its spring
127			Tension pulley subassembly	Spring breaks or loses its spring
128			Tension pulley subassembly	Spring breaks
129	P00-00091	4-20 x 0.25 L Trilobular Screw	Securing of the Delrin top front slider plate	Screws back out
130	P00-00092	0.375 Dia x 1.31 L Clevis Pin	Lower Push rod pivot pin	Pin shears or falls out
131	P00-00093	Footrest Tube Plug 0.625	Covers tube ends of footrest	Fall out
132	P00-00094	Hollow Rivet (.125 dia x .25 long)	Holds the nylon washer on the back lock bar	None Identified
133	P00-00095	JPPH 1910 Flange Weld Pin	Back lock bar pin	Shear
134	P00-00096	JPPH 1906 Flange Weld Pin	Bridge pivot pin	Shear
135	P01-00001	0.375 Dia x 1.31 L Clevis Pin with Center Tapped Hole	Upper push rod pivot pin	Pin shears or falls out
136	P01-00002	Makita LPXH01 Motor & Gearbox	Motor	Burn up motor
137	P01-00003	Makita Housing	Motor	None Identified
138	P01-00004	Makita Chuck Screw (Left Handed)	Motor	Screw backs out
139	P02-00001	Brake Pad	Brake Subassembly	None Identified
140	P02-00002	Back Lock Bar	Back lock subassembly	Yielding
141	P02-00003	Back Bridge Slide	Bridge sliding surface on backrest	None Identified
142	P02-00004	Back Bar Outer Plate	Analyzed in welded subassembly	NA
143	P02-00005	Back Lock Delrin Slider	Sliding Interface of back lock slider assembly and seat frame	Wears thin
144	P02-00006	Back Tension Bar	Back rest rotation stop	Tensile yielding
145	P02-00007	Back Stop Shim	Back rest rotation stop	None Identified
146	P02-00008	Belt Pulley Wheel	Drive train	None Identified
147	P02-00009	Ball Nut Mounting Plate	Drive train	Pin tear out
148	P02-00010	Belt Safety Pawl	Drive train	Yielding
149	P02-00011	Belt Safety Mid Link	Drive train	None Identified
150	P02-00012	Belt Safety Gear	Drive train	None Identified
151	P02-00013	Belt Safety Gear Retainer	Drive train	None Identified
152	P02-00014	Belt Safety Center Link	Drive train	None Identified
153	P02-00015	Bridge Bracket	Bridge assembly	Analyzed in its welded assembly
154	P02-00016	Bridge	Bridge assembly	Excessive Deflection
155	P02-00017	Chassis Leg Axle	Chassis/Leg Attachment	Yielding
156				Thread Back Out
157	P02-00018	Fixed Bearing Standoff	Analyzed as part of Welded subassembly	NA

158	P02-00019	Drive Train Spring Pin	Tensioner spring hooks on this to put tension on belt	Spring comes off of pin
159	P02-00020	Front Chassis Rail	Chassis	Bending, yielding
160	P02-00021	Front Leg Seat Axle	Analyzed as part of Welded subassembly	NA
161				Nut falls off
162	P02-00022	Grooved Idler Pulley Shaft	Main shaft for idler for grooved side of belt	Idler pulley breaks off
163	P02-00023	Idler Pulley Shaft	Used on idler pulleys	None Identified
164	P02-00024	Main Chassis Rail	Analyzed as part of Welded subassembly	NA
165	P02-00025	Leg Axle	Seat/leg Attachment	Yielding
166	P02-00026	Main Foot Pivot Insert	Footrest	Fall out
167	P02-00027	Main Drive Pulley Axle	Drive train	Main pulley breaks off
168	P02-00028	Lower Back Axle Sleeve	Analyzed as part of Welded subassembly	NA
169	P02-00029	Rear Leg Seat Axle Sleeve	Analyzed as part of Welded subassembly	NA
170	P02-00030	Power Train Chassis Rail	Analyzed as part of Welded subassembly	NA
171	P02-00031	Slider	Analyzed as part of Welded subassembly	NA
172	P02-00032	Upper Back Axle Sleeve	Analyzed as part of Welded subassembly	NA
173	P02-00033	Tension Pulley Arm	Drive train	None Identified
174	P02-00034	Tension Pulley Axle	Drive train	None Identified
175	P03-00001	Back Bar Right Half	Analyzed as part of Welded subassembly	NA
176	P03-00002	Back Bar Left Half	Analyzed as part of Welded subassembly	NA
177	P03-00003	Back Rest Limit Actuator	Drive train	Ultimate
178	P03-00004	Back Slider Bracket	Back lock mechanism	Yielding
179	P03-00005	Brake Bracket	Brake Subassembly	Yielding
180	P03-00006	Back Lock Surface Extension	Analyzed as part of Welded subassembly	NA
181	P03-00007	Backrest Support Bracket	Analyzed as part of Welded subassembly	NA
182	P03-00008	Main Caster Bracket	Analyzed as part of Welded subassembly	NA
183	P03-00009	Main Caster Brace	Analyzed as part of Welded subassembly	NA
184	P03-00010	Chassis Leg Pivot Flange	Analyzed as part of Welded subassembly	NA
185	P03-00011	Center Chassis Support	Analyzed as part of Welded subassembly	NA
186	P03-00012	Front Cross Brace Gusset	Analyzed as part of Welded subassembly	NA
187	P03-00013	Front Seat Support	Seat	Yielding
188	P03-00014	Front Push Rod Bracket	Analyzed as part of Welded subassembly	NA
189	P03-00015	Left Back Support	Backrest	Bridge slot section yielding

190				Ultimate failure of pivot hole
191	P03-00016	Right Back Support	Backrest	Yielding
192	P03-00017	Left Footrest Pivot Bracket	Footrest	Yielding
193	P03-00018	Right Footrest Pivot Bracket	Footrest	Yielding
194	P03-00019	Left Footrest Caster Bracket	Footrest	Yielding
195	P03-00020	Right Footrest Caster Bracket	Footrest	Yielding
196	P03-00021	Left Footrest Latch Bracket	Footrest	Yielding
197	P03-00022	Right Footrest Latch Bracket	Footrest	Yielding
198	P03-00023	Left Outer Seat Frame	Analyzed as part of Welded subassembly	NA
199	P03-00024	Right Outer Seat Frame	Analyzed as part of Welded subassembly	NA
200	P03-00025	Middle Seat Brace	Analyzed as part of Welded subassembly	NA
201	P03-00026	Rear Seat Hanger	Seat	Yielding
202				Hole tear out at backrest pivot
203	P03-00027	Sheet Metal Push Rod	Main Kinematics	Buckling
204				Yielding
205	P03-00028	Slider Caster Bracket	Analyzed as part of Welded subassembly	NA
206	P03-00029	Drive Train Cover	Drive train	None Identified
207	P04-00001	Ball Screw End Support	Drive train	
208	P04-00002	Bottom Slide Plate	Slider	Wears Thin
209	P04-00003	Bottom Front Slide Plate	Slider	Wears Thin
210	P04-00004	Top Slide Plate	Slider	Wears Thin
211	P04-00005	Top Front Slide Plate	Slider	Wears Thin
212	P04-00006	Footrest Axle Plug	Footrest	None Identified
213	P04-00007	Headrest Tray	Backrest	None Identified
214	P04-00008	Leg	Main Kinematics	Yielding
215	P04-00009	Left Seat Shroud	Seat	None Identified
216	P04-00010	Right Seat Shroud	Seat	None Identified
217	P04-00011	Left Outer Back Shroud	Backrest	None Identified
218	P04-00012	Right Outer Back Shroud	Backrest	None Identified
219	P04-00013	Left Inner Back Shroud	Backrest	None Identified
220	P04-00014	Right Inner Back Shroud	Backrest	None Identified
221	P04-00015	Drive Train End Cap	Drive train	None Identified
222	P05-00001	Upholstered Back Rest	Backrest	None Identified
223	P05-00002	Foot Stirrup	Footrest	None Identified
224	P05-00003	Upholstered Headrest Subassembly	Backrest	None Identified
225	P05-00004	Upholstered Seat Subassembly	Seat	None Identified

226	P05-00005	Upholstered Shoulder Pad Subassembly	Backrest	None Identified
-----	-----------	--------------------------------------	----------	-----------------

## Column 2

BACKGROUND					
LINE NUMBER	POTENTIAL EFFECT OF FAILURE	ROOT CAUSES	ANALYTICAL METHOD	CALCULATED FOS	RATING JUSTIFICATION
1	NA	NA	NA	NA	NA
2	NA	NA	NA	NA	NA
3	NA	NA	NA	NA	NA
4	Backrest will deflect excessively and may lay permanently at a different height than designed	Load in excess of design	FEA	MA0(Part) - Welded Backrest Subassembly (Revision 2).modfem	May interfere with the limit switch system
5	NA	NA	NA	NA	NA
6	NA	NA	NA	NA	NA
7	NA	NA	NA	NA	NA
8	NA	NA	NA	NA	NA
9	NA	NA	NA	NA	NA
10	Backrest falls out	Load in excess of design	Hand Calc.	3.8	High risk to user, and very difficult to detect
11	NA	NA	NA	NA	NA
12	NA	NA	NA	NA	NA
13	NA	NA	NA	NA	NA
14	NA	NA	NA	NA	NA
15	NA	NA	NA	NA	NA
16	NA	NA	NA	NA	NA
17	NA	NA	NA	NA	NA
18	NA	NA	NA	NA	NA
19	NA	NA	NA	NA	NA
20	NA	NA	NA	NA	NA
21	NA	NA	NA	NA	NA
22	NA	NA	NA	NA	NA
23	NA	NA	NA	NA	NA
24	NA	NA	NA	NA	NA
25	NA	NA	NA	NA	NA
26	NA	NA	NA	NA	NA
27	NA	NA	NA	NA	NA



28	Backrest will deflect excessively and may lay permanently at a different height than designed	Load in excess of design	FEA	NA: See FEA No. 3	May interfere with the limit switch system
29	Casters will not roll properly, chair less stable	Load in excess of design	FEA	MA0 - A02-00002 Caster Bracket.modfem	Very low risk to user, and very simple detection
30	Cosmetic or minor interference with another component	Load in excess of design	DVT	Not analyzed due to lack of RPN, even with an extremely high OCC Rating	Very low risk to user, easy to detect damage
31	Cosmetic or minor interference with another component	Load in excess of design	DVT	Not analyzed due to lack of RPN, even with an extremely high OCC Rating	Very low risk to user, easy to detect damage
32	Bridge will not function properly and may lead to other failures	Load in excess of design	FEA	A0 - A02-00005 Bridge Bracket Welded Subassembly.X_T	Major risk to the system, moderate to the user
33	NA	NA	DVT	NA	
34	Ball screw fixed bearing will float freely in assembly	Load in excess of design	Hand Calc.	7.1	Major risk to the system, moderate to the user
35	Function or integrity of the system is affected	Load in excess of design	FEA	MA0 - A02-00008 Chassis Welded Subassembly (STEP 102).modfem	Critical component to system functionality on many levels, may be difficult to detect a failure
36	Leg may detach from the chassis, chair becomes unstable or falls	Load in excess of design	Hand Calc.	5.9	High risk to user and difficult to detect
37	NA	NA	NA	NA	NA
38	Function or integrity of the system is affected	Load in excess of design	FEA	A1 - A02-00012 Left Welded Seat Bar Subassembly.modfem	High risk to user and difficult to detect, some redundancies in place from hardware attached
39	NA	NA	NA	A1 - A02-00012 Left Welded Seat Bar Subassembly.modfem	High risk to user and difficult to detect, some redundancies in place from hardware attached
40	Backrest poor functioning	Exceed yield strength of material	FEA	0.0	Mild risk to user, simple to detect
41	Potential propagation and disconnection from lead screw	Exceed yield strength of material	FEA	A1.3 - A02-00015 Slider Welded Subassembly (Rear).modfem	High risk to user and difficult to detect
42	Poor caster motion	Exceed yield strength of material	FEA	A1.2 - A02-00015 Slider Welded Subassembly.modfem	Mild risk to user, simple to detect after damage is done

43	Backrest poor functioning	Exceed yield strength of material	FEA	A1.4 - A02-00015 Slider Welded Subassembly (Beam).modfem	Mild risk to user, simple to detect
44	Damage to drive belt, belt safety lock system becomes ineffective	Improper torque, vibration	DVT	NA	Not likely that the bolt will contact the belt
45	Releases tension on drive belt, belt comes off or slips, safety system ineffective	Improper torque, vibration	DVT	NA	Will lead to failure of the belt safety lock system
46	Chair will fall, potentially unevenly	Too much load on the belt, excessive wear, over use	Hand Calc.		A user with physical disabilities may become immobilized, OCC based on over use
47	cause bridge to rub on the vinyl material	Excessive friction load on the slide strip	DVT	NA	Cosmetic damage to system, 3 screws, for redundancy
48	Get stuck, not be able to get back up	Use in excess of equipment work life, exceed mfr specifications	Hand Calc.	3.9	Low risk to user, significant function loss, may occur if not properly cared for, sound detectable
49	Wear, galling on the axles	Use in excess of equipment work life, exceed mfr specifications	Hand Calc.	8.9	Low risk to user, moderate function loss, may occur if not properly cared for, detectable by slop in the up position
50	Gear slips	Improper torque, vibration	DVT	NA	Low risk to user, moderate function loss, may occur if not properly cared for, detectable by slop in the up position
51	NA	NA	DVT	NA	NA
52	Unit rocks, or doesn't sit flat or roll properly	Exceed manufacturer specifications	Hand Calc.	3.3	Very low risk to user and easy to see and feel what's happening
53	Upper part of backrest is not contained as tightly	Impact or non-normal load to the washer	DVT	NA	very low risk to user, very unlikely to happen, and difficult to detect
54	Back lock bar may fall off of its pin, and not function properly	Impact or non-normal load to the washer	DVT	NA	Difficult location to have an impact to, failure of other systems, may be noticeable problem
55	Back lock bar rubs on push rod	Impact or non-normal load to the washer, or excessive use	DVT	NA	Difficult location to have an impact to, no failure of other systems, may be noticeable problem

56	Chair will fall, potentially unevenly	Loads in excess of manufacturer specs	Hand Calc.	3.9	Moderate risk to user, failure of subsequent systems, difficult to detect until too late
57	Chair will fall, potentially unevenly	Cyclic fatigue of shaft from belt tension	Hand Calc.	2.5	Moderate risk to user, failure of subsequent systems, difficult to detect until too late
58	Chair will fall, potentially unevenly	Loads in excess of manufacturer specs	Hand Calc.	3.9	Moderate risk to user, failure of subsequent systems, difficult to detect until too late
59	Excessive movement of pawls on bolts,	Impact or non-normal load to the washer, or excessive use	DVT	NA	Difficult location to have an impact to, no failure of other systems, unperceivable
60	Tension bars free to slide back and forth on pin	Impact or non-normal load to the washer	DVT	NA	Difficult location to have an impact to, no failure of other systems, unperceivable
61	Lock bar free to slide back and forth on pin	Impact or non-normal load to the washer	DVT	NA	Difficult location to have an impact to, no failure of other systems, unperceivable
62	Increased slop in bridge base, increase in wear on pins or holes	Impact or non-normal load to the washer, or excessive use	DVT	NA	Difficult location to have an impact to, potential failure of other systems
63	Increased slop in back rest lock if user pushes back, increase in wear on back lock bar	Impact or non-normal load to the washer, or excessive use	DVT	NA	Difficult location to have an impact to, no failure of other systems, unperceivable
64	Chair may feel more sloppy/unstable	Normal Use, or exceeding manufacturer specs	Hand Calc.	8.8	Easy to perceive chair getting looser, not a risk to user injury
65	Chair may feel more sloppy/unstable	Normal Use, or exceeding manufacturer specs	Hand Calc.	5.8	Easy to perceive chair getting looser, not a risk to user injury
66	Over torqueing the system	Switch wears out	DVT	NA	Redundancy used, not a risky failure to the user, however, moderate system damage possible
67	Heating of plastic end support, and subassembly failure inside slide	Over use	Hand Calc.	63.3	No significant function failure, should be able to hear the failure easily
68	Run slider into bearing at rear, over torqueing the system	Switch wears out	DVT	NA	Redundancy used, not a risky failure to the user, however, moderate system damage possible

69	Ceasing of drive system	Over use, exceeding manuf. specs	Hand Calc.		15.1	Significant function failure, should be able to hear the failure easily
70	Ceasing of drive system	Over use, exceeding manuf. specs	Hand Calc.		20.9	Significant function failure, should be able to hear the failure easily
71	Chair may feel more sloppy/unstable	Over use, over compression	Hand Calc.		3	Easy to perceive chair getting looser, not a risk to user injury
72	Chair may feel more sloppy/unstable	Over use, over compression	Hand Calc.		3	Easy to perceive chair getting looser, not a risk to user injury
73	Footrest doesn't roll smoothly	Exceed manufacturer specifications	Hand Calc.		5.7	Very low risk to user and easy to see and feel what's happening
74	Screw comes out of limit switch and it doesn't activate when needed	Vibration	DVT	NA		Redundancy used, not a risky failure to the user, very unlikely to occur
75	Caster falls off	Twisting of a sticky caster, vibration	DVT	NA		One caster falling off at a given time will not make the assembly unstable, it's probably noticeable when loose
76	Seat falls, dumps person from chair	Excessive load on screw	Hand Calc.		4	User could be injured,
77	Footrest becomes loose or detached from the creeper	Excessive load on screw	DVT	NA		Insignificant amount of weight/force on footrest, 2x the screws and less load than the above analysis
78	NA	NA	NA	NA		NA
79	NA	NA	NA	NA		NA
80	brackets come free from corresponding panels	Exceed work load of screw, soft spot in wood	DVT	NA		Several redundancies, no subsequent failures, no detection
81	Shroud no longer securely seated against push rod pivot pin	rotating surfaces	DVT	NA		Low risk, simple to catch and not likely to occur with Loctite
82						
83	Head rest slides	Vibration, or force on headrest	DVT	NA		No risk, simple to catch
84	Back rest lays a bit lower, and perhaps makes a bit of noise when contacting the chassis	Excessive or effects of cyclic load on bumper	DVT	NA		No risk, simple to catch, not analyzed
85	Improper tension on belt, failure of belt safety system	No lubrication	DVT	NA		Low risk, may lead to other system failure

86	Footrest doesn't lock in place	Pin gets sticky, spring wears out	DVT	NA	No risk, simple to see, and not likely under normal use
87	Brake pad falls out	Excessive load on screw	DVT	NA	Low risk, simple to see, astronomical safety factor
88	Brake pad falls out	Excessive load on screw	DVT	NA	Low risk, simple to see, astronomical safety factor
89	Screw comes part way out	None Identified	DVT	NA	Low risk, simple to see
90	Caster bracket comes off	rotating surfaces	DVT	NA	Low risk, simple to catch and not likely to occur with Loctite, 3 redundancies
91	Bumper potentially falls out, making the limit switches unreachable during the recline motion	Vibration	DVT	NA	Low risk, difficult to catch and not likely to occur with Loctite
92	No resistance fall of one or both sides of the chair	Vibration or excessive tensile load	Hand Calc.	22.5	High risk, difficult to catch, backing out not likely with Loctite
93	Spring pin falls off	Vibration	DVT	NA	Low risk, simple to catch and not likely to occur with Loctite, plus redundancy
94	NA	NA	NA	NA	NA
95	Limit switch falls off and fails to perform its function	Switch failed to cut power before being run through	DVT	NA	Redundancy limit switch
96	NA	NA	NA	NA	NA
97	NA	NA	NA	NA	NA
98	Leg/seat axles work their way out, and chair can fall	rotating surfaces	DVT	NA	High risk to user, likely to occur without thread locker
99	Back is no longer constrained from rotating forward	Excessive load on screw	Hand Calc.	401	High risk to user, and very difficult to detect
100	Potential damage done to system in the recline position	Bumper is damaged, or missing	DVT	NA	Low risk to user, moderate to system, and simple to detect after potential moderate damage
101	Back is no longer constrained from rotating forward	Excessive load	Hand Calc.	17.6	High risk to user, and very difficult to detect
102	Back is no longer constrained from rotating forward	Retaining ring falls off	DVT	NA	High risk to user, and very difficult to detect, however very unlikely to occur under normal use

103	Backrest pad falls	Excessive load	Hand Calc.	34	Moderate risk to user, and very difficult to detect, but somewhat of a redundancy with 2 sides
104	Backrest pad falls	Retaining ring falls off	DVT	NA	Moderate risk to user, and very difficult to detect, but somewhat of a redundancy with 2 sides
105	Bumper falls off	Excessive load or effects of cyclic load on bumper	DVT	NA	See FMEA for P00-00049
106	NA	NA	NA	NA	NA
107	Pulley becomes sloppy and misaligned with belt	bearing is loose with shaft	DVT	NA	May lead to belt failure, extremely unlikely since it sits in rigid body motion with center of bearing
108	Pulley becomes sloppy and misaligned with belt, or falls out	shaft turning when it should not, bearing friction or ceasing	DVT	NA	May lead to belt failure, extremely unlikely since it sits in rigid body motion with center of bearing
109	Brake pad is not as rigidly attached to the leg, allows more movement of the chair	Cyclic loading of screw	DVT	NA	Several redundancies, no subsequent failures, no detection
110	NA	NA	NA	NA	NA
111	NA	NA	NA	NA	NA
112	Back lock bar may fall off of its pin, and not function properly	Non-normal load to the washer or ring damage	DVT	NA	Difficult location to sustain damage, failure of other systems, may be noticeable problem
113	Back lock bar becomes unusable and may cause other failures	Excessive load	DVT	NA	Astronomical factor of safety here although potential for other failures
114	belt safety system will not be held at the proper position, inadvertent actuation or failed actuation when needed	Improper press-fit into tension arm	DVT	NA	Potential for other failures, low risk for user, detection very difficult before moderate damage is done
115	belt safety system will not be held at the proper position(s), inadvertent actuation or failed actuation when needed	Improper press-fit into members	DVT	NA	Potential for other failures, low risk for user, detection very difficult before moderate damage is done
116	NA	NA	NA	NA	NA

117	Belt failure	Improper press fit onto shaft	DVT	NA	May lead to belt failure, but belt safety system in place
118	Decreased function of the system, may not raise back up with load on it	Improper press fit onto shaft	DVT	NA	Not high risk of sudden failure, easy to perceive
119	Chair may fall or skip teeth during use	Lack of lubrication	DVT	NA	If not cared for by user, risk increases
120	Bridge falls	Excessive load	DVT	NA	Redundancy for complete failure prevention, moderate risk to user
121	Back is no longer constrained from rotating forward	Screw backs out of nut from cyclic loading	DVT	NA	High risk to user, and very difficult to detect, but redundancies help here
122	bearing comes out of end support, causes vibration and mild damage to surrounding parts	Improper fit of ring in opening	DVT	NA	Low risk to user, moderate to system, and easy to detect after mild damage
123	Belt skips over timing pulley	Over use, exceeding manuf. specs	Hand Calc. Bearing Calculations	7.2	Significant function failure, should be able to hear the failure easily
124	NA	NA	NA	NA	NA
125	Drive screws lose synchronization, system immobilization	Vibration, wear	DVT	NA	Moderate risk to user, failure of subsequent systems, difficult to detect until too late, one redundancy
126	Back lock bar does not fall into place on pin to provide locking feature, backrest falls over backward	Over use or stretching beyond recommended limits	Hand Calc.	3.1	High risk to user, moderate to system, and difficult to detect after mild damage
127	Tension on belt released	Over use or stretching beyond recommended limits	Hand Calc. Misc Hardware Calculations	3	Will lead to failure of the belt safety lock system, as well as potential falling of chair
128	Tension on belt released	Spring rubs on chassis due to small clearance	DVT	NA	Will lead to failure of the belt safety lock system, as well as potential falling of chair, low clearance creates very real possibility this will happen
129	Slider plate either falls out or gets sucked up into the chassis rail	Cyclic loading of screws	DVT	NA	3 redundancies, and low risk to user, easy to catch without much damage
130	Sudden drop of chair	Excessive load	Hand Calc. Pins Analysis	15.1	High risk to user injury, difficult to detect

131	None, cosmetic	Bumps to it, lose fit	DVT	NA	Extremely low risk to user and system
132	NA	NA	NA	NA	NA
133	Back lock will not be able to perform its proper function	Excessive load	DVT	NA	The potential load here is very low, this feature is to protect against high movement low force type motion.
134	Bridge falls	Excessive load	FEA	A1 - A02-00005 Bridge Bracket Welded Subassembly.modfem	Major risk to the system, moderate to the user, FEA minimum FOS
135	Sudden drop of chair	Excessive load	Hand Calc. Pins Analysis	15.1	High risk to user injury, difficult to detect
136	Stuck in place	Exceed manufacturer specs	Hand Calc. Misc Hardware Calculations	NA	Unit will become unusable until new motor is put on, but the torque/RPM curve is far below the motor's torque/speed line
137	NA	NA	NA	NA	NA
138	Main drive gear may work off the shaft and hit the bearing in front of it	rotating surfaces	DVT	NA	Audible issue and flawed performance before too much harm done.
139	NA	NA	FEA	NA	FEA used to identify hardness of rubber
140	The backrest over rotates backward with the seat following the rotation	Load too high for design	FEA	A0 - P02-00002 Back Lock Bar.modfem	Relatively high risk to user without the ability to counter the motion, Low risk to the system. Obvious to feel something wrong.
141	NA	NA	NA	NA	NA
142	NA	NA	NA	NA	NA
143	Slider subassembly becomes loose and sloppy	Excessive use	DVT	NA	Easy for user to recognize, low risk to user
144	Backrest over rotates on user	Load in excess of design	FEA	P02-00006 Back Tension Bar	High risk to user, and very difficult to detect, but redundancies help here
145	NA	NA	NA	NA	NA
146	NA	NA	NA	NA	NA
147	Slider becomes detached from the lead screw, chair falls	Load in excess of design	FEA	A0 - P02-00009 Ball Nut Mounting Plate.modfem	High risk to user, and very difficult to detect, but redundancies help here
148	Pawl no longer lines up correctly with gear	Load in excess of design	FEA	A0 - P02-00010 Belt Safety Pawl.modfem	Failure may create hazard for the user, not easy to detect
149	NA	NA	DVT	NA	NA
150	NA	NA	DVT	NA	NA



151	NA	NA	DVT	NA	NA
152	NA	NA	DVT	NA	NA
153	NA	NA	NA	NA	NA
154	Cause harm to pivot components and risk of falling out	Load on bridge	FEA Hand Calc.	A0 - A01-00003 Bridge Subassembly.modfem	Major risk to the system, moderate to the user, and simple for user to detect
155	Ultimate failure may result in leg detachment at chassis, and chair falling or becoming unstable	Excessive load from leg	Hand Calc. Pins Analysis	17.1	User and equipment at high risk
156	Screw Falls out and leg becomes detached from chassis	Rotational load on axle from leg pivoting	DVT	NA	User and equipment at high risk
157	NA	NA	NA	NA	NA
158	Chair will fall, potentially unevenly	Spring got pulled up and out of the pin groove	DVT	NA	Nothing for the spring to catch on
159	Rotation of the side rail tubes at the front end	Caster bracket moment	FEA	>3	Low User risk, but chassis damage could be difficult to repair
160	NA	NA	NA	NA	NA
161	Screw Falls out and leg becomes detached from seat	Rotational load on axle from leg pivoting	DVT	NA	User and equipment at high risk
162	If only one fails the tensioner will allow all to continue working properly, but idler pulley bouncing around inside may damage or derail belt	Cyclic bending stress fatigue	FEA Hand Calc.	A0.1 - P02-00022 Grooved Idler Pulley Shaft.modfem	Should be obvious to user something is wrong, belt safety system , redundant grooved pulley
163	NA	NA	DVT	NA	NA
164	NA	NA	NA	NA	NA
165	Ultimate failure may result in leg detachment at seat, and chair falling or becoming unstable	Excessive load from leg	Hand Calc. Pins Analysis	18.9	User and equipment at high risk
166	Main footrest assembly will become detached from the strut and caster	Bad press fit or improper use	DVT	NA	Low risk to equipment, and user, and very obvious to detect a problem
167	Belt loses tension, system cannot move by motor	Cyclic bending stress fatigue	FEA Hand Calc.	A0 - P02-00027 Main Drive Pulley Axle.modfem	Should be obvious to user something is wrong, belt safety system
168	NA	NA	NA	NA	NA
169	NA	NA	NA	NA	NA
170	NA	NA	NA	NA	NA
171	NA	NA	NA	NA	NA

172	NA	NA	NA	NA	NA
173	NA	NA	DVT	NA	NA
174	NA	NA	DVT	NA	NA
175	NA	NA	NA	NA	NA
176	NA	NA	NA	NA	NA
177	Change the location at which the backrest stops in the recline direction	Material forced beyond its ultimate stress	FEA	A3 - P03-00003 Back Rest Limit Actuator.modfem	Difficult for user to detect however, user not at risk
178	Change the location at which the backrest stops in the incline direction	Material forced beyond its yield stress	FEA	A0.1 - P03-00004 Back Slider Bracket.modfem	Difficult for user to detect however, user not at risk
179	Brake does not contact ground with as much force as needed for holding unit still	Material forced beyond its yield stress	FEA	A2 - P03-00005 Brake Bracket.modfem	Difficult for user to detect, user may fall during transfer
180	NA	NA	NA	NA	NA
181	NA	NA	NA	NA	NA
182	NA	NA	NA	NA	NA
183	NA	NA	NA	NA	NA
184	NA	NA	NA	NA	NA
185	NA	NA	NA	NA	NA
186	NA	NA	NA	NA	NA
187	Seat sags or becomes deformed	Material forced beyond its yield stress	FEA	A0 - P03-00013 Front Seat Support.modfem	More cosmetic, but may become troublesome to the user
188	NA	NA	NA	NA	NA
189	Bridge may fall out the back	Material forced beyond its yield stress	FEA	A1 - P03-00015 Left Back Support.modfem	Major risk to the system, moderate to the user
190	Backrest may fall out	Material forced beyond its ultimate strength	FEA	0.0	
191	Bridge may fall out the back	Material forced beyond its yield stress	FEA	A1 - P03-00015 Left Back Support.modfem	Major risk to the system, moderate to the user
192	Footrest caster no longer travels level, footrest becomes unlatched swings out	Material forced beyond its yield stress	FEA	A0 - P03-00017 Left Footrest Pivot Bracket.modfem	Low to moderate risk to equipment, and user, and very obvious to detect a problem
193	Footrest caster no longer travels level, footrest becomes unlatched swings out	Material forced beyond its yield stress	FEA	A0 - P03-00017 Left Footrest Pivot Bracket.modfem	Low to moderate risk to equipment, and user, and very obvious to detect a problem
194	Footrest caster no longer travels level	Material forced beyond its yield stress	FEA	A0 - P03-00019 Left Footrest Caster Bracket.modfem	Low to moderate risk to equipment, and user, and very obvious to detect a problem

195	Footrest caster no longer travels level	Material forced beyond its yield stress	FEA	A0 - P03-00019 Left Footrest Caster Bracket.modfem	Low to moderate risk to equipment, and user, and very obvious to detect a problem
196	Footrest caster no longer travels level, footrest becomes unlatched swings out	Material forced beyond its yield stress	FEA	A0 - P03-00021 Left Footrest Latch Bracket.modfem	Low to moderate risk to equipment, and user, and very obvious to detect a problem
197	Footrest caster no longer travels level, footrest becomes unlatched swings out	Material forced beyond its yield stress	FEA	A0 - P03-00021 Left Footrest Latch Bracket.modfem	Low to moderate risk to equipment, and user, and very obvious to detect a problem
198	NA	NA	NA	NA	NA
199	NA	NA	NA	NA	NA
200	NA	NA	NA	NA	NA
201	Seat sags or becomes deformed at rear, bridge functions poorly	Material forced beyond its yield stress	FEA	A0 - P03-00026 Rear Seat Hanger (Left Half).modfem	More cosmetic, but may cause trouble or failure of the bridge
202	Backrest becomes detached at seat	Material forced beyond its yield stress	FEA	A1 - P03-00026 Rear Seat Hanger (Left Half).modfem	Becomes a certain hazard to the user, and very difficult to detect
203	Kinematic movements become unsynced, not able to lift user back up	Material forced beyond its yield stress in buckling	FEA	MA0 - P03-00027 Sheet Metal Push Rod (Symmetry).modfem	Major risk to system and moderate to user, user will likely recognize the issue after it's too late
204	Kinematic movements become unsynced, not able to lift user back up	Material forced beyond its yield stress	FEA	0.0	Major risk to system and moderate to user, user will likely recognize the issue after it's too late
205	NA	NA	NA	NA	NA
206	NA	NA	DVT	NA	NA
207					
208	Slider becomes sloppy potentially to the point of metal on Metal	Friction	DVT	NA	Mild repair, moderate loss of function, user at low risk
209	Slider becomes sloppy potentially to the point of metal on Metal	Friction	DVT	NA	Mild repair, moderate loss of function, user at low risk
210	Slider becomes sloppy potentially to the point of metal on Metal	Friction	DVT	NA	Mild repair, moderate loss of function, user at low risk
211	Slider becomes sloppy potentially to the point of metal on Metal	Friction	DVT	NA	Mild repair, moderate loss of function, user at low risk
212	NA	NA	DVT	NA	NA
213	NA	NA	DVT	NA	NA

214	Kinematic movements become unsynced, not able to lift user back up	Material forced beyond its yield stress causing buckling	FEA	2.4	Major risk to system and moderate to user, user will likely recognize the issue after it's too late
215	NA	NA	DVT	NA	NA
216	NA	NA	DVT	NA	NA
217	NA	NA	DVT	NA	NA
218	NA	NA	DVT	NA	NA
219	NA	NA	DVT	NA	NA
220	NA	NA	DVT	NA	NA
221	NA	NA	DVT	NA	NA
222	NA	NA	DVT	NA	NA
223	NA	NA	DVT	NA	NA
224	NA	NA	DVT	NA	NA
225	NA	NA	DVT	NA	NA
226	NA	NA	DVT	NA	NA

Column 3

LINE NUMBER	PRE-RATINGS				RISK MITIGATION			END RATINGS			
	SEV	OCC	DET	RPN	ACTION NEEDED	ACTION TAKEN	RATING CHANGE JUSTIFICATION	SEV	OCC	DET	RPN
1				0	No						0
2				0	No						0
3				0	No						0
4	4	8	3	96	No						0
5				0	No						0
6				0	No						0
7				0	No						0
8				0	No						0
9				0	No						0
10	9	1	9	81	No						0
11				0	No						0
12				0	No						0
13				0	No						0
14				0	No						0
15				0	No						0
16				0	No						0
17				0	No						0
18				0	No						0
19				0	No						0
20				0	No						0
21				0	No						0
22				0	No						0
23				0	No						0
24				0	No						0
25				0	No						0
26				0	No						0
27				0	No						0
28	5	2	5	50	No						0
29	3	10	3	90	No						0
30	2	9	5	90	No						0
31	2	9	5	90	No						0
32	7	7	7	343	Yes	P02-00015 Bridge Bracket thickened	New FOS = 3.1	7	1	7	49
33				0	No						0
34	7	1	7	49	No						0
35	6	1	7	42	No						0



62	6	2	5	60	No							0
63	4	4	3	48	No							0
64	3	1	5	15	No							0
65	3	1	5	15	No							0
66	5	2	5	50	No							0
67	4	1	3	12	No							0
68	6	2	5	60	No							0
69	6	1	3	18	No							0
70	6	1	3	18	No							0
71	3	1	5	15	No							0
72	3	1	5	15	No							0
73	2	1	3	6	No							0
74	6	1	5	30	No							0
75	1	4	3	12	No							0
76	9	1	7	63	No							0
77	2	1	3	6	No							0
78				0	No							0
79				0	No							0
80	3	3	3	27	No							0
81	3	2	3	18	No							0
82				0	No							0
83	1	5	2	10	No							0
84	1	7	3	21	No							0
85	4	4	3	48	No							0
86	2	4	2	16	No							0
87	4	1	3	12	No							0
88	4	1	3	12	No							0
89	2	2	3	12	No							0
90	3	2	3	18	No							0
91	5	2	5	50	No							0
92	9	1	8	72	No							0
93	2	2	2	8	No							0
94				0	No							0
95	3	2	8	48	No							0
96				0	No							0
97				0	No							0
98	9	6	9	486	Yes	Thread locker must be used			9	1	9	81
99	9	1	9	81	No							0
100	6	3	5	90	No							0
101	9	1	9	81	No							0

102	9	4	9	324		If failure mode presents itself through DVT, use Loctite Quicktite 39202 to secure retaining ring	Reduces occurrence probability	9	1	9	81
103	7	1	9	63	No						0
104	7	4	9	252		If failure mode presents itself through DVT, use Loctite Quicktite 39202 to secure retaining ring	Reduces occurrence probability	7	1	9	63
105	1	5	3	15	No						0
106				0	No						0
107	7	1	8	56	No						0
108	7	1	8	56	No						0
109	3	1	3	9	No						0
110				0	No						0
111				0	No						0
112	4	4	5	80	No						0
113	6	1	7	42	No						0
114	5	2	5	50	No						0
115	5	2	5	50	No						0
116				0	No						0
117	7	1	8	56	No						0
118	4	3	4	48	No						0
119	7	7	5	245		Put safety feature in software that will remind the user when to verify lubrication		7	7	2	98
120	7	3	3	63	No						0
121	8	2	8	128		Thread locker must be used to ensure nut remains		8	1	8	64
122	4	3	4	48	No						0
123	6	1	3	18	No						0
124				0	No						0





160	9		9	0	No							0
161	9	8	9	648	Yes							
162	7	1	5	35	No							0
163				0	No							0
164				0	No							0
165	9	1	9	81	No							0
166	2	5	3	30	No							0
167	7	1	5	35	No							0
168				0	No							0
169				0	No							0
170				0	No							0
171				0	No							0
172				0	No							0
173				0	No							0
174				0	No							0
175				0	No							0
176				0	No							0
177	4	5	7	140	No							0
178	5	1	7	35	No							0
179	8	1	8	64	No							0
180				0	No							0
181				0	No							0
182				0	No							0
183				0	No							0
184				0	No							0
185				0	No							0
186				0	No							0
187	3	9	3	81	No							0
188				0	No							0
189	7	1	7	49	No							0
190	7	1	7	49	No							0
191	7	1	7	49	No							0
192	5	4	3	60	No							0
193	5	4	3	60	No							0
194	5	6	3	90	No							0
195	5	6	3	90	No							0
196	5	10	3	150	Yes	Design adjusted on footrest pivot brackets to allow load to be shared between both flanges	New FOS = 1.5	5	8	3		120

197	5	10	3	150		Design adjusted on footrest pivot brackets to allow load to be shared between both flanges					
					Yes	New FOS = 1.5	5	8	3	120	
198				0	No					0	
199				0	No					0	
200				0	No					0	
201	6	7	3	126	No					0	
202	9	1	9	81							
203	7	1	8	56	No					0	
204	7	1	8	56	No						
205				0	No					0	
206				0	No					0	
207				0	No					0	
208	4	8	3	96	No					0	
209	4	8	3	96	No					0	
210	4	8	3	96	No					0	
211	4	8	3	96	No					0	
212				0	No					0	
213				0	No					0	
214	7	4	8	224	Yes	Leg beefed up in high stress area New FOS = 3.0	7	1	8	56	
215				0	No					0	
216				0	No					0	
217				0	No					0	
218				0	No					0	
219				0	No					0	
220				0	No					0	
221				0	No					0	
222				0	No					0	
223				0	No					0	
224				0	No					0	
225				0	No					0	
226				0	No					0	

## Appendix I. Part Level Bill of Materials

**Table 13: Complete component level bill of materials for top-level assembly**

ITEM NO.	PART NUMBER	PART REVISION	DESCRIPTION	QTY.
1	P02-00030	00	Power Train Chassis Rail	1
2	P02-00018	00	Fixed Bearing Standoff	2
3	P02-00024	00	Main Chassis Rail	2
4	P03-00010	00	Chassis Leg Pivot Flange	4
5	P02-00020	00	Front Chassis Rail	1
6	P03-00011	00	Center Chassis Support	1
7	P03-00008	00	Main Caster Bracket	4
8	P03-00009	00	Main Caster Brace	4
9	P03-00012	00	Front Cross Brace Gusset	2
10	P01-00003	00	Makita Housing	1
11	P01-00002	00	Makita LPXH01 Motor & Gearbox	1
12	P01-00004	00	Makita Chuck Screw (Left Handed)	1
13	P00-00061	00	M5 Fender Washer	1
14	P00-00081	00	Hubless Spur Gear 1 in PD .375 bore	2
15	P00-00006	00	Thin 0.5-28 Nut	1
16	P00-00036	00	Flanged Ball Bearing 0.25 bore	3
17	P00-00035	00	Flanged Bearing 0.375 bore	1
18	P00-00085	00	0.25 ID .5 OD Flanged Ball Bearing	4
19	P02-00027	00	Main Drive Pulley Axle	1
20	P02-00022	00	Grooved Idler Pulley Shaft	2
21	P02-00023	00	Idler Pulley Shaft	2
22	P00-00070	00	0.375 Shaft Retaining Ring	1
23	P00-00071	00	0.25 ID Retaining Ring	12
24	P00-00087	00	35mm PD Flanged HTD Pulley for 15mm Belt	3
25	P00-00080	00	19.1mm PD HTD Pulley for 15mm belt	2
26	P00-00023	00	SFU1204-900	2
27	P00-00004	00	FK10 Bearing	2
28	P00-00033	00	8mm ID Flanged Bearing	2
29	P04-00001	00	Ball Screw End Support	2
30	P00-00084	00	0.75 Internal Retaining Ring	2
31	P02-00012	00	Belt Safety Gear	2
32	P02-00013	00	Belt Safety Gear Retainer	2
33	P02-00008	00	Belt Pulley Wheel	2
34	P02-00033	00	Tension Pulley Arm	1

35	P00-00050	00	Drill Bushing	1
36	P02-00019	00	Drive Train Spring Pin	1
37	P02-00034	00	Tension Pulley Axle	1
38	P00-00059	00	0.25DIA 0.25L Shoulder Bolt	6
39	P02-00010	00	Belt Safety Pawl	2
40	P02-00014	00	Belt Safety Center Link	1
41	P02-00011	00	Belt Safety Mid Link	2
42	P00-00025	00	0.252 ID 0.472 OD 0.059L Nylon Washer	5
43	P00-00002	00	HTD 25mm WD x 1135mm PL Timing Belt	1
44	P00-00088	00	Spring 9654K211	3
45	P00-00078	00	0.1875 DIA x .375L Pin	3
46	P00-00077	00	0.1875 DIA x .4375L Pin	1
47	P00-00013	00	Caster Assembly	6
48	P04-00005	00	Top Front Slide Plate	2
49	P04-00003	00	Bottom Front Slide Plate	2
50	P03-00003	00	Back Rest Limit Actuator	1
51	P00-00065	00	Actuator Bumper	1
52	P00-00056	00	0.25-20 x .3125 Socket Button Head	1
53	P00-00042	00	Self-Tap PH 6-32 0.375L	33
54	P00-00032	00	Snap Action Plunger Limit Switch	2
55	P00-00040	00	Lock Nut 2-56	8
56	P00-00060	00	2-56 x 0.75 L Pan Head Screw	8
57	P00-00069	00	2-56 x .1875 L Standoff	4
58	P00-00074	00	#2 Washer	4
59	P00-00034	00	Snap Action Roller Limit Switch	2
60	P00-00049	00	Rubber Bumper 0.25 tall	2
61	P00-00068	00	#5 x .31 L Sheet Metal Screw	2
62	P00-00079	00	0.3125 Washer	8
63	P00-00041	00	Acorn Nut 0.3125-18	8
64	P00-00091	00	4-20 x 0.25 L Trilobular Screw	28
65	P00-00001	00	Grade 5 0.25-20 Hex Nut	6
66	P04-00017	00	Motor Cover	1
67	P04-00018	00	Belt Cover	1
68	P00-00009	00	Truss Head Screw 6-32 x 0.25 L Black Oxide Stainless	2
69	P02-00017	00	Chassis Leg Axle	4
70	P00-00063	00	0.375-16 thin nut	8
71	P02-00031	00	Slider	2
72	P03-00014	00	Front Push Rod Bracket	2
73	P03-00028	00	Slider Caster Bracket	2
74	P02-00028	00	Lower Back Axle Sleeve	2
75	P02-00009	00	Ball Nut Mounting Plate	2

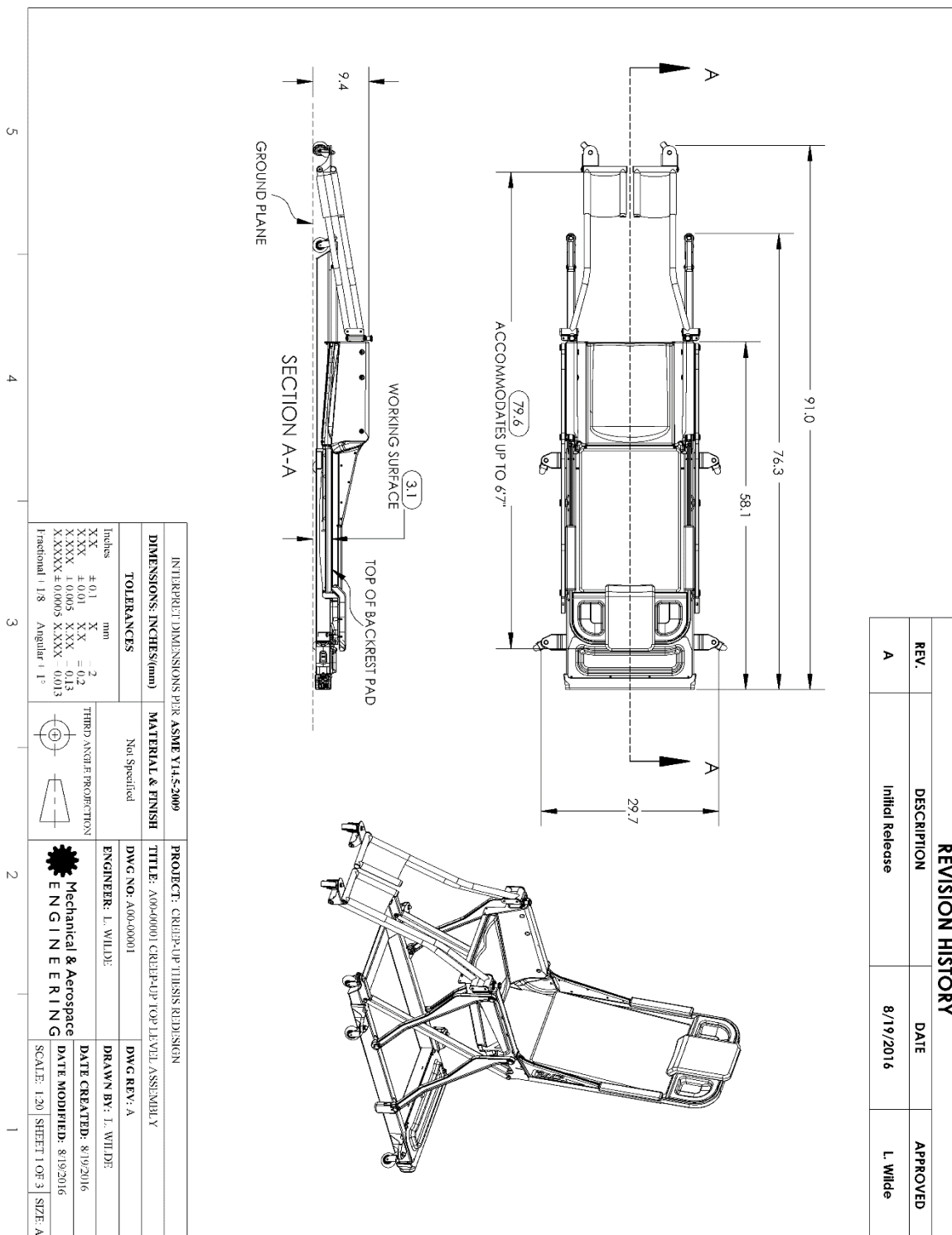
<b>76</b>	P00-00024	00	Ball Nut	2
<b>77</b>	P04-00004	00	Top Slide Plate	2
<b>78</b>	P04-00002	00	Bottom Slide Plate	2
<b>79</b>	P00-00057	00	M4x18 Socket Head	12
<b>80</b>	P00-00030	00	0.377 ID 0.563 OD 1.0 L Bushing	4
<b>81</b>	P04-00008	00	Leg	4
<b>82</b>	P00-00005	00	Roller Bearing 0.5ID 0.5L	8
<b>83</b>	P00-00037	00	Bronze Thrust Bearing 0.5ID 1.0OD 0.062T	22
<b>84</b>	P00-00007	00	Leg Spacer 0.686OD 0.513ID 0.25L	8
<b>85</b>	P03-00005	00	Brake Bracket	2
<b>86</b>	P02-00001	00	Brake Pad	2
<b>87</b>	P00-00008	00	FHS 6-32 x 0.3125L	12
<b>88</b>	P03-00027	00	Sheet Metal Push Rod	2
<b>89</b>	P00-00092	00	0.375 Dia x 1.31 L Clevis Pin	2
<b>90</b>	P01-00001	00	0.375 Dia x 1.31 L Clevis Pin with Center Tapped Hole	2
<b>91</b>	P05-00005	00	Upholstered Shoulder Pad Subassembly	2
<b>92</b>	P00-00045	00	Pan head wood screw #6 x 0.5L	37
<b>93</b>	P00-00038	00	Bronze Thrust Bearing 0.375ID 0.75OD 0.125T	4
<b>94</b>	P00-00031	00	0.377 ID 0.563 OD 0.75 L Bushing	2
<b>95</b>	P00-00066	00	0.25 Dia x 0.875 L Clevis Pin	4
<b>96</b>	P00-00026	00	0.5OD 0.257ID 0.375L Nylon Washer	2
<b>97</b>	P04-00013	00	Left Inner Back Shroud	1
<b>98</b>	P00-00021	00	0.187 ID 0.500 OD 0.062L Nylon Washer	6
<b>99</b>	P00-00062	00	#8 Fender Washer	2
<b>100</b>	P00-00046	00	PH Screw 8-32 x 0.375L	2
<b>101</b>	P04-00011	00	Left Outer Back Shroud	1
<b>102</b>	P04-00014	00	Right Inner Back Shroud	1
<b>103</b>	P04-00012	00	Right Outer Back Shroud	1
<b>104</b>	A01-00004	00	Back Rest Frame Tube Welded Subassembly	1
<b>105</b>	P03-00002	00	Back Bar Left Half	2
<b>106</b>	P03-00001	00	Back Bar Right Half	2
<b>107</b>	P02-00004	00	Back Bar Outer Plate	4
<b>108</b>	P02-00028	00	Lower Back Axle Sleeve	2
<b>109</b>	P02-00032	00	Upper Back Axle Sleeve	2
<b>110</b>	P03-00007	00	Backrest Support Bracket	2
<b>111</b>	P04-00007	00	Headrest Tray	1
<b>112</b>	P00-00067	00	0.1875D x 0.625L Clevis Pin	2
<b>113</b>	P05-00003	00	Upholstered Headrest Subassembly	1
<b>114</b>	P00-00043	00	Black Oxide 18-8 Stainless Steel Flat Washer	2
<b>115</b>	P00-00048	00	Studded Knob 10-32 x 0.75L	2
<b>116</b>	P02-00016	00	Bridge	1

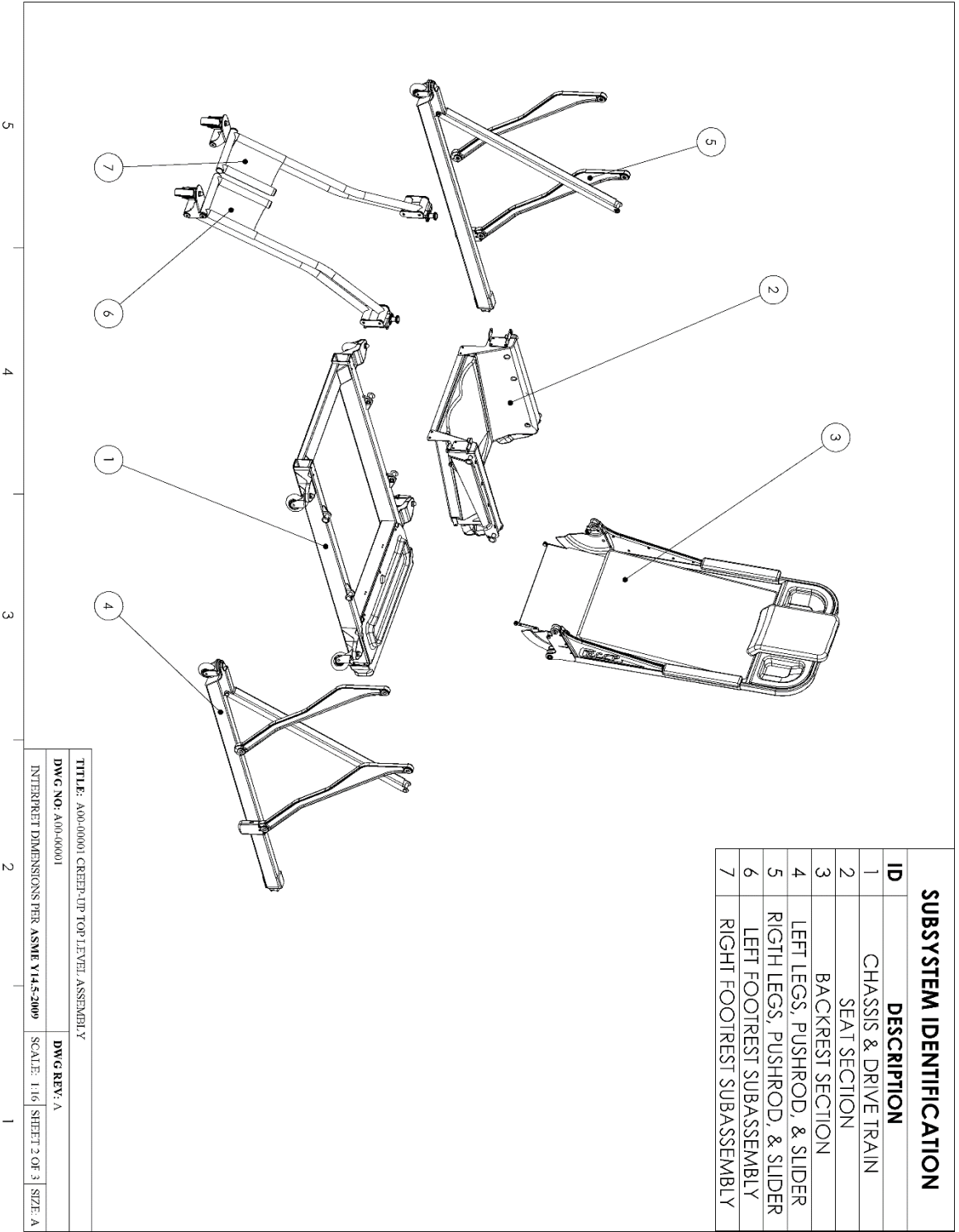
117	P02-00015	00	Bridge Bracket	2
118	P00-00096	00	JPPH 1906 Flange Weld Pin	2
119	P00-00082	00	#10 Tilobular Screw	4
120	P00-00028	00	0.19ID 0.25OD 0.156L 0.49FD 0.062FT Nylon Flanged Washer	2
121	P05-00001	00	Upholstered Back Rest	1
123	P00-00003	00	#6 x 0.625L Flat Head Wood Screw	6
124	P02-00003	00	Back Bridge Slide	2
125	P03-00004	00	Back Slider Bracket	4
126	P02-00005	00	Back Lock Delrin Slider	4
127	P00-00064	00	0.25-28 x 0.625 Socket Button Head	4
128	P00-00027	00	0.433OD 0.256ID 0.22L Nylon Washer	4
129	P00-00076	00	0.25DIA x 0.875L Pin	2
130	P02-00007	00	Back Stop Shim	2
131	P00-00083	00	0.25-28 Square Nut	4
132	P02-00006	00	Back Tension Bar	4
133	P02-00002	00	Back Lock Bar	2
134	P00-00022	00	0.125 ID 0.500 OD 0.125L Nylon Washer	2
135	P00-00094	00	Hollow Rivet (.125 dia x .25 long)	2
136	P03-00013	00	Front Seat Support	1
137	P03-00023	00	Left Outer Seat Frame	1
138	P03-00025	00	Middle Seat Brace	2
139	P02-00021	00	Front Leg Seat Axle	2
140	P03-00006	00	Back Lock Surface Extension	2
141	P02-00029	00	Rear Leg Seat Axle Sleeve	2
142	P00-00095	00	JPPH 1910 Flange Weld Pin	2
143	P00-00029	00	0.189ID 0.25OD 0.249L 0.5FD 0.062FT Nylon Flanged Washer	2
144	P00-00075	00	0.187 Dia Press-on Retaining Ring	2
145	P03-00024	00	Right Outer Seat Frame	1
146	P03-00026	00	Rear Seat Hanger	1
147	P02-00025	00	Leg Axle	4
148	P05-00004	00	Upholstered Seat Subassembly	1
149	P04-00009	00	Left Seat Shroud	1
150	P04-00010	00	Right Seat Shroud	1
151	P00-00010	00	#6 Aluminum Washer	6
152	P00-00011	00	0.254ID 0.375OD 0.187L 0.63FD 0.062FT Nylon Flanged Washer	4
153	P03-00021	00	Left Footrest Latch Bracket	1
154	P03-00022	00	Right Footrest Latch Bracket	1
155	P03-00017	00	Left Footrest Pivot Bracket	1
156	P00-00051	00	Spring Pin	2

<b>157</b>	P00-00058	00	6-32 x 0.31 Flat Head Screw	4
<b>158</b>	P00-00073	00	3in x 0.25DIA Aluminum Standoff	6
<b>159</b>	P00-00055	00	8-32 x 0.5L Socket Button Head	18
<b>160</b>	A02-00003	00	Welded Foot Rest Subassembly	2
<b>161</b>	P04-00006	00	Footrest Axle Plug	8
<b>162</b>	P00-00093	00	Footrest Tube Plug 0.625	4
<b>163</b>	P02-00026	00	Main Foot Pivot Insert	6
<b>164</b>	P05-00002	00	Foot Stirrup	2
<b>165</b>	A02-00004	00	Welded Foot Rest Strut Subassembly	2
<b>166</b>	P03-00019	00	Left Footrest Caster Bracket	1
<b>167</b>	P00-00086	00	Bronze Bushing	6
<b>168</b>	P00-00044	00	No. 8 Washer 0.75 OD	6
<b>169</b>	P00-00039	00	Caster 100# 2in	2
<b>170</b>	P03-00018	00	Right Footrest Pivot Bracket	1
<b>171</b>	P03-00020	00	Right Footrest Caster Bracket	1



### Appendix J. Top-level Mechanical Drawing





**SUBSYSTEM IDENTIFICATION**

ID	DESCRIPTION
1	CHASSIS & DRIVE TRAIN
2	SEAT SECTION
3	BACKREST SECTION
4	LEFT LEGS, PUSHROD, & SLIDER
5	RIGHT LEGS, PUSHROD, & SLIDER
6	LEFT FOOTREST SUBASSEMBLY
7	RIGHT FOOTREST SUBASSEMBLY

TITLE: A00-00001 GREEN-UP TOP LEVEL ASSEMBLY  
 DWG NO: A00-00001  
 DWG REV: A  
 INTERPRET DIMENSIONS PER ASME Y14.5-2009  
 SCALE: 1:16 SHEET 2 OF 3 SIZE: A

5 4 3 2 1

